2-Element Horizontal Beams

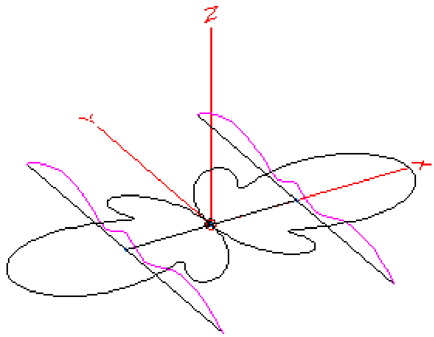

Volume 1

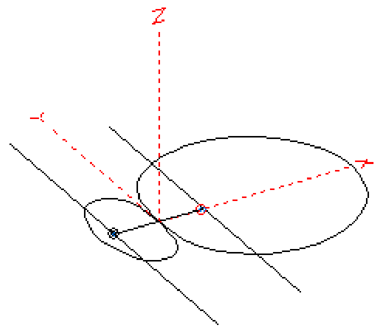

Phased Arrays

L. B. Cebik, W4RNL

Published by
antenneX Online Magazine
http://www.antennex.com/
POB 72022
Corpus Christi, Texas 78472 USA

ISBN: 1-877992-81-X

Table of Contents

Dedication

This volume of studies of 2-element beam antennas is dedicated to the memory of Jean, who was my wife, my friend, my supporter, and my colleague. Her patience, understanding, and assistance gave me the confidence to retire early from academic life to undertake full-time the continuing development of my personal web site (http://www.cebik.com). The site is devoted to providing, as best I can, information of use to radio amateurs and others–both beginning and experienced–on various antenna and related topics. This volume grew out of that work–and hence, shows Jean's help at every step.

Introduction to 2-Element Arrays

If one element is good, then two must be better. This credo underlies most amateur understanding of 2-element (and n-element) arrays. However, as we advance in our understanding of antennas, we must gain an appreciation of what it means to have more than one element and how to arrange the elements to achieve a goal. In fact, we must appreciate what it is to have an element in the first place.

Elements. These notes will address only horizontal elements and combinations of elements. Vertical antennas and arrays call for specialized treatment that is largely outside the scope of the present material. A horizontal element becomes horizontal when it is roughly parallel to the surface of the earth. A vertical antenna is one that is at right angles to the earth's surface. In between the two orientations, we find sloping elements that are neither purely vertical not purely horizontal. They, too, call for special treatment.

For our purposes, we shall call an element any wire structure that is about ½-λ long. There are shorter elements, and there are longer elements—but not much longer. Consider the two antenna structures in **Fig. 1**.

Fig. 1

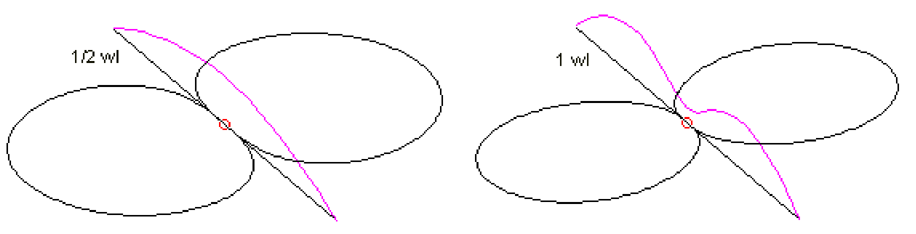

An Element and a Collinear Array of 2 Elements

The structure on the left consists of a single ½-λ element. Note the graph of the current magnitude distribution along the element. The figure also includes the free-space azimuth (or E-plane) pattern produced by the element. Since the pattern is a far field at an indefinitely large distance from the antenna, think of the element as a virtual dot at the pattern center. We have enlarged the element to show multiple facets of the element's performance at the same time.

At the right, we have a structure that appears similar in shape to the one at the left. However, it is 1-λ long. For some purposes, we might still call this structure a single element, but note the current distribution along the structure. We find 2 complete excursions of current along the wire. We have in fact 2 half-wavelength structures, end-to-end. In common antenna terms, we have a collinear array of two half-wavelength elements. The result of this collinear array is a far-field pattern that is narrower and stronger at its maximum than the pattern of the single element.

Therefore, we shall take as our basic element unit a half-wavelength structure. Most of our work will be with these units, although we shall briefly look at a pair of arrays that typically use collinear elements. Each element consists of a length of conductive material. The material may be relatively thin wire or relatively fat tubing. In all cases, the diameter of the material will be a very small fraction of the length, so the general principles that govern the operation of the antennas with which we shall deal will not change just because we change the element's diameter. Hence, for compactness, we shall often refer to elements as wires (and sometimes as tubes), but these shorthand expressions for the physical structure should not confuse us.

The idea of an element is frequency-specific. An element is about ½-λ long only over a fairly small range of frequencies. To keep an element at ½-λ as we change frequency, we shall have to change its physical length. Alternatively, if we keep the same physical structure, we shall have to change its classification. In **Fig. 1**, we may think about the two structures as being at the same frequency. Then the structure on the right becomes twice as long as the one on the left. If we view the two structures as being physically identical, then the frequency for the one on the right is twice the frequency of the one on the left.

Depending on the context, elements may go under other names. We often call the ½-λ element, especially when fed at its center, a dipole. A dipole can never be longer than ½-λ. Although many folks commonly call the antenna at the right a dipole, a better name is the doublet. A doublet is any center-fed structure, regardless of length or of the operating frequency. A 135' dipole for 80 meters becomes a doublet the moment we use the antenna on a higher amateur band, such as 40 or 20 meters.

Fig. 2

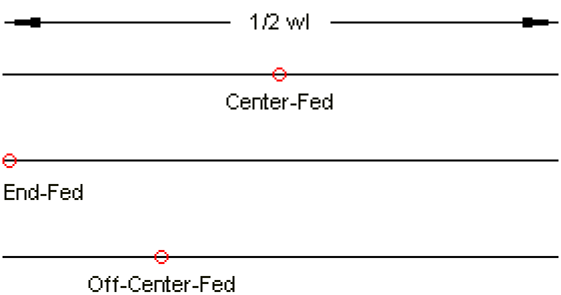

Element Feedpoint Positions

A doublet is a center-fed wire structure, and so too is a dipole. However, compare the possible feedpoints in **Fig. 2** with the right side of **Fig. 1**. The doublet is center-fed physically, but each of the two (1/2-λ) elements within it is end-fed. With only a few exceptions, the antennas with which we shall deal in these notes are based on the ½-λ element and will use a center feedpoint.

Arrays. Whenever we have more than one element in a total structure that we call the antenna, we have an array. The 1-λ wire in **Fig. 1** is already an array, a collinear array. Having 2 elements end-to-end modifies the radiation pattern in ways that are sometimes useful (and sometimes not). We can extend the length of the wire to many wavelengths (or, what amounts to the same thing, raise the operating frequency by a large amount) and achieve a "long-wire" collinear array. When we speak in the most general terms, there are only 3 possibilities for arrays, and being collinear is one of them.

Fig. 3

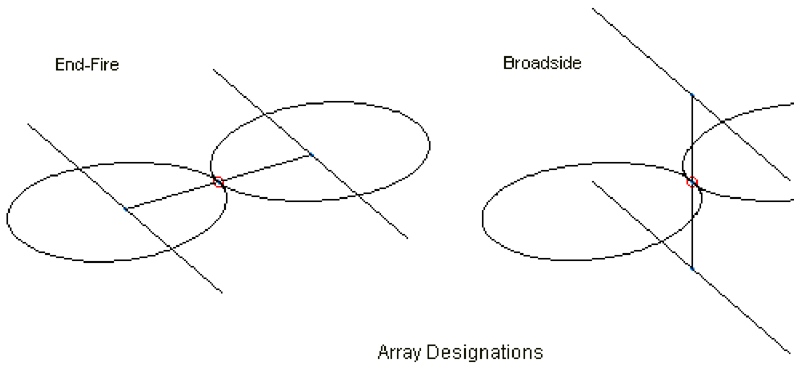

Array Designations

The other 2 classifications appear in **Fig. 3**. If we have at least 2 separate wires in the array, then they will form a plane. If the main radiation is in the plane of the wires, then we have an end-fire array. All Yagis are end-fire arrays. If the main radiation is at right angles to the plane formed by the wires, then we have a broadside array. All quad beams based on the 1-λ loop are broadside arrays.

The classifications are not mutually exclusive. Suppose that we make each wire in the structure on the left in **Fig. 3** at least 1-λ long. Next, suppose that we stack two of these arrays vertically. We shall also bring all of the connecting feedlines together in order to have a single feedpoint. The result might look like the antenna in **Fig. 4**.

The length of the wires places this array in the collinear category. The radiation pattern is in the plane of pairs of wires, making it an end-fire array. However, it is also at right angles to the plane of wire pairs, when we change our perspective. Hence, it is a broadside array. Because the method of connecting the elements together gives us no reason to prefer one category over another, we end up calling this a collinear-broadside-end-fire array. Fortunately, we shall not deal with this antenna in these notes. However, the array does give us a sense of the limits of our classifying scheme.

Fig. 4

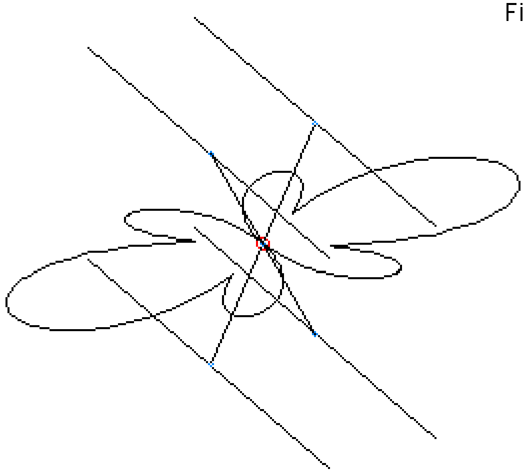

A Collinear-Broadside-End-Fire Array

Radiation Patterns. All of the samples of elements and arrays have shown free-space azimuth (E-plane) patterns. Free-space has no up or down to define an azimuth pattern, which uses the earth's surface as a reference. Since we are working with patterns in the plane of one or more elements, the patterns are in the antenna's E-plane or electrical plane. The plane at right angles to the wire(s) would be the H-plane or magnetic plane. If we took an azimuth pattern of a vertical monopole or dipole, the pattern would be at right angles to the wire and be an H-plane pattern. Because all of our antennas will be horizontal relative to the earth's surface, they will also be E-plane patterns.

As we have seen in the samples, every pattern has lobes (strong directions) and nulls (weak directions). The lobe or lobes with the strongest radiation are called the main lobes. The name for the remaining lobes depends on another classification of arrays and their patterns.

Except for omni-directional patterns that we might obtain from a vertical antenna (and a few special designs for horizontal antennas), horizontal antennas will show one or more main lobes. Simple center-fed long doublets may show many lobes at higher frequencies, and up to 4 of them may be of equal and maximum strength. However, when we create arrays, one of the goals is to reduce the number of main lobes to either one or two lobes at right angles to the wire. **Fig. 5** presents examples of each of these types of patterns.

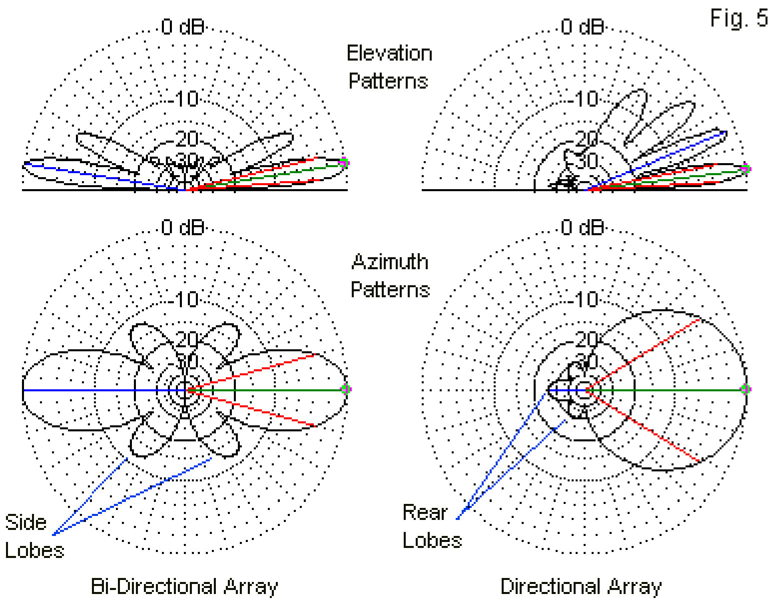

Some Radiation Pattern Types, Features, and Parts

The azimuth patterns for the antenna on the left show a bi-directional characteristic. Each main lobe is of equal strength. The smaller lobes at an angle to the main lobe or lobes become side lobes. The azimuth pattern to the right has only one main lobe. Although we probably should call this antenna uni-directional, most literature (including these notes) will shorten the word to just directional. Some antenna designs may have side lobes on the main lobe, but this example has a single lobe in the favored direction. Since we now have a forward direction, the remaining lobes in the rearward quadrant become rear lobes. (In Volume 2, we shall draw some finer distinction among the lobes and the structures of directional beam patterns.)

We shall measure the gain of a directional or a bi-directional antenna in terms of the strongest point on the strongest lobe. The unit of measure will be the decibel isotropic, or dBi. Measuring gain in decibels always requires a reference, and for antenna patterns, the most common reference is the isotropic source. An isotropic source is one that—in free space—radiates equally well in all directions, including left, right, up, down, etc. (In Volume 2, we shall look at some alternative references.) On occasion, we shall also check the gain of side or rear lobes. In most cases, we shall simply note how much weaker they are (in dB) relative to the maximum gain of the main lobe or lobes.

Fig. 6

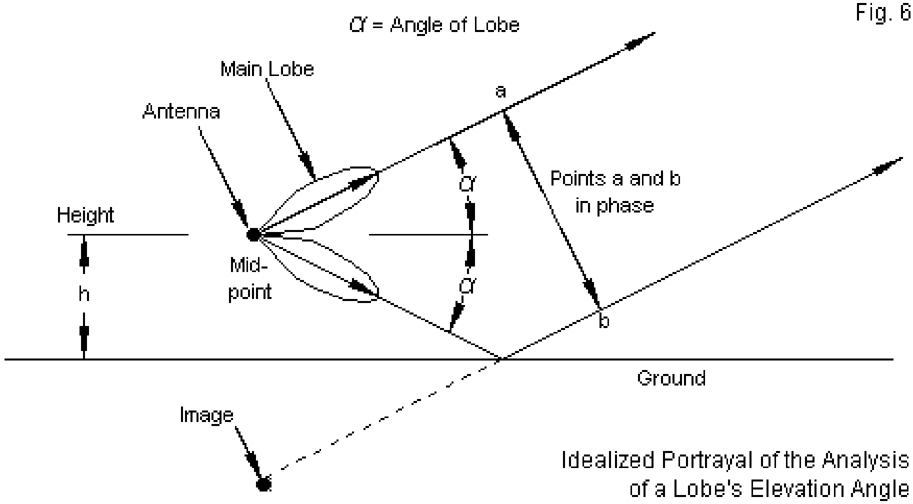

Idealized Portrayal of the Analysis of a Lobe's Elevation Angle

In free space, finding the maximum gain of a horizontal array only requires reference to one pattern. However, over ground, the main lobe will have an elevation angle as well as an azimuth direction. The radiation that in free space would go downward, over real ground encounters the earth and reflects (with some loss) upward. For a given height of the antenna above ground, the incident (upward) wave and the reflected wave will add in phase and produce a stronger lobe. **Fig. 6** shows how many texts portray this condition. As we check the radiation at various elevation angles, we find that the wave may add in phase to produce lobes or may add out of phase to produce nulls—or something in between.

The elevation patterns in **Fig. 5** give us two examples of the lobe and null structure above ground. The strength of each elevation lobe—both the main or primary lobe and the secondary lobes—depends on the antenna configuration. However, the angle of the lobes in degrees above the horizon (α) is determined ideally by the simple height of the horizontal antenna above ground. (Note that I have excluded vertical antennas from this analysis.) Let's count lobes and nulls in order from the ground up, assigning odd numbers to lobes and even numbers to nulls. The lowest lobe will be 1, while the second lobe will be 3. The null between them will be 2. These are values of N. Next, let's measure the height of the antenna above ground in wavelengths at the operating frequency (h). If the ground were perfectly reflective, then we could calculate the angle of any lobe or null:

$$\alpha = \sin^{-1} (N / 4\ h)$$

Most rudimentary calculators have a $\sin^{-1}$ or arcsin function. If we place a horizontal antenna 2 λ above perfect ground (h) and we wish to know the elevation angle (α) of the lowest lobe (N=1), the answer is 7.2°.

As antennas become longer from front-to-back, the idealized picture of how waves intercept the ground changes slightly. Therefore, longer antennas tend to exhibit elevation angles slightly lower than the equation's answer. As well, the ground is not perfect, but introduces losses that depend on its quality. This factor introduces two modifications to the elevation pattern. First, poorer ground tends to reduce the elevation angle of the lobes—again by a small amount. Second, as the ground becomes poorer, the amount of energy in the reflection decreases. Ideally, that is, above a perfectly reflecting ground, the main lobe of a horizontal antenna will show about 6 dB more gain relative to its free-space gain (where there is no reflection). Over average ground, the added gain from ground reflections drops to between 5 and 5.5 dB.

One facet of elevation patterns that most amateurs do not think about concerns the relationship of the elevation pattern to the free-space H-plane pattern. **Fig. 7** shows the 2 patterns together, with both patterns normalized. Normalization means setting the two different gain values to the same limiting value—in this case, maximum gain.

The Relationship between a Free-Space H-Plane Pattern and an Elevation Pattern above Ground

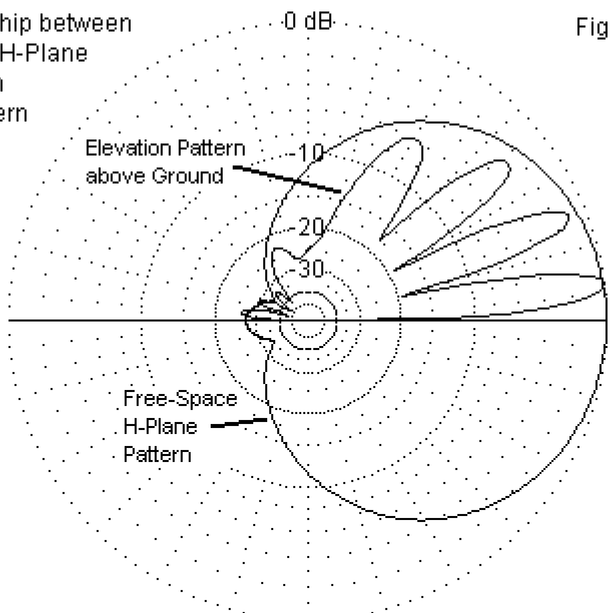

Fig. 7

Note that the elevation pattern has the same overall shape as the free-space pattern if we connect the tips of the lobes. If we average the high and low values for any small segment of the elevation pattern, we would arrive at the contour of the free-space pattern, minus the ground losses, of course.

Element Phase and Phasing. The next step in our progression through basic concepts leads us back from the radiation patterns that antennas produce to the antenna itself and how it produces that pattern when we have more than one element. Suppose that we have two elements that are parallel to each other. As shown in **Fig. 8**, the elements may or may not be the same length. Since we have defined no task for them, we may simply designate them as element 1 and element 2. The only condition that the two elements must meet is that they are within the near fields of each other. In practice, this distance is rarely more than 5/8-λ, and much close spacing is normal for most cases.

Fig. 8

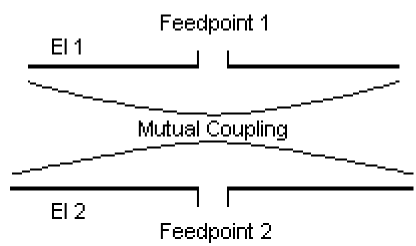

Note: Under some circumstances, one of the 2 feedpoints may be optional.

Providing Energy to the Elements of a 2-Element Array

Under this condition, the elements in the sketch receive energy from 2 sources. One source is the direct feeding of energy at their center points. All feedpoints are in series with the element. Some configurations may use only one of the two feedpoints as a direct source of energy for both elements.

Because the elements are within the near fields of each other, they also receive energy by mutual coupling. The sketch over-simplifies the field, but it does point out that each fed element transfers energy to the other. Even if an element does not receive energy directly, it still radiates and therefore transfers energy via mutual coupling back to the fed element. (As a result, a resonant driven element in a 2-element parasitic beam or Yagi is rarely the same length as an independent resonant dipole made from the same material.)

To obtain any desired and possible radiation pattern from a pair of elements with a fixed set of lengths and a fixed spacing, we must create a set of conditions at the center of each element. As shown on the left in **Fig. 9**, we describe those conditions in terms of the relative current magnitude and phase angle on each element. Very often, we arbitrarily designate the relative current on element 1 (I1) as 1 (A), and set the phase angle at 0°. For the desired pattern, the relative current magnitude on element 2 (I2) may be higher than, lower than, or the same as the current magnitude on element 1. The phase angle of the current on element 2 might be the same as on element 1, or it might be higher or lower than that angle. In some cases, the phase angle at element 2 might be 180° out of phase with the phase angle at element 1.

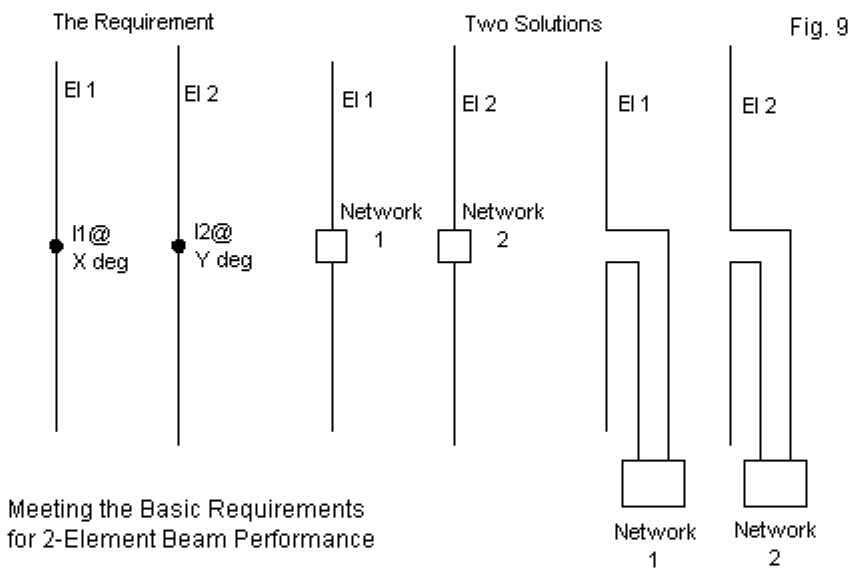

Although not much used for amateur horizontal antennas, many commercial and amateur vertical phased arrays employ networks at the feedpoints of the elements. We most often think of networks, such as the L, the π, and the T, as circuits for transforming impedances. However, every such circuit introduces a phase difference between its input and its output. By judicious calculation of the elements, we can set the two elements so that they have the correct relative current magnitudes and phase angles. Because installing and maintaining a circuit with multiple components at the element feedpoint may range from inconvenient to problematical, we often place the networks at remote locations and use transmission lines to transfer the energy to the element, as shown on the right in **Fig. 9**. If both lines are a multiple of ½-λ at the operating frequency, the current magnitude and phase angle relationships established at the network terminals will be preserved at the feedpoints.

Fig. 10

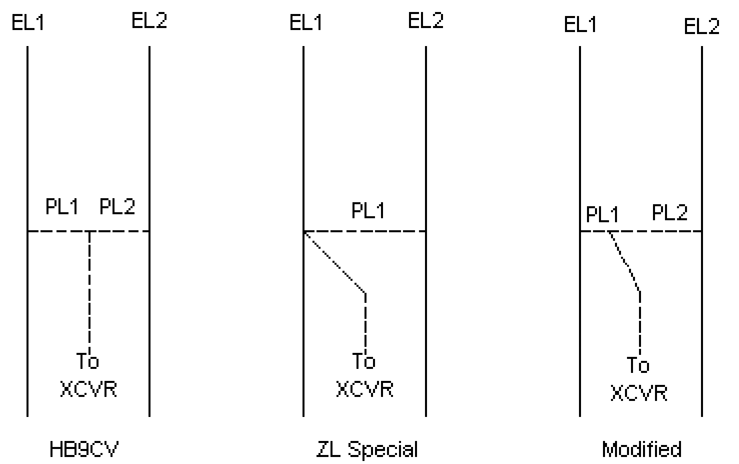

3 Ways to Phase-Feed a 2-Element Array

Most amateur horizontal 2-element phased arrays employ a different means of establishing the required relative current magnitude and phase-angle relationships: one or more transmission lines. **Fig. 10** shows three common configurations.

The arrangements on the left and in the middle are the oldest, dating back to the late 1940s and early 1950s. The HB9CV arrangement uses equal transmission line lengths to a center junction that we may call the array feedpoint. This arrangement calls for a careful selection of the element lengths to obtain the desired pattern. As well, it also calls for gamma or T matching systems at the individual element feedpoints. The ZL-Special arrangement uses a single transmission line between elements. Like the HB9CV system, the ZL-Special divides power at the junction with the main feedline. However, one side of the junction goes directly to element 1, while the other goes to element 2 via the transmission line. The third system has seen lesser use, but may be ultimately more flexible. By using different lengths of transmission line from the main feedline junction to each element, the designer can often make use of common transmission lines to achieve the required balance between the element current magnitudes and phase angles.

For nearly 3 decades, amateur designers of phased arrays—especially the ZL-Special—worked on a false set of assumptions. Builders presumed that the length of the phase-line, that is, the transmission line between elements, determined the properties of the two elements with respect to radiation. However, in the 1980s, both Les Moxon, G6XN, and Roy Lewallen, W7EL, pointed out that not the line impedance, but the relative current magnitude and phase angle were the keys to a successful horizontal phased array of the ZL-Special type. See Moxon, *HF Antennas for All Locations* (RSGB, 1982), pp. 77, 222, and Lewallen, "Try the 'FD Special' Antenna," *QST* (Jun., 1984), 21-24. Because understanding the fundamentals of transmission lines is critical to understand phased arrays (and to much else in antenna systems), let's pause to look at what the shift in viewpoint means to these antennas.

Suppose that we have an element 2 that shows a feedpoint impedance of 50 +/- j0 Ω. Let us also suppose that we need to have the same impedance at the junction with element 1. How long should we make the line to achieve this goal?

Values of I, E, Phase Angles, R, and X for Frequency 30 MHz Table 1

Ant I.... 1.00 A. @ 0 °	Ant E.... 50 v. @ 0 °	
Ant R.... 50 Ω	Ant X.... 0 Ω	Power... 50.0 watts
Line Zo.. 50 Ω	Vel.Fctr. 1.00	Freq.... 30 MHz

Line Length										
Degrees	Feet	Metres	E(in)	Phase	I(in)	Phase	R(in)	X(in)	Z Phase	Z
0°	0.00	0.00	50.00	0	1.00	0	50.00	0.00	0.00	50.00
5°	0.46	0.14	50.00	5	1.00	5	50.00	0.00	0.00	50.00
10°	0.91	0.28	50.00	10	1.00	10	50.00	0.00	0.00	50.00
15°	1.37	0.42	50.00	15	1.00	15	50.00	0.00	0.00	50.00
20°	1.82	0.56	50.00	20	1.00	20	50.00	0.00	0.00	50.00
25°	2.28	0.69	50.00	25	1.00	25	50.00	0.00	0.00	50.00
30°	2.73	0.83	50.00	30	1.00	30	50.00	0.00	0.00	50.00
35°	3.19	0.97	50.00	35	1.00	35	50.00	0.00	0.00	50.00
40°	3.64	1.11	50.00	40	1.00	40	50.00	0.00	0.00	50.00
45°	4.10	1.25	50.00	45	1.00	45	50.00	0.00	0.00	50.00
50°	4.55	1.39	50.00	50	1.00	50	50.00	0.00	0.00	50.00
55°	5.01	1.53	50.00	55	1.00	55	50.00	0.00	0.00	50.00
60°	5.46	1.67	50.00	60	1.00	60	50.00	0.00	0.00	50.00
65°	5.92	1.80	50.00	65	1.00	65	50.00	0.00	0.00	50.00
70°	6.37	1.94	50.00	70	1.00	70	50.00	0.00	0.00	50.00
75°	6.83	2.08	50.00	75	1.00	75	50.00	0.00	0.00	50.00
80°	7.29	2.22	50.00	80	1.00	80	50.00	0.00	0.00	50.00
85°	7.74	2.36	50.00	85	1.00	85	50.00	0.00	0.00	50.00
90°	8.20	2.50	50.00	90	1.00	90	50.00	0.00	0.00	50.00
95°	8.65	2.64	50.00	95	1.00	95	50.00	0.00	0.00	50.00
100°	9.11	2.78	50.00	100	1.00	100	50.00	0.00	0.00	50.00
105°	9.56	2.91	50.00	105	1.00	105	50.00	0.00	0.00	50.00
110°	10.02	3.05	50.00	110	1.00	110	50.00	0.00	0.00	50.00
115°	10.47	3.19	50.00	115	1.00	115	50.00	0.00	0.00	50.00
120°	10.93	3.33	50.00	120	1.00	120	50.00	0.00	0.00	50.00
125°	11.38	3.47	50.00	125	1.00	125	50.00	0.00	0.00	50.00
130°	11.84	3.61	50.00	130	1.00	130	50.00	0.00	0.00	50.00
135°	12.29	3.75	50.00	135	1.00	135	50.00	0.00	0.00	50.00
140°	12.75	3.89	50.00	140	1.00	140	50.00	0.00	0.00	50.00
145°	13.21	4.02	50.00	145	1.00	145	50.00	0.00	0.00	50.00
150°	13.66	4.16	50.00	150	1.00	150	50.00	0.00	0.00	50.00
155°	14.12	4.30	50.00	155	1.00	155	50.00	0.00	0.00	50.00
160°	14.57	4.44	50.00	160	1.00	160	50.00	0.00	0.00	50.00
165°	15.03	4.58	50.00	165	1.00	165	50.00	0.00	0.00	50.00
170°	15.48	4.72	50.00	170	1.00	170	50.00	0.00	0.00	50.00
175°	15.94	4.86	50.00	175	1.00	175	50.00	0.00	0.00	50.00
180°	16.39	5.00	50.00	180	1.00	180	50.00	0.00	0.00	50.00

Table 1 calculates for lossless lines the values of voltage, current, and impedance along a line that runs from 0° to 180° (with arbitrary physical lengths based on the use of 30 MHz as the test frequency). Because the load impedance at element 2 matches the line impedance, the impedance at every point along the line is 50 Ω. The impedance is a function of the voltage and current at each point along the line. For this very special case, the phase angle of the voltage and the phase angle of the current are the same, so the

impedance does not show any change in its phase angle. That is, the reactance remains zero.

However, at the input end of the line, at the junction with the main feedline, we must be able to use the current magnitude and phase angle in parallel with the current magnitude and phase angle required by element 1 to establish the correct relative current magnitudes and phase angles for the two elements. At a spacing of 1/8-λ (45°), the rear element requires a phase angle of 315° (or -45°) to form a directional pattern. So we might use a 45° length of our 50-Ω phase line and achieve the goal—if we put a half-twist in the line.

Now let's suppose that the rear element presents a different impedance, perhaps 200 +/- 0 Ω. If we use a 50-Ω line, we would obtain the results shown in **Table 2**.

I specifically chose a large difference in the resistive impedance of the element-2 load and the phase-line characteristic impedance. Even without any reactance in the element-2 load impedance, we can see several differences from the results in **Table 1**. First, the voltage and the current are not in phase with each other except at each 180° interval along the line. Second, the phase angle of the line impedance values does not coincide with the phase angle of either the voltage or the current except at 1-λ (360°) intervals. For intermediate line lengths (between 0° and 180°), the rate of change of the impedance phase-angle does not coincide with the rate of change of the current phase angle. There are other differences, but these are enough for the moment.

The key to understanding what the table is telling us lies in the unreliability of the impedance columns to guide us when we need to set the current magnitude and phase angle at both ends of a phase line. If we had introduced a reactive component into the element-2 impedance, the table would have shown additional departures from a correlation between impedance and current values. In the end, anyone who seeks to create a phased array, which requires complex values at each end of a phase line, must begin by calculating currents along the line, not impedances. (We shall have a chance later on to take a longer look at these calculations.)

Values of I, E, Phase Angles, R, and X for Frequency 30 MHz — Table 2

Ant I.... 1.00 A. @ 0 °	Ant E.... 50 v. @ 0 °	
Ant R.... 50 Ω	Ant X.... 0 Ω	Power... 50.0 watts
Line Zo.. 200 Ω	Vel.Fctr. 1.00	Freq.... 30 MHz

Line Length Degrees	Feet	Metres	E(in)	Phase	I(in)	Phase	R(in)	X(in)	Z Phase	Z
0°	0.00	0.00	50.00	0	1.00	0	50.00	0.00	0.00	50.00
5°	0.46	0.14	52.77	19	1.00	1	50.36	16.40	18.03	52.96
10°	0.91	0.28	60.26	35	0.99	3	51.45	33.00	32.67	61.13
15°	1.37	0.42	70.80	47	0.97	4	53.35	50.02	43.15	73.13
20°	1.82	0.56	82.99	56	0.94	5	56.16	67.68	50.32	87.95
25°	2.28	0.69	95.90	62	0.91	7	60.06	86.26	55.15	105.11
30°	2.73	0.83	108.97	67	0.88	8	65.31	106.04	58.37	124.54
35°	3.19	0.97	121.81	70	0.83	10	72.30	127.39	60.42	146.47
40°	3.64	1.11	134.14	73	0.78	12	81.61	150.70	61.56	171.38
45°	4.10	1.25	145.77	76	0.73	14	94.12	176.47	61.93	200.00
50°	4.55	1.39	156.54	78	0.67	17	111.15	205.24	61.56	233.40
55°	5.01	1.53	166.32	80	0.61	20	134.80	237.50	60.42	273.09
60°	5.46	1.67	175.00	82	0.54	23	168.42	273.48	58.37	321.18
65°	5.92	1.80	182.49	83	0.48	28	217.45	312.32	55.15	380.56
70°	6.37	1.94	188.71	85	0.41	34	290.42	350.02	50.32	454.81
75°	6.83	2.08	193.62	86	0.35	43	399.04	374.10	43.15	546.98
80°	7.29	2.22	197.15	87	0.30	55	550.85	353.25	32.67	654.39
85°	7.74	2.36	199.29	89	0.26	71	718.17	233.83	18.03	755.28
90°	8.20	2.50	200.00	90	0.25	90	800.00	-0.00	-0.00	800.00
95°	8.65	2.64	199.29	91	0.26	109	718.17	-233.83	-18.03	755.28
100°	9.11	2.78	197.15	93	0.30	125	550.85	-353.25	-32.67	654.39
105°	9.56	2.91	193.62	94	0.35	137	399.04	-374.10	-43.15	546.98
110°	10.02	3.05	188.71	95	0.41	146	290.42	-350.02	-50.32	454.81
115°	10.47	3.19	182.49	97	0.48	152	217.44	-312.32	-55.15	380.56
120°	10.93	3.33	175.00	98	0.54	157	168.42	-273.48	-58.37	321.18
125°	11.38	3.47	166.32	100	0.61	160	134.80	-237.50	-60.42	273.09
130°	11.84	3.61	156.54	102	0.67	163	111.15	-205.24	-61.56	233.40
135°	12.29	3.75	145.77	104	0.73	166	94.12	-176.47	-61.93	200.00
140°	12.75	3.89	134.14	107	0.78	168	81.61	-150.70	-61.56	171.38
145°	13.21	4.02	121.81	110	0.83	170	72.30	-127.39	-60.42	146.47
150°	13.66	4.16	108.97	113	0.88	172	65.31	-106.04	-58.37	124.54
155°	14.12	4.30	95.90	118	0.91	173	60.06	-86.26	-55.15	105.11
160°	14.57	4.44	82.99	124	0.94	175	56.16	-67.68	-50.32	87.95
165°	15.03	4.58	70.80	133	0.97	176	53.35	-50.02	-43.15	73.13
170°	15.48	4.72	60.26	145	0.99	177	51.45	-33.00	-32.67	61.13
175°	15.94	4.86	52.77	161	1.00	179	50.36	-16.40	-18.03	52.96
180°	16.39	5.00	50.00	180	1.00	180	50.00	0.00	0.00	50.00

Fortunately, for some kinds of 2-element phased arrays, the required values of current magnitude are the same, and the relative phase angle is either 0° or 180°. Even though simple to implement, these values result in bi-directional arrays. If we wish to create a directional (that is, a uni-directional) array, then we lose the elegance of simplicity.

Even if we do not use a phase line and feed only one of the 2 elements, phasing considerations will be important. Let's set up to different configurations of arrays with only one driven element each. **Fig. 11** shows the two arrangements. By tradition, we call then the reflector-driver and the driver-director forms of 2-element parasitic beams (also known as Yagi-Uda arrays or Yagis, for short). The term "parasitic" applies to the element that is not directly fed (even via a phase-line) and therefore receives its energy only through mutual coupling with the driver.

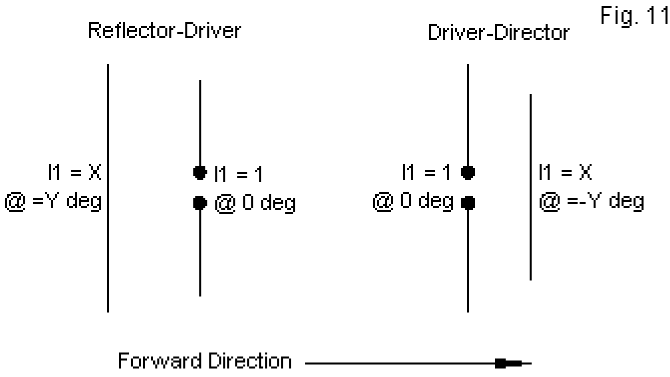

Parasitic Beam (Yagi) Phase Considerations

Although the reflector in the left version and the director in the right version of the 2-element Yagi receive energy via mutual coupling, they meet in a very general and limited way the conditions established by the use of a phase line. For a fixed direction of the main directional lobe of the pattern, the parasitic element current will show the same sort of magnitude and phase angle as the comparable element in an array that uses a phase line. A reflector element is one that shows a certain current magnitude with a positive phase angle relative to the driven element. Ordinarily, a reflector is long relative to resonance at the operating frequency. In contrast, a director is short relative to resonance at the operating frequency and will show a current with a negative phase angle relative to the driven element. 2-element Yagis are simply a special case of the 2-element phased array.

The Plan for Volume 1

The basic concepts and terminology that we have examined set the stage for the initial part of our work in this volume (as well as the next): an exploration of 2-element phased arrays. We shall confine our efforts to exploring the types of arrays most used by radio amateurs, that is, arrays that establish the phasing conditions through the use of transmission lines. As well, as indicated in the general title, we shall look only at horizontal arrays. Vertical arrays and the use of networks will have to await some future date.

Part 1 of this volume will examine two bi-directional arrays based on the use of 2 elements. The phasing requirements for such arrays are seemingly simple and seemingly similar. However, as we shall see, simplicity is not so simple as it may appear, and there are distinct differences between the two types of bi-directional arrays.

The W8JK flattop sets two elements in a horizontal plane. By feeding the two elements in a way that places them 180° out of phase with each other (with equal current magnitudes), we may obtain a bi-directional pattern with significantly more gain than we can obtain with a single dipole element. The antenna is extremely flexible. It may use elements that range from ½-λ to 1.25-λ long. The spacing between elements may range from very close (less than 1/8-λ) to perhaps 5/8-λ. In addition, the array in certain configurations may serve as a multi-band array covering a 2:1 frequency range. Nevertheless, the arrangement that we use for the element phasing system will deserve close scrutiny.

The lazy-H is a related array of 2 elements that may also run from ½-λ to 1.25-λ long. As well, the lazy-H may use spacing values from about 1/4-λ up to 5/8-λ. However, the lazy-H is a broadside array with the element set in a vertical plane relative to the earth. In addition, we feed the two elements with equal current magnitudes and in-phase with each other. Like its out-of-phase flattop cousin, the lazy-H is capable of forming a multi-band bi-directional beam that covers at least a 2:1 frequency range. Once more, the transmission lines that form the phasing network for the lazy-H will eventually take center stage in our examination.

Ultimately, most amateurs prefer directional to bi-directional beams. Eliminating QRM from the rear quadrants improves operation. Hence, amateurs tend to focus their interest on 2-element phased arrays of directional types. To explore this territory, we shall look at the basics of 2-element directional phased arrays and at some of the methods used to obtain the desired element current phasing conditions. Four of the next five chapters have their origins in a study of phased elements that originally appeared in the *National Contest Journal* between November, 2001, and May, 2002. I have revised and expanded the coverage.

Chapter 3 begins with a basic question: what kind of performance can we expect from 2 elements if we could control the current magnitude and phase angle on each element. Although this condition is difficult to replicate with prototypes, antenna-modeling software (NEC-4 in this case) provides a relatively easy way to explore the territory. Typically, we design arrays for one of two conditions: maximum gain or maximum front-to-back ratio. Since the two goals are not coincident with the same phasing conditions, we shall look at each one to see how the phasing conditions differ.

As we have briefly noted here, we may obtain element phasing without a physical phasing network or line. We might refer to this mode as geometric phasing. In Chapter 4, we shall look at the limits of geometric or parasitic element phasing. Indeed, these very limits originally led designers to move from the Yagi to the phased array. Therefore, understanding the limits is essential to understanding the design of arrays that use physical phasing lines.

The most favored array used by Commonwealth and U.S. amateurs is the ZL-Special. Based initially on a misunderstanding of the requirements for phasing, the antenna has undergone many transformations in an effort to achieve the performance of which it is capable. It uses a single phasing line that runs from the rear element to a junction with the forward element. Amateurs have produced versions using linear elements, folded dipole elements, and even in a version that uses “trombone” elements. **Fig. 12** shows the outline of some of the early attempts to design a ZL-Special.

Fig. 12

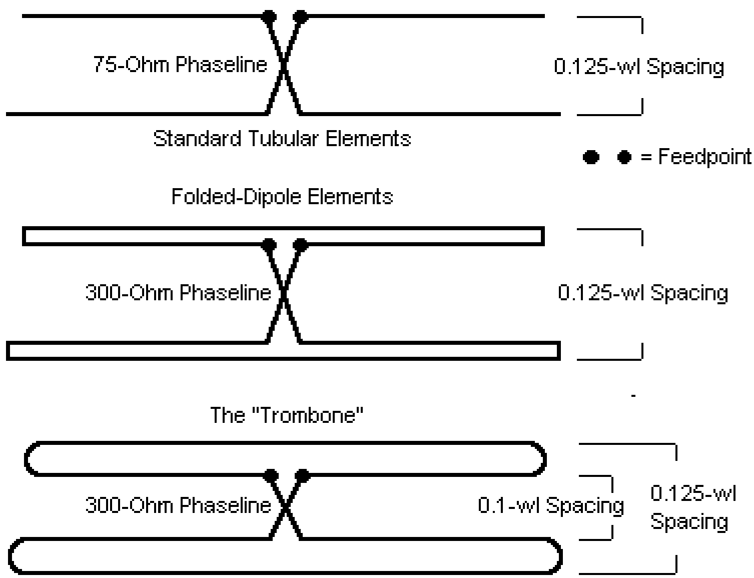

Early ZL-Special Designs

As we shall discover in Chapter 5, one of the chief limitations of the ZL-Special is the relative difficulty of finding dimensions that will permit the use of common transmission lines. W7EL found the correct dimensions for a version using folded dipoles. As well, a relatively simple modification of the phasing system allows the use of common lines and linear elements with quite good results. **Fig. 13** provides a foreshadowing of these designs.

Fig. 13

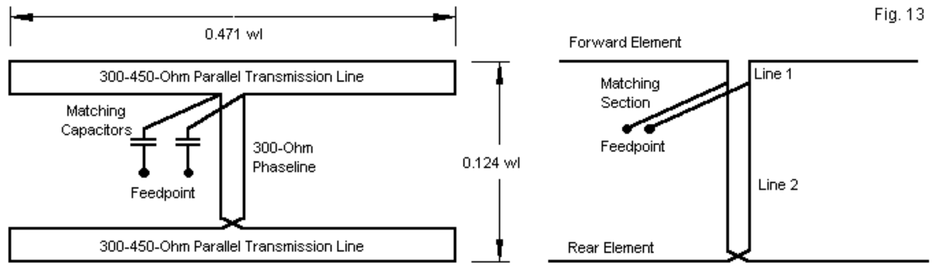

A Practical Folded-Dipole ZL-Special

A Dual-Phaseline ZL-Special

Some Practical ZL-Specials

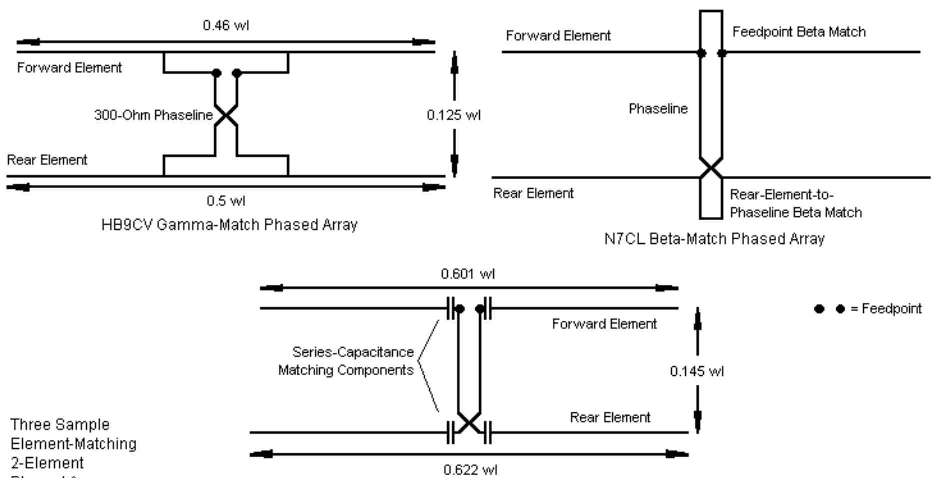

HB9CV Gamma-Match Phased Array

N7CL Beta-Match Phased Array

Three Sample Element-Matching 2-Element Phased Arrays

Capacitive Element-Matching Phased Array

Fig. 14

Because phasing lines have been so misunderstood, Chapter 6 will pause in our progression through phased arrays to examine the more proper way to calculate the phasing conditions for a 2-element array. The treatment will be based on some early work that I did in "The ZL-Special," which appeared in *Communications Quarterly* (Winter, 1997), pp. 72-90. I have recast the treatment for a more orderly look at the necessary equations for calculating the phasing conditions.

Chapter 7 will return to the practical and look at several ways of overcoming some of the limitation in basic phased-array design by element matching, as illustrated by **Fig. 14**. The HB9CV array is perhaps the oldest example of this technique through its use of gamma matching networks on each element. However, more recently, N7CL developed a beta-match system for the pair of shortened elements. Several years ago I developed a design that uses longer elements with a capacitive matching system. The diversity of techniques will show that perhaps we have only begun to scratch the surface of 2-element horizontal phased arrays.

The final chapter will examine a small sample of extended uses of the 2-element phased array when used as the driver section of a more elaborate beam.

Antenna Models Used in These Notes

My chief analytical tool will be NEC-4 antenna-modeling software. To form a common reference line, most of the models will use either a free-space environment or a set distance above average ground conditions (conductivity 0.005 S/m, permittivity 13). Limiting the conditions of modeling allows us to compare directly any two models. We shall also set up a common test frequency range and use comparable material throughout. The linear elements will generally use aluminum tubing, while a few models may use wire—for example, ZL-Special constructed with folded-dipole elements and the bi-directional arrays.

For each chapter, I shall designate the models used by the chapter number and a model number as we proceed through the progression of material. The model designations in the text will allow you to look at the model on your own. A special section of the CD-Rom will contain all of the models used in this volume.

Although you may access the model directly from the CD-Rom, I recommend that you copy the entire set into your hard drive in a special directory. Once on the hard drive, you can not only access the model, but as well you may modify it and save any results, either as a modification of the initial model or under a modified file name. All of the models will use the EZNEC format (.EZ extension). For example, you may wish to scale a design from the test frequency to frequencies in which you have a particular interest. Or, perhaps you may wish to develop for a given model that uses uniform-diameter elements a more practical version that uses stepped-diameter elements.

The potential uses of the models may be almost as endless as the possibilities for creating phased arrays.

Part I: Bi-Directional Arrays

1. The W8JK "Flat-Top" Array

The 1930s proved to be one of the most productive decades for antenna innovations. Many of the basic antennas that today are commonplace originated in this era. The decade records the names of many antenna originators. Among that group is John D. Kraus, W8JK. Among his innovations is the corner reflector array. Our interest here will be in the antenna that bears his name: the W8JK "flattop" (sometimes called simply the 8JK).

The W8JK results from a 1937 Kraus insight, and some 50 years further work on the potentials of the design. Perhaps the best single popular source of information is Kraus' article, "The W8JK Antenna: Recap and Update," *QST* (June, 1982), 11-14. Early on, Kraus worked with very closely spaced ½-λ elements that promised higher gain than more widely spaced elements. However, in later years he developed numerous variations on the design, including versions with 1-λ elements and other versions for multi-band operation over a 3:1 frequency ratio.

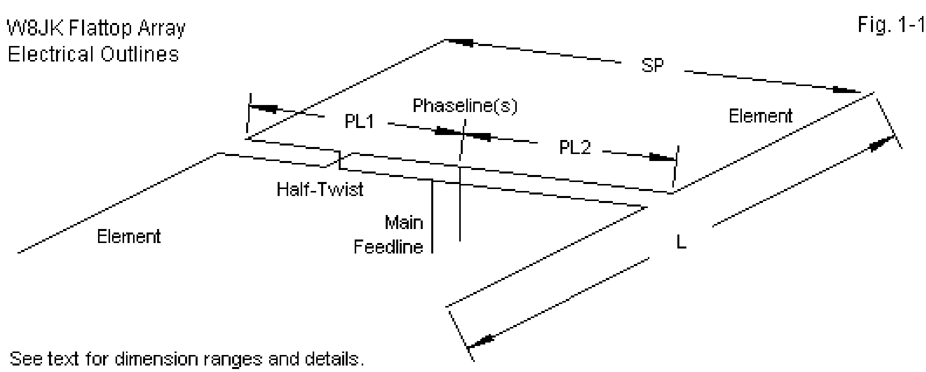

Fig. 1-1 provides an outline of the W8JK layout. The basic principle of the

design is that two parallel elements fed 180° out-of phase with respect to each other will yield considerable gain over a single wire of the same length (L) as one of the elements. The equal lengths of phaseline (PL1 and PL2) in the basic design ensure equal current magnitude on each element. Giving one (and only one) section of the phaseline a half twist suffices to set those currents 180° out-of-phase with each other.

Before we close the book on the W8JK antenna, we shall do some extensive systematic exploration of potentials. However, as a start, let's build a model of the array, step by step. We shall begin with a free-space model of just the elements, since NEC allows us to install a source on each one of them. The model will arbitrarily use copper elements that are 1-λ long (that is, 2 collinear half-wavelength elements). We shall set the spacing at ¼-λ. We shall build the model in a series of steps in order to understand how each antenna component contributes to the full model. **Fig. 1-2** shows the steps that we shall take.

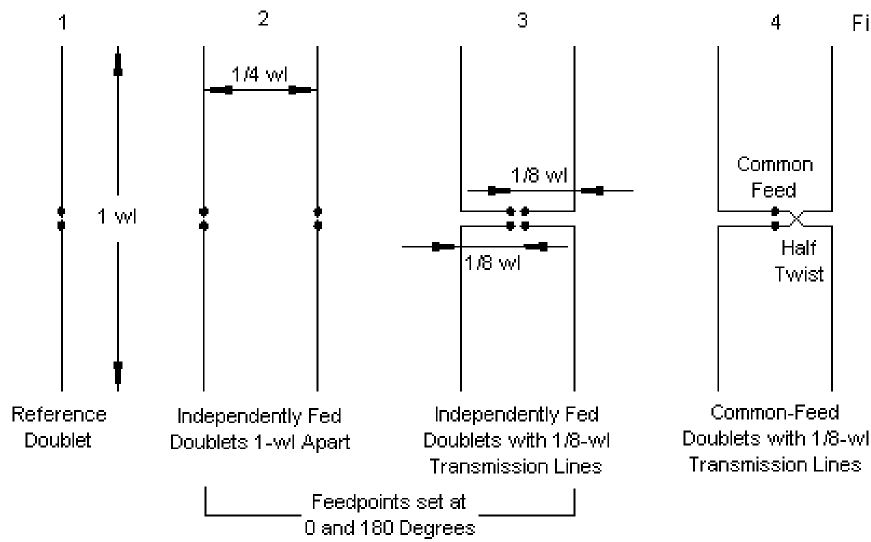

Fig. 1-2

Progressive Steps in Building a Model W8JK Flattop

We should begin with a 1-λ center-fed doublet to use for basic comparisons. The doublet shows a maximum gain in opposite directions of 3.88 dBi with a half-power beamwidth of 47°. The feedpoint impedance is about 2700 – j2100 Ω. Because we used a physical length of 1-λ, the electrical length is slightly longer. We may compare these values to a dipole that is half as long. The dipole gain is 2.14 dBi with a beamwidth of 77°. As shown in **Fig. 1-3**, we obtain the added gain largely by shrinking the beamwidth of the 1-λ doublet. (Model 1-1)

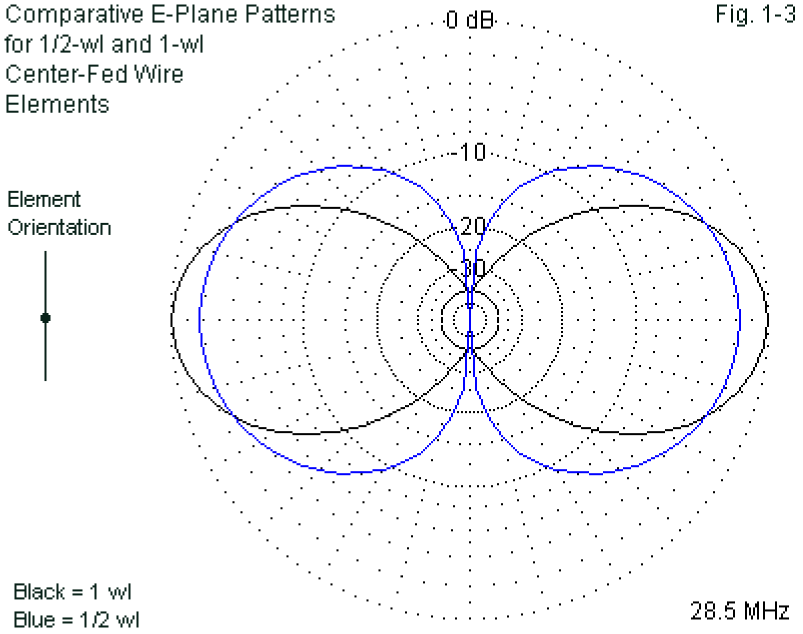

Step 2 involves modeling two elements that are ¼-λ apart. We shall feed each element separately, but we shall set the phase angle of one of the elements to 180° so that the elements are out of phase with each other. The maximum gain in opposite directions climbs to 7.05 dBi, even though the beamwidth only shrinks a small amount: to 42°. Because the element exhibit mutual coupling, the impedance at each feedpoint differs from the single 1-λ element. Each doublet in our pair shows an impedance of 1500 – j3600 Ω. **Fig. 1-4** compares the pattern of the rudimentary W8JK with the pattern of the 1-λ doublet. (Model 1-2)

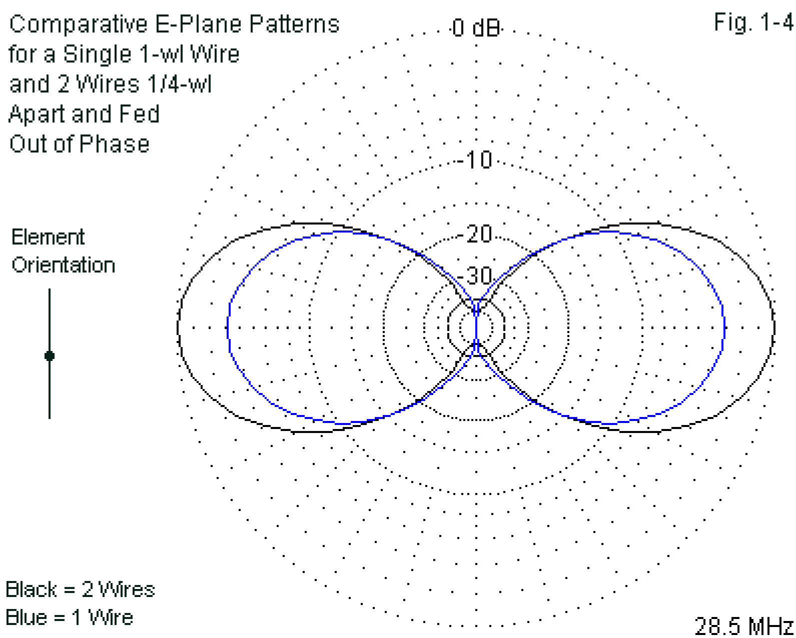

The gain and the radiation pattern of the W8JK will not change as we add further embellishments to the assembly. However, we might pause to ask what would happen if we were to feed the two wires in phase rather than out of phase. **Fig. 1-5** provides the answer to the question. The two patterns show H-plane patterns at right angles to the plane of the element pair. The pattern for the out-of-phase feeding system puts the major lobes along the plane of the wires. However, if we feed the elements in phase with each other, the main lobes of the pattern are broadside to the plane of the wires. In fact, the gain in the plane of the wires drops to 2.0 dBi, less than the gain of a single (1/2-λ) dipole.

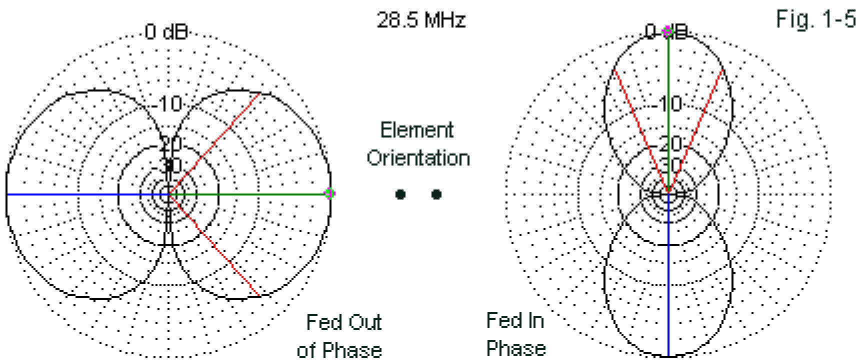

Why In-Phase Feeding Does Not Work for the W8JK Flattop

We normally feed the W8JK by using identical lengths of a parallel transmission line. We usually bring these lines to a single point between the elements. One, and only one, of the two lines receives a single half-twist to reverse the relative phase of the feedpoint current on one element. Initially, we shall not combine the two lines, but feed each one separately. 450-Ω transmission line is perhaps the most commonly used line. For this example, we shall ignore the velocity factor of a real line and use a 0.125-λ electrical length for each line in step 3 of our progression. (Model 1-3)

The radiation performance of the antenna does not change. However, the feedpoint impedance changes considerably. For each independent feedpoint, the model reports an impedance of 31.9 – j356 Ω. Because the line is not matched to the feedpoint impedance, the line acts as an impedance transformer. The element resistive impedance is high, and the reactive component is very high. In fact, the element shows an SWR of about 22.5:1 relative to the 450-Ω phase line characteristic impedance. Under these conditions, even a short length of transmission line shows a very large change in both the resistance and the reactance. **Fig. 1-6** shows the resistance and reactance changes over the 1/8-λ line section. If we were to make the lines longer, we would not see very large changes until the line approached ½-λ.

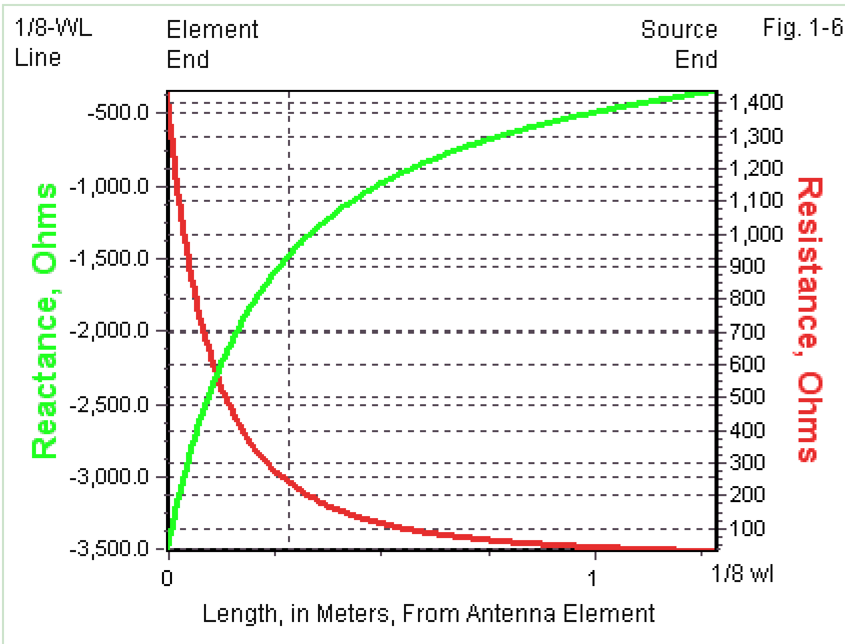

W8JK Element Impedance Transformation Along a 1/8-Wavelength Section of 450-Ohm Transmission Line

The impedance that appears at the ends of the phaselines is subject to several variables. The length of the elements in the array will very slowly change the element feedpoint impedance—and therefore the impedance at the end of the phaseline. We have already seen that the length of the phaseline also results in different impedance values. Finally, the characteristic impedance of the phaseline itself will produce perhaps the largest changes. A 600-Ω transmission line with the same length as the 450-Ω line will yield an impedance that is about 70% higher. A 300-Ω phaseline will result in an impedance that is only about half the values shown by the 450-Ω line. Once we know the element impedance (and account for the mutual coupling between wires), we can calculate the source impedance for each phase line by specifying its electrical length and its characteristic impedance (Zo). In this sample, we have let the modeling program perform the calculations for us.

Step 4 in the process simply joins the two independent lines in a parallel connection to produce a single feedpoint. A parallel connection of two impedances given as series values (R +/- jX Ω) results in resistance and reactance values that are simply half the values of the independent feedpoint impedances. In this case, the model reports an impedance of 16 – j179 Ω. (Model 1-4)

One of the difficulties associated with the W8JK flattop is the fact that the resistive component of the net feedpoint impedance is so low, while the reactive component is about 10 times the resistive component. Many W8JK users wish to use the same feedline (in this case, 450-Ω) from the feedpoint to the antenna tuner. The result is a 32:1 SWR relative to the line Zo. At this SWR level, even low-loss parallel transmission line will show significant losses. An alternative might be to introduce a network to transform the impedance to a usable value with a very low SWR—perhaps 50 Ω. The ratio of reactance to resistance in the impedance to be transformed usually results in a narrow window of low SWR on the main feedline. As well, this technique is not applicable for eventual multi-band use of the flattop array. As a consequence, most W8JK users simply use parallel transmission line and do not even calculate the losses.

The Range of W8JK Possibilities

Although Kraus developed over the years some fairly complex arrangements for the antenna, the basic configuration shown in **Fig. 1-1** is subject to 3 main variables.

1. The element length is variable from about ½-λ up to about 1.25-λ. The

3 most popular element lengths are ½-λ, 1-λ, and 1.25-λ.

2. Typically, the spacing between elements ranges from about 1/8-λ up to about 5/8-λ. Values between these extremes are popular and usually occur in increments of 1/8-λ.
3. The phaseline material normally uses 1 of 3 common parallel transmission lines Zo values: 300 Ω, 450 Ω, and 600 Ω.

The first two factors affect the performance of the array in terms of the maximum gain and the beamwidth of the lobes. The different phaseline Zo values show up only in the common feedpoint impedance. Therefore, we may develop a fairly simple survey of W8JK potentials across the most commonly used dimensions for the array.

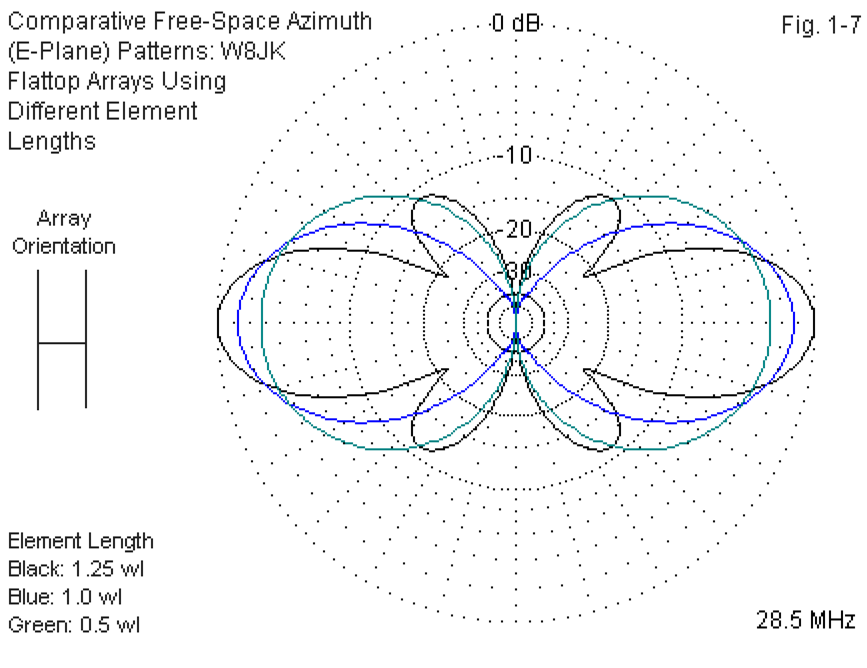

For the samples, we shall employ AWG #12 copper wire at 28.5 MHz. The comparisons will be fair using free-space models for each sample in the collection. The three different element length values will produce three distinct radiation patterns, although the basic shape for each element length will not change with changes in spacing. **Fig. 1-7** overlays the patterns for 3/8-λ spacing.

W8JK Performance Using Different Element Lengths and Different Spacings								Table 1-1
	All models in free space using AWG #12 copper wire							
Element Length = 0.5 wl								
Space wl	Gain dBi	BW deg	R300	X300	R450	X450	R600	X600
1/8	5.69	60.2	7.04	92.97	6.73	123.7	6.6	154.9
1/4	5.64	61.9	69.25	250.9	56.45	322.1	51.42	396.7
3/8	5.21	65.4	610.8	216.6	624.4	709.4	544.2	1017
1/2	4.46	72.2	275.3	-225.6	602.1	-510.7	1028	-913.9
5/8	3.21	84.8	127.2	-151.6	176.9	-310.3	208.8	-479.7
Element Length = 1.0 wl								
Space wl	Gain dBi	BW deg	R300	X300	R450	X450	R600	X600
1/8	7.09	42	8.71	-316.8	17.62	-446.9	28.34	-560.5
1/4	7.05	42.2	7.74	-129.2	16.22	-179.7	26.94	-222
3/8	6.68	43.2	8.48	-47.88	18.43	-61.56	31.69	-68.74
1/2	5.99	45.5	10.88	12.21	24.52	27.57	43.69	48.84
5/8	4.8	50.2	16.42	74.49	38.19	120.7	70.18	172.6
Element Length = 1.25 wl								
Space wl	Gain dBi	BW deg	R300	X300	R450	X450	R600	X600
1/8	8.18	30	3.32	-149.3	4.78	-160.7	5.9	-158.1
1/4	8.27	29.8	5.49	-60.38	9.37	-49.68	13.08	-24.21
3/8	7.9	30	8.35	2.05	16.29	41.28	25.43	99.63
1/2	7.2	31	13.8	63.34	31.29	143.1	56.25	255.7
5/8	6.04	32.8	27.4	146.6	76.92	303	175.4	539.3
Notes	Space wl = element spacing in wavelengths							
	Gain dBi = free-space gain in dBi							
	BW deg = beamwidth in degrees							
	R300, R450, R600 = feedpoint resistance with phaseline os 300, 450, and 600 Ohms							
	X300, X450, X600 = feedpoint reactance with phaseline os 300, 450, and 600 Ohms							

The patterns are directly related to the elements from which they derive. The pattern for 0.5-λ elements is a standard dipole figure-8, while the pattern for the 1-λ elements is an elongated version of a dipole pattern. 1.25-λ elements are standard of extended double-Zepp wires, and the W8JK array that uses them shows the side lobes that we expect to find. The side lobes warn us that any further elongation of the elements would show a decrease in the strength of the main lobe and an increase in side-lobe strength. Hence, an element length of about 1.25-λ is close the maximum usable size for an effective W8JK array.

Table 1-1 provides the modeling data for the collection of models. The table lists the free-space gain and the beamwidth for each model. (See models 1-5a through 1-7e.) The following columns list the feedpoint impedance as values of resistance and reactance for each of the 3 most popular transmission-line characteristic impedance values. However, each phaseline uses a velocity factor of 1.0 for this exercise. Hence, the recorded impedance values are indicative of feedpoint impedances, but will not replicate reality with precision.

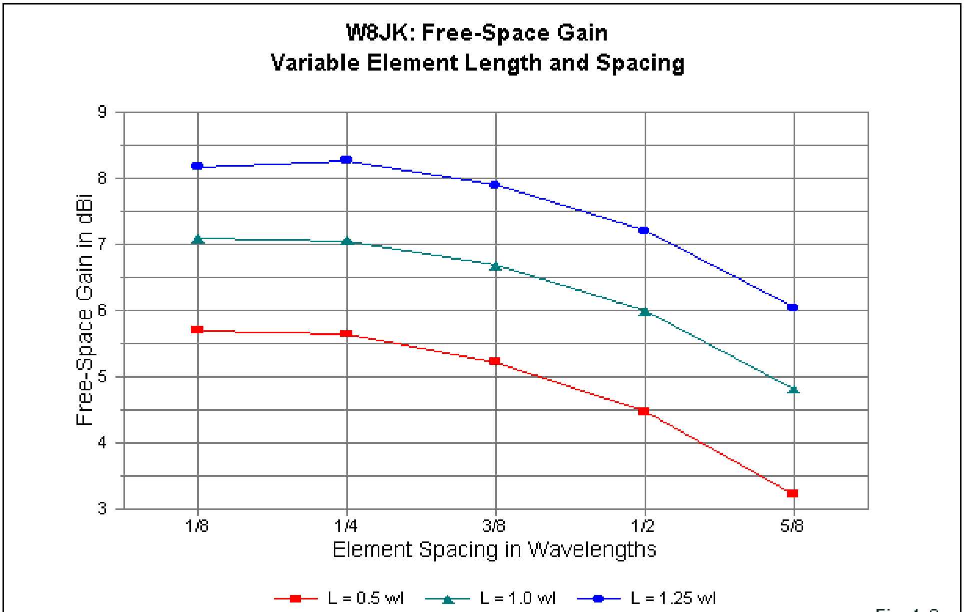

Fig. 1-8

Fig. 1-8 graphs the gain curves as the spacing value changes in 1/8-λ-increments from 1/8-λ up to 5/8-λ. For each spacing value, the curves reflect the gain of the longer element over its shorter neighbor. Classical literature on the W8JK calls attention to the fact that gain decreases as the element spacing increases. The one anomaly in the pattern occurs with the 1.25-λ elements, where the gain for a spacing of ¼-λ is higher than for 1/8-λ spacing.

The curves for the array's beamwidth show the opposite curves, since, for any given element length, the array increases gain directly as the beamwidth decreases. **Fig. 1-9** graphs the beamwidth data for the model collection. The curves do not display the near congruence of the gain curves because beamwidth does not change in the same manner. A 20-dBi-gain 14-λ-boom Yagi will still have a beamwidth between 14° and 17°. As gain increases, the rate of beamwidth decrease slows.

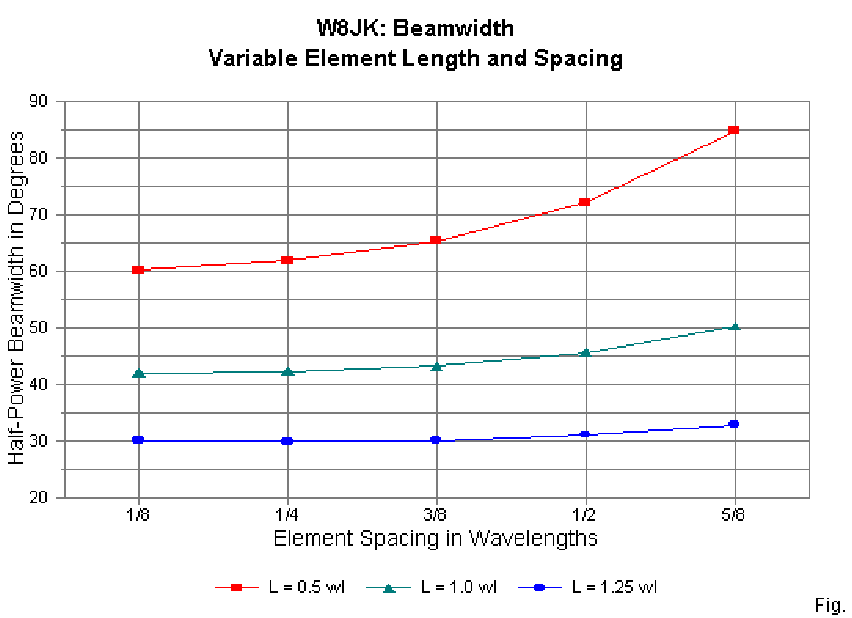

Fig. 1-9

Unfortunately for clear visualization, the data for the feedpoint impedance values do not graph neatly. For example, if we use 0.5-λ elements, then between spacing values of 3/8-λ and ½-λ, the feedpoint reactance goes in one step from a very high inductive reactance to a very high capacitive reactance. However, in assessing the practicality of any of the W8JK designs in the model collection, there are two key elements to inspect carefully. First, note how many of the feedpoint resistance values are well below the 15-20-Ω range. For most purposes, these values are quite impractical. Second, notice the ratio of reactance to resistance. The higher the ratio, the more difficult a match may be to obtain—or to obtain with any usable operating bandwidth.

Selecting a set of W8JK dimensions thus forces on us a compromise between the maximum bi-directional gain and a practical feedpoint impedance for a proposed main feedline type and characteristic impedance. The models use copper wire, the most common material for W8JK arrays. However, for many upper-HF and even VHF frequencies, tubular elements are completely usable. Expect to find differences primarily in the feedpoint impedance values. As a practical example, **Table 1-2** shows models using AWG #12 copper wire and 0.5"-diameter aluminum tubing at the 28.5-MHz test frequency.

A Comparison of W8JK Performance Using Different Element Diameters								Table 1-2
	AWG #12 models use copper wire; 0.5"-diameter models use aluminum wire.							
	Element spacing is 0.5-wavelength							
Element Length = 0.5 wl								
Element	Gain dBi	BW deg	R300	X300	R450	X450	R600	X600
AWG #12	4.46	72.2	275.3	-225.6	602.1	-510.7	1028	-913.9
0.5"	4.49	71.8	264.8	-211.1	580.2	-478.4	993.6	-856.9
Element Length = 1.0 wl								
Element	Gain dBi	BW deg	R300	X300	R450	X450	R600	X600
AWG #12	5.99	45.5	10.88	12.21	24.52	27.57	43.69	48.84
0.5"	6.05	45	17.34	23.51	39.13	52.94	69.86	94.21
Element Length = 1.25 wl								
Element	Gain dBi	BW deg	R300	X300	R450	X450	R600	X600
AWG #12	7.2	31	13.8	63.34	31.29	143.1	56.25	255.7
0.5"	7.19	30.4	23.6	92.22	53.73	208.6	97.09	373.7

The gain values are very close for the pairs of models using the same element length. Equally small is the difference in beamwidth in each pair. However, as we increase the element length, we find a growing differential between the feedpoint impedances for thin and fat elements. Note also that the differences within any pair are roughly proportional to the characteristic impedance of the phaselines. To the collection of variables that may have an effect on the feedpoint impedance at the junction of the phaselines, we may now add another: the element diameter.

The Multi-Band Potential of the W8JK Flattop Array

The exercise that we have just completed showed the W8JK array to be a capable bi-directional antenna over a considerable range of element length and spacing values. If we were to build a certain array configuration, then we might arrive at changes in the configuration simply by changing the operating frequency. For example, if we design a 20-meter W8JK with ½-λ elements and a spacing of ¼-λ, then at 10 meters, we would have a W8JK with 1-λ elements and a spacing of ½-λ. Both sets of values will work.

In fact, one of the better starting points for creating a multi-band W8JK is to use 1.25-λ elements with a 5/8-λ spacing value at the highest desired operating frequency. We may then cover at least a 2:1 frequency range. If we begin at 10 meters, we can obtain coverage for 20 through 10 meters from the same array. Let's round the construction figures in feet. For the next set of notes, **Fig. 1-10** will define the two critical dimensions. Each of the two phaselines will be ½ the spacing values—with the required half-twist in one of those two lines.

We may start at the highest frequency with the largest practical dimensions. For example, 1.25 λ at 28.5 MHz is about 44'. 5/8 λ will be about 22'. We may easily scale this 20-10-meter design for other bands, as suggested by **Table 1-3**. As we change the operating frequency, the dimensions in wavelengths change. **Table 1-4** shows the values of L and SP for each of the operating frequencies that we shall consider with our 44' by 22' W8JK array.

Fig. 1-10

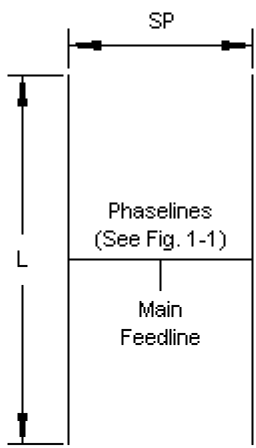

See Table 3 for dimensional possibilities.

General Outline of a
Multi-Band W8JK Array

Dimensions and Potential Band Coverage				Table 1-3
for Multi-Band W8JK Arrays				
See Fig. 1-10 for dimension designations				
L (feet)	SP (feet)	Top Band	Bottom Band	
44	22	10 m	20 m	
66	33	15 m	30 m	
88	44	20 m	40 m	

44' by 22' W8JK Dimensions in			Table 1-4
Wavelengths for Each Band Covered			
Freq MHz	L wl	SP wl	
28.5	1.275	0.638	
24.94	1.116	0.558	
21.225	0.948	0.474	
18.118	0.812	0.406	
14.175	0.634	0.317	

The array will use AWG #12 copper wire for consistency with earlier models. At the 10-meter test frequency, the value of L is slightly longer than the optimal 1.25-λ value, but we shall accrue some slight advantages by using it. (See model 1-9.) The advantages will not show up in the gain column, but they will appear in the impedance data.

If we run the model in free space, we obtain the data that appear in **Table 1-5**. The slightly lower gain value at 28.5 MHz relative to the gain at 24.94 MHz confirms that we have passed the optimal element length on 10 meters. However, the difference is too small to be operationally significant. Therefore, we shall retain our round numbers for the dimensions.

Free-Space Performance Data: 44' by 22' Multi-Band W8JK Array								Table 1-5
Freq MHz	Gain dBi	BW deg	R300	X300	R450	X450	R600	X600
28.5	5.88	37.6	36.12	174.6	109.5	374	275.1	690.6
24.94	6.15	39.8	12.59	58.42	29.51	112	54.75	183.1
21.225	5.91	48	10.15	-7.52	22.78	-7.94	40.41	-6.1
18.118	5.76	53.8	12.28	-64.76	28.54	-111.5	52.42	-168.2
14.175	5.66	59.2	46.95	-234.5	166	-519.7	510.2	-1002
10.125	5.54	62.7	13.18	71.8	15.05	133	16.14	196
Note: 10.125 MHz is not a recommended frequency; see text.								

Because the element length changes as we change operating frequencies, the pattern shape and the beamwidth also change. **Fig. 1-11** provides a gallery of free-space azimuth (E-plane) patterns. The patterns reflect the element length at each frequency. The gain values in the table also reflect the element spacing. One of the more interesting facets of this multi-band version of the W8JK is that the gain is remarkably consistent from one band to the next. Excluding 30 meters (10,125 MHz), the gain changes by less than 0.5-dB from 20 through 10 meters.

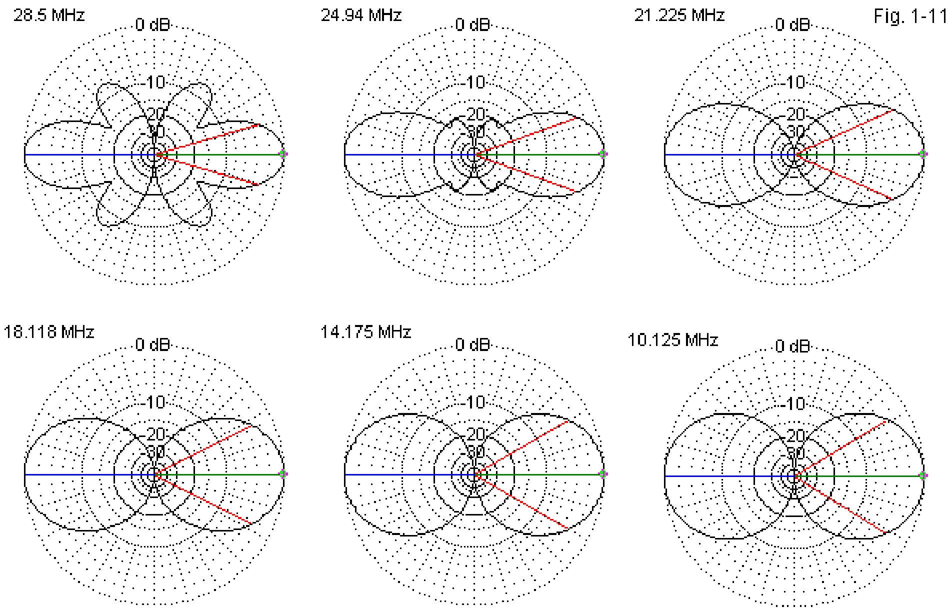

Free-Space Patterns from 10 to 30 Meters: 44' by 22' AWG #12 W8JK Flattop Array

The table and the gallery include information on 30-meter operation of the array, although I do not necessarily recommend operating the antenna on this band. The performance data and the pattern suggest quite adequate operation. However, we cannot neglect the feedpoint impedance data in **Table 1-5**. This data uses a velocity factor of 1.0 for all lines and therefore only approximates the values that would emerge at the junction of real lines. The data for 300-Ω phaselines suggest that we not use this type of line for the phaselines. In most installations, the main feedline will be either 450-Ω or 600-Ω parallel transmission line. The 300-Ω feedpoint values indicate that the lines might show SWR values that result in significant losses along the main feedline.

The 450-Ω and the 600-Ω columns show higher values for the resistive components. As well, they also show reactance values that rarely exceed the resistance by more than 3:1. In most cases, these values fall within the lower-loss range for parallel feedlines. In fact, it might be wise to use 600-Ω material for the phaselines, but to use a 450-Ω main feedline to obtain the lowest SWR values along the main feedline.

The difficulty that we obtain on 30 meters is that, regardless of the characteristic impedance of the phaselines, we obtain a very low feedpoint resistance and a reactance that is 5 times the resistance value. Therefore, obtaining a good match, even with a wide-range antenna tuner, may not be easy, and the lines losses—even with parallel transmission lines—may be significant. However, the individual operator can give the band a try and see if the results are acceptable.

Placing the 44' by 22' W8JK array above ground will, of course, modify some of the performance numbers. For samples, I have selected heights of 35' and 70' above average ground. At 10 meters, these heights are about 1-λ and 2-λ, respectively. However, at 20 meters, the heights are only ½-λ and 1-λ. Hence, we shall see band-to-band differences in the take-off (TO) angle, that is, the elevation angle of maximum gain. **Table 1-6** lists the modeled results of these tests. (See models 1-9a and 1-9b.) The table omits the impedance information, since it varies by only slight amounts from the free-space data.

W8JK Performance at Two Different Heights above Ground					
Element Length = 44'; Element Spacing 22'					
	Height = 35'			Height = 70'	
Freq MHz	Gain dBi	TO Angle		Gain dBi	TO Angle
28.5	11.45	14		11.63	7
24.94	11.46	16		11.91	8
21.225	11.26	18		11.47	9
18.118	10.84	21		11.32	11
14.175	9.8	25		10.9	14
Gain dBi = gain in dBi					
TO Angle = elevation angle of maximum gain in degrees					
					Table 1-6

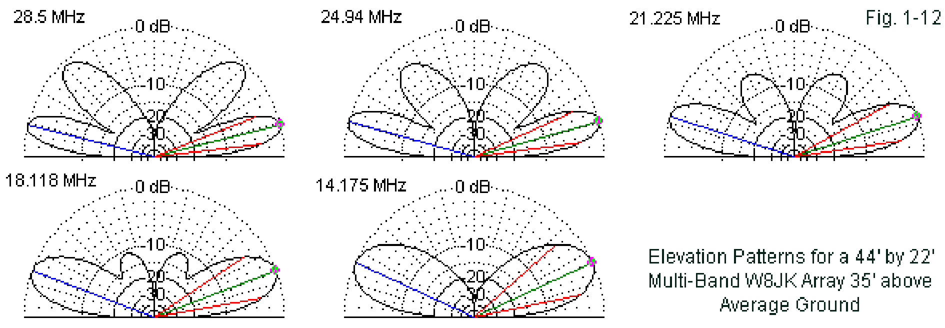

Fig. 1-12 provides us with a gallery of elevation plots along the line that marks the peak gain in both directions with a height of 35' above ground. I do not show the corresponding azimuth patterns because they will have the shape of the free-space patterns in **Fig. 1-11**. Among the notable features of elevation patterns for 20-10 meters is the absence of very high-angle lobes that we might find in the patterns for a single wire.

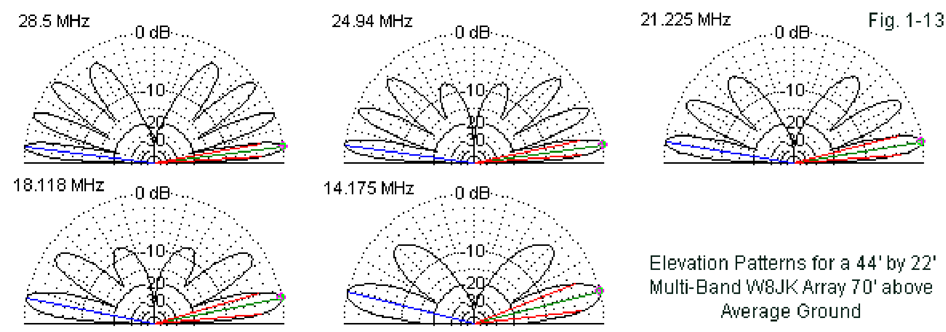

Fig. 1-13 shows the corresponding patterns for a height of 70' above ground. At this height, the TO angles are more nearly optimal for most skip signals. As well, the effects of ground are less notable in the maximum gain range. At 35' the range was nearly 1.7 dB. At 70', the range is only 1 dB.

This design exercise is not the only way to create a multi-band W8JK with nearly equal gain potential across a 2:1 frequency range. For example, the sample uses wire and presumes a fixed installation with communications targets in both directions at right angles to the wires. Although the elements are long for tubular construction, a rotatable version of the array is certainly within the range of possibility. With very significant increases in the element diameter, the builder might have to experiment with the precise element length and spacing to achieve workable feedpoint impedances on all bands.

As well, one might easily set the high-band limit to 12 or to 17 meters and work downward from that point. As we lower the frequency of the high-band limit, we shall encounter two challenges. A 2:1 frequency range will include fewer amateur bands, reducing the versatility of the array. Also, lower frequency ranges will require much higher antenna mounting heights to achieve the gain and TO values shown for the 44' by 22' model.

Nevertheless, the multi-band W8JK array promises excellent performance. Its gain is consistent from band-to-band and rivals the gain of a 2-element Yagi, but in two directions at the same time. The cost is beamwidth relative to a Yagi, especially as the element length approaches and passes 1 λ. As well, for some operations, having a front-to-back ratio, that is, having maximum gain in only one direction, is an advantage.

Conclusion

This discussion is only an introduction to the W8JK array. We have limited ourselves to center-fed elements, even though we allowed the elements to extend beyond ½-λ into the collinear range. In fact, Kraus examined many variations of the array, including multi-sectional variations. As shown in **Fig. 1-14**, he also explored end-fed versions of the array. For some applications, handling a single high-impedance feedpoint may prove simpler than handling the values that appear with a center-fed version of the antenna. See Kraus, *Antennas*, 2nd ed. (1988), p. 458, for other possibilities.

Fig. 1-14

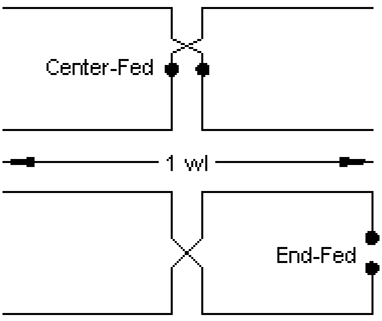

A Sample Alternative
W8JK Configuration

Nevertheless, these notes have aimed at showing the basic operating principles of the W8JK, the trends in performance with various sets of dimensions, and the flexibility of the array when pressed into multi-band duty. The W8JK flattop array remains the paradigm of phase-fed end-fire bi-directional arrays.

However, for a 2-element horizontal bi-directional array, we are not limited to a flattop configuration. Our next stop on this journey will examine 2-element broadside arrays.

2. The Lazy-H Array

While we were exploring the properties of the W8JK flattop array, we briefly experimented with feeding the 2 elements in phase. We discovered that this method of feeding produced major radiation lobes broadside to the wires, a disastrous situation for a beam from which we wanted end-fire radiation. However, we may make good use of the broadside pattern yielded by in-phase feeding of the elements if we make a single change in the arrangement of elements. Rather than setting both elements at the same height and separating them in the plane that is parallel to the earth's surface, let's arrange the element vertically, one above the other. Then we shall have an array that looks like the sketch in **Fig. 2-1**.

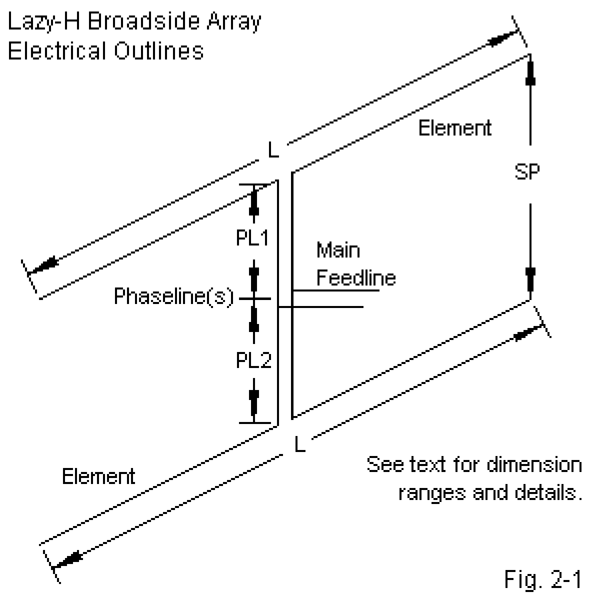

Fig. 2-1

Traditionally, we call the array the "lazy-H." The name derives from much earlier times in amateur radio when names often simply reflected the appearance of the components, in this case, the elements and the phaselines. If we add a bit of American western lore, with the many ways in which we named the figures that ranchers used to brand cattle, then the tipped-over or reclining H-shape becomes the lazy-H.

Unlike the W8JK, we generally do not trace the history of the lazy-H to a single individual. Instead, the lazy-H emerged from the realization that any two identical horizontal elements stacked vertically and fed in phase increased the overall gain relative to the gain from a single element. The original lazy-H used 1-λ elements with a spacing of ½-λ. This configuration eventually gave way to the realization that the gain improvement applied to elements of any length. Hence, we find lazy-H configurations using the 3 most common elements lengths in amateur circles: 0.5-λ, 1-λ, and 1.25-λ. The longest element length, accompanied by a 5/8-λ space between elements yielded a special name: the expanded or extended lazy-H. Although we see fewer lazy-H arrays that use ½-λ elements, we find extended use of the lazy-H principle in stacks of horizontal Yagis. (However, as we increase the gain and the front-to-back dimension of the individual antennas in a stack, the vertical separation required for maximum stack gain begins to grow larger than the values that apply to simple or collinear elements. We shall confine our attention to these more fundamental cases.)

The patterns produced by the 3 element lengths have the same inter-relationship that we saw in the lengths for the W8JK. **Fig. 2-2** overlays patterns for the 3 element lengths with the same vertical spacing between the elements. The ½-λ dipole elements produce the typical figure-8 pattern, while the 1-λ center-fed collinear elements produce an elongated figure-8 with more gain and a narrower beamwidth. The longest element in the set, the 1.25-λ (extended double-Zepp) element, produces the familiar high-gain, narrow-beamwidth main lobe with two side lobes, each of which has a strength about 10 dB lower than the main lobe. If we increase the element length much farther, the main lobe will diminish and the side lobes will strengthen until they dominate the pattern. At that point, we lose the potential for a bi-directional array.

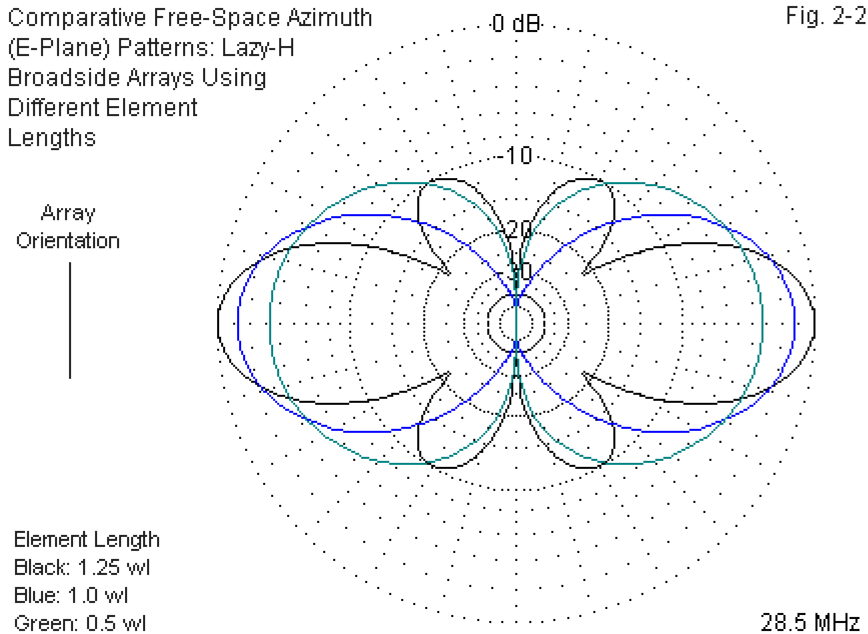

The fundamental operating principles of the lazy-H resemble those of the W8JK array. We provide the center feedpoint of each element in the pair with energy that has the same current magnitude. However, unlike the W8JK, we keep the current phase angles the same to create the broadside pattern of the elements. The simplest, but not the only, way to achieve this goal is to use equal lengths of parallel transmission line from each element to a central main feedpoint. The phaselines from the element centers to the main feedpoint will transform the impedance values at the element centers to a different value, depending on the element impedance, the characteristic impedance of the phase line and the length of each of the phaselines. The impedance that appears at the junction of the phaselines is the parallel combination of the transformed element impedance values. As we change the element length, the spacing between elements, or the characteristic impedance of the line, we find different feedpoint impedance values. Remember, however, that changing the phaseline characteristic impedance does not change that gain or radiation pattern of the pair of elements. Those values derive from the element length and the spacing value used.

Lazy-H Performance Using Different Element Lengths and Different Spacings								Table 2-1
	All models in free space using AWG #12 copper wire							
Element Length = 0.5 wl								
Space wl	Gain dBi	BW deg	R300	X300	R450	X450	R600	X600
1/8	2.43	77.4	94.32	65.18	93.46	103.2	92.7	137.7
1/4	3.23	77.5	111.5	115.1	119	204.3	121.6	287.7
3/8	4.5	77.6	212.7	220.7	261.8	434.1	284.7	642.9
1/2	5.95	77.6	658.3	-159.2	1472	-374.9	2595	-707
5/8	6.91	77.4	98.5	-235.3	119.8	-411.4	132	-589.7
3/4	6.73	77.4	39.18	-97.15	44.01	-170.6	46.65	-244.7
Element Length = 1.0 wl								
Space wl	Gain dBi	BW deg	R300	X300	R450	X450	R600	X600
1/8	4.17	46.8	77.27	-284.4	144.8	-371	215.6	-428.6
1/4	5.01	47.6	30.79	-136	65.92	190.9	111.2	-235.6
3/8	6.41	47.8	15.72	-59.49	35.11	-86.63	61.93	-111.5
1/2	8.05	47.4	9.18	1.67	20.66	3.76	36.74	6.67
5/8	8.99	46.8	8.08	67.15	18.42	104.4	33.16	144
3/4	8.52	46.4	14.98	164.8	35.45	258.2	66.28	358.8
Element Length = 1.25 wl								
Space wl	Gain dBi	BW deg	R300	X300	R450	X450	R600	X600
1/8	5.2	32	37.08	-158.6	54.21	-172	67.54	-170.3
1/4	6.14	32.8	20.82	-71.68	36.62	-680.6	52.26	-48.86
3/8	7.63	33	13.38	-11.05	26.79	15.61	42.68	59.34
1/2	9.21	32.6	10.17	50.33	22.93	113.4	40.87	201.8
5/8	9.94	32	12.97	135.9	35.11	274.9	76.58	480.6
3/4	9.39	31.4	44.16	331	202.7	788.7	1007	1769

We may usefully run the same exercise that we performed on the W8JK for the plausible versions of the lazy-H. We can use element lengths of 0.5-λ, 1.0-λ, and 1.25-λ at spacing values from 1/8-λ to 5/8-λ in 1/8-λ increments. In fact, I shall extend the spacing range to ¾-λ for a reason that will emerge as we examine the data. Then we can check the feedpoint impedance for 300-Ω, 450-Ω, and 600-Ω phaseline impedance values, with the understanding that each line uses a velocity factor of 1.0. Hence the feedpoint impedance values only indicate what might emerge in reality, but are not precise, since most real transmission lines have a velocity factor that range from perhaps 0.98 down to about 0.80. **Table 2-1** shows the results of the modeling survey. (See models 2-1 to 2-3 in variations a through f.)

The gain column for this free-space exercise with AWG #12 copper wire arrays shows one very significant way in which lazy-H performance differs from the W8JK performance. The W8JK lost gain as we increased the element spacing. The lazy-H increases gain with increased vertical spacing between elements. For all three element-lengths, the gain peaks with a spacing close to 5/8-λ. Including the values for ¾-λ spacing shows the limits of element spacing for maximum gain performance. The rate of gain change is very similar for all three curves in **Fig. 2-3**. Only above the 5/8-λ spacing value do we find a small departure from complete congruence.

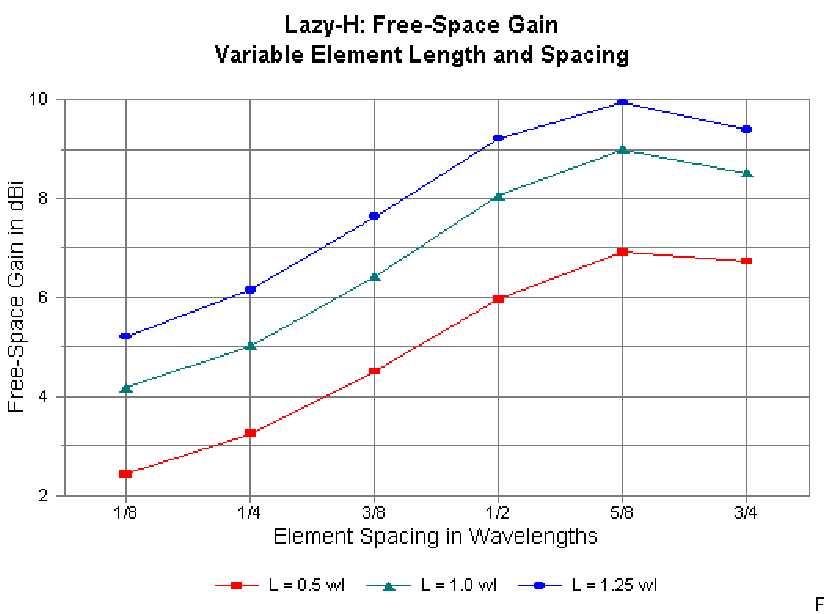

Fig. 2-3

When we surveyed W8JK possibilities, we noticed that for any given element length, increasing the spacing between elements produced wider beamwidth values as the gain decreased. However, as shown in **Fig. 2-4**, changing the element spacing produces almost no change in the half-power beamwidth of the two main lobes in this bi-directional array. Indeed, it is a fundamental property of vertical stacking and in-phase feeding that the beamwidth does not change significantly from the use of a single element.

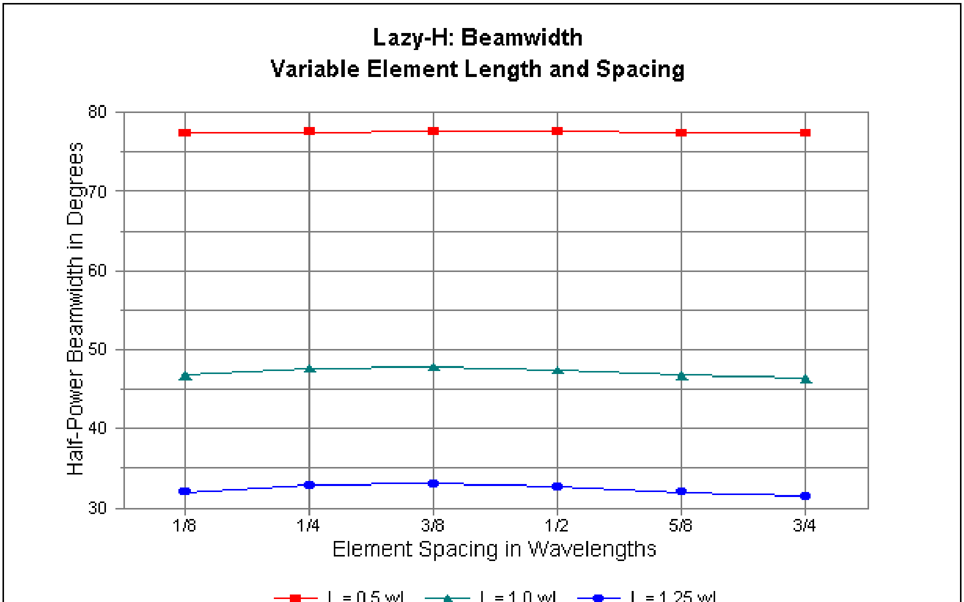

Fig. 2-4

The impedance figures shown in **Table 2-1** are not the same as those we found for the W8JK array, even though we are using the same element lengths, the same spacing values, and the same free-space environment. Since the phaseline transformation properties would also be constant, the source of the differences must lie in the element phasing. Not only does in-phase vs. out-of-phase feeding change the dominant direction of the radiation lobes, it also changes the impedance values at the center of each element. Hence, the transformed and combined impedance values change between the two arrays.

The specific optimal combination of phaseline impedance and main feedline impedance will vary from one proposed design to another. However, for the ½-λ elements, a 300-Ω phaseline may provide the best match to a 450-Ω main feedline. The goal is to provide the main feedline with the lowest feasible SWR relative to its characteristic impedance to minimize losses on the long run from the array to the antenna tuner. SWR values less than 10:1 tend to favor lower losses. As we increase the element length, higher characteristic impedances for the phaselines tend to provide the desired relationship. Indeed, for most monoband lazy-H arrays, 600-Ω phaselines work well with a 450-Ω main feedline.

A Special Monoband Lazy-H Design

The version of the lazy-H that we have used for our initial survey of potentials employs a central main feedpoint with 2 equal phaselines. As we shall see, this arrangement is necessary if we wish to use the lazy-H for multi-band operations. For single-band operation, we can use a different arrangement among the components. **Fig. 2-5** shows the outlines of our possibilities.

The first step is to re-examine two 1-λ elements that are spaced 0.5-λ apart. If we feed these elements separately and in phase, we obtain a free-space gain of 8.05 dBi, with a beamwidth of 47.4°. These values will not change as we look at the ways in which we may feed the antenna. (See model 2-4.)

The second option is the one used in the survey. If we use 600-Ω phaseline, then we obtain a feedpoint impedance of 36.7 + 6.7 Ω. (See model 2-2d.) Although this impedance seems almost right for a 50-Ω coaxial cable, the cable weight at the center of the array is a mechanical challenge. Therefore, many builders have sought some alternative arrangement that might place the feedpoint at the level of the lower element. One simple expedient is to replace the centered-feed arrangement with a single phaseline that ½-λ long and that has a single half-twist as it runs from the lower element to the upper element.

Both of the lower outlines in **Fig. 2-5** use this arrangement.

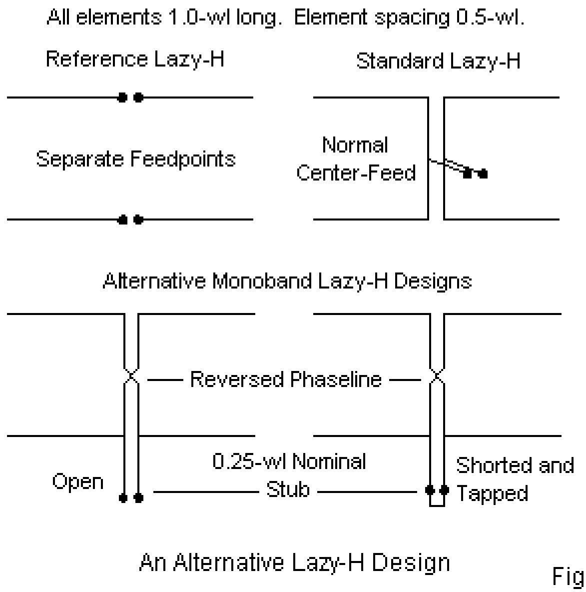

Fig. 2-5

We need the half twist in the single long phaseline because of the basic properties of current along a transmission line. A half-wavelength of transmission line replicates the load impedance because both the voltage and the current undergo a 180° phase shift for each half-wavelength of line. Hence, voltage and current do not return to their original phase angle until the line reaches a full wavelength. To obtain in-phase current feeding of elements that are ½-λ apart, we need the half-twist to effect a phase reversal along the line between the upper and the lower elements.

The impedance at the junction of the phaseline and the lower element will be very high—usually in excess of 3000 Ω. Let's add a stub from the junction and let it hang downward. One way to form the stub is to prune it, as shown in the lower left sketch. However, this method of obtaining a desired feedpoint impedance may require a very specific stub characteristic impedance and length for a desired feedpoint impedance. For example, with the AWG #12 copper wire model used in this exercise, the line required a characteristic impedance of 350 Ω with a length of 0.245-λ to produce the 50-Ohm SWR curve that appears in **Fig. 2-6**. A length of 0.235-λ produced a nearly perfect 50-Ω resistive impedance at the 28.5-MHz design frequency, but the SWR curve shifted upward in frequency. Hence, for the purposes of the sample, I used the shorter stub length. (See model 2-5.)

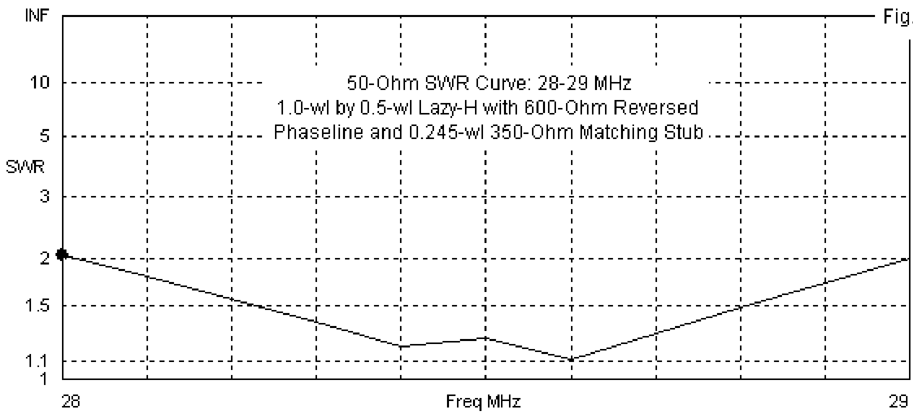

Fig. 2-6

Somewhat less finicky is the use of a shorted stub that is a full ¼-λ, as shown at the lower right in **Fig. 2-5**. In general, the required field adjustment consists in finding the correct tapping point to effect an acceptable match to a 50-Ω main feedline.

The Multi-Band Potential for the Lazy-H Broadside Array

The special arrangement of array components that we have just explored is quite satisfactory for a monoband array. However, since the phaseline provides in-phase feeding for only a single frequency (or a narrow band of frequencies), we must return to the centered-feeding system if we wish to operate the lazy-H on more than one amateur band. Moreover, we must set the element length to the practical maximum at the highest band that we intend to use—if we wish to have a bi-directional array rather than a mere multi-directional antenna. As well, we have seen that 5/8-λ is the widest spacing we may use before losing peak gain, and so we shall also employ this spacing at the highest band that we intend to operate. **Fig. 2-7** shows the general outline of our projected multi-band lazy-H.

Fig. 2-7

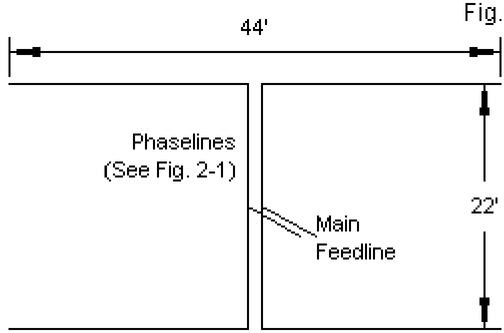

General Outline of a Sample
Lazy-H Multi-Band Broadside Array

The sketch projects that the highest frequency is 10 meters (or 28.5 MHz). The element length and the spacing are the same values that we assigned to the sample multi-band W8JK in the first chapter. You may scale the antenna for coverage of other bands than the ones we shall examine. As we saw with the W8JK array, 44’ is very slightly long for 28.5 MHz. **Table 2-2** shows the element lengths and the spacing values as a function of the operating frequency. Note that **Table 2-2** includes 30 meters. One reason that we excluded 30 meters from the multi-band 44’ by 22’ W8JK array was the potential for high main feedline losses. We shall wish to see if the lazy-H yields the same result at 10 MHz.

44' by 22' Lazy-H Dimensions in Wavelengths for Each Band Covered			Table 2-2
Freq MHz	L wl	SP wl	
28.5	1.275	0.638	
24.94	1.116	0.558	
21.225	0.948	0.474	
18.118	0.812	0.406	
14.175	0.634	0.317	
10.125	0.453	0.226	

Free-Space Performance Data: 44' by 22' Multi-Band Lazy-H Array								Table 2-3
Freq MHz	Gain dBi	BW deg	R300	X300	R450	X450	R600	X600
28.5	9.79	30.6	17.05	163.1	49.6	343	118.4	627.9
24.94	9.38	40.2	7.34	49.52	16.97	91.37	31.02	145.2
21.225	7.42	50.6	10.15	-18.28	22.9	-32.15	40.83	-49.14
18.118	5.82	59.6	20.62	-79.65	49.37	-146.1	93.49	-231.5
14.175	4.17	70.4	151.7	-234.6	501.9	-390.6	1099	-271.8
10.125	2.94	79.8	42.96	40.34	52.66	98.14	58.67	159.3

Table 2-3 provides the free-space modeling data for the 44’ by 22’ lazy-H on all bands from 10 down to 30 meters. The impedance values with a phaseline of about 450 Ω are satisfactory for a 450-Ω main feedline, although a few values are close the 10:1 SWR limit that we earlier set as most desirable. Even 30 meters is usable in this regard. (See models 2-6, 2-6a, and 2-6b.)

However, since the gain decreases as the frequency decreases (given that the element length and the spacing both shrink as measured in wavelengths), we do not necessarily have favorable performance conditions below 17 meters. The 18.118-MHz performance level is about the same as provided by the W8JK flattop. Above 17 meters, gain performance goes up, with a 4-dB advantage on 10 meters over 17. However, below 17 meters, the gain decreases. At 30 meters, the gain is less than 1-dB higher than a standard dipole. For an installation that permits only 1 antenna, the 44’ by 22’ lazy-H provides inexpensive coverage, but the gain is superior only above 17 meters.

Fig. 2-8 provides a gallery of free-space azimuth (E-plane) patterns for the

6-band coverage of the lazy-H. The evolution of the lobes from the triple-lobe extended double-Zepp pattern down to the dipole's figure-8 is clearly apparent as we reduce the operating frequency. When we place the antenna above ground, the azimuth patterns at the TO angle will have the same shape as the patterns in free space.

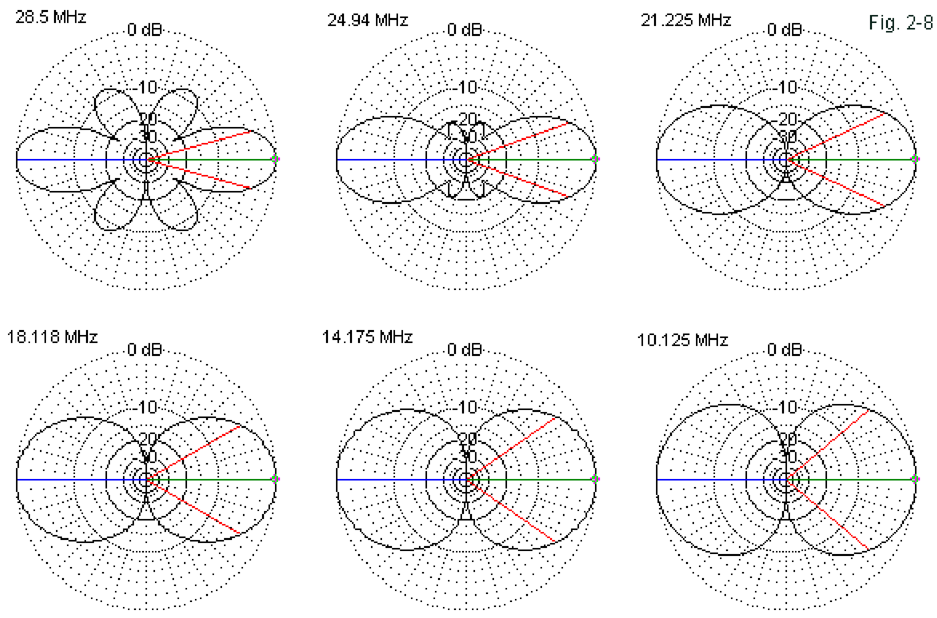

Free-Space Patterns from 10 to 30 Meters: 44' by 22' #12 Lazy-H Broadside Array

In the preceding chapter, we placed the W8JK at heights of 35' and 70' above ground to approximate heights of 1-λ and 2-λ at the highest frequency. We may perform the same test with the lazy-H, but with a proviso. If we place the lower element at 35' and at 70', then in both cases, the upper element will be 22' higher, that is, will be at 57' and 92' above ground. The lazy-H gives back the horizontal space occupied by the W8JK, but requires an equivalent vertical space in exchange.

Table 2-4 provides the data for the antenna at both heights. As we found with the W8JK, the impedance values do not change from their free-space values by enough to warrant a repetition of that part of the table. Therefore, the new table only provides the reports of gain and take-off angle.

Lazy-H Performance at Two Different Heights above Ground					
Element Length = 44'; Element Spacing 22'					
	Base Height = 35'			Base Height = 70'	
Freq MHz	Gain dBi	TO Angle		Gain dBi	TO Angle
28.5	14.64	10		15.24	6
24.94	14.34	11		14.94	7
21.225	12.28	13		12.93	8
18.118	10.57	15		11.25	9
14.175	9.09	20		9.66	12
10.125	7.4	28		7.91	16
Gain dBi = gain in dBi					
TO Angle = elevation angle of maximum gain in degrees					
					Table 2-4

The data are not surprising considering the additional gain provided by ground reflections. As always, the test ground quality is average (conductivity 0.005 S/m, permittivity 13). However, we may make a few comparisons. On 30 meters, the bi-directional gain is about the same as a dipole. The 17-meter gain is just below the level provided by a directional 2-element Yagi. The gain on 12 and 10 meters is greater than the gain provided in only 1 direction by a 3-element Yagi.

The TO angles for the arrays are uniformly lower than for the W8JK. The greater overall height of the array, relative to the height of the lower element or the height of the W8JK in similar modeling tests accounts for the lower angles. In fact, for any two element vertically stacked, the TO angle of the stack is equivalent to a single wire's TO angle if that wire is about 2/3 the way up between the actual wires. The equivalent height for the lower of the two arrays—with elements at 35' and 57'—is about 50'. For the higher array—with elements at 70' and 92'—the equivalent height is about 85'.

Fig. 2-9 presents a gallery of elevation patterns for the lower of the two test arrays. The corresponding gallery of plots for the higher array appears in **Fig. 2-10**. Compare these elevation plots to the ones for the W8JK arrays with an eye toward the development of high-angle lobes.

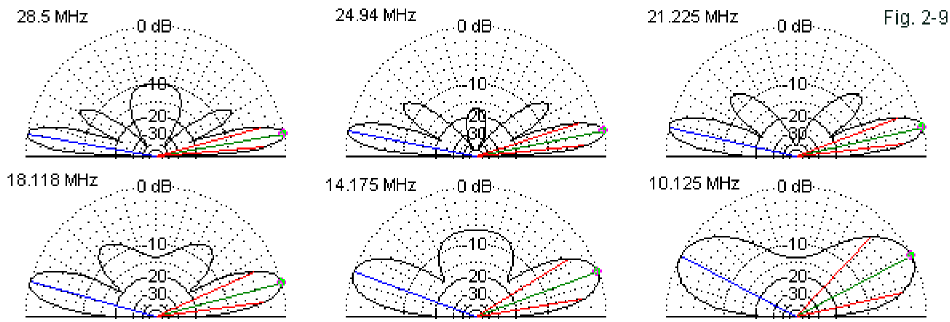

Elevation Patterns for a 44' by 22' #12 Lazy-H Broadside Array 35' above Average Ground

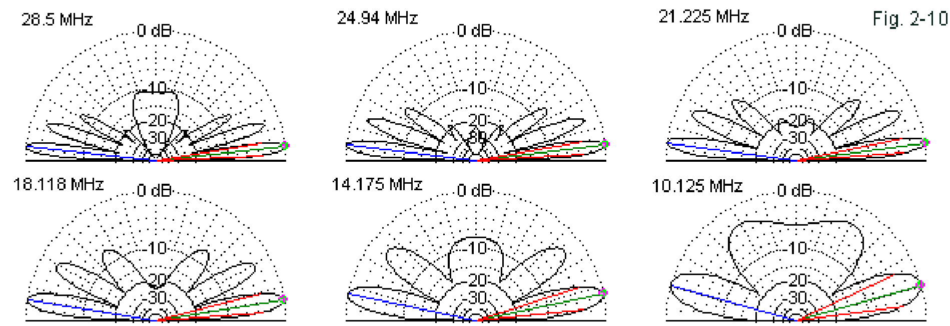

Elevation Patterns for a 44' by 22' #12 Lazy-H Broadside Array 70' above Average Ground

With the W8JK array, we found an absence of very-high-angle lobes in all of the elevation plots. However, the lazy-H suppresses straight-up lobes only on 15 meters, where the spacing between the wires is very close to ½-λ. As we move away from 15 meters in either direction, the vertical radiation grows stronger. It does not ever reach dominant levels, but is sufficient to show clearly how W8JK and lazy-H patterns differ at various frequencies as a function of out-of-phase vs. in-phase feeding.

Whether we are working with a W8JK or a lazy-H array, the old adage that height is everything to a horizontal antenna certainly applies. If one chooses to scale either array to cover lower bands, the benefits of the gain potential of the arrays may well be lost unless the antenna is high enough above ground.

The Quad Loop as a Phased Array

The lazy-H is perhaps the paradigm for 2-element broadside phase-fed arrays. However, the antenna has cousins with which we are familiar—although we may not realize their kinship to the lazy-H. Consider the 1-λ quad loop. **Fig. 2-11** confirms that when the circumference of a loop is about 1-λ and the loop is fed at either to bottom or at the top, the pattern is broadside to the loop and horizontally polarized.

The Quad Loop as a 2-Element Broadside Array

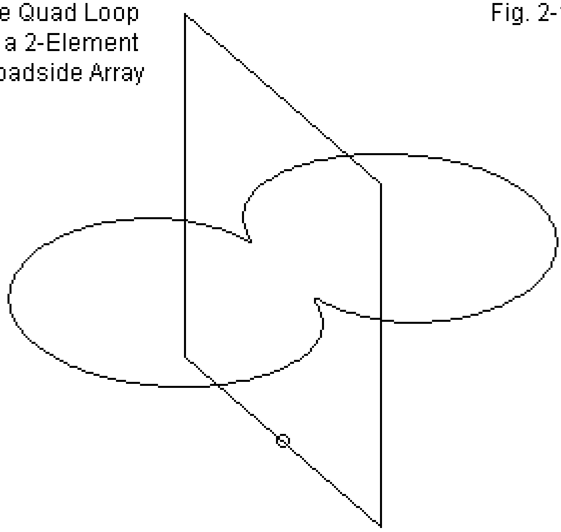

Fig. 2-11

When we model a closed loop, as shown in the sketch with 1 feedpoint, we generally construct wires in a continuous progression so that the upper horizontal element reverses the positions of end-1 and end-2 relative to the lower horizontal wire. This very functional modeling method tends to obscure that fact that a quad loop is actually two ½-λ elements with their ends bent to meet in the middle.

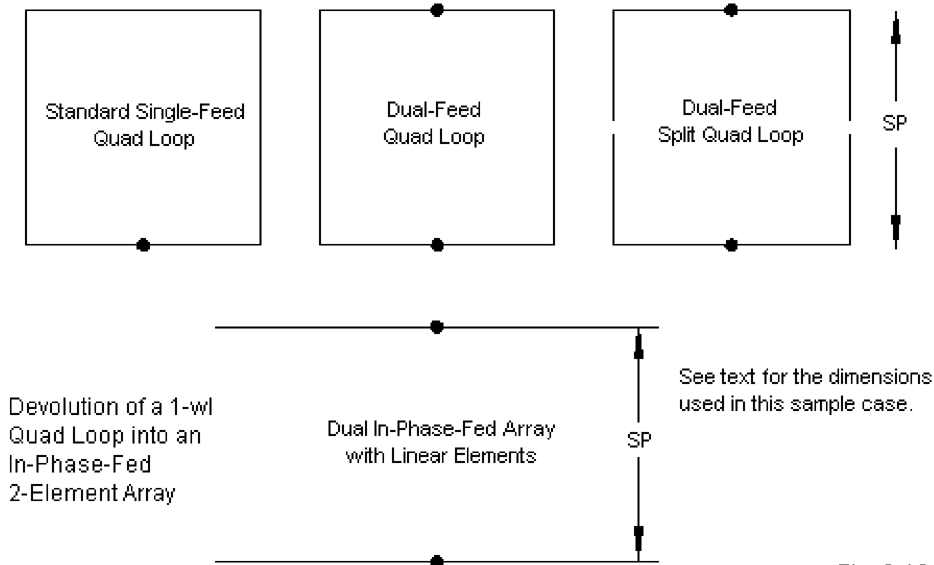

Fig. 2-12

Let's devolve the closed quad loop through several models back to its lazy-H form, as suggested by the progression in **Fig. 2-12**. (See models 2-7 through 2-7c.). The next step after the initial closed loop is to provide the loop with separate upper and lower feedpoints. Then, we may split the element at the center points of the vertical sides and compare the results to the closed version. The actual split will be much smaller than the sketch suggests so that we may preserve the dimensions of the overall loop. Finally, we may unbend the element ends but retain the spacing between the upper and lower elements.

There are a number of so-called cutting formulas for quad loops, most of which are simply erroneous. Our AWG #12 copper-wire loop requires a total length of just about 1.06-λ to be resonant at the design frequency of 28.5 MHz. This value translates into a cutting formula in which the length in feet is equal to 1043 divided by the frequency in MHz. In fact, the required circumference is a function of frequency and the diameter of the conductor. Fatter elements require larger circumferences (in contrast to linear elements, where fatter elements require shorter lengths). Volume 2 of *Quad Notes* provides an algorithm for determining with very high accuracy the required side length or circumference of a single quad loop for any reasonable element diameter over frequencies from 3 to 300 MHz. The three loop versions of our antenna will require no size adjustment as we alter the details of the configuration. Each side will be 0.265-λ. **Table 2-5** provides the results of our little exercise in loop devolution.

Loop-to-Linear-Element Devolution: Free-Space Data			Table 2-5
All loops 0.265-wl per side. Linear elements 0.496-wl long.			
Antenna Version	Gain dBi	BW deg	R +/- jX Ohms
Closed: 1 Feed	3.26	84.2	126.9 - j0.17 (x1)
Closed: 2 Feeds	3.27	84.2	63.56 + j0.62 (x2)
Split: 2 Feeds	3.27	84.2	63.58 + j0.97 (x2)
Linear: 2 Feeds	3.35	77.8	114.3 - j 0.84 (x2)

The closed loop with dual feedpoints shows individual feedpoint impedance values that are half the value of the impedance when we use a single feedpoint. Effectively, the two feedpoints are in series with each other, or—from another perspective—the single feedpoint is the series sum of the two individual feedpoint impedance values. When we split the center points of the sides by a small amount, we do not alter the impedance value of the individual feedpoints on each of the elements relative to the closed version of the dual-feedpoint loop. Note that the gain and beamwidth have not changed in this progression.

The final step in the devolution consists of straightening the elements. In the process, we lose the high mutual coupling between wire sections at the loop corners. Hence, the total length of the element diminishes. The length of each half-loop is 0.53-λ, while the linear elements for resonance are only 0.496-λ. Due to mutual coupling between the upper and lower wires at a spacing of 0.265-λ, the feedpoint impedance on each wire is about 114 Ω, in contrast to the 63.5-Ω impedance at the feedpoint of each half-loop. The gain of the linear elements is very slightly higher (0.08-dB) since the entire current distribution is in the horizontal plane, compared to the bent elements of the loops.

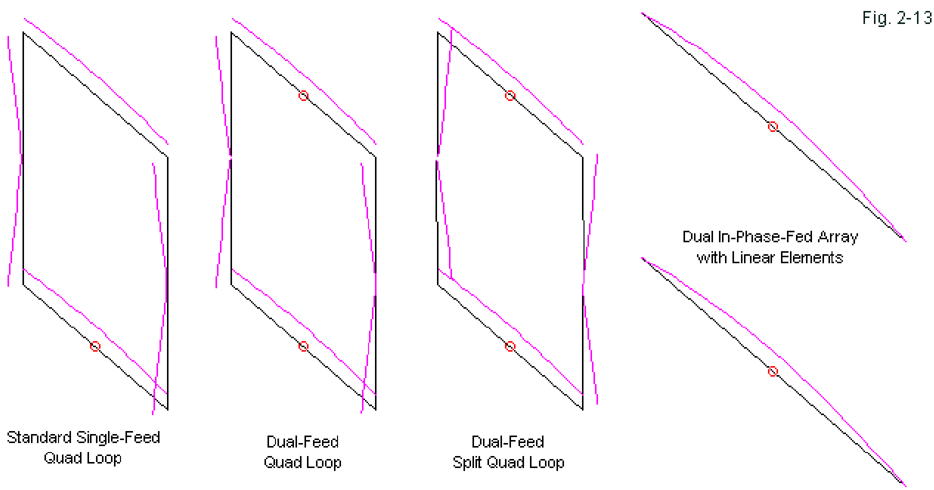

Current Magnitude and Distribution on the Sample Models in the Devolution Exercise

Perhaps the final step in showing the fundamental equivalence between the lazy-H and the quad loop is to show the current distribution along each wire in the four steps of the progression. **Fig. 2-13** provides the graphic evidence. The direction of the current curves on the side portions of the loops is not important. What is significant is the fact that for both the upper and the lower loops, the current shows the same phase direction.

Before we leave the quad loop, let's carry the exercise one step further. We shall create a closed loop and a split loop. For each model, we shall use a single center feedpoint and phaselines, just like those we use with the normal lazy-H configuration. See **Fig. 2-14**. If our work so far has been correct, then we should obtain the same performance from the closed loop and the split loop.

Fig. 2-14

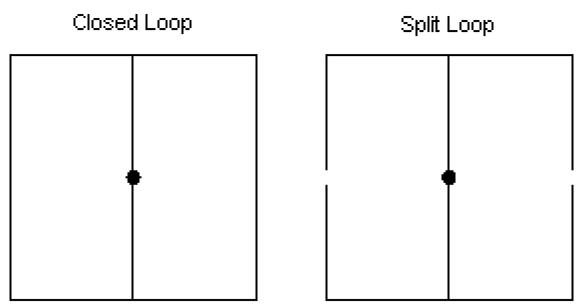

Phase-Feeding Loops with Transmission Lines

Feeding Closed and Split Loops with Phaselines								Table 2-6
Version	Gain dBi	BW deg	R300	X300	R450	X450	R600	X600
Closed	3.27	84.2	67.33	150.4	69.51	238.6	70.47	324.8
Split	3.27	84.1	67.35	150.4	69.52	238.6	70.48	324.8

Table 2-6 provides the final step in our genetic research. (See models 2-8a and 2-8b.) The performance of the closed loop and the split loop are the same, regardless of the phaseline characteristic impedance.

The quad loop and the lazy-H arrays are the foundation of numerous more complex directional beams. As the three volumes of *Quad Notes* show, we may form complex parasitic arrays using quad-loop elements. The resulting beams form combined broadside-end-fire arrays with considerable directional capabilities. It is possible to use the lazy-H in a similar way. However, one popular form of lazy-H directional array results from placing a screen behind the driven array. The screen forms a planar reflector with properties derived from optical considerations rather than from parasitic element theory. (See *Planar and Corner Reflector Notes* for more information on these types of arrays.) In fact, if we place the screen on or very near to the ground and place the lazy-H above it, then we obtain an array that radiates directly upward for high-gain NVIS operations. Quad loops above ground-level screens also make good NVIS antennas.

A More Distant Relative of the Lazy-H: the Bi Square Array

One reason that we restricted the circumference of the quad loop to about 1-λ is a simple fact of radiation from a loop. When the circumference falls very much lower than 1-λ, the radiation is primarily in the plane of the loop and no longer broadside to it. If we retain a closed structure and increase the circumference above about 1.5-λ, then the radiation returns from a broadside orientation to being in the loop's plane.

Let's consider a loop that is 2-λ in circumference. If we use a closed loop, then we find the strongest lobes in the loop's plane, as shown on the right in **Fig. 2-15**. However, if we split the loop at the top, as is the case with the sketch on the left in **Fig. 2-15**, the radiation is broadside to the loop's plane. We call this configuration, split and all, a bi-square array. (See models 2-9 and 2-9a.)

Fig. 2-15

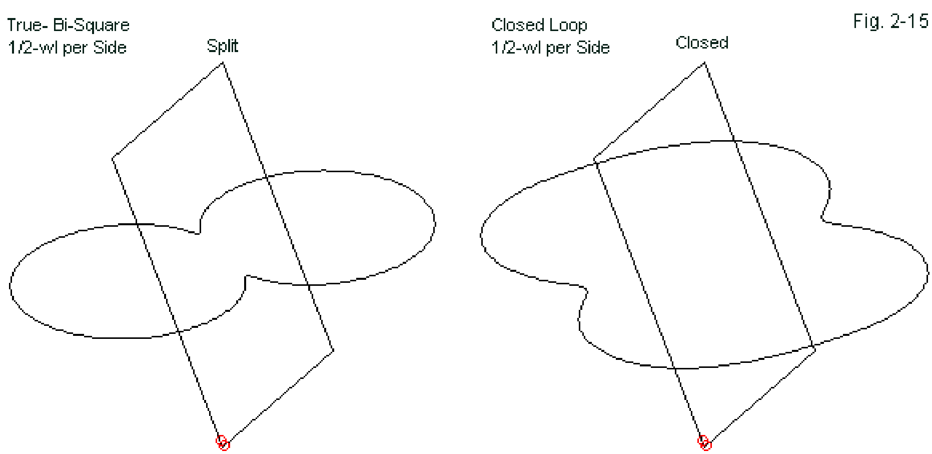

2-Wavelength "Loops" as a Broadside Array

The bi-square has several interesting facets. First, the views show it in a diamond rather than a square configuration. Any quad loop has essentially the same free-space performance whether set up as a diamond or as a square, so long as we feed the loop in the same relative place. The bottom point feed for the diamond is equivalent to a mid-element feedpoint for a square version. (The performance over ground might change due to the variables of coupling with the earth's surface.) The bi-square uses the diamond configuration for practical reasons that will shortly become evident.

Second, the sketch shows both diamonds fed at the bottom point. We might as easily have used a pair of phaselines between the side midpoints for a centered feedpoint. However, again for practical reasons, the move is unnecessary, since the collinear structure of the four 1/2-λ sides provides exactly the phasing that we wish to obtain for the broadside pattern.

In free-space and using AWG #12 copper wire, the broadside bi-directional gain is 5.83-dBi at 28.5 MHz, with a beamwidth of about 62°. The doubled circumference provides about 2.5-dB additional gain relative to a 1-λ closed quad loop. With the feedpoint shown, the impedance is very high, above 3000 Ω. Therefore, the most common method of feeding the bi-square uses a ¼-λ stub tapped for a good match to a 50-Ω feedline.

Fig. 2-16 shows the outlines of a practical bi-square installation. If we use a non-conductive support mast that is 1-λ tall, then we can fit the bi-square against the mast with nearly 0.3-λ between the feedpoint and ground. If we drop a ¼-λ stub down from the feedpoint, then the taps will place the main feedline very close to ground level. The sketch shows two guy ropes that establish the shape of the array. If the support mast is tall enough to require further stiffening, we can run two more guy ropes into and out of the sketch for 4-point guying.

As set up in its more common form, the bi-square provides 10.27 dBi modeled bi-directional gain broadside to the array. The TO angle of the horizontally polarized radiation is 19°. Perhaps the only drawback of this simple array is that it leaves a number of ropes in the yard over which someone may trip in the dark. (See model 2-9b.)

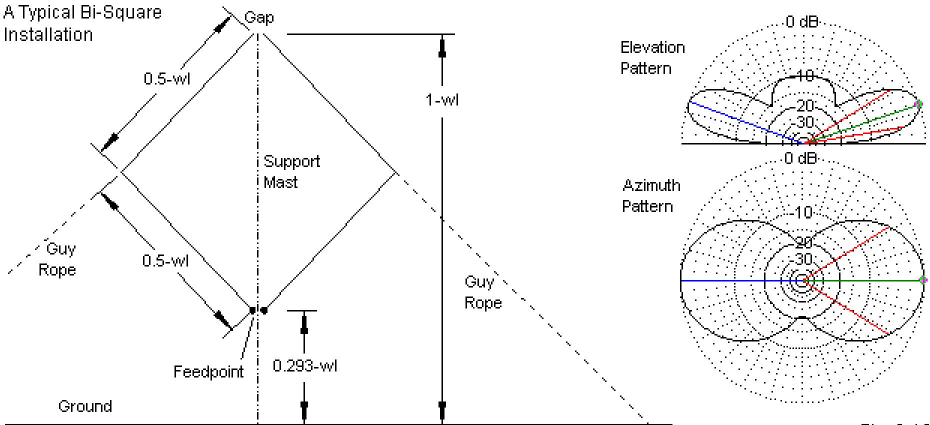

Fig. 2-16

Conclusion

In this chapter, we have examined a variety of 2-element bi-directional broadside arrays. Although the lazy-H is perhaps the most fundamental form for such arrays, we have also briefly looked at a few kindred configurations.

The lazy-H is a flexible and versatile array for both monoband and multi-band use. However, its in-phase feeding gives it properties that are the reverse of the W8JK studied in the preceding chapter. Up to 5/8-λ, gain increases with element spacing. However, the beamwidth of a lazy-H is the same as the beamwidth of a single element having the same length. In multi-band service, the lazy-H shows exceptional gain at the highest frequencies of use, but the gain decreases with the frequency. Even though the lazy-H may be usable for one band lower than a W8JK flattop, the gain on that band is not much more than the gain of the simple resonant dipole.

The W8JK and the lazy-H are both bi-directional beams. Their simplicity of construction and feeding gives them both attractiveness and utility. Nonetheless, many amateurs prefer a directional (or uni-directional) beam in order to reduce interference from the rear. Therefore, we shall leave the world of bi-directional phased arrays and turn to directional phased arrays.

Part II: Directional Arrays

3. The Limits of Performance

Although the pioneering work on parasitic directional arrays goes back to the original papers of Yagi and Uda in the late 1920s, amateur development of directional beams only began in earnest with the conclusion to World War II. Amateurs latched onto the Yagi as perhaps the premier directional beam design. The decade following the war saw many individual and commercial designs, all based on empirical experimentation.

The directional 2-element horizontal phased array achieved notoriety in the 1950s with builder claims that one or another variation on the basic design outperformed 3- and even 4-element Yagis. Although we now know that the appearance of high performance owed much to Yagi deficiencies of the period, horizontal phased arrays have retained much of their mid-century aura of magic. Since magic and an understanding of antennas are mutually exclusive, perhaps we should begin again.

The notes in this series of chapters will begin with some basic modeling data that tends to set limits to the performance expectations that we may logically have of 2-element phased arrays. In the next chapter, we shall explore the degree to which the geometry of the parasitic array can capture the potential of phased element performance. Chapter 5 will examine one of the two classic methods of array phasing: the ZL-Special with its single phaseline. We shall pause in Chapter 6 to examine the calculation of phaseline requirements for the ZL-Special. In Chapter 7, we shall look at two different ways of phasing a pair of elements using element-matching techniques, one by R. Baumgartner, HB9CV, the other by Eric Gustafson, N7CL. Throughout, we shall try to integrate specific design strategies into an overall picture of the performance of which 2-element phased arrays are capable.

A Few Preliminaries

The idea of a 2-element phased array contains an ambiguity. At the most general level, the notion can refer to the relative phasing of the elements in any 2-element array. Under this heading, we may include arrays with a single driven element as well as two driven elements. The perspective offered by this most general idea of a phased array will be useful in seeing where some antennas fit into a larger picture.

Alternatively, the concept of a 2-element phased array often refers specifically to an "all-driven" antenna, that is, to an array in which both elements receive power directly from the source. The key question that immediately arises within this view of phased arrays is how we may get energy to the individual elements in the correct magnitude and phase to effect a desired set of performance characteristics. The most common means is via a "phasing line" composed of a length or lengths of transmission line. Indeed, this means of conveying energy from the array source to the individual elements has been the basis of numerous misconceptions about how phased arrays operate.

The phasing-line system of energy transfer, of course, is quite unnecessary. As Brian Egan, ZL1LE, demonstrated with a 15-meter phased array in the 1990s, one may create a phasing network of lumped components and then use separate lines to each element so long as they preserve the relative values of current magnitude and phase created by the network.

The key to understanding 2-element horizontal phased arrays is the fact—stressed by Roy Lewallen, W7EL, in many writings—that the relative current magnitude and phase angle between the two elements determines the operating characteristics of the antenna. In the early days of phased-array popularity, most builders thought in terms of the impedance transformation along a transmission line linking the elements. However, the impedance along a mismatched line does not track with the current magnitude and phase transformations along the line. Impedance values repeat on a lossless line twice for each wavelength of line. However, current magnitude and phased values appear only once per wavelength.

From this misunderstanding others emerged. Although the most popular line lengths interconnecting elements were in the vicinity of 1/8 λ, most folks thought in terms of a 135° phase shift. However, with or without a half twist in the short line, the current can only make an approximate 45° phase shift. (The number is a crude marker, since we have already noted that the current phase may change more or less than 45° in a line that is 45° long.) If a straight line yields a 45° phase shift in current, then a line with a half twist yields a -45° phase shift. Antenna patterns may be identical to those produced by feeding the elements 135° out of phase, but the current behavior and the consequences for evaluating means of obtaining the correct phasing of the elements will depend upon adopting the -45° perspective. Because we shall be looking at close-spaced element systems, we shall adopt this orientation throughout these notes.

A further constraint upon our understanding of 2-element horizontal arrays has been the magic associated with 1/8-λ spacing. In fact, no particular spacing between elements holds any theoretically superior place in the scheme of 2-element arrays. We shall discover that in some respects, almost any spacing will do, although specific spacing values between elements can result in arrays that are easier to implement.

A Modeling Project

I want to expand our appreciation of phased array performance parameters, although space will not allow an absolutely complete account. We have already examined some bi-directional arrays, so in the following chapters, the idea of an array will point to beams with only one major (forward) lobe. We shall continue to abide by the title restriction and work with 2 and only 2 elements.

Fig. 3-1 presents the basic parts of a 2-element phased array, as we shall model it in NEC-4. We shall assign to each element a current source, specifying both the magnitude and phase angle. By convention, the designated forward element will have a current magnitude of 1.0 and a phase angle of 0.0°. The designated rear element will then be assigned the values of current magnitude and phase that yield a desired performance limit. Since we are working with directional arrays with a single main forward lobe, the forward element will always be the element in the direction of that lobe. Assigning separate values of current magnitude and phase angle to each element is an analog of what we accomplish with a phasing network. Such networks cannot yield performance that exceeds the limits of separate sources for each element, no matter the ingenuity of the system.

Fig. 3-1

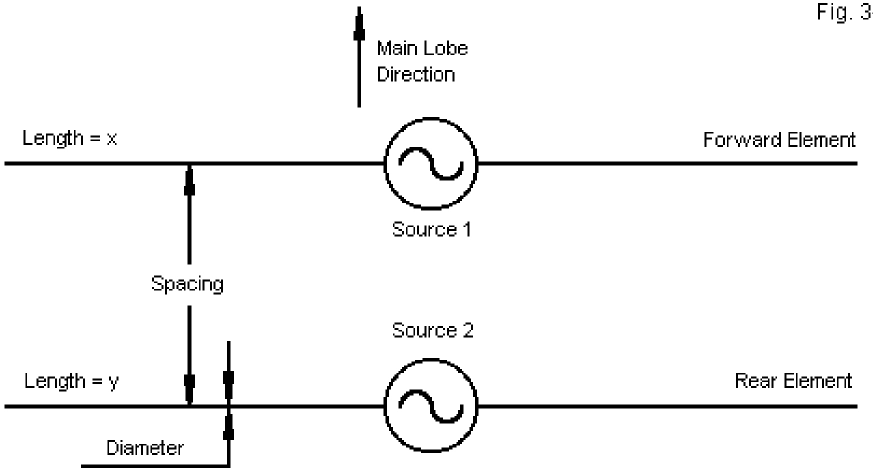

Phased Horizontal Array Parts and Variables

For the notes in this section, we shall reduce the total number of variables to a manageable number. We shall vary the spacing between elements systematically. We shall also examine some variations in element length, using both equal-length and unequal-length elements in the study. However, these results will change if we alter the diameter of the elements. For convenience, we shall employ 10-meter (28.5-MHz) elements made from 0.5" diameter aluminum. These elements give us a reasonably realistic model that scales easily to other amateur bands. With a fixed element diameter, we shall not explore variations that result from selecting other diameter materials.

If the forward element has a source current of 1.0 at 0°, then usual conventions will assign the rear element a current with a certain magnitude and a positive phase angle in the vicinity of 135°. However, we may obtain the same results with a rear-element current phase of 315° or -45° relative to the forward element. We shall adopt the negative phase angle notation within these notes. To convert the angle to a more conventional appearance, add 180°.

The basic element for our exploration is a resonant dipole of the specified material. In a NEC-4 model, such a dipole is 197.6" long or about 0.4771 λ long at 28.5 MHz. (The half-inch diameter element is 0.001207 λ across.) The subject dipole has a resonant impedance of 72.1 + j 0.5 Ω.

A special note on the models associated with this chapter: there are only 5 models used in this chapter. They have special designations to coincide with the designations in the tabular data and with the array's structure.

- RES-E Ideal phased array with equal-length "resonant" elements
- SHT-E Ideal phased array with equal-length short elements
- LNG-E Ideal phased array with equal-length long elements
- RES-UF Ideal phased array with unequal-length elements: forward element longer
- RES-RF Ideal phased array with unequal-length elements: rear element longer

Now we are finally ready to examine a 2-element phased array.

Maximum Front-to-Back Ratio Configurations

The basic model consisted of two self-resonant dipoles of the type just described set at various distances apart. The exercise spacing values ranged from 0.05 λ to 0.2 λ in 0.025-λ increments. This range covers—with some interesting but practically useless excess—the element spacing used in virtually all recorded directional phased array construction. In addition to using equal-length self-resonant elements, I also made up pairs that are 10% shorter and 10% longer than the basic model. The short elements are 177.84" long (0.4294 λ), while the long elements are 217.36" long (0.5249 λ). As we shall see, resonance is not a requisite for a phased pair of elements. (We shall look at unequal-length elements soon.)

The first exercise attempted to arrive at the rear element relative current magnitude and phase angle necessary to achieve a maximum 180° front to back ratio. Although the pursuit of a perfect null can go on indefinitely, it proved fairly easy to obtain a rear null greater than 60 dB lower than the forward lobe maximum value. Since the maximum null is a very narrow-bandwidth phenomenon, -60 dB seemed deep enough to show general trends when we set 2-element phased arrays for a maximum front-to-back ratio.

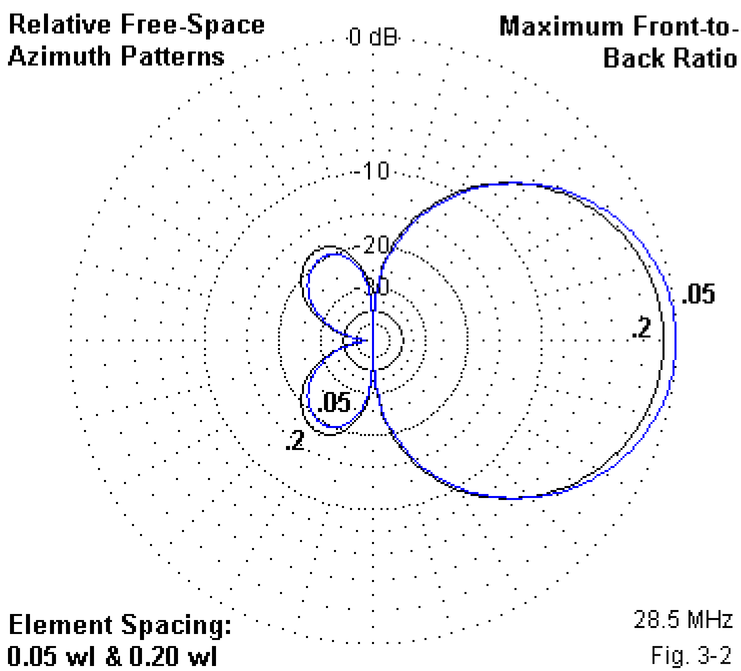

Fig. 3-2 shows typical patterns for the narrowest element spacing and the widest element spacing used. Although only one set of patterns appear in the figure, the general properties apply to all three of the subject models. As element spacing increases beyond 0.1 λ, gain drops off. More notable are the rear lobes. The deep null occurs within a rearward lobe, leaving angled side

lobes. The lobes are weakest at the narrowest spacing levels and increase with wide spacing. To some degree, then, aiming at the maximum 180° front-to-back ratio may be practically misdirected, although it serves to set operational limits for the 2-element array.

Table 3-1 provides full data for the short, resonant, and long element pairs. As we might expect, the maximum gain for any spacing is partly dependent upon the element lengths. Consistent among the three test models is the occurrence of maximum gain at the closest spacing levels: 0.05 and 0.075 λ. Thereafter, gain decreases steadily. The front-to-back values are simply for the record to verify that the model obtained the requisite depth of rear null. At a spacing of 0.125 λ, a popular element separation for 2-element Yagis and phased arrays, the forward gain of the maximum-null phased arrays do not differ significantly from the gain of a well-designed Yagi. In the maximum front-to-back configuration, then, the phased array's claim to fame is only its rearward null and not its gain.

Of primary interest to us are the rear element relative values of current magnitude and phase angle necessary to yield the deep null. **Fig. 3-3** graphically portrays the data of **Table 3-1**. Of immediate notice is that the change in element lengths between models has almost no effect on the requisite phase angles. The graphs of the three lines overlap and proceed in a virtually linear curve from about -17° at 0.05-λ spacing to about -73° at 0.2-λ spacing. Equally notable is the fact that we may obtain a rearward null for any spacing in this range. What does change with the length of the elements is the relative current magnitude required on the rear element. The longer the element pair, the higher the required value of relative rear element current to achieve. The differentials for 10% changes in element length are between 2% and 3%.

Not all element spacing values will be easy to implement with standard means of element phasing. The tabulated data shows negative resistance values in some entries for very close-spaced elements. These values are correct and simply mean that the mutual coupling between elements is providing more energy to the affected element than the source itself.

Equal-Length 2-Element Phased Array Performance
Maximum 180° Front-to-Back Configuration

Model SHT-E — Element Length (Front and Rear): 0.2147 λ
Frequency: 28.5 MHz — Diameter: 0.001207 λ (0.5")

Space λ	Gain dBi	Front-to-Back Ratio dB	Z1 (Rear) R +/- jX Ohms	Z2 (Forward) R +/- jX Ohms	Rear I Magnitude	Rear I Phase
0.05	6.41	65.58	3.9 - j110.3	3.2 - j 78.8	1.024	-17.4
0.075	6.42	66.13	7.9 - j117.1	7.5 - j 71.8	1.035	-26.4
0.1	6.36	73.68	11.9 - j120.7	14.7 - j 64.0	1.045	-35.6
0.125	6.25	61.40	15.7 - j122.8	24.4 - j 57.6	1.051	-44.9
0.15	6.11	65.41	19.1 - j123.8	35.7 - j 53.7	1.056	-54.3
0.175	5.92	68.86	22.3 - j124.3	47.7 - j 53.0	1.057	-63.8
0.2	5.69	65.46	25.7 - j124.2	59.1 - j 55.8	1.057	-73.2

Model RES-E — Element Length (Front and Rear): 0.2386 λ
Frequency: 28.5 MHz — Diameter: 0.001207 λ (0.5")

Space λ	Gain dBi	Front-to-Back Ratio dB	Z1 (Rear) R +/- jX Ohms	Z2 (Forward) R +/- jX Ohms	Rear I Magnitude	Rear I Phase
0.05	6.50	63.70	10.7 - j 35.5	-1.6 + i 7.0	1.033	-17.0
0.075	6.50	88.97	15.9 - j 37.5	4.6 + j 24.2	1.049	-26.0
0.1	6.44	60.36	20.7 - j 38.4	15.3 + j 39.4	1.063	-35.2
0.125	6.33	64.42	25.1 - j 38.8	29.8 + j 51.2	1.074	-44.7
0.15	6.18	66.73	29.1 - j 38.6	46.8 + j 58.2	1.080	-54.3
0.175	5.99	61.47	32.8 - j 38.2	64.6 + j 60.1	1.083	-64.0
0.2	5.76	63.34	36.0 - j 37.6	81.3 + j 56.7	1.080	-73.6

Model LNG-E — Element Length (Front and Rear): 0.2624 λ
Frequency: 28.5 MHz — Diameter: 0.001207 λ (0.5")

Space λ	Gain dBi	Front-to-Back Ratio dB	Z1 (Rear) R +/- jX Ohms	Z2 (Forward) R +/- jX Ohms	Rear I Magnitude	Rear I Phase
0.05	6.59	66.90	18.9 + j 39.0	- 7.3 + j 95 5	1.045	-16.6
0.075	6.59	74.73	25.9 + j 41.8	1.0 + j125.3	1.067	-25.5
0.1	6.52	63.87	32.0 + j 43.8	16.4 + j150.6	1.087	-34.9
0.125	6.41	65.07	37.4 + j 45.5	37.7 + j169.4	1.101	-44.5
0.15	6.26	66.57	42.3 + j 47.0	62.8 + j180.7	1.110	-54.4
0.175	6.08	72.84	46.7 + j 48.6	88.8 + j183.6	1.113	-64.3
0.2	5.85	67.24	50.7 + j 50.0	113.3 + j178.5	1.110	-74.3

Note: All gain values are for free-space. Rear current (I) magnitude and phase values are relative to forward element values of 1.0 and 0.0°. Model RES-E uses elements of equal length to an independent resonant dipole at the test frequency. Models SHT-E and LNG-E use elements that are 10% shorter and 10% longer, respectively.

Table 1. Performance and operating conditions of three 2-element phased arrays in a maximum 180° front-to-back ratio configuration.

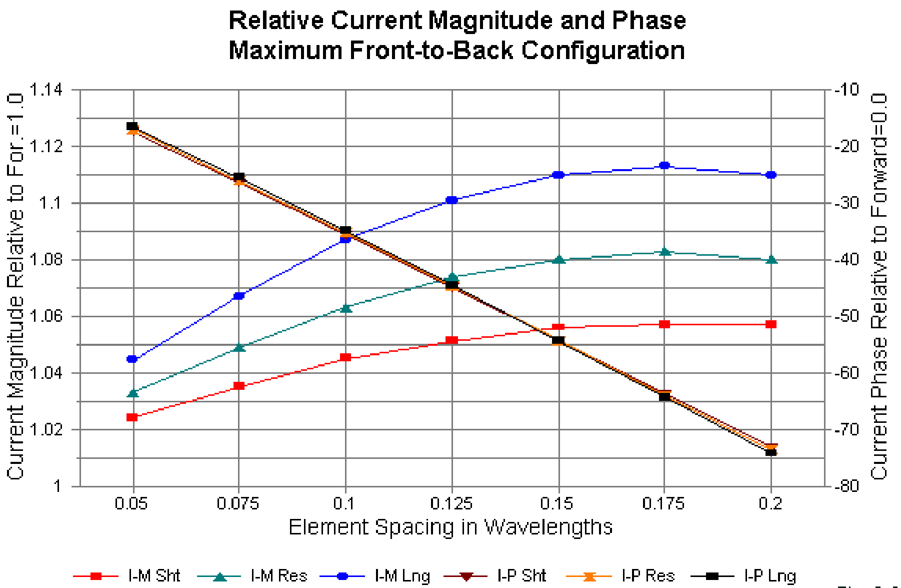

Fig. 3-3

A Test of Equal vs. Unequal Element Lengths

There are three possible element arrangements for a 2-element horizontal phased array. As we have just examined, both elements may be equal in length. However, **Fig. 3-4** shows two more configurations. The forward elements may be shorter than the rear element, and the forward element may be longer than the rear element. Our familiarity with the requirements for parasitic beams makes one of the arrangements natural and the other almost unthinkable. However, the Yagi-Uda array is limited to achieving its directional characteristics by virtue of geometry—a subject that we shall explore in the next chapter. If we can devise means (and we often can) to control the relative current magnitudes and phase angles on the two elements, then having a longer element in the direction of the main forward lobe is not only feasible, but has also been used in some practical antennas.

Fig. 3-4

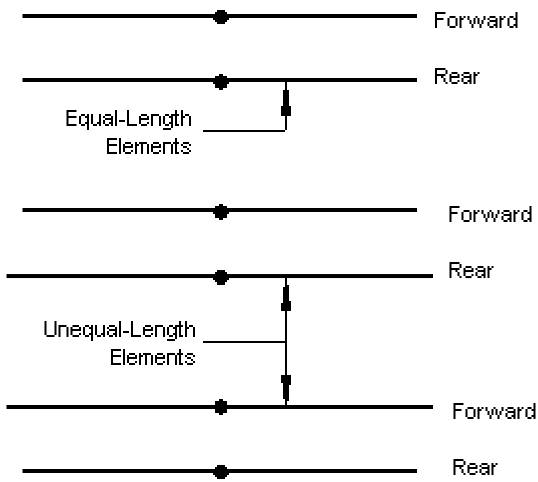

Three Element Length Options
for a Horizontal Phased Array

Both types of unequal-length element arrays are fully functional in a phased array, both in reality and in models. All that we need to do is provide the two elements with the correct relative current magnitudes and phase angles. For our ideal models, the task is one of assignment.

Table 3-2 provides the complete modeling data on the test runs. The equal-length model is the same as used for the earlier runs. Each of the unequal-length arrays has one element that is the same as our original self-resonant dipole and a second element that is 5% longer: 207.48" or 0.5010 λ. As the table shows, there is no significant difference in the maximum forward free-space gain. Once more, at the closest element spacing modeled, a negative resistive component on the forward element is possible.

Unequal-Length 2-Element Phased Array Performance
Maximum 180° Front-to-Back Configuration

Model RES-UF | Element Length: Front: 0.2505 λ; Rear: 0.2386λ
Frequency: 28.5 MHz | Diameter: 0.001207 λ (0.5")

Space λ	Gain dBi	Front-to-Back Ratio dB	Z1 (Rear) R +/- jX Ohms	Z2 (Forward) R +/- jX Ohms	Rear I Magnitude	Rear I Phase
0.05	6.52	62.19	12.1 - j 38.7	-3.6 + j 53.5	1.114	-16.9
0.075	6.52	69.26	17.3 - j 39.5	3.5 + j 75.7	1.139	-25.9
0.1	6.45	63.68	22.0 - j 39.7	16.4 + j 95.2	1.160	-35.3
0.125	6.34	65.22	26.2 - j 39.5	34.0 + j109.8	1.175	-44.9
0.15	6.20	63.14	30.1 - j 39.0	54.6 + j118.6	1.185	-54.6
0.175	6.02	67.19	33.5 - j 38.4	76.1 + j120.6	1.186	-64.4
0.2	5.79	68.90	36.6 - j 37.6	96.3 + j116.4	1.184	-74.2

Model RES-UR | Element Length: Front: 0.2386 λ; Rear: 0.2505λ
Frequency: 28.5 MHz | Diameter: 0.001207 λ (0.5")

Space λ	Gain dBi	Front-to-Back Ratio dB	Z1 (Rear) R +/- jX Ohms	Z2 (Forward) R +/- jX Ohms	Rear I Magnitude	Rear I Phase
0.05	6.52	63.77	13.3 + j 4.5	-2.4 + j 3.7	0.962	-16.9
0.075	6.52	61.79	19.3 + j 3.7	3.7 + j 22.1	0.974	-25.9
0.1	6.45	67.19	24.8 + j 3.6	14.5 + j 38.0	0.985	-35.1
0.125	6.35	62.79	29.7 + j 3.7	29.2 + j 50.1	0.992	-44.5
0.15	6.20	65.18	34.2 + j 4.2	46.2 + j 57.4	0.997	-54.1
0.175	6.01	65.28	38.4 + j 4.9	64.0 + j 59.3	0.998	-63.7
0.2	5.78	63.36	42.1 + j 5.9	80.8 + j 56.3	0.998	-73.3

For comparative data on Model RES-E, see Table 1.

Note: All gain values are for free-space. Rear current (I) magnitude and phase values are relative to forward element values of 1.0 and 0.0°. Model RES-E uses elements of equal length to an independent resonant dipole at the test frequency. Models RES-UF and RES-UR use elements that are 5% longer than those in RES-E at the forward and at the rear elements, respectively.

Table 2. Performance and operating conditions of 2 unequal-length element 2-element phased arrays in a maximum 180° front-to-back ratio configuration.

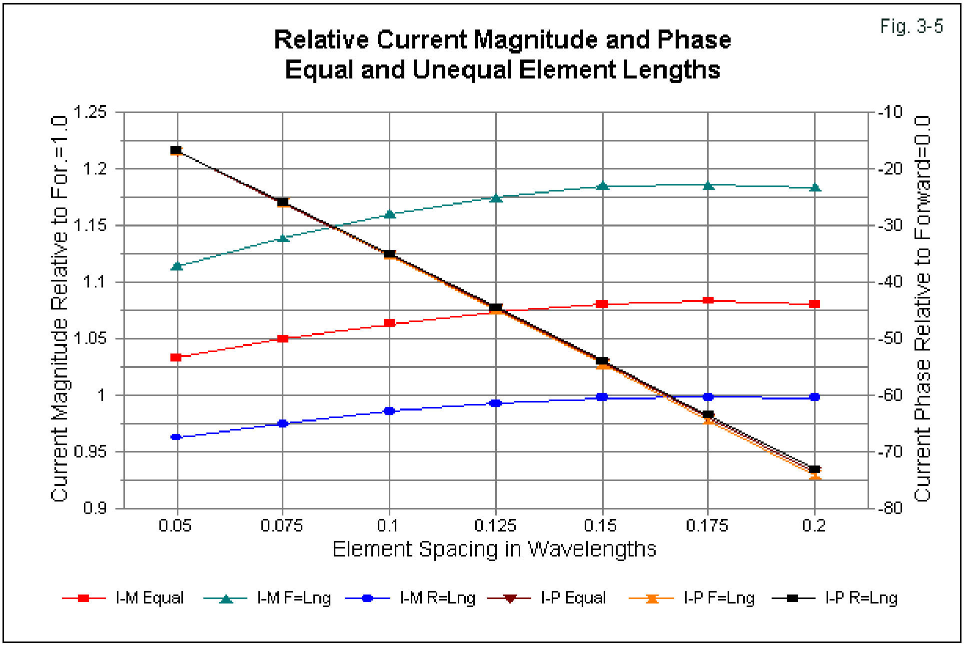

Fig. 3-5 shows the relative current magnitude on the rear element, along with the relative phase angle. As with the three equal-element-length arrays, the phase angles required to achieve a 180° front-to-back ratio in excess of 60 dB overlap with considerable precision. The differences are almost solely in the realm of the required relative current magnitude for the rear element. In this figure and in **Fig. 1-3**, you will note a slight decrease in the rear element current magnitude at the maximum spacing used (0.2 λ). The reversal of direction in current magnitude is consistent for all models in the series, both the ones used here and others in my collection.

These models cannot guarantee that any particular element arrangement will provide an adequate basis for a practical array. However, when experimenting with phased arrays and various phasing schemes, it pays not to overlook the potential of a longer forward element.

Maximum Gain Configurations

The maximum front-to-back ratio configuration of a phased array represents one limit of performance, a limit marked by moderate gain and a deep rearward null. We may also set the relative current magnitudes and phase angles to achieve maximum forward gain, letting the front-to-back ratio become whatever it will be. In general, the conditions for maximum forward gain in a 2-element horizontal phased array do not favor high front-to-back ratios. **Fig. 3-6** shows a typical maximum gain pattern, with a front-to-back ratio well below 10 dB.

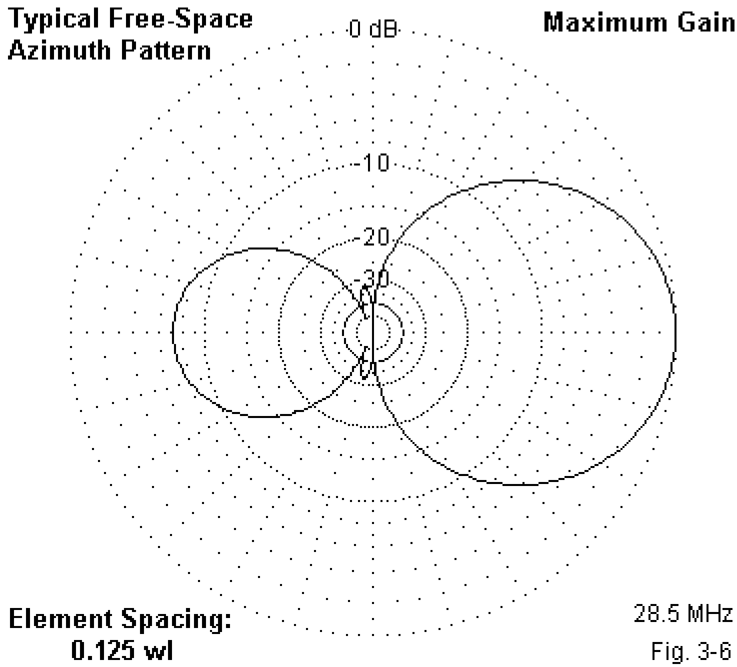

Fig. 3-6

For the 5 models that we previously examined, **Table 3-3** provides the necessary data. Note especially the relationships among the element spacing, the forward gain, and the front-to-back ratio.

Equal-Length and Unequal-Length 2-Element Phased Array Performance
Maximum Gain Configuration

Model SHT-E
Frequency: 28.5 MHz
Element Length (Front and Rear): 0.2147 λ
Diameter: 0.001207 λ (0.5")

Space λ	Gain dBi	Front-to-Back Ratio dB	Z1 (Rear) R +/- jX Ohms	Z2 (Forward) R +/- jX Ohms	Rear I Magnitude	Rear I Phase
0.05	7.10	8.57	1.8 - j102.1	1.5 - j 87.4	1.010	- 8.0
0.075	7.23	7.57	3.5 - j104.5	3.2 - j 85.1	1.015	-11.0
0.1	7.24	7.42	5.4 - j105.0	6.2 - j 80.1	1.020	-14.8
0.125	7.21	7.01	7.0 - j103.8	10.5 - j 75.5	1.020	-18.0
0.15	7.15	6.67	8.8 - j101.9	15.5 - j 70.4	1.025	-21.3
0.175	7.06	6.33	10.6 - j 99.7	21.4 - j 66.5	1.025	-24.5
0.2	6.96	5.95	12.6 - j 97.2	27.7 - j 63.4	1.030	-27.5

Model RES-E
Frequency: 28.5 MHz
Element Length (Front and Rear): 0.2386 λ
Diameter: 0.001207 λ (0.5")

Space λ	Gain dBi	Front-to-Back Ratio dB	Z1 (Rear) R +/- jX Ohms	Z2 (Forward) R +/- jX Ohms	Rear I Magnitude	Rear I Phase
0.05	7.19	8.17	4.9 - j 24.6	-0.7 - j 5.7	1.015	- 7.5
0.075	7.31	7.72	7.0 - j 21.8	2.0 + j 5.1	1.020	-11.0
0.1	7.31	7.38	9.5 - j 18.1	6.2 + j 15.9	1.030	-14.5
0.125	7.28	7.08	11.8 - j 14.2	12.3 + j 25.5	1.038	-18.0
0.15	7.21	6.75	13.7 - j 10.2	20.3 + j 33.7	1.035	-21.5
0.175	7.13	6.46	16.1 - j 6.3	28.9 + j 40.6	1.040	-25.0
0.2	7.02	5.97	18.3 - j 1.7	37.9 + j 45.1	1.040	-27.8

Model LNG-E
Frequency: 28.5 MHz
Element Length (Front and Rear): 0.2624 λ
Diameter: 0.001207 λ (0.5")

Space λ	Gain dBi	Front-to-Back Ratio dB	Z1 (Rear) R +/- jX Ohms	Z2 (Forward) R +/- jX Ohms	Rear I Magnitude	Rear I Phase
0.05	7.28	8.48	9.3 + j 52.5	- 3.8 + j 78 0	1.025	- 7.5
0.075	7.39	7.71	11.8 + j 62.1	0.3 + j 98.1	1.030	-10.8
0.1	7.39	7.47	14.5 + j 69.9	7.0 + j116.4	1.035	-14.5
0.125	7.35	7.11	17.5 + j 77.5	15.6 + j132.1	1.045	-18.0
0.15	7.29	6.77	20.3 + j 84.5	26.6 + j145.2	1.050	-21.5
0.175	7.20	6.43	23.4 + j 91.1	39.2 + j155.7	1.055	-25.0
0.2	7.10	6.03	26.1 + j 97.6	53.0 + j162.6	1.050	-28.3

Equal-Length and Unequal-Length 2-Element Phased Array Performance
Maximum Gain Configuration
(continued)

Model RES-UF — Element Length: Front: 0.2505 λ; Rear: 0.2386λ
Frequency: 28.5 MHz — Diameter: 0.001207 λ (0.5")

Space λ	Gain dBi	Front-to-Back Ratio dB	Z1 (Rear) R +/- jX Ohms	Z2 (Forward) R +/- jX Ohms	Rear I Magnitude	Rear I Phase
0.05	7.21	8.19	5.2 - j 28.3	-1.1 + j 38.7	1.085	- 7.5
0.075	7.33	7.74	7.6 - j 24.2	1.7 + j 53.1	1.100	-11.0
0.1	7.33	7.36	9.7 - j 19.8	7.1 + j 66.5	1.110	-14.5
0.125	7.30	7.04	11.9 - j 15.3	14.3 + j 78.6	1.120	-18.0
0.15	7.23	6.70	13.7 - j 11.0	23.7 + j 88.6	1.120	-21.5
0.175	7.15	6.40	16.0 - j 6.7	34.1 + j 96.9	1.125	-25.0
0.2	7.04	6.02	18.5 - j 2.4	45.1 + j102.8	1.130	-28.3

Model RES-UR — Element Length: Front: 0.2386 λ; Rear: 0.2505λ
Frequency: 28.5 MHz — Diameter: 0.001207 λ (0.5")

Space λ	Gain dBi	Front-to-Back Ratio dB	Z1 (Rear) R +/- jX Ohms	Z2 (Forward) R +/- jX Ohms	Rear I Magnitude	Rear I Phase
0.05	7.21	8.60	6.6 + j 16.5	-1.4 - j 8.8	0.950	- 7.8
0.075	7.33	7.80	8.8 + j 21.8	1.5 + j 2.8	0.950	-11.0
0.1	7.33	7.44	11.5 + j 27.0	5.9 + j 14.2	0.955	-14.5
0.125	7.30	7.13	14.1 + j 32.2	12.0 + j 24.4	0.960	-18.0
0.15	7.23	6.82	16.9 + j 37.3	19.6 + j 33.3	0.965	-21.5
0.175	7.15	6.36	19.0 + j 42.6	28.5 + j 39.7	0.960	-24.5
0.2	7.04	6.01	21.7 + j 47.6	37.9 + j 44.7	0.960	-27.8

Note: All gain values are for free-space. Rear current (I) magnitude and phase values are relative to forward element values of 1.0 and 0.0°. Model RES-E uses elements of equal length to an independent resonant dipole at the test frequency. Models SHT-E and LNG-E use elements that are 10% shorter and 10% longer, respectively. Models RES-UF and RES-UR use elements that are 5% longer than those in RES-E at the forward and at the rear elements, respectively.

Table 3. Performance and operating conditions of 5 2-element phased arrays in a maximum-gain configuration.

Maximum gain does not occur at the very closest spacing tested, but appears in the 0.75-λ to 0.1-λ region of element spacing. Front-to-back ratios show a steady decrease with increasing element spacing. The maximum gain phenomenon has a wider bandwidth than the maximum front-to-back null. Therefore, each registered data set comprises a centered set of values in the middle of the range of phase angles and the range of current magnitudes that yield the highest gain. Over this region, the front-to-back ratio may change by as much as 2 dB, and the table shows only the center value.

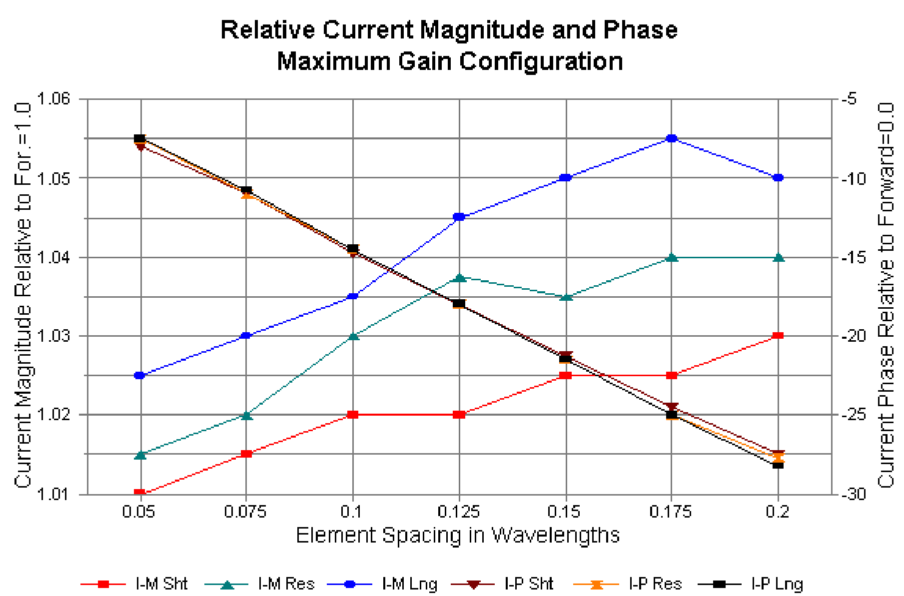

Fig. 3-7

Fig. 3-7 graphs the current magnitude and phase angle data for the 3 equal-element-length models. Once more the phase angle curves form an overlapping trio. Irregularities in the current magnitude curves arise from the simple averaging and centering procedure used to produce the curves. However, the general trend is both clear and consistent with the maximum front-to-back curves: the longer the elements, the higher the required relative current magnitude level on the rear element to achieve the desired performance curves.

The maximum gain curves represent the highest gain level that we may achieve with 2 elements of the sizes in the models. In general, the highest gain levels coincide with those for a quite short boom 3-element Yagi or a 2-element quad, both of which are designed for adequate 10-meter band coverage. The Yagi boom length would be about 8' for this gain level, with 12' boom 3-element Yagis capable of 8 dBi free-space gain across the first MHz of 10 meters. However, the phased-array data, taken at a single frequency, do not necessarily hold over an equivalent operating bandwidth.

Conclusions and Compromises

The exercise that we have presented is at most a demonstration of phased array properties and not a proof of them. What it shows is two sets of limits between which most horizontal phased arrays operate. In general, designers either consciously select or discover through experimentation phasing arrangements that yield acceptable performance with respect to gain, front-to-back ratio, and operating bandwidth. In the earliest days of amateur horizontal phased-array development, numerous successful and not-so-successful designs emerged from the misapplication of parasitic principles to phased arrays. However, access to modeling software now permits somewhat more systematic studies of the trends involved.

Table 3-4 gives us a partial view of what happens to the performance characteristics of a 2-element array as we drift away from the conditions that yield maximum front-to-back ratio. Varying the rear element relative current magnitude alone (with a fixed relative current phase angle) by about +/-10% shows a gradual decline in gain and a more rapid decrease in front-to-back ratio whether the current magnitude goes too high or too low. However, as we fix the current magnitude on the rear element and vary the phase angle, we obtain a different progression. The front-to-back ratio decreases on both sides of the optimal values. In contrast, the change in phase angle shows a single low-to-high progression in the +/-2° variation in the example.

Performance Shifts With Changes in Relative Current Magnitude and Phase Angle
Model RES-E at 3 Element Spacings

Element Spacing: 0.05 λ

1. Rear Element Relative Current Phase Angle: -17.0°

Rear I Magnitude	Gain dBi	Front-to-Back Ratio dB	Z1 (Rear) R +/- jX Ohms	Z2 (Forward) R +/- jX Ohms
0.933	6.34	15.23	3.7 - j 38.9	5.9 + j 6.1
0.983	6.47	21.48	7.4 - j 37.0	2.2 + j 6.6
1.033	6.50	63.70	10.7 - j 35.3	-1.6 + j 7.0
1.183	6.42	21.95	13.7 - j 33.8	-5.3 + j 7.5
1.133	6.28	16.30	16.4 - j 32.4	-9.0 + j 7.9

2. Rear Element Relative Current Magnitude: 1.033

Rear I Phase Angle	Gain dBi	Front-to-Back Ratio dB	Z1 (Rear) R +/- jX Ohms	Z2 (Forward) R +/- jX Ohms
-13.0	6.88	17.45	8.5 - j 30.7	-2.0 + j 1.6
-15.0	6.69	23.97	9.6 - j 33.1	-1.8 + j 4.3
-17.0	6.50	63.70	10.7 - j 35.3	-1.6 + j 7.0
-19.0	6.30	25.07	11.9 - j 37.6	-1.2 + j 9.7
-21.0	6.11	19.47	13.2 - j 39.8	-0.7 + j 12.4

Element Spacing: 0.125 λ

1. Rear Element Relative Current Phase Angle: -44.7°

Rear I Magnitude	Gain dBi	Front-to-Back Ratio dB	Z1 (Rear) R +/- jX Ohms	Z2 (Forward) R +/- jX Ohms
0.974	6.31	23.22	20.3 - j 42.5	33.8 + j 46.2
1.024	6.33	29.53	22.8 - j 40.5	31.8 + j 48.7
1.074	6.33	64.42	25.1 - j 38.8	29.8 + j 51.2
1.124	6.31	29.77	27.2 - j 37.1	27.9 + j 53.7
1.174	6.28	24.03	29.1 - j 35.7	25.9 + j 56.2

2. Rear Element Relative Current Magnitude: 1.074

Rear I Phase Angle	Gain dBi	Front-to-Back Ratio dB	Z1 (Rear) R +/- jX Ohms	Z2 (Forward) R +/- jX Ohms
-40.7	6.52	25.75	22.7 - j 35.4	26.2 + j 48.1
-42.7	6.42	31.85	23.9 - j 37.1	28.0 + j 49.7
-44.7	6.33	64.42	25.1 - j 38.8	29.8 + j 51.2
-46.7	6.23	32.45	26.4 - j 40.4	31.7 + j 52.7
-48.7	6.14	26.50	27.8 - j 41.9	33.7 + j 54.0

Performance Shifts With Changes in Relative Current Magnitude and Phase Angle
Model RES-E at 3 Element Spacings
(continued)

Element Spacing: 0.2 λ

1. Rear Element Relative Current Phase Angle: -73.6°

Rear I Magnitude	Gain dBi	Front-to-Back Ratio dB	Z1 (Rear) R +/- jX Ohms	Z2 (Forward) R +/- jX Ohms
0.980	5.76	26.01	32.5 - j 41.3	80.3 + j 51.3
1.030	5.76	32.36	34.3 - j 39.4	80.8 + j 54.0
1.080	5.76	63.34	36.0 - j 37.6	81.3 + j 56.7
1.130	5.76	32.38	37.5 - j 36.0	81.8 + j 59.3
1.180	5.75	26.68	38.9 - j 34.5	82.3 + j 62.0

2. Rear Element Relative Current Magnitude: 1.080

Rear I Phase Angle	Gain dBi	Front-to-Back Ratio dB	Z1 (Rear) R +/- jX Ohms	Z2 (Forward) R +/- jX Ohms
-69.6	5.92	28.63	33.6 - j 35.1	77.3 + j 57.3
-71.6	5.84	34.61	34.8 - j 36.4	79.3 + j 57.0
-73.6	5.76	63.34	36.0 - j 37.6	81.3 + j 56.7
-75.6	5.69	35.05	37.3 - j 38.8	83.3 + j 56.3
-77.6	5.61	28.98	38.7 - j 39.9	85.3 + j 55.8

Note: Total rear element relative current magnitude shift: +/- 10%; total rear element relative current phase angle shift: +/- 2°

Table 4. Performance shifts in model RES-E at 0.05, 0.125, and 0.2 λ element spacing with a constant rear element relative phase angle and a variable relative current magnitude and with a constant rear element current magnitude and a variable relative current phase angle.

The table shows clearly that the operating bandwidth for a set of conditions varies directly with the spacing between elements. The cost of obtaining the wider operating bandwidth is, of course, a decrease in the forward gain. However, the rate of gain decrease itself increases with spacing values above about 0.125 λ. Indeed, one of the sensible reasons for selecting an element spacing in the 0.1-λ to 0.15-λ region is that we acquire reasonable operating bandwidth while maintaining higher gain levels.

Designers of phased arrays rarely survey the potentials for practical beams by extending the systematic model variation exemplified by **Table 3-4**. There are too many variables involved in the design work for one to fix upon a set of relative current magnitudes and phase angles and then design means for obtaining them. Instead, they tend to discover configurations that meet our usual amateur standards for what counts as a "good" beam. **Fig. 3-8** shows a typical and desirable phased array pattern for a beam using equal length (self-resonant) elements that are spaced 0.125 λ. Gain does not appear on the pattern, but the triple rear lobe everywhere exceeds -20 dB relative to the forward lobe.

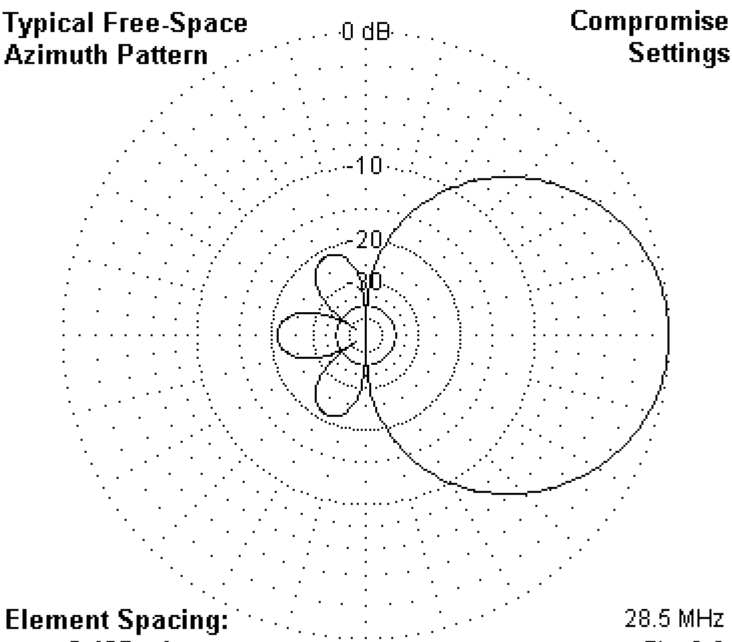

Fig. 3-8

There is no single set of values for relative current magnitude and relative phase angle that will yield patterns of this sort. **Table 3-5** lists data for a set of compromise values developed simply by taking proportional parts of the differentials between the magnitude and phase angle values for the two extreme or limiting cases. **Fig. 3-9** graphs the free-space gain and front-to-back ratio.

Performance Shifts With Changes in Relative Current Magnitude and Phase Angle
Model RES-E at 0.125 λ Element Spacing Stepped Between Front-to-Back and Gain Settings

Setting No.	Rear I Mag.	Rear I Phase	Gain dBi	Front-to-Back Ratio dB	Z1 (Rear) R +/- jX Ohms	Z2 (Forward) R +/- jX Ohms
1	1.074	-44.7	6.33	64.42	25.1 - j 38.8	29.8 + j 51.2
2	1.065	-38.0	6.64	21.05	20.8 - j 33.3	24.2 + j 45.5
3	1.056	-31.4	6.94	14.53	17.1 - j 27.4	19.5 + j 39.3
4	1.047	-24.7	7.17	10.32	14.1 - j 21.0	15.4 + j 32.6
5	1.038	-18.0	7.28	7.08	11.8 - j 14.2	12.3 + j 25.5

Table 5. Performance shifts as the relative rear element current magnitude and phase angles are shifted in proportional steps between maximum front-to-back ratio and maximum gain settings.

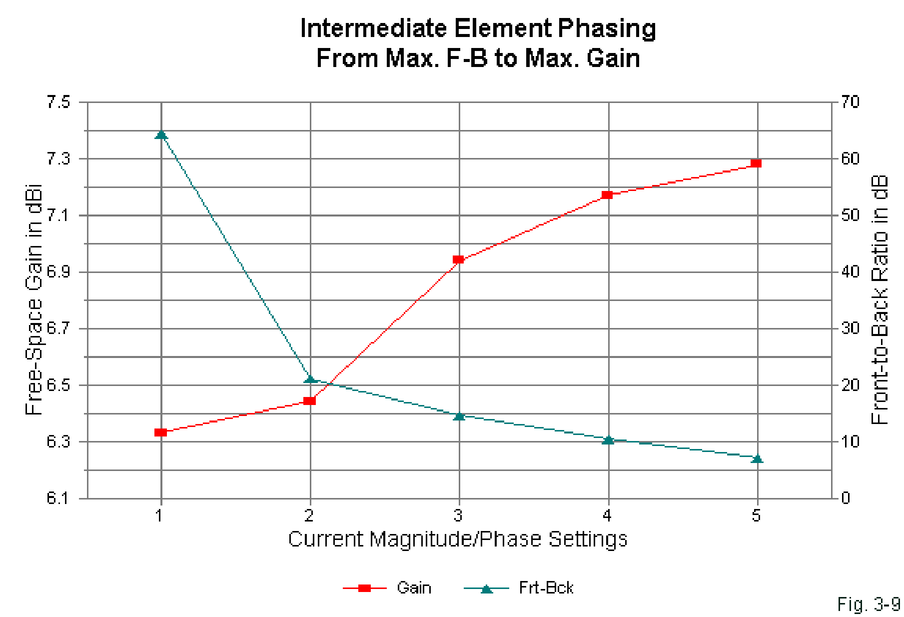

Fig. 3-9

The setting numbers on the graph's X-axis correspond to the combinations shown in the table. Variations from the combinations are possible, but the general trends shown in the graph will persist.

As noted earlier, the very high 180° front-to-back ratio decreases quickly, so that a phase angle of -38° on the rear element with a 1% decrease in current magnitude results in a front-to-back ratio just over 20 dB. However, in this increment, gain only rises by about 0.1 dB, with the steeper gain increase curve appearing between settings 2 and 3. As a result, one must accept a front-to-back ratio of less than 20 dB to achieve gain levels higher than 6.5 dBi.

The strategy used for these models can well be altered with possibly different results. We have sampled only two of many strategies in the effort to find a satisfactory set of operating conditions, and we have not explored the question of operating bandwidth—the frequency range over which the performance characteristics sustain themselves at acceptable levels. One reason for this void in our discussion is that the means by which we implement the current magnitudes and phase angles on each element play a significant role in setting the operating bandwidth. The exploration of such means is yet to come. We can only note at this stage that the number of variables involved in phased array design is high enough to preclude anything like a complete treatment.

Although the overall treatment for selecting workable compromise values for element current and phase angles may be incomplete, the earlier part of the chapter is decisive with respect to the maximum gain—on the one hand—and the maximum front-to-back ratio—on the other hand. Within the limits of NEC software to accurately model 2-element array behavior, an array of this type that uses elements in the vicinity of 1/2-λ cannot exceed the free-space gain indicated in the tables and graphs. Moreover, if any array claims a significant front-to-back ratio—perhaps greater than about 15 dBi—then the gain will be significantly lower than the maximum values shown in the tables and graphs for maximum gain performance.

Likewise, the maximum front-to-back ratio data applies only over a very narrow frequency span, one that we may measure in Hz. As we move away from the test frequency, the front-to-back deteriorates rapidly. With the ideal models, we cannot show the rapid deterioration in a frequency sweep. The assignment of individual source values for current magnitude and phase angle will remain constant. In contrast, if we were to use one of the physical means of obtain correct phase relationships at a certain frequency, those relationships would change with frequency, even within the operating passband defined by the first MHz of 10 meters. Ideal models are very useful devices, but only when we use them within their legitimate limits.

Therefore, we have only scratched the surface of horizontal phased-array understanding. The exercise has set performance limits. The data in **Tables 3-1** and **3-2**, however, are more than interesting numbers: they provide insight into the conditions that yield individual element impedances in paired combinations. For example, the pattern of impedances in the listings will take on considerable importance in later parts of this series of chapters.

As well, we have identified some of the factors affecting operating bandwidth, such as element spacing and where we set the rear element relative current magnitude and phase angle between the maximum gain and the maximum front-to-back values. Of course, we have not mentioned a third significant factor that affects operating bandwidth, namely, the diameter of the elements that we use. However, element diameter as a fraction of a wavelength will play a role in operating bandwidth, especially as one examines wire and tubular implementations of 2-element phased arrays.

Perhaps one sample case may suffice to show that element diameter does make a difference. See **Table 3-6**. The sample case uses the model with equal element lengths and a spacing of 0.125-λ. The only change among the three models is the diameter of the elements. The table shows values for 0.25”, 0.5”, and 1.0” elements. The gain shows a very slight rise with increasing diameter, largely as a result of decreasing losses from the aluminum elements. The front-to-back ratio simply verifies that the models have met the conditions set earlier in this chapter for qualifying as maximum front-to-back ratio values. The most interesting entries are the rear element current magnitude and phase angle values. The required phase angle does not change with the change in element diameter. However, the rear-element current magnitude changes by about 3% in the move from the smallest to the largest element diameter. In practical terms, the table makes clear that if we desire to replicate a phased array—regardless of the means of arriving at a desired set of phasing condition—we must replicate the element diameter as well as the remaining dimensions. If we do not do so, then we must anticipate performance changes.

Maximum Front-to-Back Ratio Performance Shifts With Changes in Element Diameter
Model RES-E at 0.125 λ Element Spacing Using Different Element Diameters

Element Diameter	Gain dBi	Front-to-Back Ratio dB	Rear I Magnitude	Rear I Phase
0.25"	6.30	62.26	1.061	-44.7
0.5"	6.33	64.42	1.074	-44.7
1.0"	6.34	66.56	1.092	-44.7

Table 6. Changes in the required rear element current magnitude and phase angle as a result of changing element diameter. Element lengths and spacing remain constant.

So far, we have not explored how close we may come to a nearly perfect array with the ordinary design means available to us. One of those ordinary means that we usually overlook is antenna geometry. We shall explore the nature and limitations of that design route in the next chapter.

4. The Limits of Geometric Phasing

In Chapter 3, we noted that there are two ways of looking at the idea of a phased array. One perspective views the phased array as a combination of elements, all of which are fed. The other perspective is more general: it examines the relative current magnitude and phase angle of element combinations, regardless of which one or more of them may be fed. From this latter perspective, a 2-element parasitic array is phased in the sense that the unfed element will display a relative current magnitude and phase angle.

Fig. 4-1

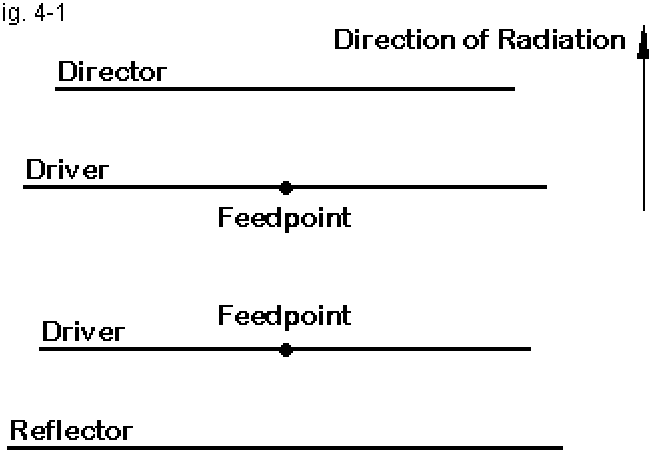

Options for 2-Element Parasitic Arrays

The parasitic array, of course, has a more common name: the Yagi-Uda beam. The Yagi (for short) may have as many parasitic elements as a designer can put to good use. Our interest will be in the smallest of such arrays: 2-

element models. **Fig. 2-1** shows the options that we have for creating 2-element Yagis. We may either use a director or forward parasitic elements with a driven element, or we may use a reflector or rear parasitic element with a driven element.

The names "director" and "reflector" are simply conventional tags by which we identify a given parasitic element. The names do not themselves indicate how a parasitic array operates. Indeed, among those new to antennas, we find numerous misconceptions concerning reflectors, including the idea that they function similarly to the mirrored surface behind the light source in a flashlight. Directors, by the same analogy, appear to function in the manner of optical lenses by focusing the beam of RF.

Let's approach 2-element Yagis from a different point-of-view. The close proximity of the 2 elements provides significant inter-element coupling such that the unfed element will show at its center a relative current magnitude and phase angle. By adjusting the element diameters, spacing, and lengths, we may alter the unfed element relative current magnitude and phase angle. However, this process is limited by the basic geometry of the array. It is composed of parallel linear elements. Hence, the three variables of length, diameter, and spacing can only go so far in yielding on the unfed element a relative current magnitude and phase angle that corresponds with those identified in Chapter 3 as able to produce a desired radiation pattern.

In this chapter, we shall look more closely at the basic properties of 2-element Yagis in both the reflector-driver and the driver-director configuration. Our efforts will be to understand the limitations that geometry alone, as a set of design variables, places on the performance of 2-element arrays, especially compared to independently feeding both elements. When we are done, we should be able to correlate typical Yagi patterns with the relative phasing conditions for the two elements. At the end, we shall look at some alternative 2-element geometries designed to improve those conditions.

The Reflector-Driver and Driver-Director 2-Element Arrays

The earliest detailed study of 2-element Yagis using method-of-moments modeling software is the work of Jerry Hall, K1TD, whose results appear in the 15th and 16th editions of *The ARRL Antenna Book* (pp. 11-2 through 11-8). I shall replicate his work in part, using the modeling constraints applied in Part 1. The test frequency will be 28.5 MHz. The array elements will use 0.5" (0.001207 λ) diameter elements. Throughout our simplified examination of 2-element Yagis, I shall aim for two simultaneous goals: maximum front-to-back ratio and driver resonance. A driver will be considered resonant when the source reactance is +/-j1 Ω or less. Using these twin goals will not yield the absolute maximum 180° front-to-back ratio possible with two elements, but it will be close. As well, the results will permit easier graphing of the source impedances of corresponding reflector-driver and driver-director arrays.

We shall also limit our samples to the same increments of element spacing that we used in Chapter 3: from 0.05 λ to 0.2 λ in 0.025-λ increments. Where our interest will depart from the earlier study is in the recording of the relative current magnitude and phase angle on the parasitic element when the driver has a current magnitude of 1.0 and a phase angle of 0.0°. (See model yrd.ez and adjust both the element lengths and spacing as necessary.)

Table 4-1 provides the basic performance data for the models of a reflector-driver parasitic array meeting the conditions we have just specified. In addition to the usual performance data (free-space gain in dBi, 180° front-to-back ratio in dB, and the source impedance in Ω), the table provides element lengths as a function of a wavelength at the test frequency. Unlike the models in Chapter 3, which used a relatively arbitrary but consistent set of dimensions for each model, the parasitic array must have different element lengths at each increment of spacing to achieve the maximum front-to-back ratio at a resonant driver impedance.

The dimensions themselves hold some interest. As you scan the table, note that the reflector length required to meet the twin modeling objectives reaches a peak length at a spacing of 0.125 λ and then decreases. In contrast, the required driver length decreases until the element spacing is 0.175 λ and then increases.

2-Element Reflector-Driver Performance
Set for Maximum 180° Front-to-Back Ratio and Resonance

Element Spacing λ	Reflector Length λ	Driver Length λ	Gain dBi	Front-to-Back Ratio dB	Feedpoint Z R +/- jX Ω
0.05	0.2505	0.2387	6.24	11.36	8.1 + j 0.1
0.075	0.2507	0.2356	6.36	11.40	15.4 - j 0.2
0.1	0.2511	0.2334	6.32	11.33	24.3 - j 0.1
0.125	0.2514	0.2310	6.25	11.18	33.8 + j 0.0
0.15	0.2513	0.2312	6.18	10.96	42.9 - j 0.1
0.175	0.2513	0.2310	6.06	10.69	52.1 + j 0.0
0.2	0.2511	0.2312	5.91	10.36	60.2 - j 0.0

Note: All elements 0.5" (0.001207 λ) aluminum

Table 1. 2-element reflector-driver Yagi performance when set for maximum 180° front-to-back ratio and driver resonance.

Fig. 4-2 graphs the gain and front-to-back ratio data as a convenient way to examine the trends. Within the limitations of the increments of element spacing used here, the gain and the front-to-back ratio reach their peak values with an element spacing of 0.075 λ. There are two good reasons why we rarely, if ever, design 2-element reflector-driver Yagis with this particular spacing. One of those reasons is the low source impedance: just above 15 Ω. The other reason is the narrowness of the operating bandwidth at this spacing, a facet of 2-element Yagi design that we shall examine more thoroughly in a moment.

The low level of the front-to-back ratio of the reflector-driver design has struck many antenna enthusiasts and has occasioned two responses. One is the design of 3-element and larger Yagis. The second is the design of arrays that feed both elements. The front-to-back ratio with an element spacing of 0.125 λ is about 11.18 dB. We can increase this level to about 11.50 dB largely by shortening the driver and thereby changing the mutual coupling between the elements. However, in the process, the gain begins to decrease, and the source impedance reaches a value of about 30 - j 52 Ω. Hence, draining the reflector-driver design of the last modicum of front-to-back ratio tends to result in relatively impractical source impedance values.

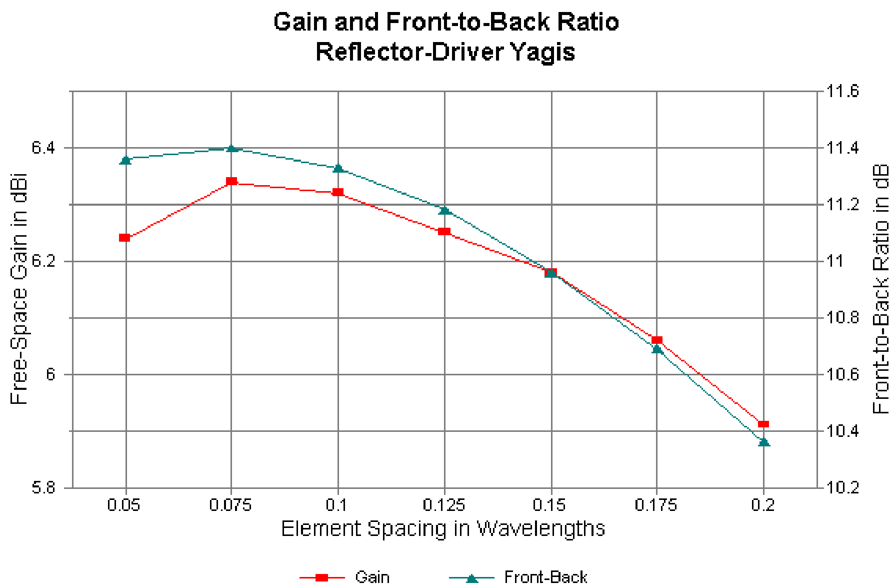

Fig. 4-2

Table 4-2 reveals the reason for the low levels of front-to-back ratio associated with reflector-driver Yagi designs. The table lists the modeled rear element relative current magnitude and phase angle values, along with the values needed for the same set of elements to achieve more than 60 dB front-to-back ratio. (The ideal front-to-back ratio models show the same deep 180° null as those in Chapter 3, along with the rearward side lobes that result in worst-cast front-to-back ratios between 17 and 22 dB.) The gain of the models using two sources appears in the right-most column. The ideal phase angles have been converted from the negative angles typical of models in Chapter 3 to values that correspond to those yielded by models of Yagis. To convert either value to one that is more suited to phasing networks, simply subtract 180° from the listed value.

Actual vs. Ideal Rear Element Relative Current Magnitude and Phase Angle
2-Element Reflector-Driver Yagis

	Actual		Ideal		
Element Spacing λ	Relative I Mag.	Relative I Phase	Relative I Mag.	Relative I Phase	Gain dBi
0.05	0.833	165.1	0.963	163.1	6.51
0.75	0.774	158.1	0.953	154.1	6.51
0.1	0.719	150.7	0.944	144.9	6.44
0.125	0.670	143.1	0.938	135.6	6.33
0.15	0.636	136.5	0.938	126.1	6.18
0.175	0.603	129.3	0.936	116.6	6.00
0.2	0.576	122.4	0.937	107.1	5.77

Note: all phase angles adjusted for positive values. For negative angle values corresponding to those in Part 1, subtract 180 from the listed value. All "ideal models" set to a 180° front-to-back ratio greater than 60 dB.

Table 2. Actual vs. ideal rear element relative current magnitude and phase angle values for maximum 180° front-to-back ratios for 2-element reflector-driver Yagis in Table 1.

In concert with the curves that we saw in **Fig. 4-2**, the relative current magnitude and the phase angle of the optimized Yagi both depart more radically from the ideal numbers with the widening of the spacing between elements. Coincidence is closest at the narrowest spacing values. However, the narrower the spacing between elements, the more exact the coincidence must be to yield the ideal maximum front-to-back value of more than 60 dB. Hence, the closeness of the values at a spacing of 0.05 λ is still not close enough to yield the highest front-to-back ratio. As well, the ideal model shows its highest gain at the narrowest spacing, although the Yagi does reach maximum gain until the spacing is 0.075 λ. Interestingly, the ideal models have a higher gain potential only until the spacing reaches 0.15 λ, after which the Yagi shows slightly higher gain.

The data that we have scanned thus far does not take into account an important factor in amateur use of 2-element beams: operating bandwidth. The first MHz of 10 meters is one of the widest HF amateur bands (excluding the 80-75-meter band). Hence, examining the bandwidth characteristics of sample driver-reflector Yagis can be illuminating in terms of telling us how rapidly the test-frequency optimized condition may deteriorate. **Table 4-3** provides the data. However, I shall reserve commentary on this data until we have explored the alternative Yagi configuration.

Bandwidth Characteristics for 2-Element Reflector-Driver Yagis
At 0.1, 0.125, and 0.15 λ Element Spacing

Element Spacing: 0.1 λ

Frequency MHz	Gain dBi	Front-to-Back Ratio dB	Feedpoint Z R +/- j X Ω	SWR Relative to 24.3 Ω
28.0	6.84	9.53	16.3 - j 23.1	3.20
28.25	6.58	10.94	20.2 - j 11.3	1.71
28.5	6.32	11.33	24.3 - j 0.1	1.01
28.75	6.07	11.01	28.4 + j 10.4	1.53
29.0	5.86	10.41	20.5 + j 20.5	2.16

Element Spacing: 0.125 λ

Frequency MHz	Gain dBi	Front-to-Back Ratio dB	Feedpoint Z R +/- j X Ω	SWR Relative to 33.8 Ω
28.0	6.72	9.92	24.7 - j 21.4	2.19
28.25	6.48	10.91	29.3 - j 10.3	1.43
28.5	6.25	11.18	33.8 + j 0.0	1.00
28.75	6.04	10.94	38.1 + j 9.8	1.35
29.0	5.85	10.45	42.3 + j 19.2	1.73

Element Spacing: 0.15 λ

Frequency MHz	Gain dBi	Front-to-Back Ratio dB	Feedpoint Z R +/- j X Ω	SWR Relative to 33.8 Ω
28.0	6.61	9.89	33.3 - j 20.0	1.78
28.25	6.39	10.71	38.1 - j 9.7	1.31
28.5	6.18	10.96	42.9 - j 0.1	1.00
28.75	5.98	10.80	47.4 + j 9.0	1.25
29.0	5.80	10.41	51.7 + j 17.7	1.52

Table 3. Bandwidth characteristics for 2-element reflector-driver Yagis at 0.1, 0.125, and 0.15 λ element spacing.

If we shift to driver-director models of parasitic arrays, we do not get the same picture of results. **Table 4-4** lists the element lengths and the basic performance figures for the driver-director configuration. Unlike the reflector-driver dimensions, the driver-director element lengths continuously decrease with increased spacing between elements. (See model ydd.ez and adjust element lengths and spacing as necessary.)

2-Element Driver-Director Performance
Set for Maximum 180° Front-to-Back Ratio and Resonance

Element Spacing λ	Driver Length λ	Director Length λ	Gain dBi	Front-to-Back Ratio dB	Feedpoint Z R +/- jX Ω
0.05	0.2498	0.2378	6.48	26.03	11.0 - j 0.0
0.075	0.2486	0.2335	6.52	23.60	21.1 + j 0.2
0.1	0.2465	0.2298	6.44	14.85	29.7 + j 0.2
0.125	0.2443	0.2263	6.22	10.66	36.6 + j 0.1
0.15	0.2423	0.2234	5.98	7.94	41.2 + j 0.2
0.175	0.2407	0.2202	5.62	5.96	45.9 + j 0.1
0.2	0.2395	0.2170	5.23	4.45	50.0 + j 0.2

Note: All elements 0.5" (0.001207 λ) aluminum

Table 4. 2-element driver-director Yagi performance when set for maximum 180° front-to-back ratio and driver resonance.

The table also confirms the general proposition that a driver-director array develops a significant gain and front-to-back superiority over the reflector-driver array when the spacing is fairly narrow—under 0.1 λ. **Fig. 4-3** tracks the gain and front-to-back ratio values. Above 0.1-λ-element spacing, the front-to-back ratio drops rapidly to the reflector model values and below. The gain values start their drop above 0.75-λ spacing. Since the 21-Ω impedance of the 0.075-λ model is manageable with a matching network, this element spacing region is among the most popular for driver-director arrays.

The flatted curve between 0.05-λ and 0.075-λ element spacing hides a surprise for those not familiar with Jerry Hall's study. The slope of the curve beyond the 0.075-λ mark suggests that in the lowest region of spacing, there is a peak in the front-to-back value. In fact, at a spacing of 0.0625 λ, the front-to-back ratio can reach nearly 47 dB with a free-space gain of 6.52 dBi and a source impedance of about 16.5 + j 7.9 Ω. Such an array also comes closest to meeting the ideal conditions for maximum front-to-back ratio, with a relative magnitude of 0.964 and a phase angle (adjusted) of 158.6° (or -21.4°). For single-frequency use, such an array might well fill a need.

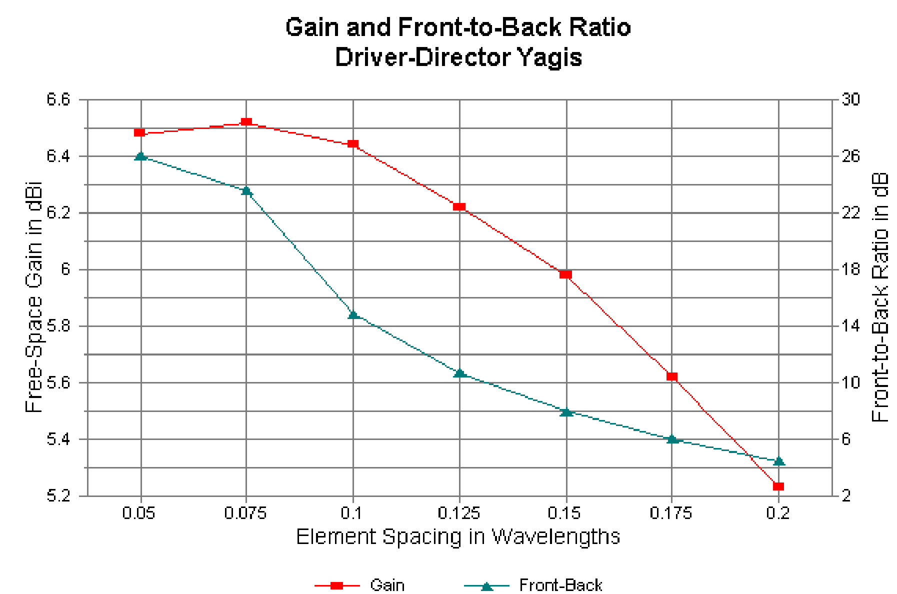

Fig. 4-3

Table 4-5 provides data comparing the modeled relative current magnitude and phase angle for the unfed element. The data has been adjusted to coincide in form with other data that we have examined. The negative phase angles of the director have been made positive, as if the forward element had a value of 0.0°. As well, the current magnitude has been adjusted as if the director had a value of 1.0. This set of adjustments allows the ideal data to correspond with all other dual-source models we have so far examined, where all forward elements are set to a magnitude of 1.0 and a phase angle of 0.0°, and the rear element values are presented for comparison. In concert with the curves of **Fig. 4-3**, **Table 4-5** makes evident the rapid departure from ideal phasing conditions for maximum front-to-back ratio above 0.075-λ element spacing. Equally evident, in comparison with the data for the reflector-driver Yagi, is the relative uselessness of the driver-director array as a directional beam above about 0.1-λ-element spacing.

Actual vs. Ideal Rear Element Relative Current Magnitude and Phase Angle
2-Element Driver-Director Yagis

	Actual		Ideal		
Element Spacing λ	Relative I Mag.	Relative I Phase	Relative I Mag.	Relative I Phase	Gain dBi
0.05	0.934	162.8	0.961	163.1	6.51
0.75	1.006	149.5	0.951	154.1	6.51
0.1	1.140	149.7	0.948	144.9	6.43
0.125	1.333	146.1	0.943	135.5	6.31
0.15	1.555	145.6	0.939	126.1	6.16
0.175	1.845	145.8	0.926	116.7	5.96
0.2	2.188	147.3	0.910	107.3	5.72

Note: all phase angles adjusted for positive values. For negative angle values corresponding to those in Part 1, subtract 180 from the listed value. In addition, actual angles are taken from the director and appear as negative angles relative to the driver to the rear. The relative current magnitude values have been adjusted to reflect the values on the rear element if the forward element is set at 1.0. All "ideal models" set to a 180° front-to-back ratio greater than 60 dB.

Table 5. Actual vs. ideal rear element relative current magnitude and phase angle values for maximum 180° front-to-back ratios for 2-element driver-director Yagis in Table 3.

Despite the radical differences in gain and front-to-back behavior between reflector-driver and driver-director Yagis, the resonant impedances of the two arrays do not differ greatly for any given element spacing. **Fig. 4-4** tracks the source resistance of the two array designs as optimized for each element spacing increments. An interesting property of reflector-driver designs is that the impedance curve is nearly linear, in contrast to the curve for the driver-director array.

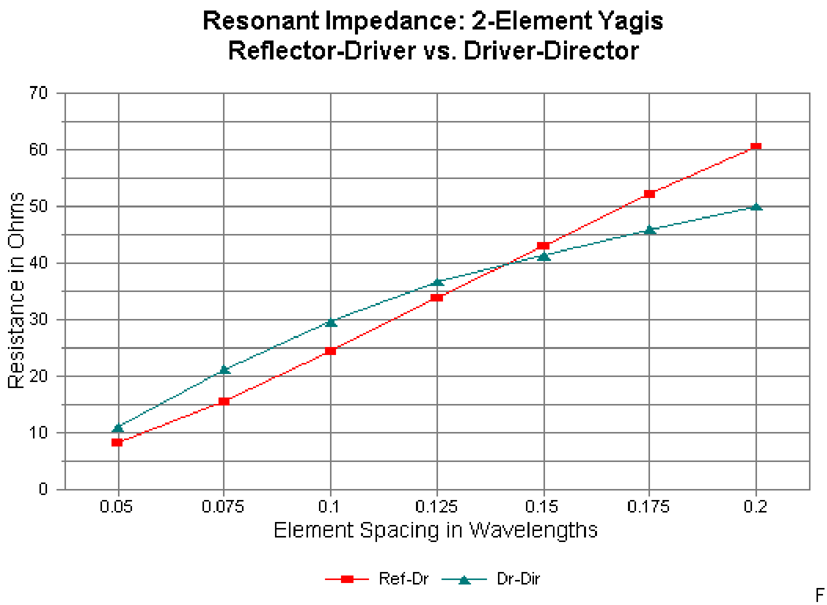

Fig. 4-4

In our exploration of the two types of parasitic arrays, we only passively examined **Table 4-3**. To this data, we may add the corresponding driver-director data in **Table 4-6**. These tables present modeled performance figures for each array at 3 increments of element spacing from 28.0 to 29.0 MHz. For each array, the most common element spacing values are listed: 0.1 through 0.15 λ for the reflector-driver array and 0.75 through 0.125 λ for the driver-director Yagi. As expected, operating bandwidth increases with increased element spacing. The reflector-driver Yagi's SWR curves, shown in **Fig. 4-5**, can be adjusted to cover the entire 1-MHz bandwidth by selecting a design frequency of about 28.35 rather than the 28.5-MHz figure used in this study. At a slightly wider element spacing of 0.15 λ, the 2-element reflector-driver design can be designed to cover the entire 10-meter band. At each level of element spacing, the gain and the front-to-back values tend to show the same sort of curve broadening with each increase in spacing, although the peak values decrease along the way.

Bandwidth Characteristics for 2-Element Driver-Director Yagis
At 0.075, 0.1, and 0.125 λ Element Spacing

Element Spacing: 0.075 λ

Frequency MHz	Gain dBi	Front-to-Back Ratio dB	Feedpoint Z R +/- j X Ω	SWR Relative to 21.1 Ω
28.0	5.59	12.31	33.0 - j 21.6	2.47
28.25	6.03	16.75	27.0 - j 11.6	1.72
28.5	6.52	23.60	21.1 + j 0.2	1.01
28.75	7.00	15.47	15.7 + j 13.9	2.22
29.0	7.30	8.87	11.6 + j 29.2	5.66

Element Spacing: 0.1 λ

Frequency MHz	Gain dBi	Front-to-Back Ratio dB	Feedpoint Z R +/- j X Ω	SWR Relative to 29.7 Ω
28.0	5.64	11.39	39.2 - j 19.5	1.87
28.25	6.03	13.54	34.7 - j 10.3	1.43
28.5	6.44	14.85	29.7 + j 0.2	1.01
28.75	6.84	12.96	24.6 + j 12.4	1.63
29.0	7.15	9.28	20.1 + j 26.4	2.98

Element Spacing: 0.125 λ

Frequency MHz	Gain dBi	Front-to-Back Ratio dB	Feedpoint Z R +/- j X Ω	SWR Relative to 36.6 Ω
28.0	5.55	9.35	43.2 - j 18.7	1.64
28.25	5.87	10.24	40.2 - j 9.8	1.31
28.5	6.22	10.66	36.6 - j 0.1	1.00
28.75	6.56	10.05	32.7 + j 11.1	1.40
29.0	6.84	8.36	28.8 + j 23.7	2.11

Table 6. Bandwidth characteristics for 2-element driver-director Yagis at 0.075, 0.1, and 0.125 λ element spacing.

The SWR curves have been adjusted to use as the reference impedance value the resonant impedance of each test array. The curves presume that for any reasonable driver impedance, a builder may construct a matching network to transform the impedance to a value that is compatible with a selected main feedline. The naturally low impedance values of Yagi antennas provide one of many reasons for the dominance of 50-Ω cable as the main feedline for amateur antennas.

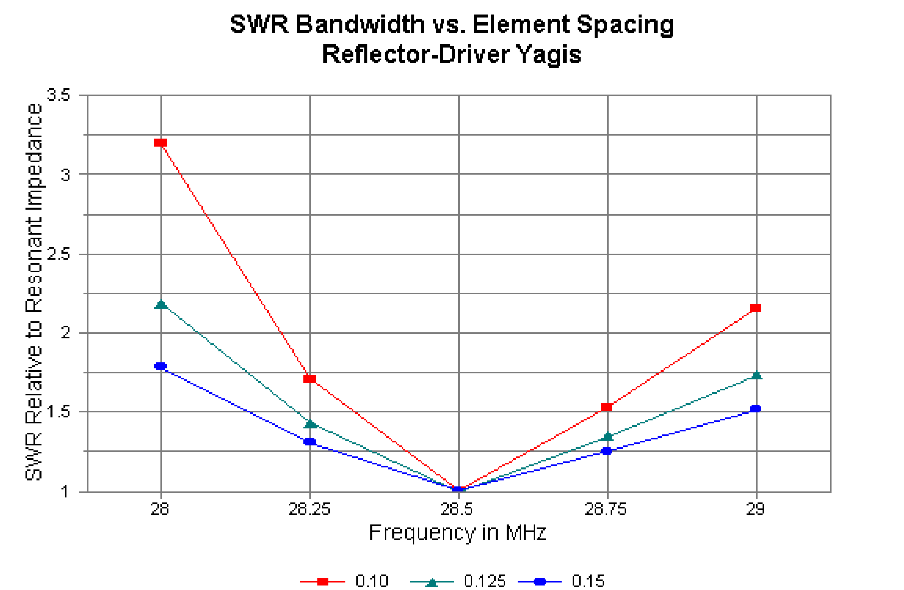

Fig. 4-5

The driver-director Yagi SWR curves, shown in **Fig. 4-6**, are naturally steeper, given the narrower element spacing values involved. The most notable feature of the SWR graph is its reversal from the one for the reflector-driver array: here, more rapid increases occur above the design frequency rather than below it. Likewise, gain increases with rising frequency (rather than with decreasing frequency in the case of the reflector-driver array). The source impedance of the driver-director array shows an increasing reactance with frequency in accord with the relative shortening of the element. However, the resistive component of the impedance decreases with rising frequency (in contrast to the resistance curve of the reflector-driver Yagi). At the spacing increments generally used in driver-director designs, narrow bandwidth is a condition of maximizing performance.

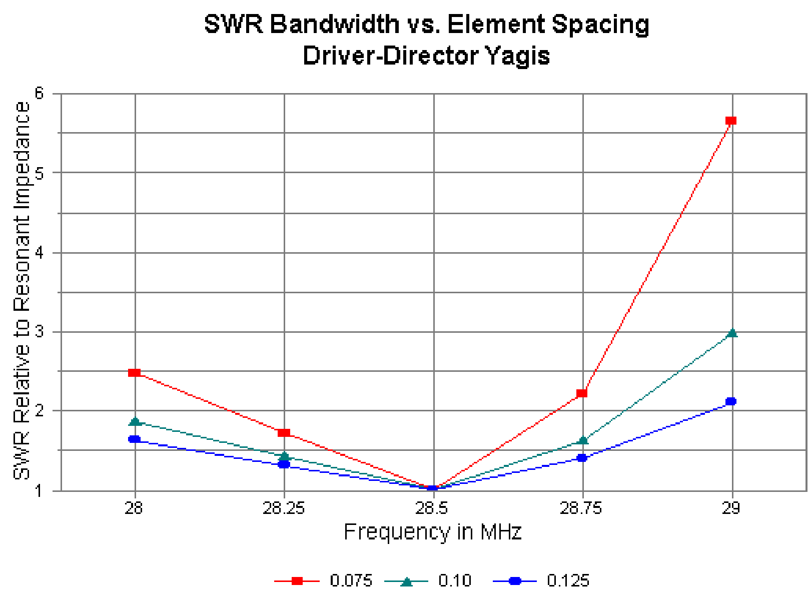

Fig. 4-6

Understanding basic 2-element Yagi-Uda performance limitations is a necessary condition of understanding the urge to design phased arrays in which both elements are fed. In principle, the dual source phased array is capable of higher gain and better front-to-back performance than all but the most closely spaced parasitic arrays. The reason is simple: the wider the spacing of a parasitic array, the further the elements get from relatively ideal conditions of element current magnitude and phase angle.

Alternative Geometries

We have omitted many details of 2-element Yagi behavior relative to the more complete data in some areas on interest that appear in Jerry Hall's study. However, we would be remiss if we did not acknowledge design efforts to overcome some of the phasing failings of 2-element parasitic arrays using linear parallel elements. Let's look in detail at only one of those efforts to use an alternative geometry: the Moxon rectangle. **Fig. 4-7** shows the basic outline of this antenna whose origin is largely due to the initial efforts of G6XN.

The Moxon rectangle owes its operating characteristics to not one, but two forms of inter-element coupling. Between the parallel portions of the elements, we encounter the same sort of mutual coupling that is almost the sole source of coupling within a standard Yagi design. However, by bending the elements toward each other, we obtain an added form of coupling, often called capacitive coupling between the element ends. The result is a broader beamwidth and an increase in the front-to-back ratio. By judicious control of the element diameter, the gap between element tails, and the other dimensions of the array, we may obtain a broadband reflector-driver array. (See model mox.ez.)

Fig. 4-7

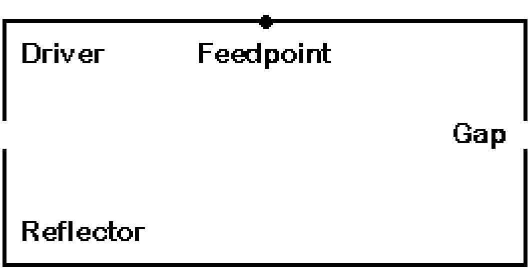

Array with Parallel and End Coupling
The Moxon Rectangle

Fig. 4-8 shows the free-space gain and front-to-back curves for a typical Moxon rectangle designed for 28.35 MHz, using 0.5" aluminum elements. The design frequency is necessary, since reflector-driver arrays decrease their front-to-back ratio and increase their SWR more slowly above the design frequency than below it. The resulting array covers the first MHz of 10 meters. The gain decreases nearly linearly across the passband, while the front-to-back ratio peaks just below the 28.4-MHz mark on the graph. **Fig. 4-9** shows the 50-Ohm SWR curve for the design.

Since Moxon rectangle designs using a variety of element materials and design frequencies are now common in antenna literature, we may turn our attention to **Table 4-7**. This table summarizes the performance data shown in the graph. In addition, it provides values for the rear element relative current magnitude and phase angle.

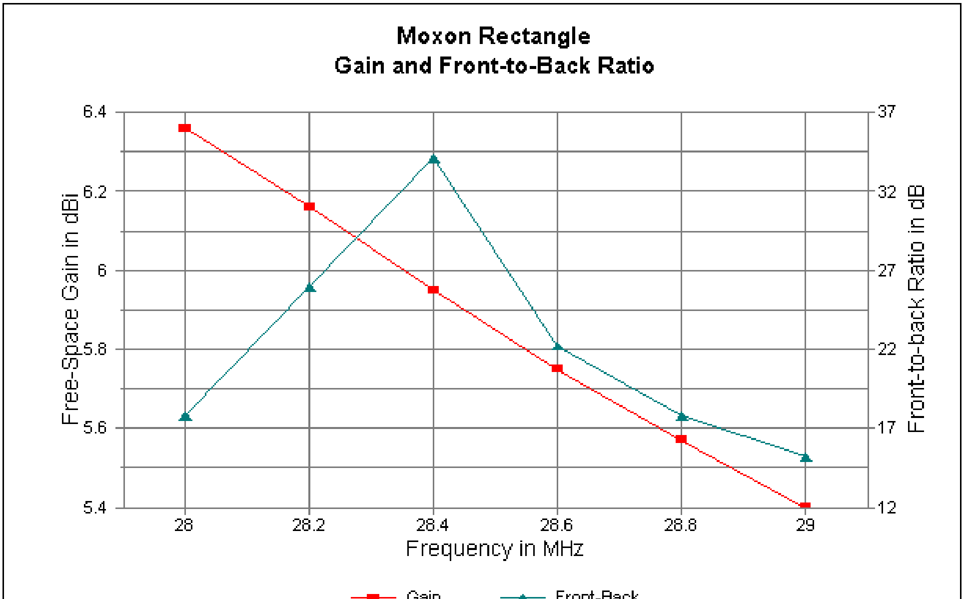

Fig. 4-8

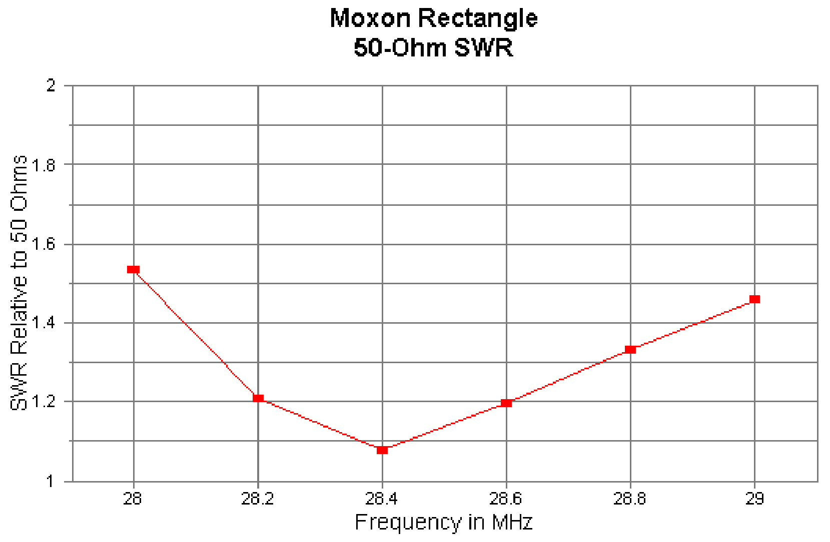

Fig. 4-9

Bandwidth Characteristics for 2-Element Moxon Rectangle

Frequency MHz	Gain dBi	Front-Back Ratio dB	Feedpoint Z R +/- j X Ω	50-Ω SWR	Refl. I Mag.	Refl. I Phase
28.0	6.36	17.79	39.2 - j 15.7	1.53	0.980	140.1
28.2	6.16	25.95	46.3 - j 8.3	1.21	0.967	134.1
28.4	5.95	34.12	53.2 - j 2.2	1.08	0.943	128.0
28.6	5.75	22.21	59.3 + j 2.9	1.20	0.911	122.5
28.8	5.57	17.81	64.6 + j 7.3	1.33	0.874	117.6
29.0	5.40	15.20	69.2 + j 11.4	1.46	0.835	113.2

Note: Aluminum element diameter: 0.5" (0.001207 λ)

Table 7. Bandwidth characteristics for 2-element Moxon rectangle, with modeled rear element relative current magnitudes and phase angles.

At the design frequency, the parallel portions of the elements are about 0.133 λ apart. At that spacing, an ideal phase angle would be about 132.5° (or -47.5°). The rear element relative current magnitude would be close to 0.94. Compare these values to the ones in the table for 28.2 (0.967 and 134.1°) and 28.4 MHz (0.943 and 128.0°). Little wonder that the Moxon rectangle achieves a maximum front-to-back ratio of well over 30 dB at its design frequency.

The cost for this improved front-to-back figure is a decrease in gain, partly resulting from the increased beamwidth relative to a standard Yagi design. Since the bent portions of the elements still have significant current levels near the array corners, their contribution to gain becomes instead a contribution to beamwidth. Hence, the Moxon rectangle has an average free-space gain of about 6.0 dBi, somewhat below the levels of the optimized Yagis and of the idealized phased arrays that we examined in Chapter 3.

The Moxon rectangle is not the only attempt to alter geometry to improve performance over parallel-element Yagis. **Fig. 10** shows some of the other arrangements tried with greater or lesser success. The VK2ABQ square was a forerunner of the Moxon rectangle. The diamond lends itself to inexpensive construction with a single non-conductive support for wire element ends. The hex and folded-X have been popular from time to time as near-ultimate compact full size designs. An interesting study, but beyond the scope of these notes, would be to investigate the relative current magnitude and phase on the unfed element in each design, noting that the most common implementation of the folded X-beam is as a driver-director array. The others are all reflector-driver arrays.

In addition to alternative configurations for 2-element paretic arrays, the years have seems innumerable attempts to shrink the 2-element beam down to much more compact dimensions. The side-to-side dimension of a 2-element driver-reflector Yagi is about 0.5-λ, but the front-to-rear or boom dimension is only between 0.1-λ and 0.15-λ. The roughly 4:1 dimensional ratio has led numerous amateurs (and commercial antenna makers as well) to try various means of shortening elements. Although one may also equip shortened elements with end “hats,” the chief method has been to inductively load each element. One may place inductive loads either at the element center or somewhere further out along the element lengths on each side of the center point. The inductive loads may take the form of solenoid coils or of shorted transmission-line stubs. We call the latter linear loads.

Fig. 4-10

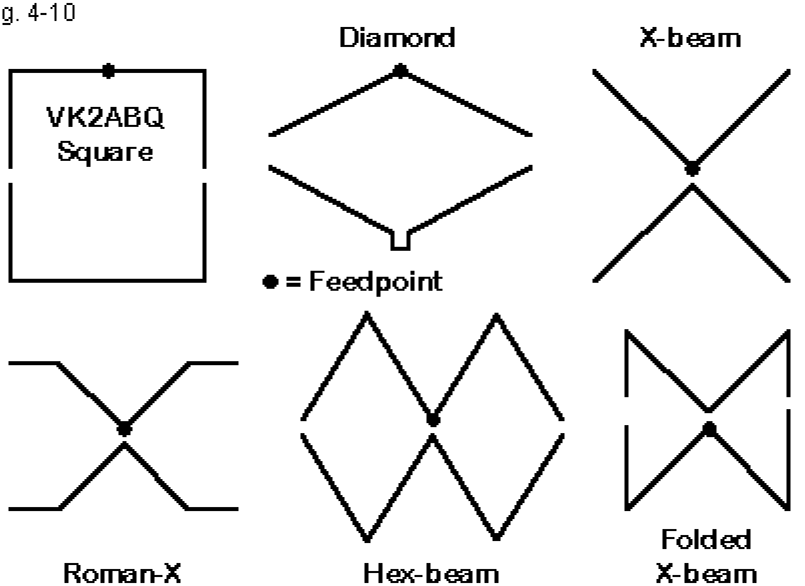

Some Alternative 2-Element Geometries

Volume 2 of this set devotes its pages to a much more extended look at parasitic 2-element beams. Besides expanding the basic coverage of the fundamental parasitic properties that we have surveyed in this chapter, the study will devote considerable space to examining the various ways of shrinking the beam—and to the consequences of the shrinking process.

Conclusions

Our goal has been to track the performance potential of parasitic arrays with only a single fed element with an eye toward understanding the limitations of using geometry alone to set the relative current magnitude and phase angle conditions between the elements. Both reflector-driver and driver-director Yagis show very serious limitations in this regard, except for very closely spaced driver-director models that are impractical for most (but not all) amateur applications. Alternative geometries, such as the Moxon rectangle, are able to overcome the problem of achieving high front-to-back ratio values by using multiple element coupling methods. However, they cannot achieve the higher gain levels (by about 0.5 dB or so) attained in principle by some ideal and compromise phased array designs.

The key to 2-element Yagi design shortcomings is also the key to 2-element horizontal phased array success. Can we find a practical way to implement a 2-element phased array with both elements fed to arrive at desired gain, front-to-back ratio, and bandwidth values? In the next chapter, we shall begin our exploration by reviewing the ZL-Special and its variants, all of which make use of what seems in principle to be the simplest phasing mechanism possible: a single phasing line that connects the two elements. More complex systems, such as the HB9CV and the N7CL systems do exist, but basic principles of phasing are often best explored by keeping the number of design variables to a minimum. The more complex systems will have their turn in a later chapter.

5. The Limits of a Single Phase Line: The ZL-Special

When George Pritchard (ZL3MH, later ZL2OQ) introduced the amateur community to the 2-element phased array, it seemed to offer magic in the form of performance up to 7 dBd (9+ dBi free-space equivalent) and up to a 40 dB front-to-back ratio. Unfortunately, the comparators of the day were relatively primitive 2- and 3-element Yagis that rarely performed up to their theoretical potentials. Nonetheless, the antenna type acquired the name "ZL-Special" and has been the subject of performance debate ever since. For a reasonably complete bibliography of ZL-Special articles in English, see the end of the next chapter.

Fig. 5-1 shows several of the variations on the ZL-Special theme. Some of them work; others do not—or at least not very well. Virtually all early work on horizontal phased arrays presumed that we needed only attend to the impedance transformation along a transmission line. Hence, with 1/8-λ spacing and a similar transmission line, a half twist would yield a 135° phase-shift with the accompanying high gain forward lobe and a deep rear null. **Fig. 5-1** shows both linear and folded elements, along with the most popular phaseline characteristic impedances. The trombone attempted to overcome the velocity factor of the common TV twinlead line (about 0.8) by making wide-spaced folded elements that were physically 1/8-λ at their outer edges but electrically 1/8-λ apart relative to the phaseline on the inner side. Although the trombone works quite well, the structure is completely unnecessary: simple folded dipoles would work as well.

Not until Roy Lewallen, W7EL, pointed out the fundamental error in amateur conceptions of the ZL-Special did we begin to re-analyze the 2-element horizontal phased array with some precision. (See Lewallen, "Try the 'FD Special' Antenna," *QST* (June, 1984), 21-24.) What controls the performance of the ZL-Special phase line is not so much the impedance transformation, but the current transformation (in terms of both current magnitude and phase angle). The current and the impedance do not change at the same rate except when the line is exactly matched to the element that forms its load. Hence, we had to take a wholly new approach to the single-line phased array. In these notes, we shall follow this lead.

Fig. 5-1

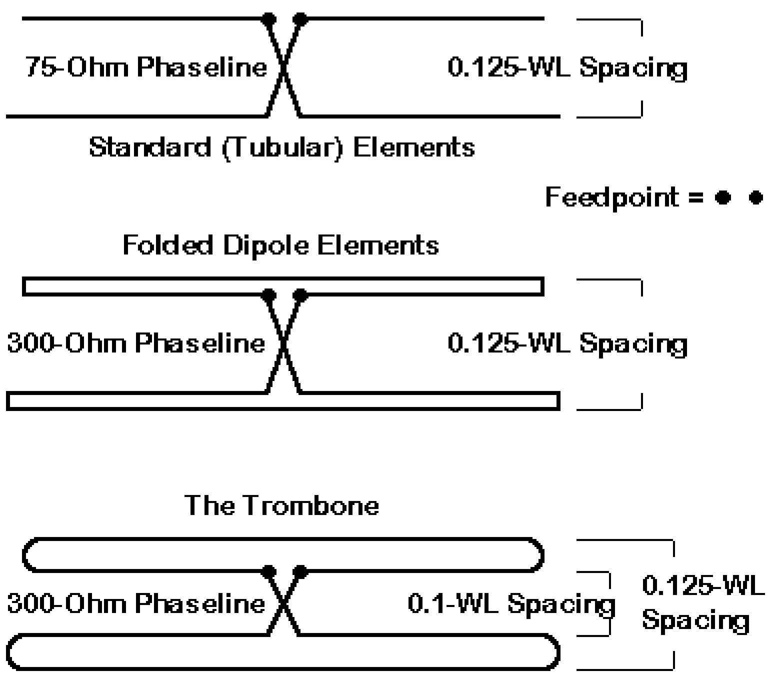

Early ZL-Special Designs

ZL-Special Basics

Fig. 5-2 shows the deceptively simple elements of a ZL-Special. The two elements bear "forward" and "rear" element labels, where the forward element indicates two things. First, the main forward lobe is in the direction of the forward element. Second, the standard ZL-Special feedpoint is at the junction of the phaseline and the forward element.

Fig. 5-2

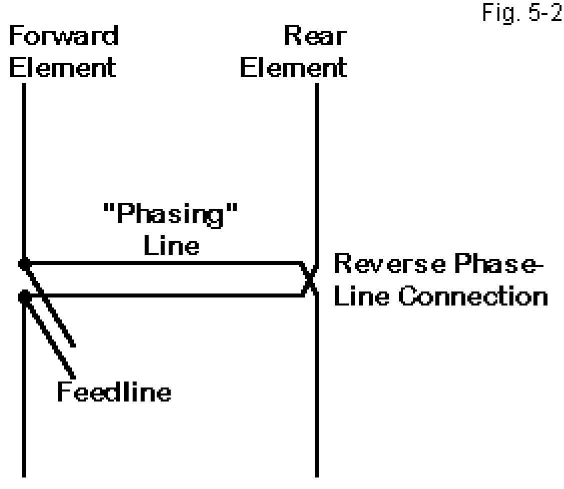

Basic Elements of a ZL-Special

Most radio amateurs do not fully appreciate how many variables are at work in this seemingly simple arrangement. First, the individual elements exhibit center-point impedances that are functions of the mutual coupling between them. The mutual coupling depends upon the element diameters, lengths, and spacing between them. Second, the feedline meets a parallel current division at the forward junction, which requires that all other variables result in the same voltage at the junction. The requisite voltage is a function of the source impedance of the forward element and the "share" of current received by that element.

Third, the rear element impedance at its center sets both a current magnitude and phase angle and a voltage magnitude and phase angle, both of which undergo transformation down the selected length of phase line. From Terman, *Radio Engineers' Handbook* (McGraw-Hill: 1943), p. 185, we have equations for the current and the voltage at any point down a transmission line from a load or antenna element. The following equations are for lossless lines, which are satisfactory for the short phasing lines used in 2-element horizontal phased arrays and which also coincide with the calculations within the TL facility of NEC-2 and NEC-4:

$$I_s = I_r \cos\left(2\pi \frac{l}{\lambda}\right) + j\,\frac{E_r}{Z_o}\sin\left(2\pi\frac{l}{\lambda}\right)$$

$$E_s = E_r \cos\left(2\pi \frac{l}{\lambda}\right) + j\,I_r\,Z_o\sin\left(2\pi\frac{l}{\lambda}\right)$$

The meaning of the terms is as follows:

E_r is the voltage at the load or antenna end of the line,
E_s is the voltage at the source end of the line,
I_r is the current at the load or antenna end of the line,
I_s is the current at the source end of the line,
Z_o is the characteristic impedance of the line, and
$(2\pi\ (l/\lambda))$ is an expression for the electrical length of the line in degrees for the frequency of interest.

Because both the voltage and the current have an associated phase angle and resolve into real and imaginary components, the use of these equations in calculations is more complex that their initial appearance may suggest. See the next chapter, which replicates some of the math in "Modeling and Understanding Small Beams: Part 5: The ZL Special," *Communications Quarterly*, (Winter, 1997), 72-90. The calculations are also available within NEC in the TL facility and in the HAMCALC suite of GW Basic utility programs from VE3ERP.

Critical to our understanding of phaseline operation is the fact that the resultant values of voltage and current (magnitude and phase) at the forward end of the phase line are interactive, as the basic equations make evident. Achieving a current level that balances with the portion of source current used by the forward element at a common voltage such that the rear element then has a current magnitude and phase angle to yield a desirable pattern requires juggling all of the variables into a usable collection.

Even if we arrive at a usable collection of values, we have several other variables to consider. First, the calculated characteristic impedance of the phase line must be one that we can acquire or build. Second, the requisite physical length of the phase line (accounting for the line's velocity factor) for the current transformation must be at least the space between the elements. As well, it should not be too much longer than that spacing in light of practical considerations for supporting the line. Since the line will be open—whether we use coax or parallel line for the task—we must isolate it from disturbances that a metallic boom might create. Designing a ZL-Special, then, requires either careful analysis or some very lucky guesses.

A Design Example

Let's analyze a single design for 28.5 MHz to see if we can make the picture clearer. We shall begin with 2 elements. Both will be our standard 0.5" (0.001207-λ) aluminum elements. The forward element will be 0.465-λ long, while the rear element is 0.506-λ long. The spacing will be 0.125-λ. However, from Part 1 of this series, we should now understand that the selected spacing is somewhat arbitrary, since for any element spacing, we may find element lengths that result in a desired phased array pattern.

Fig. 5-3 shows the 4 steps in our analysis, and the results appear in **Table 5-1**. If we arrange the elements individually in a NEC model and feed them independently with current sources, then the feed values in the table's step 1 under the relative current columns will result in the relative voltage and the individual element impedances. The models follow the system used in Chapter 3 of reversing the direction of the rear element relative to the forward element so that any phase line that we add can be in normal orientation. Notable is the similarity of the element impedances, a useful condition (but not the only such condition) for successful ZL-Special design. The tables in Chapter 3 show in a general way what conditions must exist for us to achieve such similar impedances: the relative longer length of the rear element when both elements are longer than a self-resonant dipole at the frequency of interest is a promising combination at the 1/8-λ spacing. (See models ph3-1.ez through ph3-4.ez.)

Fig. 5-3

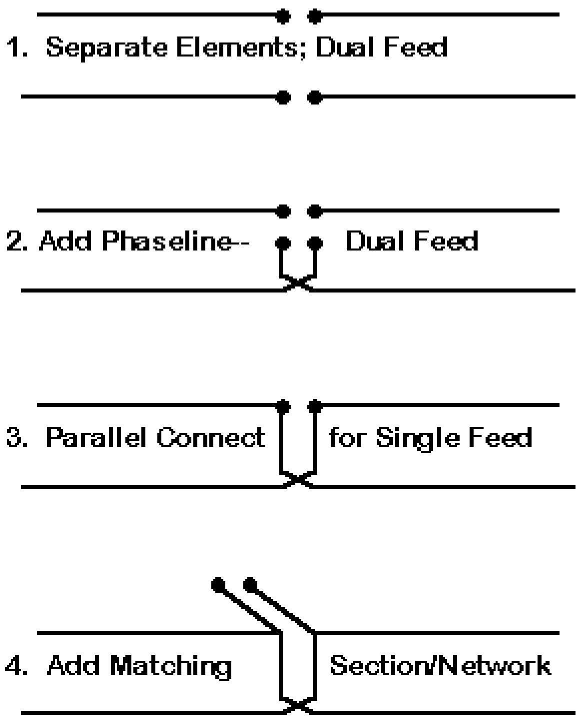

Design Steps for a ZL-Special

As **Fig. 5-4** shows, we have not striven for the highest gain or front-to-back value, but simply for highly usable values.

Sample ZL-Special Analysis Data

The following data come from NEC-2/NEC-4 models of a 2-element horizontal phased array for 28.5 MHz using 0.5" aluminum elements. The rear element is 0.506 λ long, while the forward element is 0.465 λ long. The modeling environment is free space. In all cases, the free-space gain is 6.34 dBi, and the 180° front-to-back ratio is 30.15 dB.

Step 1. Independent elements, independent sources:

Element	Rel. I magnitude	Rel. I phase angle	Rel. V magnitude	Rel. V phase angle	Impedance R +/- J X Ω
Rear	0.8935	-44.18°	26.24	-23.58°	27.49 + j 10.34
Forward	1.0	0.0°	33.53	31.94°	28.46 + j 17.76

Step 2. Independent elements, independent sources, phase line installed:

Element	Rel. I Magnitude	Rel. I phase angle	Rel. V Magnitude	Rel. V phase angle	Impedance R +/- J X Ω
Rear	0.8935	-44.15°	---	---	27.49 + j 10.34
Phaseline	0.664	44.25	33.56	32.02°	49.74 - j 8.98
Forward	1.0	0.0°	33.51	31.96°	28.43 + j 17.73

Step 3. Phase line connected to forward element, single source

Element	Rel. I Magnitude	Rel. I phase angle	Rel. V Magnitude	Rel. V phase angle	Impedance R +/- J X Ω
Rear	0.5734	-60.80°	---	---	
Forward	0.6418	-16.62°	---	---	
Feedpoint	1.0	0.0°	21.53	15.34°	20.76 + j 5.70

Step 4. Matching section added:

Element	Rel. I Magnitude	Rel. I phase angle	Rel. V Magnitude	Rel. V phase angle	Impedance R +/- J X Ω
Rear	0.9774	-133.7°	---	---	
Forward	1.0939	-89.48°	---	---	
Feedpoint	1.0	0.0°	60.67	6.14°	60.32 + j 6.49

Table 1. Sample ZL-Special analysis data from NEC models in the 4 steps of antenna analysis demonstrated in the text.

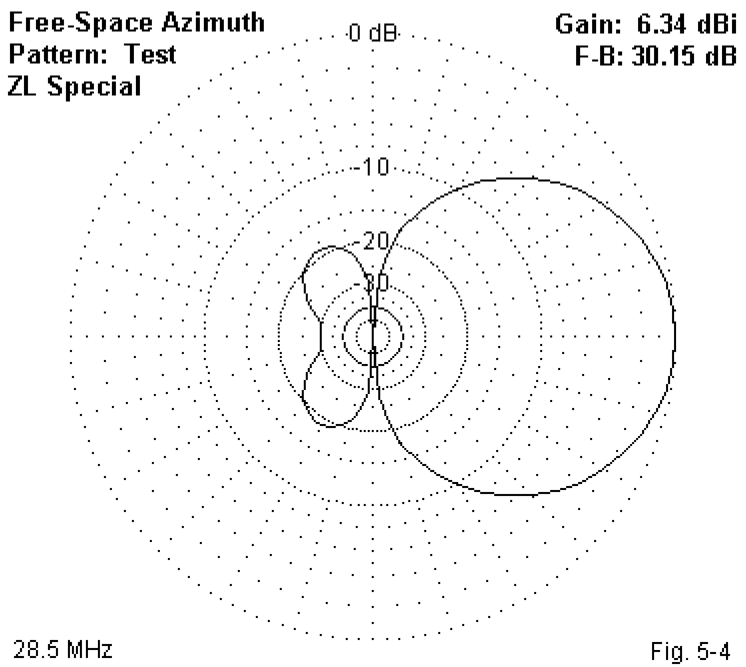

Fig. 5-4

The second step in our analysis creates a model with a transmission line attached to the rear element, but with its forward end brought to a source wire that is independent of the forward element. The selected line—from calculations, is RG-83, 35-Ω coax with a velocity factor of 0.66. The required length is 0.13-λ physically or 0.197-λ electrically. This length of the chosen line yields the correct relative rear element current magnitude and phase angle. At the same time, it yields the required forward-end voltage magnitude and phase angle to match the value for the forward element. Note that the required forward line-end current is 0.664 (relative to a forward element value of 1.0) with a phase angle of 44.25°.

Step 3 in the analysis requires that we connect the forward end of the phase line and the forward element center to create a single feedpoint for the array.

Under these conditions, supplying the feedpoint with a current of 1.0 at 0.0° phase angle, we obtain the relative element current levels and phase angles shown. The forward element phase angle is a function of the reactance at its center. Nevertheless, the net phase angle difference between the two elements is still -44.18°. At this stage, we have a complete array that we can frequency sweep from 28.0 to 29.0 MHz. **Fig. 5-5** shows the results. The gain shows a nearly linear curve upward, with a total change of about 0.9 dB. The front-to-back ratio remains above 20 dB from the lower band edge to above 28.8 MHz and is at all points superior to the front-to-back ratio of a common reflector-driver Yagi by 5 dB minimum. However, as **Table 5-1** shows, the source impedance is just above 20 Ω.

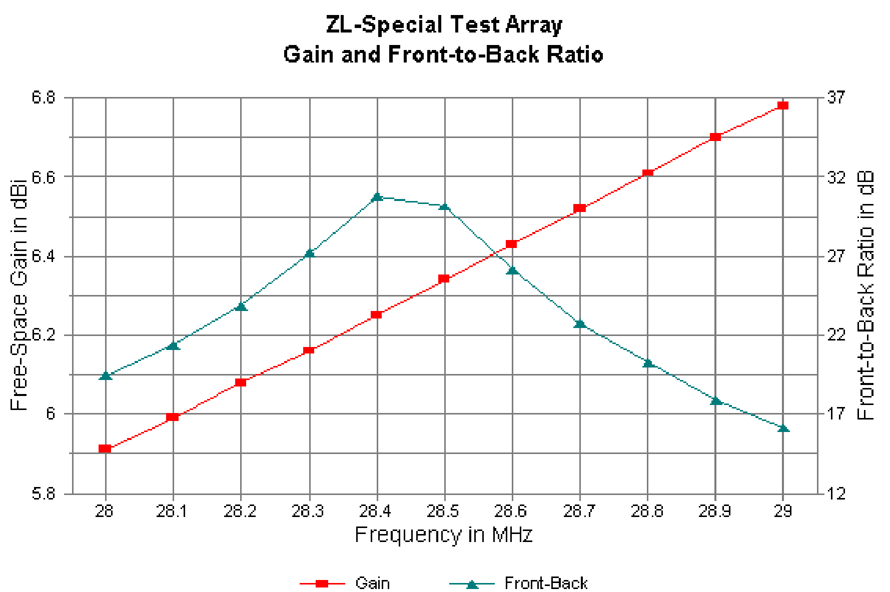

Fig. 5-5

The final step in our design is to add a matching system to raise the impedance to something compatible with common 50-Ω coaxial cable. The low source impedance reactance suggests a matching section. A 0.13-λ section of the same 35-Ω cable (RG-83) used for the phase line functions as a near-1/4-λ section to achieve the goal. With this section in place, we achieve the 50-Ω SWR curve shown in **Fig. 5-6**. One might select other lengths for the matching line to better center the SWR curve, but the values shown would be in most cases quite satisfactory.

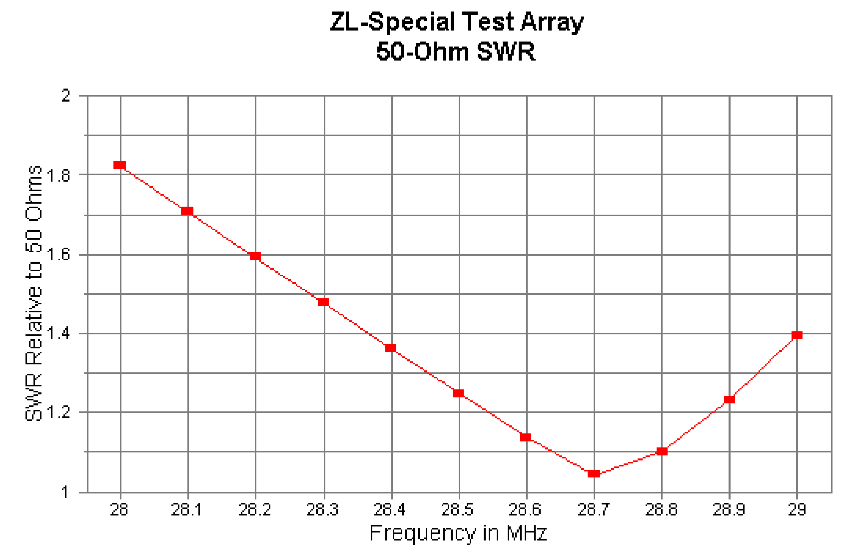

Fig. 5-6

For reference, **Fig. 5-7** shows the array patterns at 28.1 and 28.9 MHz to confirm that the patterns are usable and to show the evolution of the rear lobes as we increase frequency.

The design explored here has attempted to show the required alignment of the many variables involved in ZL-Special design. It is not the only design that will work, but it shares many characteristics with successful ZL-Specials. Most significant is the required low characteristic impedance of the phase line, calling for a coaxial cable. Such lines are vulnerable to external disruption from near-metallic contact, so a non-conductive boom is desirable without resorting to complex phaseline support construction.

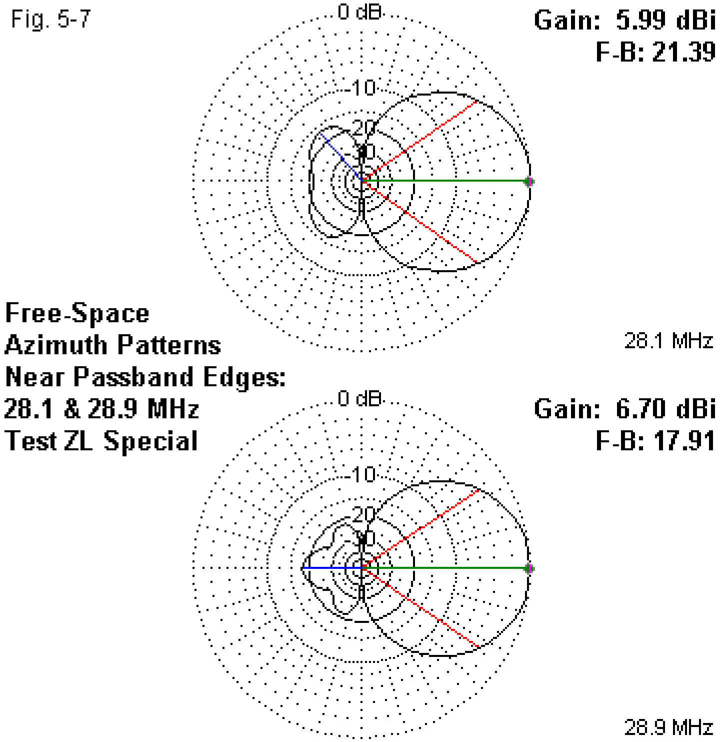

Folded-Dipole ZL-Specials

The use of folded dipoles as ZL-Special elements arose to overcome two problems: cost and the need for low-impedance phasing lines. Early versions of such designs taped the elements to bamboo horizontal supports. In general, most of these designs simply set two TV-twinlead elements 1/8-λ apart with a section of TV twinlead as the phasing line. Element lengths were a matter of trial and error experimentation.

W7EL's "Field-Day Special" rests on a different approach—an attempt to calculate the consequences of mutual impedance on the elements, with the selection of element length, spacing, and line length designed to achieve the required current magnitude and phase angle transformation. **Fig. 5-8** shows the outline of a 10-meter version of the antenna that I have built. The element lengths indicated are for modeled versions that use #18 wire at a 1" spacing (about 450 Ω impedance as a transmission line) and that use #20 wire spaced 0.375" (about 300 Ω as a transmission line). The longer length for the thinner wire that is spaced more closely is natural. The following notes are based on the 1"-spaced model. In both cases, using vinyl-covered wire shortens the physical element by 1-2% to account for the velocity factor of the insulation in antenna use. (See models ph3-5.ez.)

Fig. 5-8

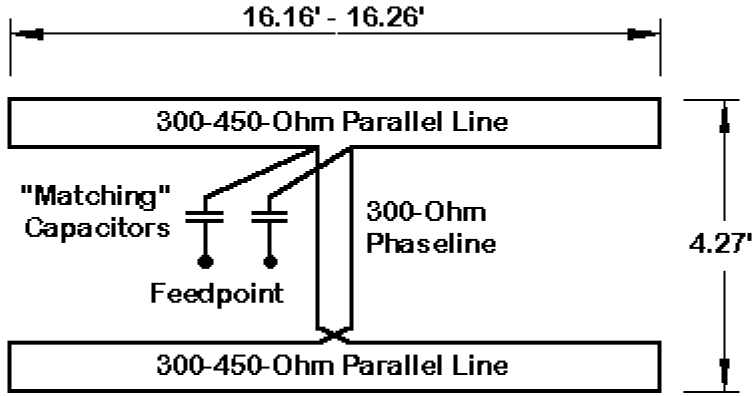

W7EL Field-Day Special: 28.5-MHz Version

Fig. 5-9

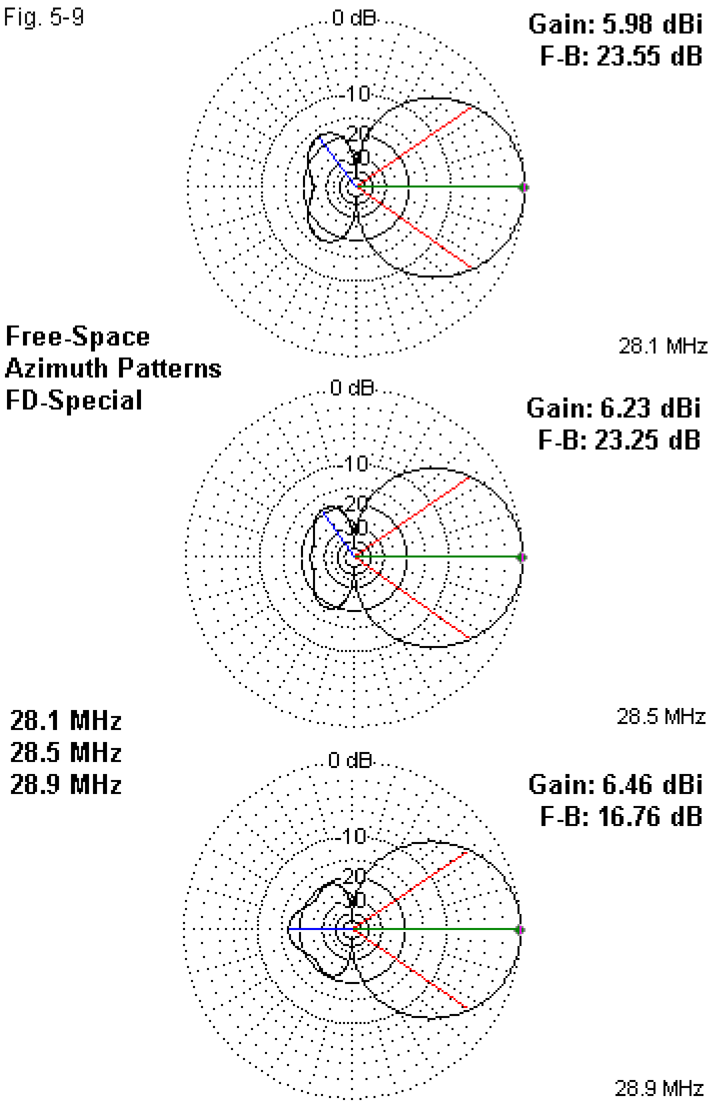
0 dB
-10
-20
-30
Gain: 5.98 dBi
F-B: 23.55 dB
28.1 MHz
Free-Space
Azimuth Patterns
FD-Special
0 dB
-10
-20
-30
Gain: 6.23 dBi
F-B: 23.25 dB
28.5 MHz
28.1 MHz
28.5 MHz
28.9 MHz
0 dB
-10
-20
-30
Gain: 6.46 dBi
F-B: 16.76 dB
28.9 MHz

Although the element spacing is 4.27' (0.1237-λ), the phase line is 4.9' (0.1420-λ) long, despite the 0.8 velocity factor of high-quality twinlead. Indeed, calculations suggest that a higher front-to-back ratio results from the use of 340-Ω line. However, as **Fig. 5-9** shows in the free-space azimuth patterns across the first MHz of 10 meters, performance with a 300-Ω line achieves similar levels to the first design that we explored. As well, with a 300-Ω line, slightly better performance is possible by lengthening the forward element slightly, although the difference is unlikely to be noted in practical operation.

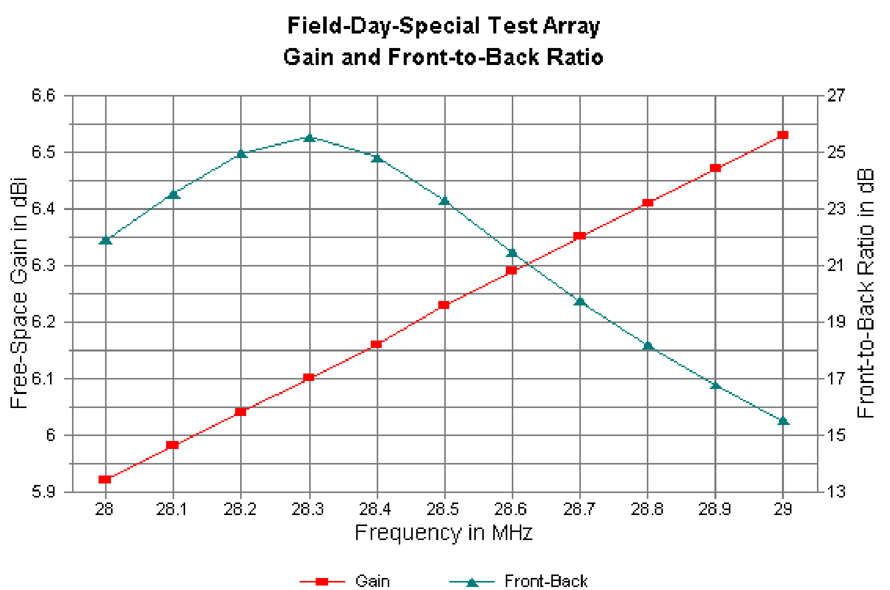

Fig. 5-10

Fig. 5-10 shows the gain and 180° front-to-back curves for the model across the 28.0 to 29.0 MHz span. Typical of ZL-Special designs of any sort, the gain rises almost linearly, while the front-to-back ratio shows a broad peak centered a bit below the center of the design passband. **Fig. 5-11** provides figures on the resistance and reactance within the design passband. The resistance range is only about 7.5 Ω. The reactance changes by a total of 56 Ω. As **Fig. 5-8** indicated, a pair of series capacitors, each with a reactance of -j110 Ω (about 50 pf at 28.5 MHz) would provide a very reasonable SWR curve across the passband.

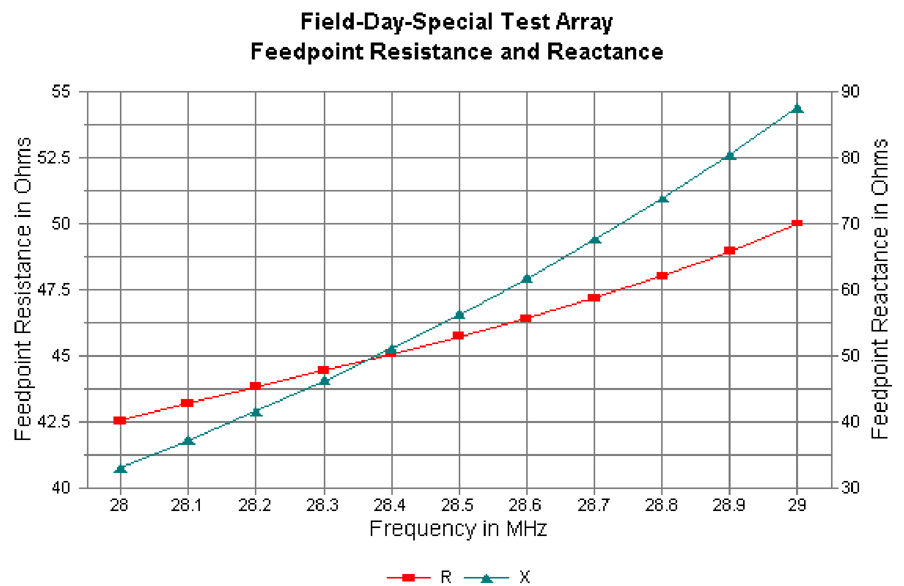

Fig. 5-11

The need for a compact portable antenna inspired the original design of the Field-Day Special. However, for our purposes, it serves additional functions. One is to illustrate that equal-length elements (each about 0.468-λ long) result in wide-band performance that is not significantly different from the use of unequal length elements in the first example. A second function is to show that folded dipole elements have no advantage or disadvantage relative to single elements in performance—although there may be differences in the physical convenience of one or another element type. Third, the elements have widely divergent impedances: forward 124 + j 84 Ω, rear 80 - j 256 Ω. Nevertheless, the right length of the right impedance phase line effects the correct current division at the feedpoint junction so that we arrive at the correct current magnitude and phase angle on the rear element to achieve proper or acceptable phased performance.

A Dual-Line ZL-Special

Before we leave the ZL-Special, let's examine a further variation on the general theme of phasing with a single transmission line section between the element. There is no rule that says that one must feed the system precisely at the junction with the forward element, even if tradition has imbedded this view in our minds. **Fig. 5-12** shows the general outline of a variant of our first ZL-Special study model. (See model ph3-6.ez.)

Fig. 5-12

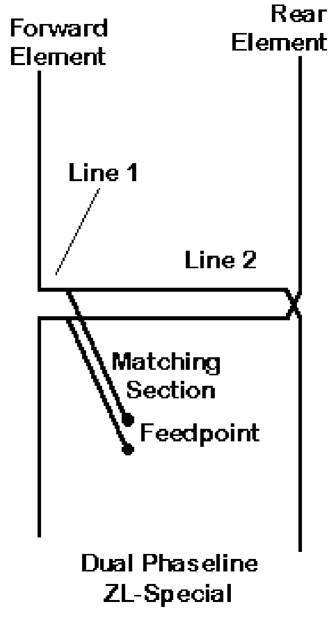

The design uses the same element lengths as our initial model. The forward element is 0.465-λ long and the rear element is 0.506 λ long. Both are 0.5" (0.001207-λ) diameter aluminum. The original design used a single phaseline length of 0.13-λ of 35-Ω, 0.66 velocity factor line. Suppose that one cannot obtain the required RG-83, but has some RG-8X with a 50-Ω impedance and a velocity factor of 0.78. The higher-impedance line at any length will not achieve in a single line the desired phasing for reasonable ZL-Special performance.

However, we may effect transformations of current magnitude and phase angle on both the forward and the rear elements by bringing lengths of transmission line from each element to a middle point. The length of line from the rear element is 0.13-λ. Although this length is physically similar to our original design, electrically, it is only 0.167-λ electrically, since the velocity factor of our new line is higher. A 0.015-λ line from the forward element is 0.192-λ electrically or about 0.52'. At the junction, given a source current of 1.0 at 0.0°, we arrive at a relative current split of these dimensions: forward 0.950 at 4.35° and rearward 0.458 at -2.1°. The resulting current ratio of rear to forward elements is 0.811 at -44.8°, close to the values for the original design.

The design shown here is similar in principle to the one used to improve front-to-back performance of a 10-meter hilltopper 2-element Yagi. (See "Two Hilltoppers for 10 Meters," *The ARRL Antenna Compendium*, Vol. 6, pp. 1-9.) Like the single-line ZL-Special, the antenna requires a non-conductive boom to ensure that the phase-line remains clear of unwanted interactions. The design is amenable to many variations in building materials. However, as we noted in Chapter 3, element diameter does play a significant role in the overall performance of a 2-element phased array. Therefore, one should carefully model a proposed variant in order to adjust the phaseline lengths, even if the modified design only requires small changes.

Fig. 5-13 shows the azimuth patterns across the 28-29 MHz span of the design passband. The differences in performance between the dual-line array and the original test array with a 35-Ω phaseline would not be noticeable in operation.

Fig. 5-13

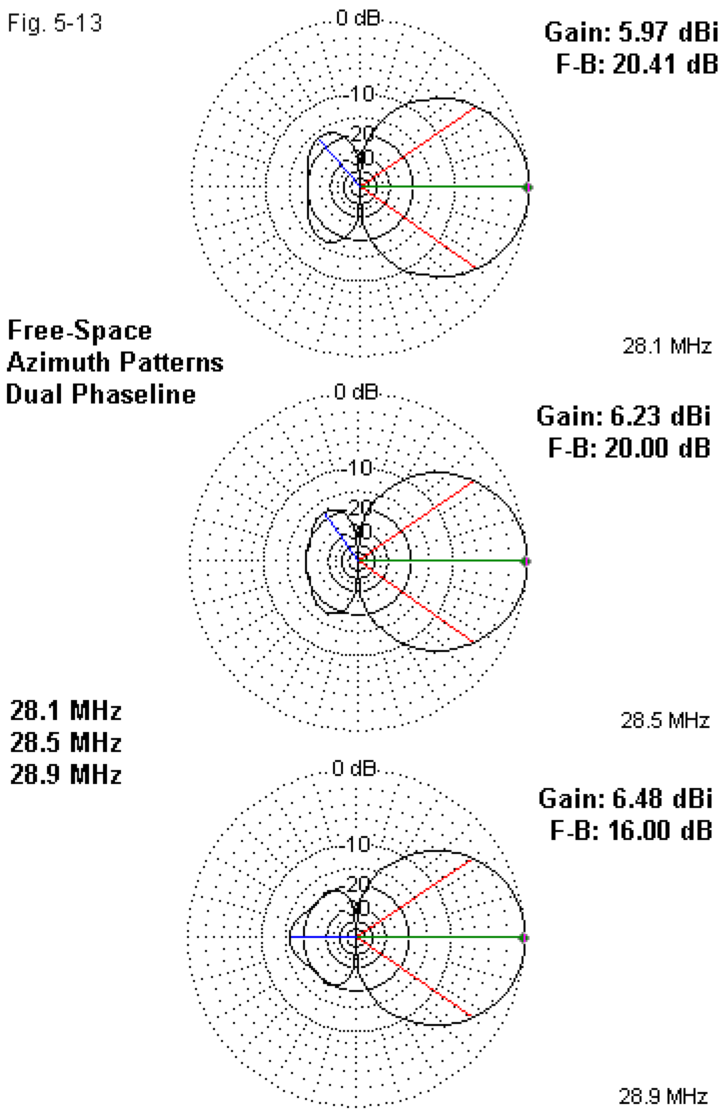
0 dB
-10
-20
-30
Gain: 5.97 dBi
F-B: 20.41 dB
28.1 MHz
Free-Space
Azimuth Patterns
Dual Phaseline
0 dB
-10
-20
-30
Gain: 6.23 dBi
F-B: 20.00 dB
28.5 MHz
28.1 MHz
28.5 MHz
28.9 MHz
0 dB
-10
-20
-30
Gain: 6.48 dBi
F-B: 16.00 dB
28.9 MHz

Only the front-to-back ratio suffers a bit relative to the more ideally phased original example, as shown in the gain and front-to-back curves in **Fig. 5-14**. A bit of element length adjustment might well have improved the numbers a bit, but that maneuver would have altered the demonstration.

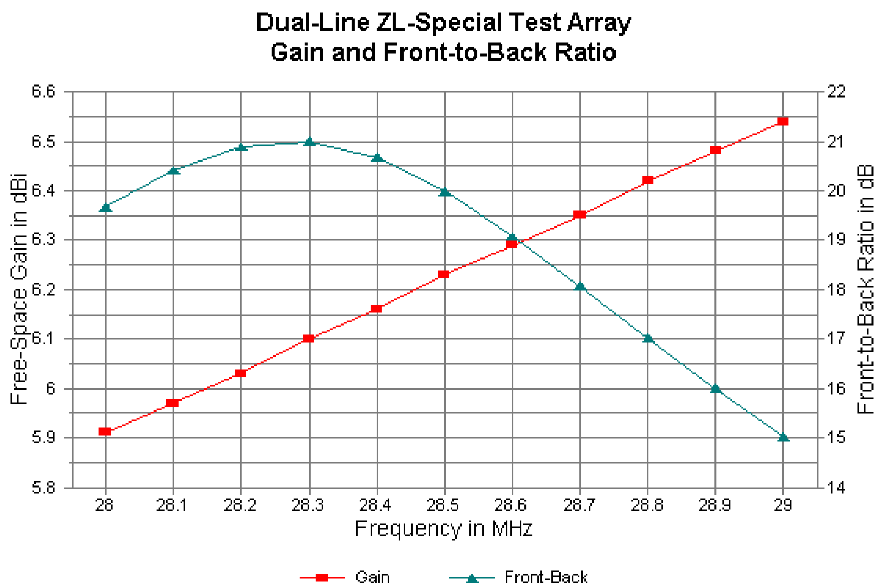

Fig. 5-14

The natural impedance at 28.5 MHz for the new phaseline arrangement is about 23.5 + j 13.1 Ω. The low reactance suggests that a modified 1/4-λ line section might effect a match. 0.167-λ (electrical) of 35 to 37 Ω line provides the broad 50-Ω SWR curve shown in **Fig. 5-15**. The line might consist of either RG-83, or in the absence of such line, a parallel section of RG-59. In each case, the line velocity factor will determine the physical length.

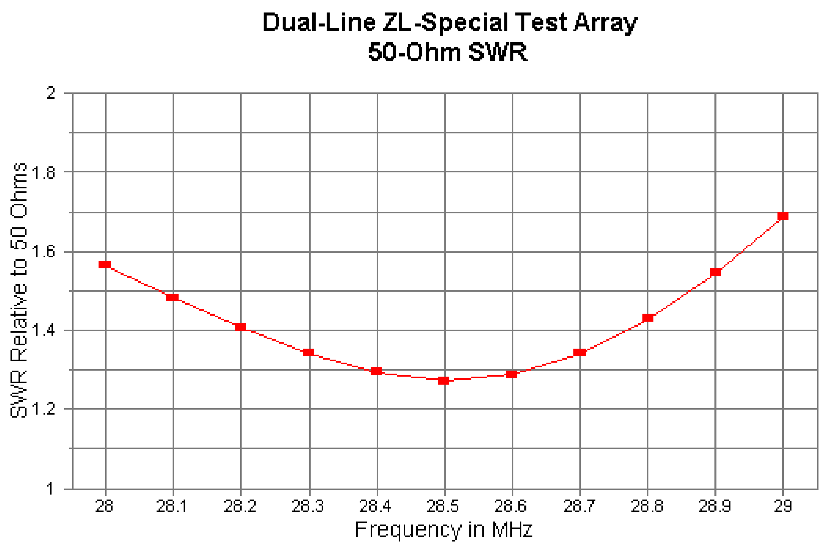

Fig. 5-15

Tentative Conclusions

We have examined the numerous variables that go into the design of a ZL-Special. The somewhat simplistic view of 2-element horizontal phased array design taken in the early years of ZL-Special building has given way to a more complete appreciation of the number of interactive variables involved, including the antenna dimensions and consequential mutual coupling. As well, the phasing work became more complex in terms of the current magnitude and phase angle transitions down a length of line having a given characteristic impedance so as simultaneously to provide each element with the correct relative current magnitude and phase angle and to effect a current division at the line junction or feedpoint that would result in those values.

Many possible ZL-Special designs prove to be unfeasible. The requisite characteristic impedance of the phasing line may not exist and cannot be constructed. The required line length may be shorter than the distance between the elements, or it may be excessively long.

The key to successful ZL-Special design is to find a set of element lengths and a spacing that meets two conditions. First, the relative current magnitude and phase angle on the individual elements must provide a satisfactory pattern in terms of gain and front-to-back ratio. Second, the impedances of the elements under the first condition must permit the design of a phasing line (or pair of lines) that employs an available or achievable characteristic impedance and that allows the requisite current division and transformation. As we saw in Part 1, there is in principle no restriction upon element spacing within the range of 0.05-λ to 0.2-λ, although element spacing in the 0.1-λ to 0.13-λ range tends to yield the most easily achieved gain and operating bandwidth levels.

There is, in principle, no restriction upon the element lengths relative to the length of a resonant dipole at the design frequency. As well, there is no restriction upon the relative lengths of the elements: the forward element may be in principle shorter than, equal to, or longer than the rear element. Some combinations may be more favorable than others, although to date, there is no complete survey of all combinations.

Perhaps the major disadvantage of the ZL-Special phasing system lies in the need to use folded dipole elements with high-impedance phaselines or to use with single tubular elements a low-impedance line. Many, if not most, builders wish to use a metallic boom and hence to have a phase line that is not susceptible to unwanted interactions. The quest for a stable phasing system has led to some interesting variants of phasing schemes for the 2-element horizontal array. The early HB9CV system—still in use today—and the recent N7CL system are two approaches to the same end. If the elements and the desired phase line do not match, let's add matching networks. As we shall see in Chapter 7, a slight increase in electrical complexity can lead to significant simplifications in the physical design of 2-element horizontal phased arrays.

However, before we examine the remaining variants on the 2-element phased array, let's pause long enough to more fully appreciate the role of the transmission line as a current and impedance transformation device. Those who wish to focus on the nuts and bolts of array design may skip the equation-laden next chapter. However, the information may prove useful further down the line and so I shall include it within a separate chapter.

6. The Analysis of the ZL-Special

In Chapter 5, I alluded to the means of and techniques for calculating the correct phaseline values to arrive at a ZL-Special that provides the desired performance. For those who may be interested, this chapter provides a method, but certainly not the only method, for calculating the phaseline values, once the designer has derived certain information from NEC models based on initial decisions about element length and spacing.

Background for ZL-Special Analysis

We can reduce the ZL-Special problem to an orderly series of propositions and explanations. The following notes are an outline of that process.

1. *The significant reason for phasing 2 horizontal half-wavelength elements is front-to-back ratio, not gain*. Two phased half-wavelength horizontal elements will not significantly exceed the gain of a 2-element Yagi. Although 2-element Yagis with high gain are possible, they sacrifice front-to-back ratio. The rationale for designing a phased array is to improve the front-to-back ratio of the antenna for QRM reduction. Phasing promises, in the abstract, to produce a deep rear null, while preserving the gain obtainable with a 2-element Yagi.

2. *We may think of the ZL-Special as a "-45°" antenna*. Traditionally, we have conceived of the ZL-Special as two parallel horizontal elements connected by a short (about 45°) phaseline with a half twist. Thinking in impedance terms, where all values reappear every half wavelength, we subtracted the half-twist line from 180° to obtain 135° phasing. However, we can make two modifications to this traditional view.

First, we may think of the antenna in terms of current phase shifts rather than impedance phase shifts. Current magnitude-phase combinations occur only once per wavelength along a transmission line. Although full-length 135°

lines will achieve the desired phasing for well-designed models, a 45° length of phaseline with a half twist is not the equivalent of a 135° line with respect to current.

Second we may for modeling purposes move the half twist of the phase line anywhere along the line, including at the point of junction with the rear element. In modeling terms, this move means twisting the element. In practical terms, if the front element is modeled in increasing length values (for example, from -8' to +8'), then the rear element is modeled in decreasing values (for example, from +8' to -8'). The two elements are 180° out of phase, and connected by an untwisted 45° length of phaseline.

With respect to the front element, the rear element is (ideally) current phased at -45° (or 315°). The model will now return correct values for calculating voltage and current along the phaseline, with no change in the impedance transformation. However, as we shall see, impedance transformation is largely incidental to understanding the ZL-Special.

3. *For any two close-spaced near-resonant elements, there is a value of current magnitude and phase for each element that will yield a deep null to the rear*. The values of current phase relative to the front element are roughly proportional to the spacing between elements. The precise angles required by the front and rear current will depend to some degree on the antenna geometry and thus may vary slightly from those graphed in Chapter 5.

The first consequence of reviewing Chapter 5 is to dispel the idea that the 2-element horizontal phased array is in any sense necessarily a 135° or a -45° antenna. Within reason, there is a continuum of usable spacing and phasing values. Consequently, using wide-spaced planar folded dipoles (trombones) for elements lacks a rationale, and computer models can detect no advantage for that geometry.

The second consequence of our work in the preceding chapter is to indicate why many hams obtain usable results from casually designed ZL-Specials, even if somewhat off the critical marks. If we arbitrarily set a 20 dB front-to-back ratio as the minimum mark of an improved 2-element array relative to the standard Yagi, then ZL-Specials may depart considerably from optimal values and still meet the criterion.

4. *NEC models using separate front and rear element sources are "forced" and may not be amenable to phaseline construction*. By judiciously arranging the antenna geometry (element length, diameter, and spacing) and the relative current magnitudes and phase angles, we may obtain a deep rear null in many antenna models. In general, such antennas rarely translate into arrays that work with phasing lines of the ZL-Special sort.

Virtually any forced or 2-source model can be built successfully under the condition that each element can be supplied with the correct magnitude and phase angle of current. Perhaps the only practical way to achieve this goal is through a lumped-constant network.

5. *Horizontal 2-element phased arrays with phaselines are heavily interactive at all points of measurement*. The basic antenna geometry consists of the element diameters and their lengths (both absolute and relative to each other) and the spacing between elements. Slight variations in any parameter will yield different values (magnitude and phase angle) of voltage, current, and impedance at the element feedpoints. The rear element values undergo transformation along the phaseline, depending upon the characteristic impedance and the velocity factor of the transmission line used. The phaseline front terminal values combine with the front-element values to produce a feedline matching situation.

NEC 2-source models calculate the feedpoint values of magnitude and phase angle for voltage, current, and impedance for each element. Moreover, for available transmission lines--and for those one might build--we know the characteristic impedance and the velocity factor. Therefore, it is possible to analyze proposed ZL-Special designs, to evaluate their feasibility and likely performance, and to adjust the design to a level of satisfactory performance. The following procedure will permit some precision in the process of design.

Analyzing ZL-Special Designs

The analysis of 2-element phased arrays with phaselines is a stepped procedure that uses the values of voltage and current magnitude and phase provided by a 2-source model derived from NEC or MININEC analysis. Most 2-source models used to obtain values for the following analysis will normally designate the element 1 current as 1 at a phase angle of 0° and the element 2 current as a set of values optimized by trial. The magnitude of the rear element current will be close to 1 and the phase angle will be close to the value corresponding to the element spacing. Alternatively, one may use a front element current value of 0.5 and a correspondingly adjusted rear element current close to 0.5. The utility of the alternative will be explained later in the discussion.

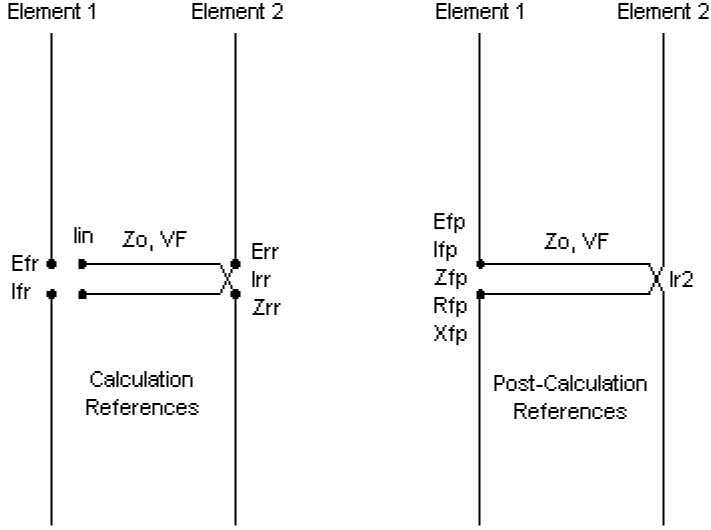

Calculation Reference Poinrs and Designations Fig. 6-1

Fig. 6-1 shows some of the designations used during the calculations and their location on a ZL-Special phased array. The following lines list the meanings of the designations in the figure. I suspect that you may refer to this listing often during the progression of the discussion.

Equation Terms

E_{fr} Voltage at the front element; appears as Element 1 voltage in modeling program outputs; corresponds to E_{in} in general equations for transmission lines

I_{fr} Current at the front element; appears as Element 1 current in modeling program outputs

E_{rr} Voltage at the rear element; appears as Element 2 voltage in modeling program outputs; corresponds to E_L in general equations for transmission lines

I_{rr} Current at the rear element; appears as Element 2 current in modeling program outputs; corresponds to I_L in general equations for transmission lines

Z_{rr} Impedance at the rear element feedpoint

I_{in} Current at the input end of the phasing transmission line; corresponds to I_{in} in general equations for transmission lines

E_{fp} Feedpoint voltage, equals E_{fr} in "perfect" models of ZL-Specials

I_{fp} Total current at the antenna system feedpoint

Z_{fp} Impedance at the antenna system feedpoint

R_{fp} Resistive component of the feedpoint impedance, Z_{fp}

X_{fp} Reactive component of the feedpoint impedance, Z_{fp}

I_{r2} Recalculated rear element current

ℓ_f, Length in feet

ℓ_m Length in meters

ℓ_d Length in electrical degrees

ℓ_r Length in radians

Z_O Characteristic impedance of the phaseline

VF Velocity factor of the phaseline

Note: Each term for E, I, and Z will have an associated phase angle, θ.

1. For any antenna geometry that yields a "perfect" ZL-Special, the voltage at the front element feedpoint will be identical to the voltage at the input end of the phaseline connected to the rear element. We may use this fact as a starting point in our analysis of the antenna design, since it provides the necessary third term (in addition to the values of voltage and current at the rear element feedpoint) for calculating either the characteristic impedance of the phaseline or its length, where the other is given. The basic formula for calculating the voltage along a lossless transmission line is given by the equation,

$$E_{in} = E_L \cos\left(2\pi\frac{\ell}{\lambda}\right) + jI_L Z_O \sin\left(2\pi\frac{\ell}{\lambda}\right)$$

where E_L and I_L are the rear element feedpoint values, E_{in} is the front element feedpoint voltage value, and the parenthetical expressions represent the phaseline length. We may simplify calculations by pre-calculating the line length into radians to obtain ℓ_r.[5]

Since we cannot calculate the line length and Z_O simultaneously, we must assume one or the other. Letting the line length equal the element spacing is most convenient. We can always set up a small utility program in BASIC to step the calculation through several plausible values of line length, each of which will require a different Z_O. We must also make a judicious guess as to the likely velocity factor of the line. In general, if the proposed ZL-Special design uses straight dipoles, use a figure in the 0.67 to 0.8 range, since the phaseline will likely have a low Z_O. If the design uses folded dipoles, then an initial velocity factor of 0.8 will serve, since the range of the phaseline Z_O will be from about 150 Ω to 350 Ω.

If we select ℓ_r and VF, rewrite the terms for front and rear element values, and solve for Z_O, we obtain the following equation:

$$Z_O = \frac{E_{fr} - E_{rr}\cos\ell_r}{jI_{rr}\sin\ell_r}$$

If the array design is "perfect," it will require a phaseline with line length ℓ_r and the characteristic impedance, Z_O to provide the correct phase and magnitude shift of current to the rear element.

2. To understand the conditions at the antenna feedpoint, we must also know the current at the input end of the phaseline. We may obtain this value from the standard equation for calculating the current along a transmission line (written here in terms of front and rear elements):

$$I_{in} = I_{rr}\cos\ell_r + j\frac{E_{rr}}{Z_O}\sin\ell_r$$

The value of current obtained, along with its phase angle, will also be crucial in evaluating the proposed array design.

3. For the array, if perfect, the total current at the feedpoint is the sum of currents in the two branches, namely, the front element and the phasing line input end, or

$$I_{fp} = I_{fr} + I_{in}$$

This equation, of course, is for a vector sum.

The phase angle of the total feedpoint current represents in "perfect" models the appropriate source current phase angle to obtain a forward element current phase angle of 0° and a rear element current phase angle of the value obtained from the original model. If fed with a current at 0° phase angle, the antenna forward element will show a phase angle shifted in the positive direction by the amount of the phase angle of I_{fp}, with the rear element current shifted positive by the same amount. The net difference between forward and rear element current phases will remain the same.

4. From the front element voltage and the feedpoint current, we may obtain

the feedpoint impedance, along with values for the resistive and reactive components:

$$Z_{fp} = \frac{E_{fr}}{I_{fp}} \qquad R_{fp} = Z_{fp}\cos\theta_{Zfp} \qquad X_{fp} = Z_{fp}\sin\theta_{Zfp}$$

The calculation of Z_{fp}, of course, is again a matter of vector division involving the subtraction of I_{fp}'s phase angle from the phase angle of E_{fr}. R_{fp} and X_{fp} provide the values of resistance and reactance to be matched to the feedline for the system.

5. The preceding steps provide the crucial data for a "perfect" phased array. To test the feasibility of the design, simply recalculate the rear element current, I_{r2}, using the calculated value of I_{in} and Z_O, along with E_{fr}. Use the standard equation (with terms rewritten for the present problem).

$$I_{r2} = I_{in}\cos\ell_r - j\frac{E_{fr}}{Z_O}\sin\ell_r$$

If the model's chosen geometry is perfect, then this calculation will simply return the current magnitude and phase angle of I_{rr}. Anything less than perfect will show a divergence between I_{r2} and I_{rr}, especially with respect to the phase angle.

Using the ZL-Special Equations

Using the equations just given for the ZL-Special requires that we expand them to account for the fact that each voltage, current, and impedance may be a complex number, that is, a magnitude with a phase angle. As a convenience to anyone who might wish to put these calculations into a utility computer program, the following expansions are provided, along with some convenient additional calculations of casual interest in the analysis of horizontal 2-element phased arrays.

First, the rear element values of E_{rr} and I_{rr}, along with their associated phase angles, yield the impedance at the rear element, Z_{rr}:

$$Z_{rr} = \frac{E_{rr}}{I_{rr}} \qquad \theta_{Zrr} = \theta_{Err} - \theta_{Irr}$$

where Z_{rr} is the rear element feedpoint impedance and θ_{Zrr} is its associated phase angle. Obtaining this figure allows one to determine the impedance phase change along the phaseline as a matter of interest.

The use of equations for determining current, voltage, or impedance transformation along a transmission line require that we first convert the physical length of the phaseline, initially identical to the spacing between elements, into radians. This is a standard two-step process that begins by converting the physical length into an electrical length in degrees:

$$\ell_d = \frac{1.2 f \ell_m}{VF} \qquad or \qquad \ell_d = \frac{.366 f \ell_f}{VF}$$

where ℓ_d is the length of the line in degrees, f is the frequency in MHz, VF is the velocity factor of the line, and ℓ_m and ℓ_f are the initial lengths in meters and feet, respectively.

Converting degrees into and out of radians requires the familiar equations,

$$\ell_r = \frac{\pi \ell_d}{180} \qquad and \qquad \ell_d = \frac{180 \ell_r}{\pi}$$

where ℓ_r is the electrical length in radians.

We derive a value of Z_O that produces the desired change of current phase with an incidental change of magnitude:

$$Z_O = \frac{E_{fr} - E_{rr}\cos\ell_r}{jI_{rr}\sin\ell_r}$$

Expanded to account for the complex numbers involved, it becomes

$$Z_O = \frac{E_{fr}\cos\theta_{Efr} + jE_{fr}\sin\theta_{Efr} - E_{rr}\cos\theta_{rr}\cos\ell_r - jE_{rr}\sin\theta_{rr}\cos\ell_r}{jI_{rr}\cos\theta_{rr}\sin\ell_r - I_{rr}\sin\theta_{rr}\sin\ell_r}$$

Gathering real and imaginary terms in the numerator allows one to split the equation into its parts. However, since the denominator is also complex, inverting the parts allows further subdivision. Each real and imaginary subdivision pair may be recombined by vector addition. Re-inverting and using vector addition once more produces the final result, the Z_O of the phaseline.

Calculating the current at the input end of the phaseline, given the phaseline Z_O, is straightforward:

$$I_{in} = I_{rr}\cos\ell_r + j\frac{E_{rr}}{Z_O}\sin\ell_r$$

This equation expands into the following form:

$$I_{in} = I_{rr}\cos\theta_{Irr}\cos\ell_r - \frac{E_{rr}}{Z_O}\sin\theta_{Err}\sin\ell_r + j\left(I_{rr}\sin\theta_{Irr}\cos\ell_r + \frac{E_{rr}}{Z_O}\cos\theta_{Err}\sin\ell_r\right)$$

where the real and imaginary parts of the equation are recombined by vector addition.

Z_{in}, the impedance at the input end of the phaseline, can be obtained from E_{fr} and I_{in} by the same calculation method used to obtain Z_{rr}. The difference in the phase angle for the two impedances is the total impedance phase angle change for the phaseline.

Since the total feedpoint current is a vector sum, that is,

$$I_{fp} = I_{fr} + I_{in}$$

the magnitude and phase angle of I_{fp} are determined from

$$I_{fp} = \sqrt{(I_{fr}\cos\theta_{Ifr} + I_{in}\cos\theta_{Iin})^2 + (I_{fr}\sin\theta_{Ifr} + I_{in}\sin\theta_{Iin})^2}$$

$$\theta_{Ifp} = \arctan\frac{I_{fr}\sin\theta_{Ifr} + I_{in}\sin\theta_{Iin}}{I_{fr}\cos\theta_{Ifr} + I_{in}\cos\theta_{Iin}}$$

Pre-calculation of various recurrent terms, of course, can simplify the programming of such equations.

Determination of the feedpoint impedance, resistance, and reactance are self-explanatory, with the addition of one item:

$$Z_{fp} = \frac{E_{fr}}{I_{fp}} \qquad \theta_{Zfp} = \theta_{Efr} - \theta_{Ifp}$$

$$R_{fp} = Z_{fp}\cos\theta_{Zfp} \qquad X_{fp} = Z_{fp}\sin\theta_{Zfp}$$

The recalculation of I_{r2}, the rear element current magnitude and phase angle, via the standard formula,

$$I_{r2} = I_{in}\cos\ell_r - j\frac{E_{fr}}{Z_O}\sin\ell_r$$

requires an expansion similar to that for calculating input current from load current, with some appropriate sign changes along the way. Expanded, the equation is

$$I_{r2} = I_{in}\cos\theta_{Iin}\cos\ell_r + \frac{E_{fr}}{Z_O}\sin\theta_{Efr}\sin\ell_r + j\left(I_{in}\sin\theta_{Iin}\cos\ell_r - \frac{E_{fr}}{Z_O}\cos\theta_{Efr}\sin\ell_r\right)$$

The equation requires completion in the same manner as the calculation of I_{in}.

Undoubtedly, these notes provide superfluous detail for many readers and insufficient detail for others. If it assists a few readers, it will have served its purpose. Those who wish precision beyond the capabilities of average home construction may replace the lossless transmission line formulas with those for lossy lines. Terman's *Radio Engineer's Handbook* and Johnson's *Antenna Engineering Handbook* provide ready references.

Fig. 6-2

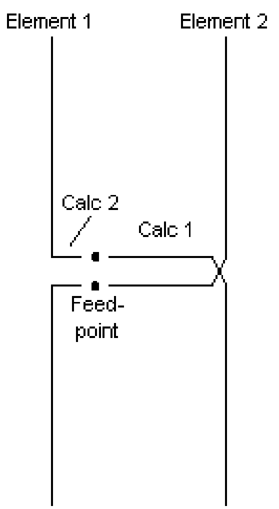

Dual-Line ZL-Special

We may also use the equations in connection with variations on the ZL-Special, since they are perfectly general in their calculation of voltages, currents, and impedances along a (lossless) transmission line. **Fig. 6-2** illustrates the dual-line version of the ZL-Special.

In general, we would perform the first calculation for the longer line and use those values to find a short line that arrives as the correct values. However, in reality, antenna modelers will likely by-pass the calculations in favor of trial-and-error antenna modeling, using the TL or transmission-line facility built into NEC-2 and NEC-4. Essentially, NEC is performing the same task as a small part of its overall calculation set.

We may also set up the calculations in a variety of ways for a variety of venues. The following pages record a simple GW Basic program that I have used and that is the kernel of the program included in the Ham-Calc suite, edited by VE3ERP and made available through *CQ*. One of the useful facets of the outmoded programming language is the transparency of it entries. Being able to see the entries allows relatively straightforward conversion of the lines into Visual Basic, C++, or some other windows-compatible programming language. As well, writing equations in Basic is almost identical to writing them within the languages used by any of the standard spreadsheet programs.

Some of the Basic utility programs that I have written in the past have found their way into various formats, including some stand-alone calculation programs for certain types of antenna. In this case, the program is strictly utilitarian and only partial in its results—a sort of halfway house on the path from an initial model to a final model. As a result, it is likely only to find incarnations in the personal computer stores of individuals.

GW Basic Program for Trial Calculations of a ZL-Special Phaseline

```
10 'FILE: "ZLSP.BAS"
20 CLS:COLOR 11,1,3:CLS
30 EIN=0:EL=0:IL=0:THIN=0:THEL=0:THIL=0:FR=0:LF=0:LD=0:LR=0:STHIN=0:
      CTHIN=0:STHEL=0:CTHEL=0:STHIL=0:CTHIL=0:SLR=0:CLR=0:ABJ=0:ABR=0:BBJ=0:BBR
      =0:ZAI=0:ZBI=0:ZA=0:ZB=0:ZO=0:VF=0:PI=3.141593
40 PRINT"                    Zo of Phaseline for Use with ZL Special":PRINT"
                              L. B. Cebik, W4RNL"
50 PRINT:PRINT" Calculates the characteristic impedance required of a phase
      line of specified     length using values for El, Il, and Ein from an
      antenna modeling program.":PRINT
55 INPUT " Enter Frequency in MHz                            ",FR
60 INPUT " Enter Rear Element Voltage in Volts               ",EL
70 INPUT " Enter Voltage Phase Angle                         ",TEL
80 INPUT " Enter Rear Element Current in Amps                ",IL
90 INPUT " Enter Current Phase Angle                         ",TIL
100 INPUT " Enter Front Element Voltage in Volts             ",EIN
110 INPUT " Enter Voltage Phase Angle                        ",TIN
112 INPUT " Enter Front Element Current in Amps              ",IIF
114 INPUT " Enter Current Phase Angle                        ",TIF
120 INPUT " Enter Element Spacing in Feet                    ",LF
125 INPUT " Enter Velocity Factor of Phase Line (decimal)    ",VF
130 PRINT:PRINT" Are these values correct?  <Y>es or <N>o"
140 A$=INKEY$:IF A$="Y" OR A$="y" THEN 200 ELSE IF A$="N" OR A$="n" THEN 10
      ELSE 140
200 CLS   'Page 2 Data Print-out
205 ZL=EL/IL:ZIL=TEL-TIL
210 PRINT"                          ZL Special Data":PRINT
220 PRINT"  Rear:E: ";EL;" at ";TEL;" I: ";IL;" at ";TIL;" Z: ";ZL;" at ";ZIL;"
230 PRINT"  Front:E: ";EIN;" at ";TIN;"  I: ";IIF;" at ";TIF
250 PRINT"  Frequency:  ";FR;" MHz      Element Spacing:  ";LF;" feet       VF:
 ";VF
255 PRINT:PRINT"       Phaseline              Phaseline Input             Rear
Element"
260 PRINT"    Length    Zo      Current  Angle   Impedance Angle    Current
Angle"
264 PRINT"  System Input:  Current  Angle         Feed: Resistance  Reactance
  I Angle"
270 M=30/FR:MA=LF:MT=LF+M:MS=M/5
280 FOR J=MA TO MT STEP MS
290 LF=J
300 GOTO 700
310 PRINT USING "######.##";LF,ZO,IPOL,IPHSD,ZIN,ZID,IZT,IZTD
315 PRINT"            ";:PRINT USING "#######.##";ITL,ITD;:PRINT"
      ";:PRINT USING "#######.##";RIN,XIN;:PRINT"     ";:PRINT USING
      "####.##";IAC
```

GW Basic Program for Trial Calculations of a ZL-Special Phaseline (continued)

```
320 NEXT
325 LF=MA
330 PRINT:PRINT"    A new Minimum Line Length <L>, a new Velocity Factor <V>,
     move on <M>?"
340 A$=INKEY$:IF A$="L" OR A$="l" THEN 120 ELSE IF A$="V" OR A$="v" THEN 125
     ELSE IF A$="M" OR A$="m" THEN 380 ELSE 340
380 PRINT:PRINT " Press <Pr Scr> for paper copy.                   Another run?
      <Y>es or <N>o"
390 A$=INKEY$:IF A$="y" OR A$="Y" THEN GOTO 10 ELSE IF A$="N" OR A$="n" THEN
      400 ELSE 390
400 End
700 'Calculation Section
705 THIN=(PI*TIN)/180:THEL=(PI*TEL)/180:THIL=(PI*TIL)/180:THIF=(PI*TIF)/180
710 LD=((.366*FR)*LF)/VF
720 LR=(PI*LD)/180
730 STHIN=SIN(THIN):CTHIN=COS(THIN):STHEL=SIN(THEL):CTHEL=COS(THEL):
     STHIL=SIN(THIL):CTHIL=COS(THIL):SLR=SIN(LR):CLR=COS(LR):STHIF=SIN(THIF):C
     THIF=COS(THIF)
740 IR=((-1*IL)*(STHIL*SLR)):IJ=(IL*(CTHIL*SLR))
750 ER=((EIN*CTHIN)-((EL*CTHEL)*CLR)):EJ=((EIN*STHIN)-((EL*STHEL)*CLR))
760 ZAIR=IR/ER:ZAIJ=IJ/ER:ZAI=SQR((ZAIR*ZAIR)+(ZAIJ*ZAIJ))
765 ZBIR=IJ/EJ:ZBIJ=IR/EJ:ZBI=SQR((ZBIR*ZBIR)+(ZBIJ*ZBIJ))
770 ZA=1/ZAI:ZB=1/ZBI:ZO=SQR((ZA*ZA)+(ZB*ZB))
780 IIM=(IL*(STHIL*CLR))+((EL/ZO)*(CTHEL*SLR)):IF IIM>-.001 AND IIM<.001 THEN
     IIM=0
790 IRL=(IL*(CTHIL*CLR))-((EL/ZO)*(STHEL*SLR)):IF IRL=0 THEN IRL=.0000001
800 IPOL=SQR((IRL*IRL)+(IIM*IIM)):IPHS=ATN(IIM/IRL):IPHSD=(IPHS*180)/PI
810 IRF=IIF*CTHIF:IIIF=IIF*STHIF
820 IRT=IRF+IRL:IIT=IIIF+IIM:IF IRT=0 THEN IRT=.0000001
830 ITL=SQR((IRT*IRT)+(IIT*IIT)):ITA=ATN(IIT/IRT):ITD=(ITA*180)/PI
840 ZIN=EIN/IPOL:ZID=TIN-IPHSD
845 IF ZID>90 THEN ZID=180-ZID ELSE IF ZID<-90 THEN ZID=-180-ZID
850 ZYS=EIN/ITL:ZYR=THIN-ITA:SZYR=SIN(ZYR):CZYR=COS(ZYR):RIN=ZYS*CZYR:
     XIN=ZYS*SZYR
860 INF=IPOL:CITF=COS(IPHS):SITF=SIN(IPHS):INR=INF*CITF:INI=INF*SITF:
     ENR=EIN*CTHIN:ENI=EIN*STHIN
870 IZR=(INR*CLR)+((ENI/ZO)*SLR):IZI=(INI*CLR)-((ENR/ZO)*SLR):
            IZT=SQR((IZR*IZR)+(IZI*IZI)):IZTH=ATN(IZI/IZR):IZTD=(IZTH*180)/PI
880 IAC=IZTD-ITD
890 GOTO 310
900 BREAK
```

Conclusion

The ZL-Special presents the most fundamental challenges in determining correct dimensions for a 2-element horizontal phased array. It uses the physically simplest means to correct element-phasing, means that turn out to have a number of electrical complexities. These notes provide one, but not the only route to their solution. Because of the ZL-Special's central place among phased arrays, I am including a bibliography of articles on the antenna and its immediate variants in English at the end of this chapter.

Additional references on some physically more complex horizontal phased arrays will appear in the next chapter. These antennas are interesting for the use of element-matching techniques to overcome the problems presented by the complex impedances at the element feedpoints.

ZL-Special Bibliography

Bluhm, "The Penny-Pincher's Dream," *QST* (Dec., 1965), 63-64.
Bradley, "The 'Half ZL-Special'--a Beam for the City Dweller," *Break-In* (Jul., 1989), 9-10.
Bradley, "The 'Half ZL-Special' Revisited," *Break-In* (Sep, 1991), 4-5.
Glover, "ZL-Special for 2m," *Break-In* (Apr, 1985), 12.
Judd, "ZL-Special 2m Beam," *Out of Thin Air*, pp. 56-59.
Judd, "The ZL-Special," *Short Wave Magazine* (Jul., 1950), 337-339.
Kear, "'Five for Five:' (Five Decibels for Five Bucks)," *QST* (Jan., 1971), 40-42.
Lewallen, "Try the 'FD Special' Antenna," *QST* (Jun., 1984), 21-24.
McCoy, "The Scotsman's Delight," *QST* (Jun., 1963),24-26.
Moxon, "Two-Element Driven Arrays," *QST* (Jul., 1952), 28.
Moxon, *HF Antennas for All Locations* (RSGB, 1982), pp. 77, 222.
Newkirk, "The 'BRD Zapper: A Quick, Cheap, and Easy 'ZL-Special' Antenna," *QST* (Jun., 1990), 28- 29.
Prichard, "A New Driven Array," *Break-In* (May, 1949), 13-14.
Prichard, "Two Beams for the Price of One," *Break-In* (Jul., 1949), 15-17.
Prichard, "Some Notes on the Driven Arrays," *Break-In* (Sep., 1949), 5-7.

Prichard, "Further Experimentation with the '3MH' Beam," *Break-In* (Dec., 1949), 13.
Prichard, "Two Element Rotary: The '3MH Special,'" *Short Wave Magazine* (Dec., 1950), 666-667.
Prichard, "The 'ZL-Special' Beams, *Break-In* (May, 1961), 129-130.
Prichard, "ZL-Specials in 1985," *Break-In* (Oct., 1985), 11.
Schick, "A Shortened ZL-Special Beam," *CQ* (Jul., 1959).
---, "Modified 'ZL' Special, *Antenna Roundup*, Vol. 2 (Cowan Publishing, 1966), pp. 65-66.

Note: Special thanks go to Elaine Richards, News and Features Editor for PW Publishing Ltd., publishers of *Shortwave Magazine* and *Practical Wireless* for her kindness in supplying me with copies of articles on the ZL-Special appearing in those journals. My thanks also go to Brian Egan, ZL1LE for providing copies of ZL-Special articles appearing in *Break-In*, and to Bridget DiCosimo of A.R.R.L. for finding similar materials that have appeared in *QST*.

7. Removing the Limits by Element Matching

The chief limitation of the ZL-Special form of a 2-element horizontal phased array has been mechanical: how to use single tubular elements with phaselines that are not susceptible to interaction with a metallic boom that supports the elements. Successful tubular-element ZL-Specials require low-impedance phaselines, while higher-impedance phaselines are more suited to folded-dipole elements.

Solutions to this problem have been available since R. Baumgartner, HB9CV, developed the array bearing his call in 1954. Interestingly, the HB9CV array has been exceptionally popular on the continent of Europe, but has met mostly silence in the English-speaking realm of amateur radio. Indeed, *Rothammels Antennenbuch* (now produced by DARC) devotes several sections to HB9CVs for various frequency ranges, and 1984 saw the production of a book devoted to the antenna (Fuchs-Collins, *HB9CV: Richtantenne mit allen Variationen* [Frech-Verlag, 1984]). This later book still insisted on favorably comparing the phased 2-element array to a 4-element Yagi.

Since the HB9CV's appearance, several other systems of overcoming the shortcomings of the ZL-Special have appeared. We shall sample only two of them: the recent N7CL phased array and a system for capacitively matching elements to the phaseline. All three systems have a common thread. If the natural impedance of the rear element does not match well with a higher impedance phaseline, we may alter the impedance of the element through the use of a matching system. The techniques that we shall examine vary chiefly in the means used to create the match.

All of the variables that we examined in the case of the ZL-Special remain in effect. Element diameter and length, and the relative lengths of the two elements, determine the required relative current magnitudes and phase angles on the individual elements for a desired level of performance within the limits set in Chapter 3. However, instead of selecting the physical dimensions that will match the phaseline we opt to use, we shall select dimensions that are appropriate for the application of a matching network to create the desired impedance on the rear element. We shall not ignore the forward element, since its dimensions must not only provide the desired rear element impedance when combined with that element, but as well, its impedance must allow the desired current division at the feedline junction and yield a feedpoint impedance that we can match to our most common feedlines.

The HB9CV

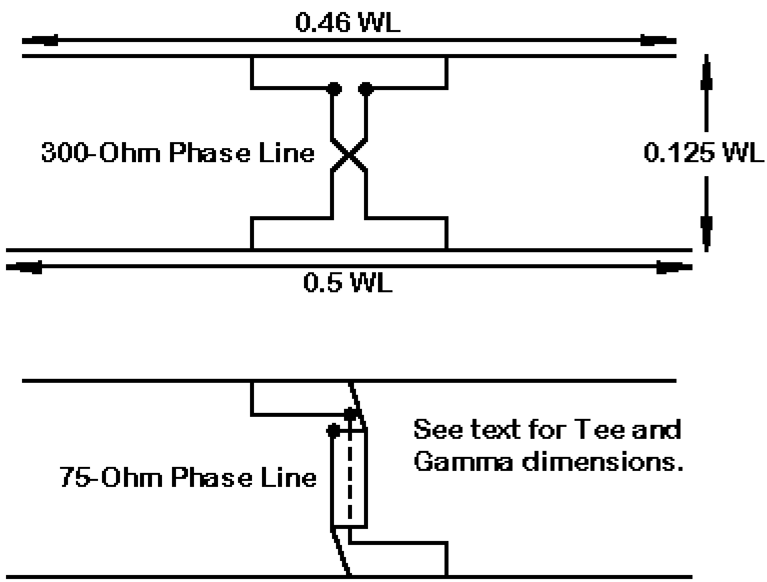

Two Versions of the HB9CV Phased Array

Fig. 7-1

The original HB9CV design, shown at the top of **Fig. 7-1**, attempted to permit the use of 300-Ohm (or other parallel line available in the 1950s) with single tubular elements by the use of Tee or double gamma-match sections. A later version, shown in the lower part of the figure, varied the feedline system for use with 75-Ω coaxial cable. By setting the gamma match in opposite directions on the two elements, the coax shield could connect to the element centers and to the boom. In fact, later versions of the HB9CV employed the boom as one of a pair of lines, with a small diameter line forming the partner. Since the smaller wire in a parallel line with different diameter wires generally determines the line impedance, a single line could run from the rear element connection to the forward element connection and serve both as half the phaseline and as the gamma section. Although the feedpoint is shown at the forward element of the illustrated versions of the HB9CV, various feedpoints between that point and the mid-point between elements are used.

HB9CV specified certain dimensions for the antenna. The rear element should be 0.5-λ long, and the forward element should be 0.46-λ long, if the element diameter is between 0.004-λ and 0.007-λ. At ten meters, 0.004-λ is well over 1.5", which is larger than most builders would use. Therefore, adjustments are natural to HB9CV design. As well, HB9CV also specified the lengths and spacing of the gamma sections for both the Tee and gamma versions. Once more, these dimensions will vary with the actual materials used in construction.

Although not fully appreciated by some antenna modelers, the HB9CV antenna is somewhat difficult to model physically. Since the gamma sections will have a different diameter than the elements, we encounter angular junctions of dissimilar diameter wires in NEC-2 and NEC-4 models, and this situation tends to yield inaccurate results. MININEC models do not suffer this problem, but require very high segmentation densities, since the wires of the antenna structure create so many sharp angles. As well, the gamma match sections are closely spaced to the elements and may need a version of MININEC having a close-wire correction factor. I have created models of the HB9CV with unreasonably high gain reports (>8.1-dBi free-space gain) by violating some of the limitations of the modeling systems.

However, the HB9CV antenna can be modeled in principle within NEC-2 or NEC-4 by using a constant diameter wire size for both the elements and the gamma sections, adequate segmentation, and a TL phaseline. In these notes, I shall examine the modeled results of both Tee and gamma versions of the HB9CV that use 1" diameter materials throughout. The forward element is 0.46-λ long, while the rear element is 0.508-λ long, with an element spacing of 0.125-λ. The gamma sections are spaced 0.0096 λ from the main element with lengths adjusted as follows: The Tees are 0.125-λ long, while the one-sided gammas are 0.053-λ long. The results do not report directly on the performance of the original designs or any specific variation of them, but they do indicate a set of reasonable expectations for performance.

These modeled dimensions vary from the original design chiefly in the spacing and length of the Tee and gamma sections. The revised model spacing is to avoid potential NEC inaccuracies of closely spaced wires of different lengths. However, the sections are only crucial to performance in setting the impedance of the elements, as seen by the phaseline, at a desired level. As long as the elements obtain the required relative current magnitudes and phase angles for a desired performance level, one may use any gamma diameter and length that will produce them.

Fig. 7-2 shows the modeled free-space gain and front-to-back performance of the Tee and gamma models. The Tee uses a 300-Ω phaseline, while the gamma uses a 75-Ω line. As with all of the models in this series, these models do not necessarily indicate the peak performance of which an array is capable. They only serve to illustrate the principles of the array designs. Hence, the relatively low gain figures for the gamma-HB9CV might well increase with further optimization.

More interesting than the precise numbers for the reported gain is the difference in the gain curves for the two types of HB9CVs. The gamma version shows the nearly linear increase in gain with frequency to which we have grown accustomed from our ZL-Special efforts. However, the balanced Tee-HB9CV shows an almost perfectly flat gain across the first MHz of 10 meters. Independent element versions of the modeled design show the rear element, with its matching section, to have an impedance of about 250 Ω with almost no reactance, a good match for the phaseline. The single-sided gamma version does not show the same closeness of match with its 75-Ω line. Indeed, measurements on an HB9CV 2-meter antenna, which uses a single-wire for the phaseline and gamma sections, indicate a line in the 200-Ω range for a direct 50-Ohm coax feed.

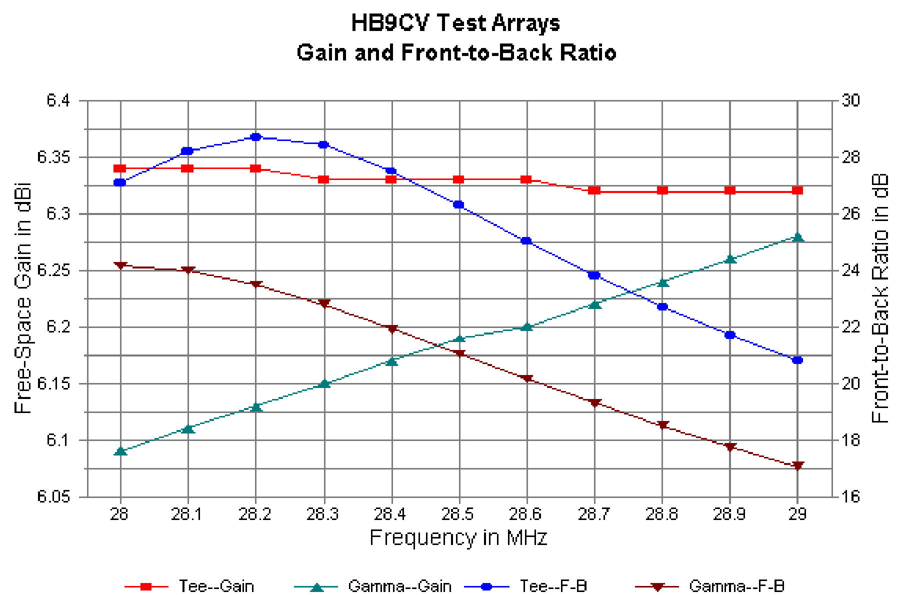

Fig. 7-2

The cost of the Tee-version's relative even performance across the first MHz of 10 meters is the feedpoint impedance. As shown in **Fig. 7-3**, the HB9CV has an SWR curve centered on about 100 Ω. A 2:1 matching network or device is required for standard coax feed. In contrast, the gamma version shows a well-behaved 50-Ω SWR curve.

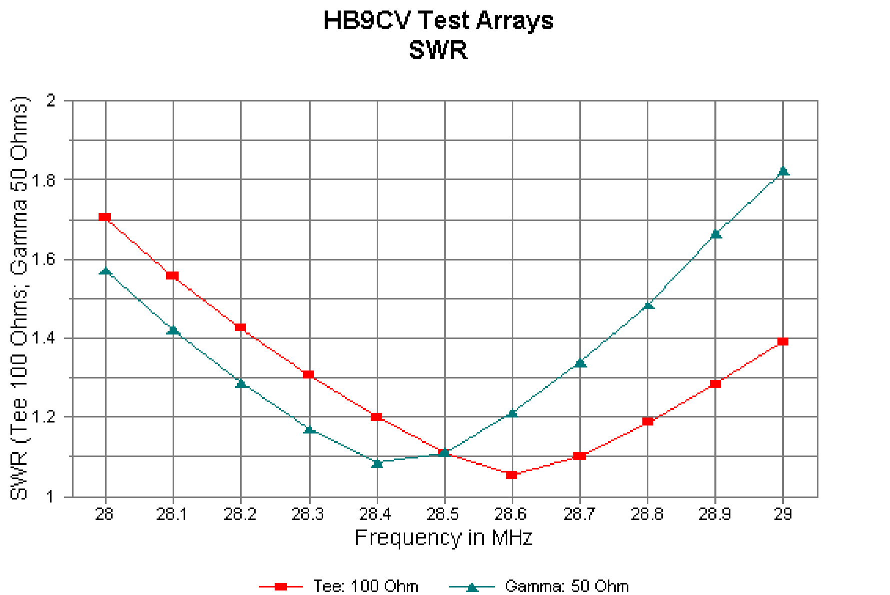

Fig. 7-3

Fig. 7-4 samples the free-space azimuth patterns of the Tee-version of the HB9CV at 28.0, 28.5, and 29.0 MHz to indicate the evolution of the pattern across the operating passband.

In the 1950s, the 1/8-λ spacing of elements and the use of element lengths similar to those of 2-element Yagis held a mystique among phased array designers. From our work with both ideal phased arrays in Chapter 3 and optimized Yagis in Chapter 4, we now understand the appeal of the 1/8-λ spacing. It represents a reasonable balance between operating bandwidth and gain. Beyond the 1/8-λ mark, gain tends to decrease ever more rapidly for elements near the ½-λ or self-resonant length. Below a spacing of 1/8-λ, the operating bandwidth decreases ever more rapidly.

Fig. 7-4

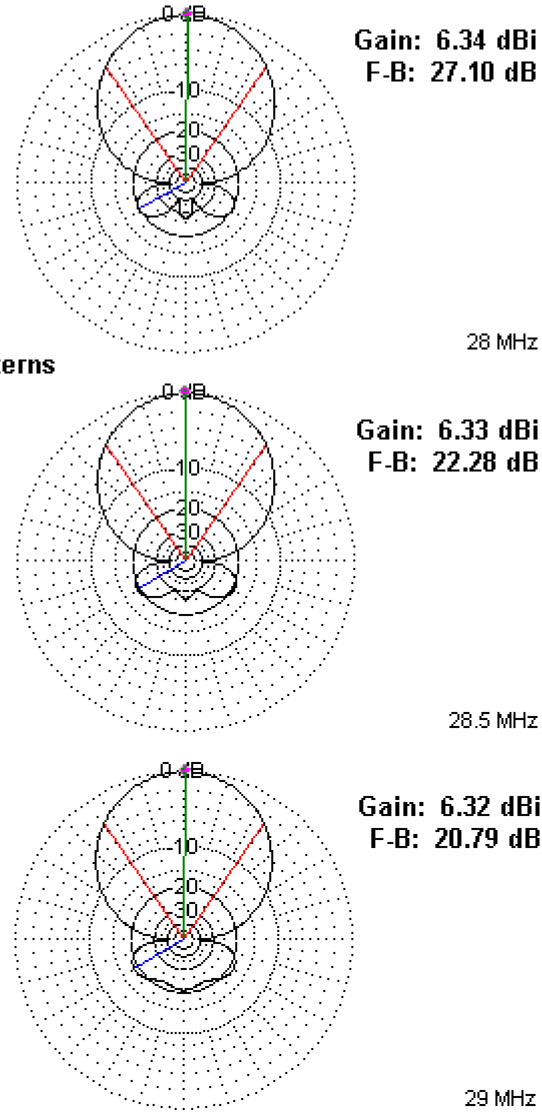

Free-Space Azimuth Patterns HB9CV with Tee-Match

28.0 MHz
28.5 MHz
29.0 MHz

However, for the proper phasing of an array to produce good performance—relative to having only 2 elements—there is no magic spacing. So long as we achieve the correct confluence of all of the variables in a phased 2-element horizontal array, we may use any spacing between 0.05-λ and 0.2-λ. The gamma and Tee matching system to bring the rear element into reasonable alignment with the impedance of a chosen phaseline and the forward element to an impedance that yields the proper current division and feedpoint impedance might well be adaptable to other element lengths and spacing values. However, the success builders have had with the original HB9CV designs has tended to suppress both experimentation and calculation that would yield new variants.

The N7CL Beta-Matching System

In the search for less complex mechanical designs of 2-element horizontal phased arrays, Eric Gustafson, N7CL, has developed within the past few years a different approach to the same end. N7CL wanted to do away with virtually the entire visible superstructure of the HB9CV while achieving similar performance capabilities. To this end, he turned to the shorted-stub form of the beta or hairpin stub, although he used coaxial cable sections for his stubs.

Fig. 7-5 shows the schematic outline of the N7CL phased array. It consists of 2 elements, a phaseline, and two stubs. For the phaseline, N7CL selected a 100-Ω line created from side-by-side (series) sections of standard coaxial cable. The shielding provided by the cable braids permit the line to ride inside the metal boom supporting the elements with no ill effects.

However, single tubular elements do not match well to 100-Ω phaselines. The key to effecting a match between the rear element and the phaseline is to change the element impedance from its natural value to something very close to 100 Ω. A beta match will do the job, but under the condition that the element impedance exhibits a sufficient capacitive reactance to form the series reactance to go with the shunt or parallel inductive reactance of the stub in classic L-network terms.

Fig. 7-5

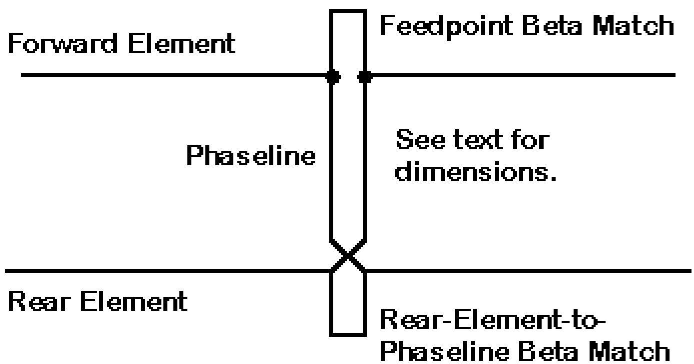

The N7CL Phased Array

We cannot simply apply a beta match to any element and expect good results. We must begin with an acceptable 2-element design using separate feedpoints. Since the rear element must show a capacitive reactance, it must be shorter than a self-resonant half-wavelength, if we are to believe the indications of the tables in Chapter 3. We shall want a net reactance on the feedline-phaseline junction that is also capacitive, which indicates a forward element that is shorter still.

For this 10-meter design example, using 0.5" aluminum elements, I selected a forward element length of 0.4446-λ and a rear element of 0.0.4772-λ. The element spacing is 0.1112-λ. With this combination and a rear element relative current magnitude of 0.8762 at -38.53°, we obtain a performance potential of 6.39 dBi free-space gain and 23.88 dB front-to-back ratio. One might further vary these values for higher performance, but for the design example, I declared them satisfactory.

The forward element impedance is 20.9 - j32.7 Ω, whereas the rear element impedance is 16.4 - j39.7 Ω. For the test model, I selected a 100-Ω

phaseline. To raise the impedance of the rear element to about 100 Ω, I added a shorted stub, the shunt component of a beta or l-network. The required value from network calculations was about j44 Ω. Since the length of a shorted stub will vary with both the desired reactance and the characteristic impedance of the line used, I arbitrarily created a 50-Ω stub with an electrical length of 0.1116-λ.

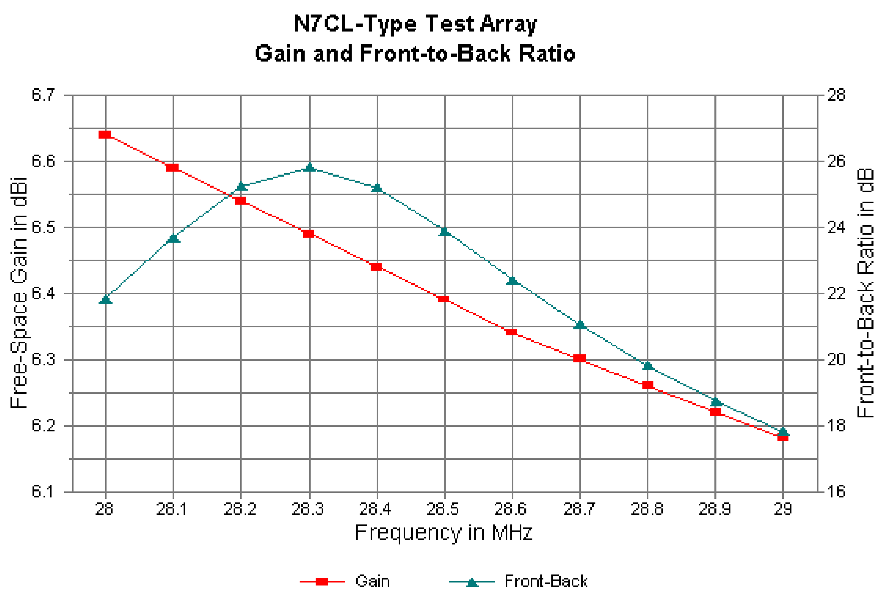

Fig. 7-6

I then created a phaseline with the specifications of 100 Ω and a velocity factor of 0.78 to simulate RG-8X or similar cable. The physical length is 0.1314-λ to ensure that there is enough cable to reach from the center of the boom tube to the elements at each end. The line has an electrical length of 0.1684-λ, the length necessary to transform the current magnitude and phase for the desire conditions on each element. With the rear stub and the 100-Ω phaseline added to the model, we obtain the desired performance indicated from the initial model with independently fed elements. However, the feedpoint impedance at the junction of the forward element and the phaseline is 21.33 - j22.45 Ω.

The capacitive reactance and low resistance at the feedpoint are ripe for a second beta match, this time a 50-Ω shorted stub with an electrical length of about 0.126 Ω. The result is a feedpoint impedance of 43.8 - j7.0 Ω at the design frequency.

Fig. 7-6 shows the free-space gain and front-to-back curves for this sample design across the first MHz of 10 meters. Because the rear-element beta match reverses the impedance progression with changing frequency relative to an element with no matching system, the gain curve shows a reverse direction relative to other phased arrays with which we have worked. The front-to-back curve peaks at about 28.3 MHz. Both progressions of values can be altered with further design refinements.

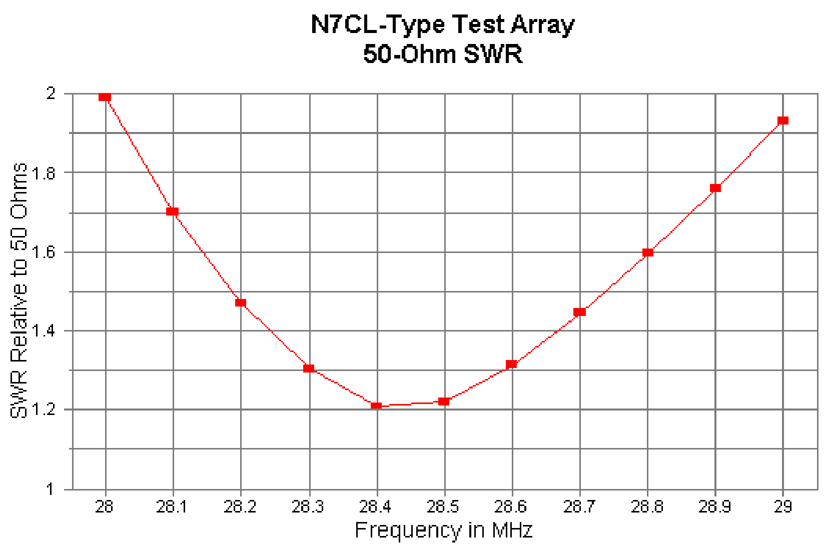

Fig. 7-7

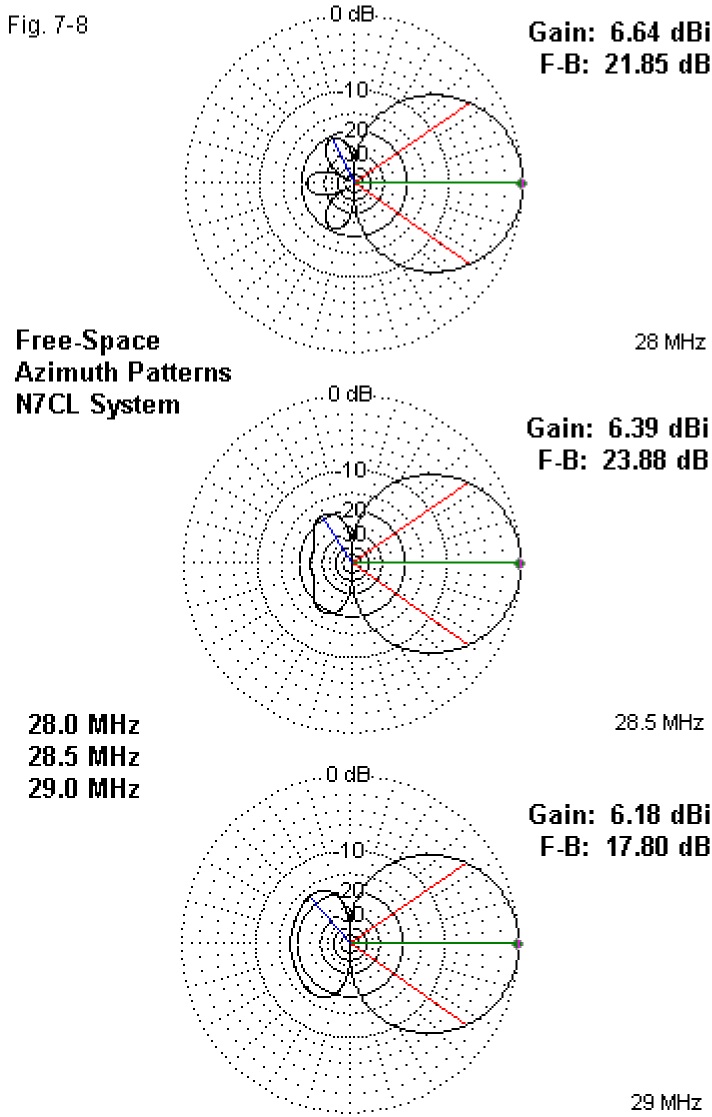
Fig. 7-8
Free-Space
Azimuth Patterns
N7CL System
28.0 MHz
28.5 MHz
29.0 MHz
0 dB
-10
-20
-30
Gain: 6.64 dBi
F-B: 21.85 dB
28 MHz
0 dB
-10
-20
-30
Gain: 6.39 dBi
F-B: 23.88 dB
28.5 MHz
0 dB
-10
-20
-30
Gain: 6.18 dBi
F-B: 17.80 dB
29 MHz

In the design example, the elements were not sufficiently optimized to yield both an SWR under 2:1 across the passband and a minimum value close to 1:1, as shown in **Fig. 7-7**. The feat may be more difficult than might appear at first sight, since any adjustment to the length of the forward element to move the SWR curve will also affect the natural—and hence, the transformed—impedance of the rear element. Moreover, the element spacing—just over 0.11-λ—also works to narrow the operating passband of the array. **Fig. 7-8** shows sample free-space azimuth patterns at both the band edges and mid-band.

The N7CL phasing system has been in use in 30-meter and 40-meter arrays under the Cal-Av label. I am grateful to Eric for permission to describe his patented matching system, although he is in no way responsible for the slant given to the explanation or for my simple design example. As I have noted, design examples do not necessarily equal production designs in performance.

Capacitive Element Loading

A few years ago (1998-99), I took a different tack in trying to overcome the problem of designing a phased array that could use a higher impedance or twin-coax phasing line. (See "The HB9CV Phased Array and Gain Comparisons" at http://www.cebik.com/phase/hb.html.) As we increase the length of a dipole, the impedance increases. If we lengthen the dipole sufficiently, the impedance approaches 100 Ω resistive, but with a considerable inductive reactive component. We may compensate for this reactance by inserting capacitors at the element feedpoint in series with the element.

When we deal with 2 elements, the problem becomes only slightly more complex due to the interaction of the elements. The result will be elements considerably longer than a self-resonant dipole. The final design result was the array pictured in **Fig. 7-9**. The forward element is 0.602-λ long, while the rear element is 0.622-λ long. The elements are 1" diameter aluminum. Because the gain of a dipole tends to increases modestly with increases in length, I used a relatively wide spacing of 0.145-λ to achieve satisfactory performance. The longer elements offset the gain reduction caused by the wider element spacing, but yielded a wider operating bandwidth.

Fig. 7-9

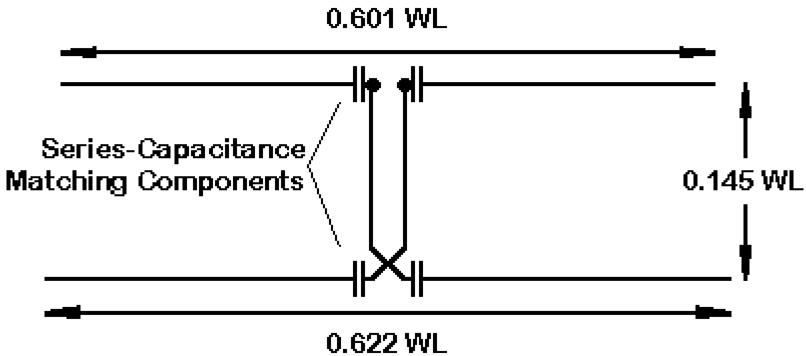

Capacitive Element Matching Phased Array

We need not bring each element to zero reactance in order to have a satisfactory array. The rear element uses a total capacitance of 25.4 pf (two 50-pf capacitors in series on each side of the feed junction). The forward element uses 15 pf (two 30-pf capacitors). When modeled as independent elements separately fed, the rear element impedance is 82.9 - j11.4 Ω, while the forward element is 102.6 + j35.7 Ω. We may now add a 100-Ω phaseline using the same 0.78 velocity factor twin 50-Ω coax construction used in the preceding example. The physical length for the design example is 0.145-λ, although in practice, some extra line may be useful for making connections. A 0.150-λ line will not significantly change performance due to the initial good match between the line and the rear element. The feedpoint junction requires no additional matching network, because the forward-element capacitors were adjusted to provide a low 50-Ω SWR.

Fig. 7-10 shows the free-space gain and front-to-back ratio potential performance across the 28.0 to 29.0 MHz spread. The system is not at all finicky, as revealed by the values obtained simply by replacing the 100-Ω line with a 150-Ω line, as might be obtained by employing 75-Ω coax lengths as shielded twinlead. However, the system is relatively optimized for the 100-Ω line. The 150-Ω line shows superior band-edge front-to-back performance, although the 100-Ω line version shows a higher peak value. Since the matching capacitors only compensate for the element inductive reactance and do not transform the impedance, the gain curve shows its normal upward trend with frequency.

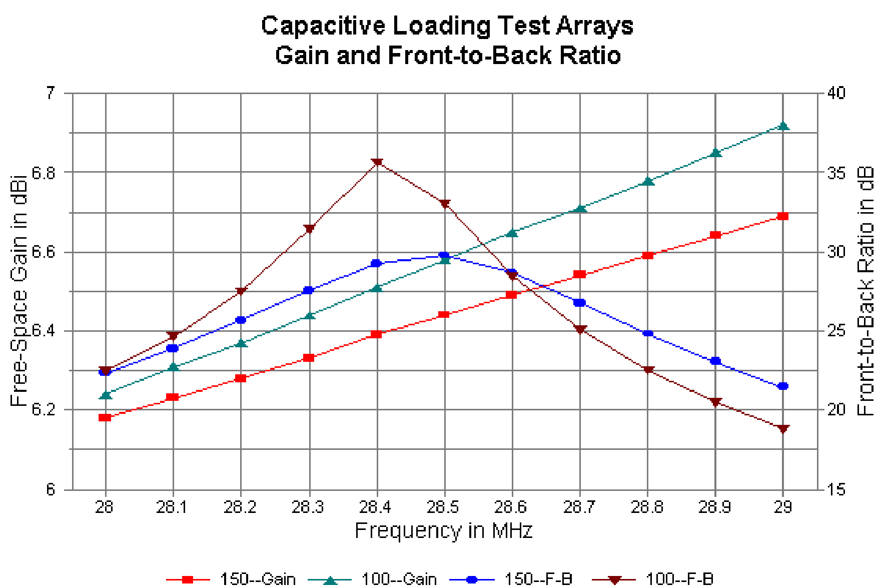

Fig. 7-10

In **Fig. 7-11**, we find the SWR curves for both the 100-Ω and the 150-Ω line versions. Both are satisfactory. However, we might classify the 100-Ω line version as somewhat "tamer."

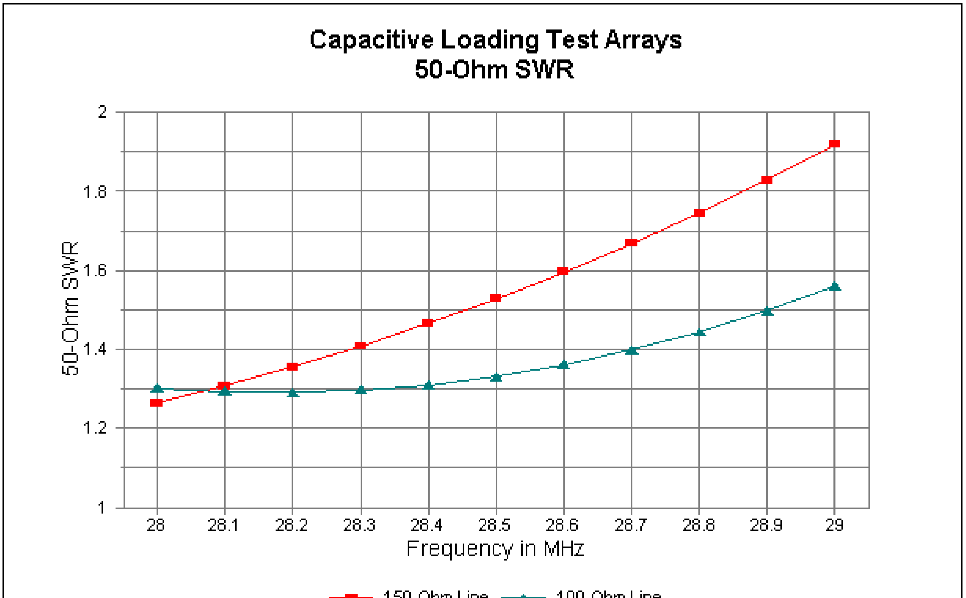

Fig. 7-11

Fig. 7-12 provides the standard 28.0, 28.5, and 29.0 MHz free-space azimuth patterns for performance reference. The array with capacitively loaded elements is an experiment and not a finished product. The elements are long by most array standards—about 20% longer than those of a standard array. However, the reward for heavier elements is a somewhat simplified structure for matching the rear element impedance to the phaseline and the array feedpoint impedance to standard coaxial cable feedlines.

Fig. 7-12

Free-Space
Azimuth Patterns
Capacitive Element
Matching

28.0 MHz
28.5 MHz
29.0 MHz

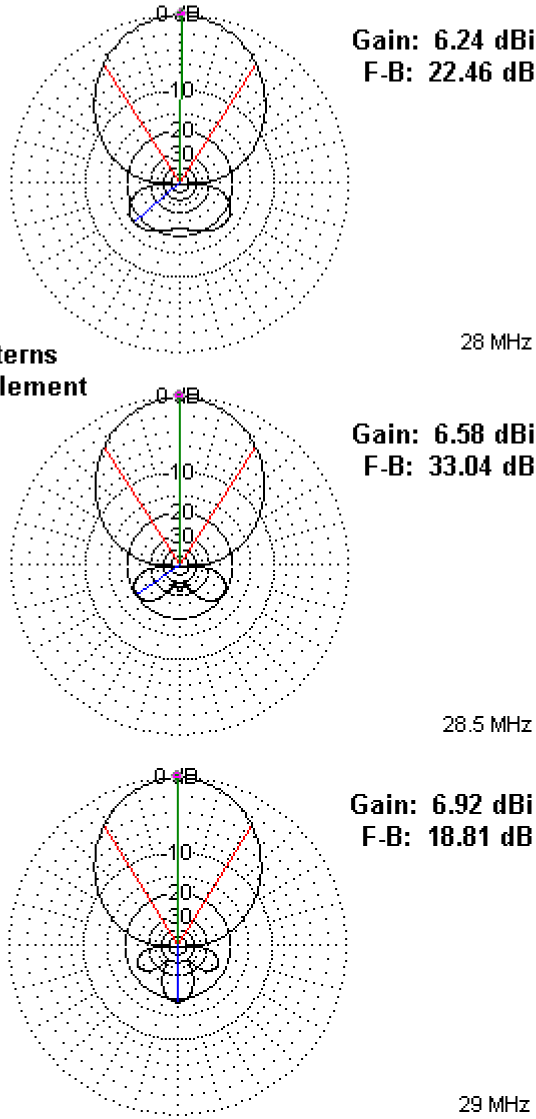

Conclusions

The three systems we have explored in this part of the series illustrate ways in which we may achieve 2-element phased arrays using normal beam constructions with a metallic boom supporting the insulated elements. In each case, the designer has matched the element impedances to a desired phaseline, using a varied assortment of techniques. Once more, our goal has not been to produce paradigm production designs, but only design examples sufficient to illustrate the principles involved. If we have gained some appreciation of the techniques of matching the rear element to the phaseline and changing everything else to align the other variables involved in a 2-element horizontal phased array, then we have gotten out of them everything intended.

Indeed, some may wish to emphasize the performance differences among the examples, but this would be a mistake. Many designs can undergo further optimization. What should strike us is the basic similarity in performance among the ZL-Special and the matched-element designs. One cannot be absolute on the basis of a sampling, but it is likely that the performance range among the models explored so far represents the main arena for 2-element horizontal phased array performance.

Free-space makes an ideal environment for comparing the potential performance of antennas of essentially the same type. However, over the years, some folks have questioned whether or not there might be a difference between the performance of phased horizontal arrays and of parasitic arrays over ground. The only free-space evidence a potential difference in performance would be a significant dissimilarity between the elevation or H-plane patterns of Yagis and phased arrays. None exists.

However, we may use a more direct demonstration by modeling sample parasitic and phased arrays over real ground. **Table 7-1** lists the critical performance parameters of two Yagis, a reflector-driver array with an element spacing of 0.125 λ and a driver-director array with 0.075-λ element spacing.

Comparative Performance Figures of Sample 2-Element Arrays
All Arrays 1 λ Above Good Ground at 28.5 MHz

1. Reflector-Driver Yagi

Dimensions:

Reflector Length λ	Driver Length λ	Element Spacing λ	Element Diameter λ
0.5028	0.4620	0.1250	0.001207 (0.5")

Performance:

Gain dBi	TO Angle degrees	Second Lobe Gain dBi	Angle degrees	Main-Second Lobe Ratio dB	Front-Back Ratio dB
11.61	14	9.35	46	-2.26	12.52

2. Driver-Director Yagi

Dimensions:

Driver Length λ	Director Length λ	Element Spacing λ	Element Diameter λ
0.4972	0.4670	0.0750	0.001207 (0.5")

Performance:

Gain dBi	TO Angle degrees	Second Lobe Gain dBi	Angle degrees	Main-Second Lobe Ratio dB	Front-Back Ratio dB
11.83	14	9.49	46	-2.34	19.58

3. ZL-Special

Dimensions:

Rear El. Length λ	Forward El. Length λ	Element Spacing λ	Element Diameter λ	Phaseline--Note 1 Length Zo	VF
0.5060	0.4650	0.1250	0.001207 (0.5")	0.1300 35	0.66

Performance:

Gain dBi	TO Angle degrees	Second Lobe Gain dBi	Angle degrees	Main-Second Lobe Ratio dB	Front-Back Ratio dB
11.68	14	9.51	47	-2.17	31.62

2. N7CL Phased-Array with Rear-Element-Matching

Dimensions:

Rear El. Length λ	Forward El. Length λ	Element Spacing λ	Element Diameter λ	Phaseline--Note 2 Length Zo	VF
0.4972	0.4670	0.0750	0.001207 (0.5")	0.1314 100	0.78

Performance:

Gain dBi	TO Angle degrees	Second Lobe Gain dBi	Angle degrees	Main-Second Lobe Ratio dB	Front-Back Ratio dB
11.74	14	9.49	46	-2.25	31.44

Note 1: ZL-Special uses a feedpoint impedance matching section.
Note 2: N7CL array uses shorted stubs for rear-element matching and for feedpoint matching.

Table 1. Comparative performance figures of sample 2-element arrays with all arrays 1 λ above good ground at 28.5 MHz.

The Yagis come from Chapter 4. The sample phased arrays are the 35-Ω phaseline model from Chapter 5 and the N7CL array from our work in this section. All arrays are 1-λ above ground. At 1-λ, a parasitic array elevation pattern shows both a lower main lobe at about 14° elevation along with a secondary lobe above. The differential in the secondary lobe is a good indicator of performance similarity or difference.

Fig. 7-13

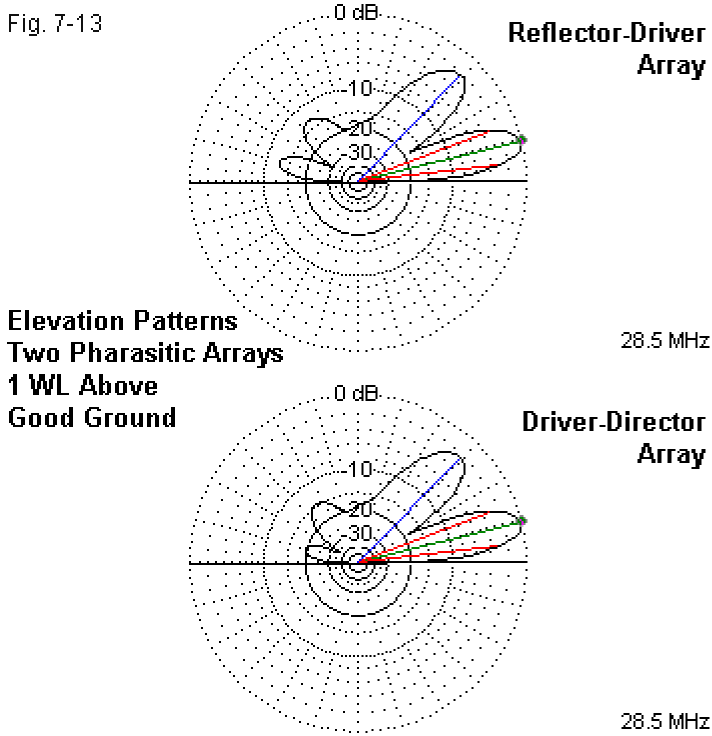

As the figures in the table show—backed up by the elevation patterns in **Fig. 7-13** and **Fig. 7-14**—the differentials are too small to support a claim of performance differential. The differentials that do exist lie in the realm of gain and front-to-back ratio. The 2-element horizontal phased array is capable of slightly higher gain than a 2-element Yagi of similar operating bandwidth. The gain advantage runs between 0.2 to 0.7 dB. However, with a reasonable front-to-back ratio, the gain of a 2-element horizontal phased array never reaches the level of a well-designed 2-element quad or a short-boom 3 element Yagi.

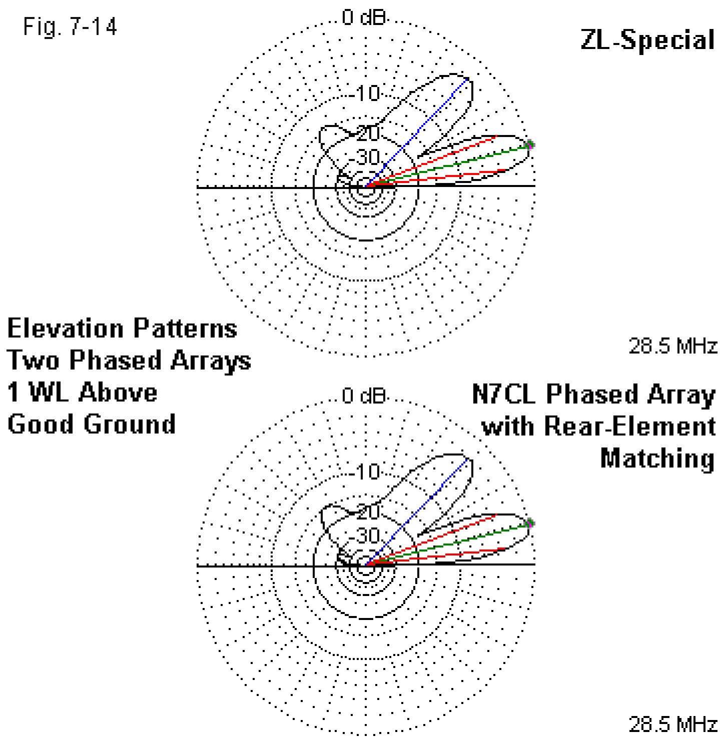

If the gain advantage of the horizontal phased array is marginal relative to parasitic arrays of similar operating bandwidth, the front-to-back advantage is significant and operationally noticeable. A reflector-driver Yagi with coverage of the first MHz of 10 meters will have a peak front-to-back ratio of about 12 dB. A similarly sized phased array with equal or greater gain is capable—when optimally designed—of nearly 20 dB across the full passband, with peak values in the 30-dB region. Whether one wishes the additional quietness from the rear of the phased array or wants to be able to hear what may be happening in the direction to which the beam is not aimed depends on the type and style of operation. In short, the desirability of one type of array over another is a user judgment.

These comparative notes relate only to full-size models of both parasitic and phased arrays. Shortened, loaded elements yield lesser gain in virtually all circumstances, although loaded reflectors may increase the front-to-back ratio of a reflector-driver Yagi. A shorter-element phased array may be capable of the full gain that its elements permit with inherently good front-to-back ratio as well. In the end, the variables involved in antenna selection—where 2 elements form the common baseline among candidates—may outnumber the variables involved in properly phasing 2-element horizontal arrays.

The seemingly marginal place of the 2-element horizontal phased array among amateur antennas might be less interesting if the array alone marked the limit of the our work. However, a closely related but much overlooked potential for the 2-element phased array is to serve as the driver section of a longer antenna. In order assess these potentials, we must—for the space of one chapter—violate the title restriction of this study. In the next chapter of Volume 1, we shall look at a few diverse samples of longer beams in which a 2-element phased array serves one or more important functions.

8. Extending the Uses of 2-Element Phased Arrays

The basic premise of this volume has been to see how 2-element phased arrays perform—as 2-element beams. However, small phased arrays have other uses in addition to their principle role as stand-alone beams. Essentially, we may add to a 2-element phased array one or more parasitic elements to create a beam with desired characteristics. In general, we use the phased array as the driver section of the antenna.

At this point, we might engage in a battle of semantics. When we combine a 2-element phased array with one or more parasitic elements, what do we have? A phased array with added parasitic elements? A Yagi-Uda parasitic beam with a dual phased driver section? The answer, of course, is that we have both. In any given context, we may prefer one name to the other. Since this volume has focused on phased horizontal arrays, the following notes will most often note that we are adding elements to the phased array that we supply with energy. However, if we encounter the same antennas in the second volume, we might reverse our perspective on the total antenna.

Beams that employ phased driver sections have received numerous claims over the years. One presumption that antenna modeling has gradually eroded is the idea that a phased driver section automatically increases the array gain over a beam of the same length that uses a single driver element. We can obtain higher gain only under some very specific circumstances, and in the course of our small foray into phased drivers, we shall look at those circumstances. More generally, the benefits of using a phased driver section accrue to the front-to-back ratio and to the operating bandwidth. The idea of operating bandwidth in this context does not just mean the 2:1 SWR curve. It also includes the smoothness of other performance factors, such as the gain and front-to-back ratio.

We shall examine three seemingly diverse examples of beams with phased-array drivers. All of the beams will use 0.5”-diameter aluminum elements for consistency with the models used throughout the volume. If you wish to replicate any one of the designs, you will need to adjust the element lengths for whatever stepped-diameter tubing schedule that you select as most suitable to your local wind and weather condition. Virtually all combinations of stepped diameter elements will result in longer elements than the uniform-diameter elements shown in the models. In addition, each beam will use a design frequency of 28.5 MHz. This frequency is convenient, since it allows us to check the bandwidth over a full MHz of the band from 28 to 29 MHz. The bandwidth of this section of 10 meters is 3.5%, larger than the bandwidth of any other upper-HF amateur band. Therefore, if a beam has satisfactory performance on 10 meters, then a scaled version of the beam will certainly cover any other upper HF band.

Two Phased Elements Plus a Director for Maximum Gain

The first sample extended array uses a single director to obtain a high gain array that uses only 3 elements. **Fig. 8-1** shows the general outline of the final design and the 2-element phased array that serves as the core. Note that the director has a position that is a fairly long distance from the forward element of the driver section.

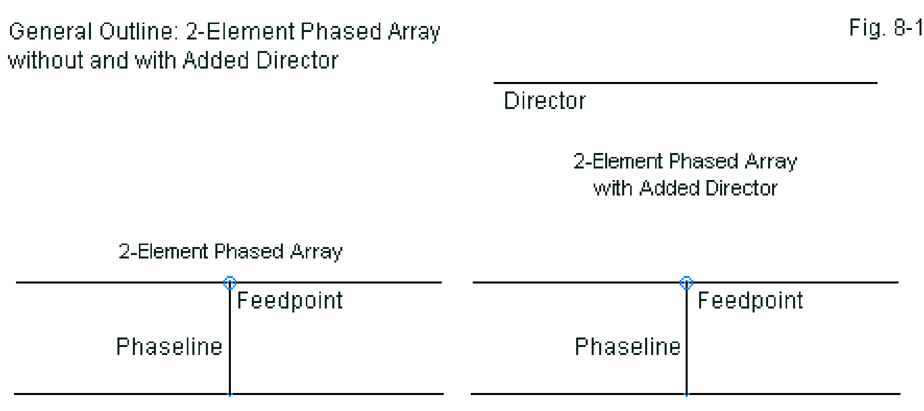

Table 8-1 lists the essential beam dimensions. As always, beams modeled within NEC assume that the elements are well insulated and isolated from a conductive boom—or that the boom uses a non-conductive material. The element spacing column uses two modes of entry so that you can see the relative spacing between elements and the overall beam length.

Table 8-1. Dimensions of a 3-element beam with a phased driver and a director
All elements are 0.5"-diameter aluminum

Element Name	Length in inches	Space from rear in inches	Space from preceding element in inches
Rear Driver	202.4	---	---
Front Driver	200.3	52.7	52.7
Director	181.3	147.6	94.9

Phaseline between rear and forward driver elements: 69.6" of 50-Ω, 0.66-VF transmission line with a half-twist. Feedpoint matching stub: open stub using 41.1" of 50-Ω, 0.66-VF transmission line.

The boom for this beam is about 12.3' long, which is typical of high-gain 3-element Yagis. However, the gain of the new design is almost a half-dB higher. The reason that we may obtain high performance from this array is, in part, that the driver section consists of a pair of phased elements set up for maximum gain, as noted in Chapter 3. **Table 8-2** provides the data on the driver alone and the full beam at 28.5 MHz. (See models 8-1.ez, 8-1a.ez, and 8-1b.ez.) The front-to-back ratio value is the 180° version of that parameter. The pre-match feedpoint impedance indicates the value prior to adding the open-ended stub.

Table 8-2. Modeled free-space performance of the 3-element beam and the driver section at 28.5 MHz

Version	Gain dBi	Front-Back Ratio dB	Feedpoint Impedance R +/- jX Ω
Driver section	7.17	9.87	25.2 + j35.8 (pre-match)
Full beam	8.58	34.80	16.5 + j23.6 (pre-match)
			50.1 + j1.9 (with open stub)

Unlike most beams that use a phased array as the driver section, this beam uses a high-gain configuration for the driver section. The director adds about 1.4-dB to the gain. However, its chief role lies in converting the mediocre front-to back ratio into a very respectable figure. **Fig. 8-2** overlays the free-space azimuth (E-plane) patterns of the driver section alone and the full beam to show the relative proportions of the radiation patterns.

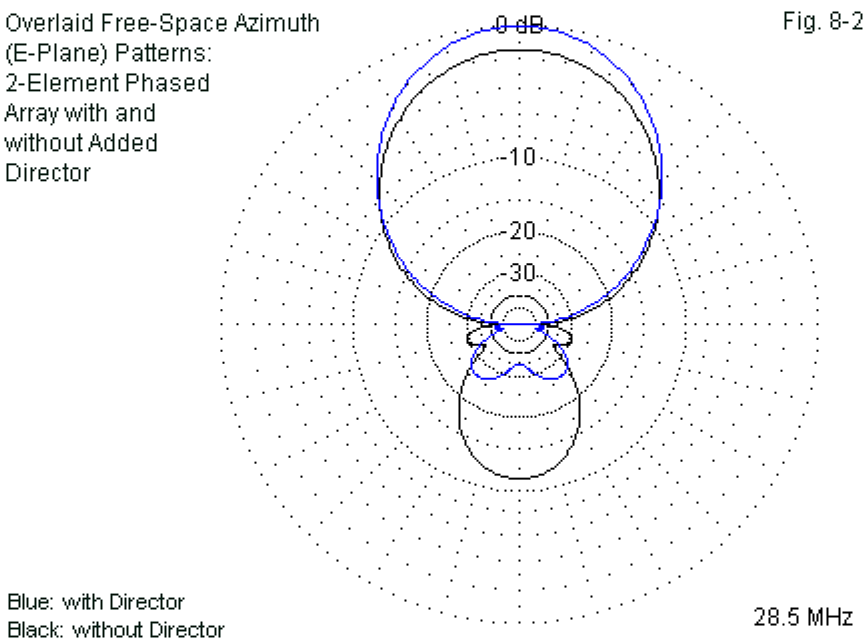

One misconception of complex beams that persists in the amateur community is the idea that reflectors set the front-to-back ratio, while directors have their greatest influence on forward gain. At fine levels of final adjustment, every element has an affect on every performance parameter. In most parasitic beams with at least 3 elements, the driver may have the least effect. However, in terms of the basic setting of the pattern, the director largely determines the gain and the front-to-back ratio. The reflector has its greatest influence on the feedpoint impedance of the driver. (2-element driver-reflector Yagis tend to have relative low front-to-back ratios.) In this design, we have no reflector. However, adding the director alone is sufficient to produce an array with very respectable performance in the rear quadrants.

Fig. 8-3 shows the free-space gain and the 180° front-to-back ratio from 28 to 29 MHz. The dimensions maximize the front-to-back ratio at the design frequency. Note that the front-to-back ratio remains above 20 dB only from about 28.2 to 28.7 MHz. Like the phased array that serves as the driver for the full beam, the operating bandwidth is somewhat narrow in terms of the usual amateur standards for 3-element beams.

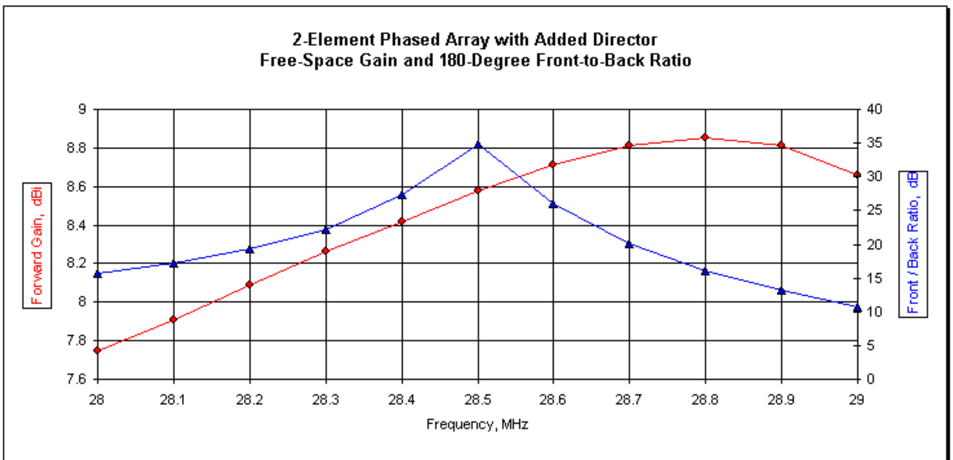

Fig. 8-3

Most arrays with a parasitic director show a rising gain figure across the operating passband. Purely parasitic beams with single driver elements tend to show a curve that remains on an upward swing as the antenna passes the upper limit of the passband. (The are some special designs that form exceptions to this generalization.) The 3-element beam with its phased drivers reaches peak gain within the overall passband. This phenomenon is useful in reducing the differential in gain between the upper and lower limits of the passband. Nevertheless, the gain peak falls just above the high performance region.

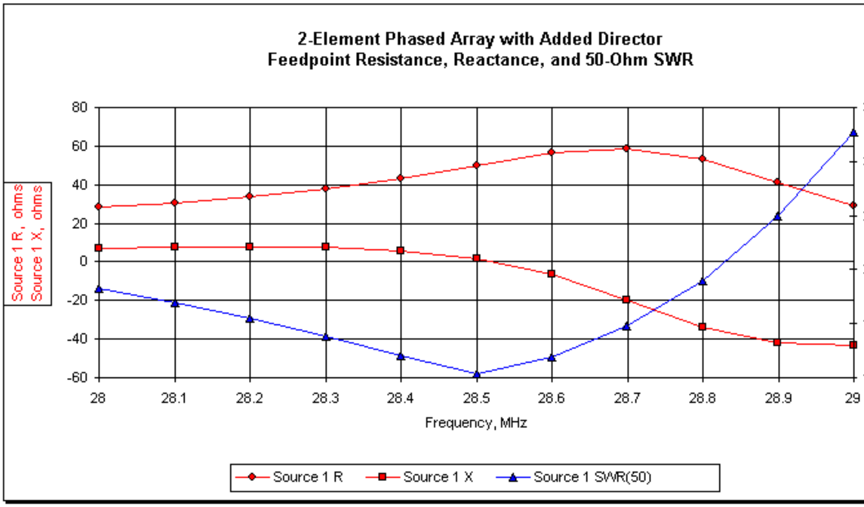

Fig. 8-4

Fig. 8-4 shows the feedpoint performance values, that is, the resistance, reactance, and 50-Ω SWR (with the open stub in place). The chief limiting factor for the array is the increasing capacitive reactance above about 28.6 MHz. As a result, the 2:1 SWR bandwidth extends only from 28.0 MHz to about 28.8 MHz. The SWR bandwidth is slightly greater than the peak-performance bandwidth, as measured by a front-to-back ratio of at least 20 dB.

The 50-Ω SWR curve and the impedance values in the graph result from the use of an open stub. This stub is a form of beta match. In most cases, we think of a beta match as requiring a shorted or closed stub. Shorted stubs apply to driver sections that show a pre-match impedance with capacitive reactance. The driver section in the full beam shows an inductive reactance at the feedpoint prior to matching. Therefore, an open stub that exhibits capacitive reactance is the appropriate parallel matching component. (See Volume 2 for further information on various matching systems for direction beams.)

All in all, the 3-element beam based on the use of a high-gain phased driver array provides relatively high performance in a reasonably straightforward mechanical package. Effective operation up to about 28.8 MHz is adequate for many applications. Still, the main services performed by this array have been to illustrate one extended use of a 2-element phased array and to show with some clarity the function of elements within a combined phased and parasitic antenna.

Two Phased Elements Plus a Director for Maximum Operating Bandwidth

Perhaps the most common reason to use a 2-element phased array (or driver section) within a larger beam is to increase the operating bandwidth. Although gain may be among the parameters involved, the main factors that most designers wish to improve are the front-to-back ratio and the SWR bandwidths. The search for designs with large operating bandwidths has gone on for decades, and in the last 2 decades of the 20^{th} century, Bill Orr, W6SAI, came up with two interesting designs: one for a 2-element driver-reflector beam and the other for a 3-element Yagi. The conditions that favored wide-band operation also favored a 50-Ω feedpoint impedance, a serendipitous finding, given the use of 50-Ω cables as standard amateur feedlines.

Fig. 8-5 shows the outlines of the 2- and 3-element Orr Yagis along with a third candidate for wide-band service: a 3-element beam in which 2 of the elements form a phased array and one is a director. In principle, the new beam is a variation of the long-boom array that we just finished exploring. However, the new beam is less than half as long as our first subject. In fact, it uses a shorter boom than the 2-element Yagi at the upper left. In addition, the spacing between the to phased elements is less than half the spacing value used by the long, high-gain array. Obviously, the phased elements are not optimized for maximum gain.

Nevertheless, at the design frequency, the short-boom array with the phased drivers acquits itself very well. **Table 8-3** compares some basic modeled performance numbers at 28.5 MHz for the 2 pure Yagis and the new candidate for wide-band 10-meter service.

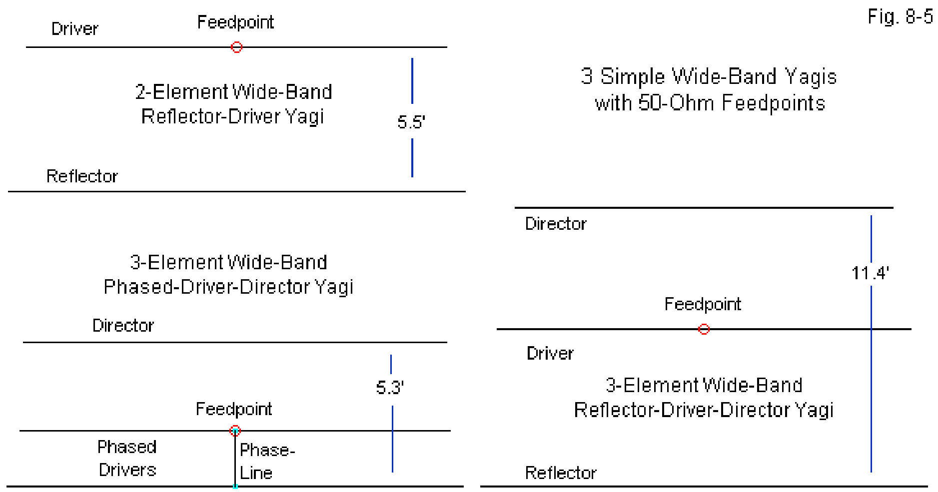

Table 8-3. Modeled free-space performance of 3 wide-band 10-meter beams

Beam Version	Gain dBi	Front-to-Back Ratio dB	Feedpoint Impedance R +/- jX Ω
2-element Yagi	5.97	10.78	49.7 + j4.0
3-element Yagi	7.05	21.71	47.5 – j4.0
Phased drivers + director	6.65	18.30	51.9 + j7.1

As the numbers suggest—confirmed by the overlaid patterns in **Fig. 8-6**—the phased driver-director beam performs more like the 3-element Yagi than the 2-element driver-reflector Yagi. The gain and front-to-back ratio are close to the values that the 3-element Yagi provides, but the boom is less than half as long. **Table 8-4** lists the dimensions of the short-boom 3-element beam. (See model 8-2.ez.) You may wish to compare the dimensions to those for the long-boom, high-gain array in **Table 8-1**. As well, note the differences in the 28.5-MHz performance values for the two different phase-driven arrays, but remember that the goal of the new design is not raw gain, but a wide-operating bandwidth.

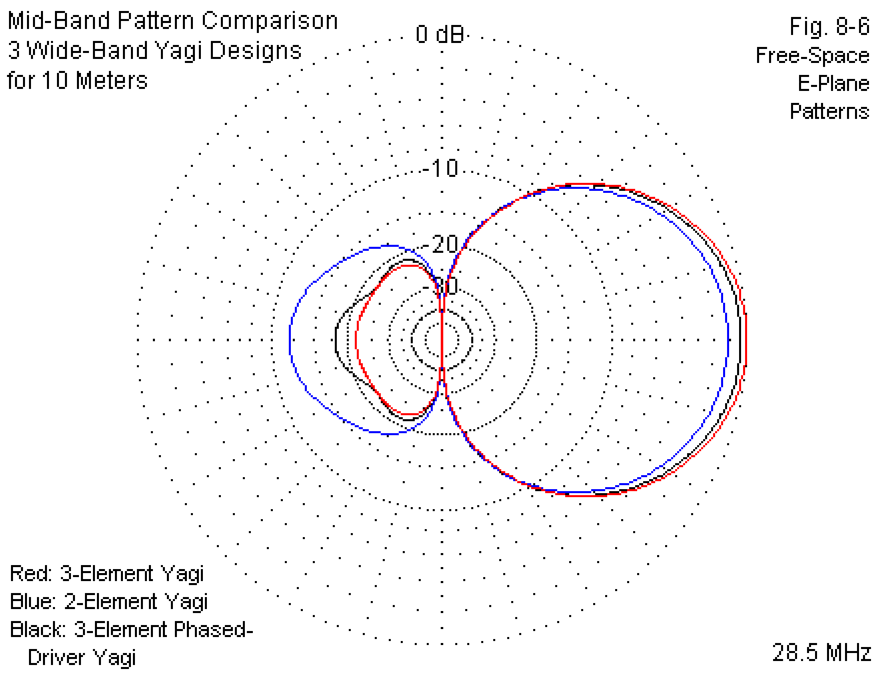

Table 8-4. Dimensions of a 3-element beam with a phased driver and a director
All elements are 0.5"-diameter aluminum

Element Name	Length in inches	Space from rear in inches	Space from preceding element in inches
Rear Driver	197.6	---	---
Front Driver	189.9	25.0	25.0
Director	186.0	64.0	39.0

Phaseline between rear and forward driver elements: 25.0" of 250-Ω, 1.00-VF (or 0.84-VF) transmission line.

There is no direct analog to the short-boom 3-element array, either with respect to the pair of phased drivers or with respect to the director placement. Perhaps the nearest analog is a 2-element Yagi that uses a driver and a director. A Yagi with this configuration and 28.5-MHz performance numbers close to those of the 3-element array would use a spacing of about 32.5” between the driver and the director, about 0.08-λ. (See model 8-2a.ez.) In free-space, such a beam would show a gain of about 6.75 dBi with a front-to-back ratio of about 18.9 dB. However, the feedpoint impedance at resonance would be close to 19.5 Ω and require one or another form of matching to a 50-Ω main cable.

The driver-director Yagi suffers one other problem. It has a very narrow operating bandwidth. **Fig. 8-7** compares the 50-Ω SWR curve of the short-boom 3-element array with the 19.5-Ω SWR curve of the driver-director Yagi. The comparison does not favor the pure Yagi as a wide-band antenna for 10 meters. In fact, the SWR curve for the 3-element short-boom array suggests that with only a little redesign, we might be able to cover all of 10 meters from 28.0 to 29.7 MHz. (Model 8.2.ez uses the alternative 0.84-VF phaseline.)

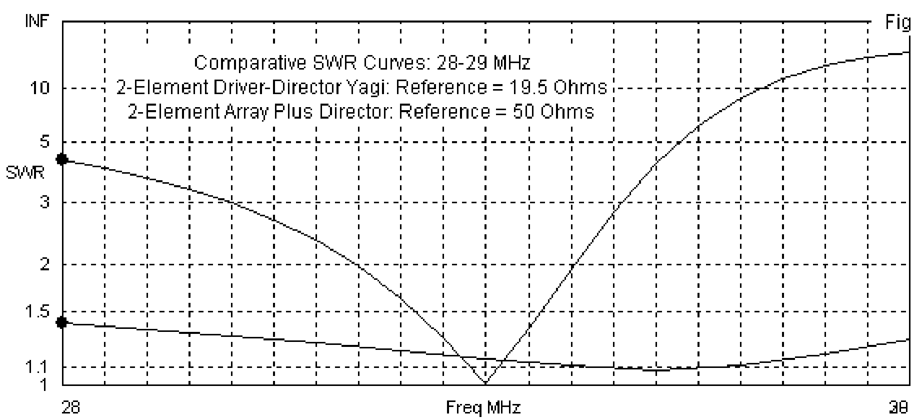

Fig. 8-7

Fig. 8-8 provides a view of the free-space gain and the 180° front-to-back ratio from 28 to 29 MHz. Like all arrays having a director, the array shows a gain curve that rises as the frequency increases. The peak of the curve occurs well above the limit of this frequency sweep.

Fig. 8-8

The front-to-back ratio peaks on the design frequency. It varies by less than 3-dB across the band, a desirable feature in a wide-band beam design.

Fig. 8-9 traces the feedpoint data, including resistance, reactance, and the 50-Ω SWR. If you compare the comparable graph for the long-boom array (**Fig. 8-4**) with the current one, you will see numerous similarities, especially in the shape of the curves. The resistance curve moves upward with frequency and then declines near the upper end of the sweep range. The reactance curve begins by being nearly flat, but eventually takes a sharper bend in the capacitive direction. The major difference between the curves for the two antennas is the values for the wide-band array change much more slowly than those for the long-boom array. As a consequence, the 50-Ω SWR never exceeds 1.4:1 across the full-MHz sweep. Indeed, by re-centering the values for the design to about 28.8 MHz or so, one may cover the entire 10-meter band with less than 2:1 50-Ω SWR. However, the gain at the lower end of the band would fall to less than 6 dBi. As well, the front-to-back ratio at both band edges would drop to about 10 dB.

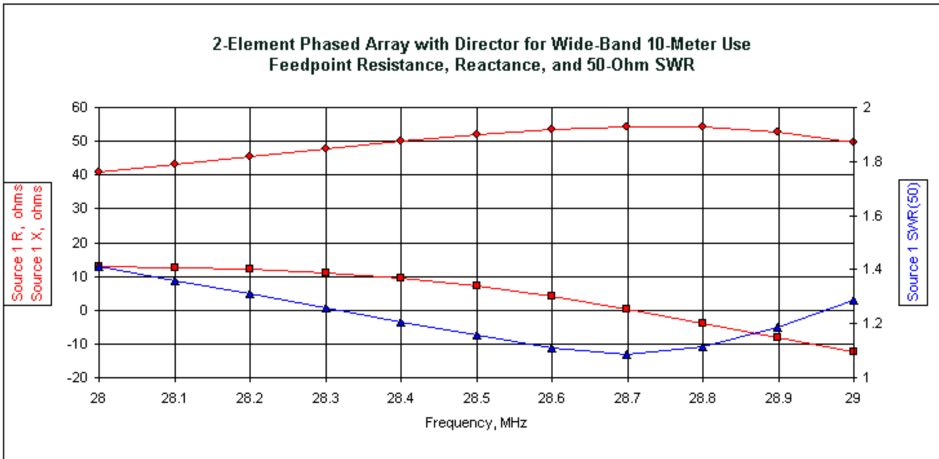

Fig. 8-9

The pair of driver elements call for a 250-Ω phaseline with a single half-twist. In this design, the proximity of the two elements—and of the director—require the relatively high line impedance to effect the proper phase relationships. The line also calls for a velocity factor of 1.0. Perhaps the best way to create the line is to fabricate it from copper wire and some periodic insulating spacers. **Table 8-5** lists some common wire sizes and the required center-to-center wire spacing needed to create a 250-Ω phaseline. With some adjustment of the element lengths, one might also press into service twin runs of RG-83 125-Ω coaxial cable, which has a velocity factor of 0.84.

The 3-element short-boom, wide-band array with a pair of phased driver elements and a single director provides good performance in a very compact package. On lower HF bands, such as 40 meters, the weight of the third element might well be an objection to implementing the antenna over and above a simpler 2-element wide-band driver-reflector design. However, in the upper

HF region (and even in the VHF region), the weight of a single extra element becomes less of a challenge (both to build and to sustain through local weather). Hence, the compact wide-band 3-element phased-driver design becomes attractive for covering bands like 10, 6, and 2 meters.

Table 8-5. 250-Ω transmission line dimensions

AWG Wire Size	Wire Diameter	Center--to-Center Spacing
#14	0.0641"	0.262"
#12	0.0808"	0.330"
#10	0.1019"	0.416"
#8	0.1285"	0.525"

A 4-Element Beam with a 2-Element Phased Array as a Driver

Fig. 8-10

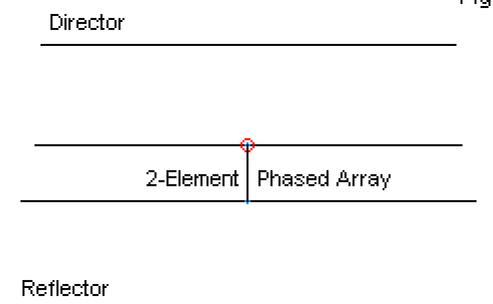

General Outline of a 4-Element Beam
Driver by a 2-Element Phased Array

In our exploration of the basic properties of beams that use phased driver elements, we noted the primary role of the director in producing additional gain relative to the drivers alone and in setting the basic rear-quadrant radiation pattern—that is, the front-to-back ratio. We noted that in a single-driver Yagi, the reflector functions primarily (but not solely) to set the feedpoint impedance of the antenna. When we use a phased-driver pair, the phasing system to a large degree sets the feedpoint impedance. Therefore, we may fairly ask whether there is any advantage to be gained by adding a reflector to the antenna.

Fig. 8-10 shows one way of answer our question. We may create a 4-element beam that consists of a 2-element phased array with an added reflector and an added director. If we cut the design for 28.5 MHz and use 0.5”-diameter aluminum tubing, we end up with the dimensions that appear in **Table 8-6**.

Table 8-6. Dimensions of a 4-element beam with a phased driver, a director, and a reflector: all elements are 0.5”-diameter aluminum

Element Name	Length in inches	Space from rear in inches	Space from preceding element in inches
Reflector	214.2	---	---
Rear Driver	201.0	48.2	48.2
Front Driver	188.2	72.8	24.6
Director	183.0	117.2	44.4

Phaseline between rear and forward driver elements: 24.6” of 250-Ω, 1.00-VF transmission line.

In many ways, the new beam is similar in its dimensions to the 3-element short-boom array, with the addition of the reflector element. Since interactions do differ with the added element, the lengths and the spacing of the elements must change to compensate and to center the performance at the design frequency. We may see at a glance the operational enhancement that we achieved by adding the fourth element by comparing the modeled free-space performance data at 28.5 MHz for the 3- and the 4-element beams in **Table 8-7**.

Table 8-7. Modeled free-space performance of 3- and 4-elementwide-band 10-meter beams using phased driver pairs.

Beam Version	Gain dBi	Front-to-Back Ratio dB	Feedpoint Impedance R +/- jX Ω
3-element array	6.65	18.30	51.9 + j7.1
4-element array	7.18	29.89	43.9 – j1.7

The extra element nearly doubles the boom length of the array, with all of the wind loading that the increase may entail for a given region of the country. For the cost in weight and wind load, we add about 0.5 dB gain and about 10-dB front-to-back ratio. **Fig. 8-10** overlays the patterns for the two arrays. As the patterns show, the average front-to-back ratio does not improve by a full 10 dB. However, the improvement is sufficient to be operationally noticeable. The gain improvement would be hard to detect in operation.

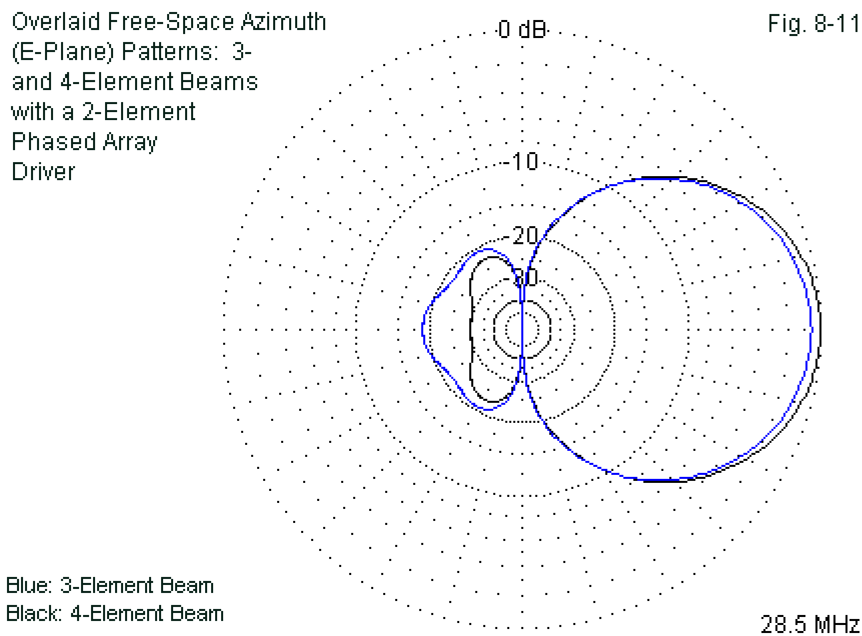

Performance at the single design frequency is not a good measure to use in evaluating a beam designed to perform across a spread of frequencies. For that reason, I have included throughout the volume frequency sweeps of virtually all of the antenna designs discussed. A comparison of the 4-element array and the earlier 3-element array requires similar treatment. Compare **Fig. 8-8** with **Fig.**

8-12 in order to see whether we acquire a uniform advantage in adding the fourth element.

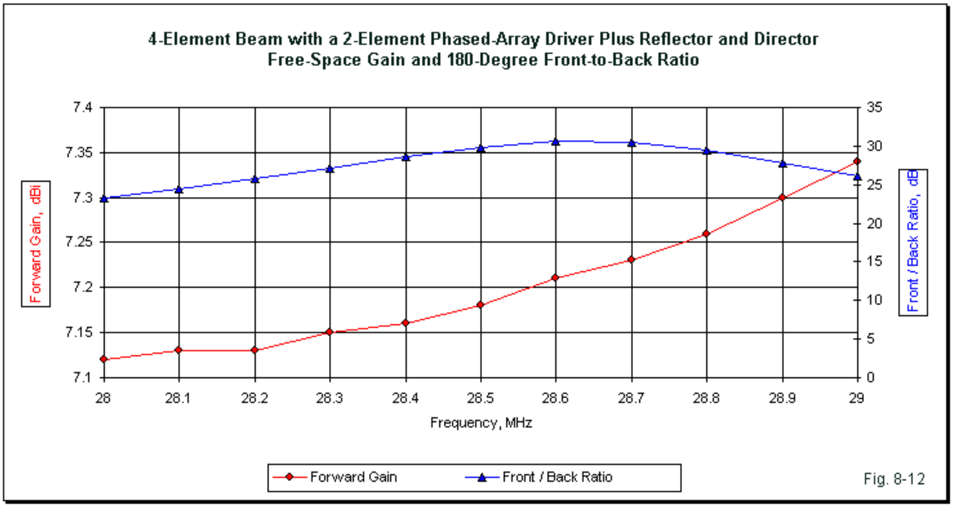

Fig. 8-12

One measure of improvement is to consider the difference of gain from one band edge to the other. In this case, the comparison is fair, since both beams show a rising gain value as the frequency increases. However, the 3-element beam shows nearly 0.75-dB difference between the values at 28 and at 29 MHz. For the same frequency spread, the 4-element array shows a difference of only about 0.3 dB.

Since the front-to-back ratio for both arrays peaks within the swept passband, we may fairly compare two values. One is the front-to-back ratio at each band edge. For the 3-element array, the band-edge values are between 15.5 and 16.5 dB. The 4-element beam shows values above 23 dB at both ends of the band. The 4-element array has a much higher maximum-to-minimum value (approaching 10 dB) largely because the 180◦ front-to-back ratio is so much higher than the worst-case value. However, across the swept passband, the 4-element array shows clearly superior performance.

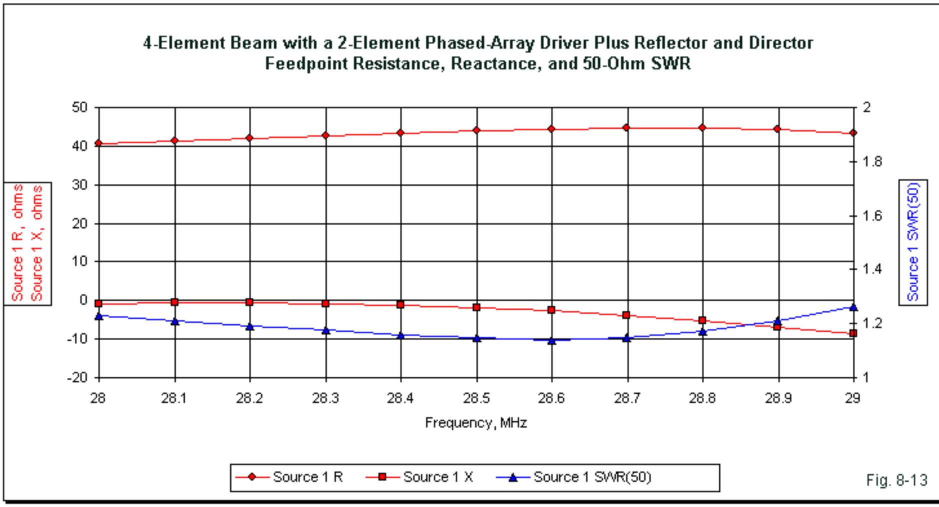

The feedpoint data for the 4-element array, shown in **Fig. 8-13**, show a further effect of adding the reflector. The resistance, reactance, and 50-Ω SWR curves all have the same general shapes that we met with the earlier 3-element arrays. However, the 4-element curves are all much flatter. For example, the reactance does not change by 10 Ω across the full MHz spread. The resistance changes by no more than 5 Ω. As a consequence, the SWR never reaches a value of 1.3:1 between 28 and 29 MHz.

The low rates of change for the array gain and for the feedpoint values strongly suggest that we might easily expand the beam's coverage to include all of 10 meters from 28.0 to 29.7 MHz with very reasonable performance throughout. Given the patterns of usage on the 10-meter band, this move might be unnecessary. However, it bodes well for a 6-meter antenna intended to cover the entire band or for a 2-meter antenna intended for coverage above and below the amateur allocation.

We now have an answer to the question of what we gain from the addition of a reflector to the 3-element array. The reflector improves the operating bandwidth by flattening the response curves. As well, it improves the overall front-to-back performance of the array. Whether or not these improvements justify doubling the boom length and adding the weight and wind load of another element defies a general answer. The user's decision will be based on the operational needs and specifications that he or she brings to the question.

More Distant Phasing Landscape

We have restricted our explorations to antennas using no more than 2 elements as a phased array to drive a larger beam that includes one or more parasitic elements. Nevertheless, the arena of phased arrays includes a considerable territory beyond the 2-element limit. As we close this volume, we can add only a few notes to indicate what lies beyond for those who wish to pursue element phasing further.

The early days of 2-element horizontal phased arrays—in the era when the ZL-Special and the HB9CV first appeared—created a misimpression that has persisted even into the 21st century. The excessive claims made for early phased arrays generated what we would now call a "sound-bite." Any 2-element parasitic beam can be improved by simply setting a phase line between the elements. As a consequence, we enjoyed many articles that created phased arrays, especially phased quad beams.

Unfortunately, most of the designs either over-estimated the improvements or began with bad beam designs in the first place. Parasitic quad beams lent themselves to mistreatment largely because we understood them so poorly. We presumed that the loops (or 2-element bent dipole arrays that formed each element) followed all of the rules applicable to 2-element beams with linear elements. That presumption proved completely unfounded.

For example, as we saw in Chapter 4, a 2-element driver-reflector Yagi has difficulty reaching a 12-dB front-to-back ratio at any spacing that yields a usable feedpoint impedance and modest forward gain. (See **Table 4-1**.) However, by designing a 2-element driver-reflector quad beam on its own ground, we can obtain a very high front-to-back ratio at the design frequency, along with quite reasonable gain. **Fig. 8-14** provides the outline and free-space pattern for such a beam. (See model 8-4.ez.)

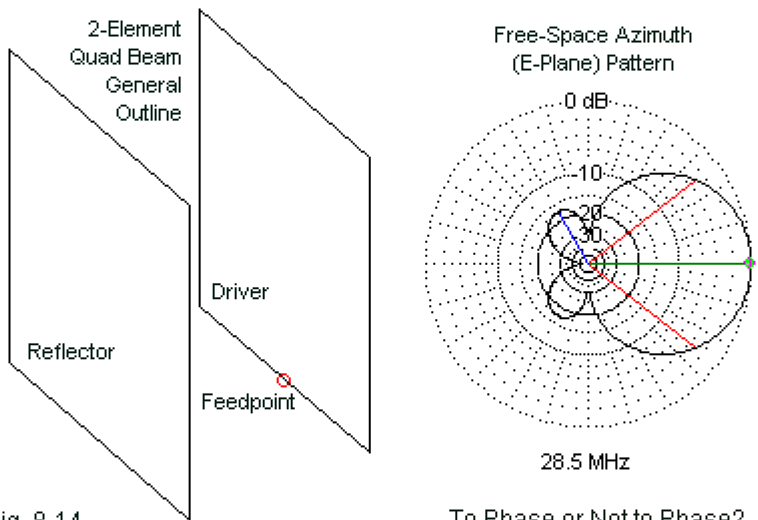

Fig. 8-14

The test beam shows a free-space gain of 7.04 dBi with a front-to-back ratio of over 57 dB at 28.5 MHz. Like all such beams with radically high 180° front-to-back ratios, the front-to-back ratio falls off rapidly, but remains respectable at whatever frequency limits that we might reasonably set. The feedpoint impedance is about 136 Ω resistive, and the SWR curve is quite good for a quad. The question that faces a designer with a penchant for phasing elements is simple: what improvements might we make to these performance specifications?

If we improve gain, the front-to-back ratio will deteriorate, and the gain increment will be very small. In the final analysis, if we begin with a well-designed parasitic array, any improvements made by successfully phasing the 2 elements will normally involve structural and adjustment complexities that far outweigh the anticipated improvements. The use of phased driver sections tends to allow design improvements most often with special cases of beams that employ linear elements in the ½-λ vicinity.

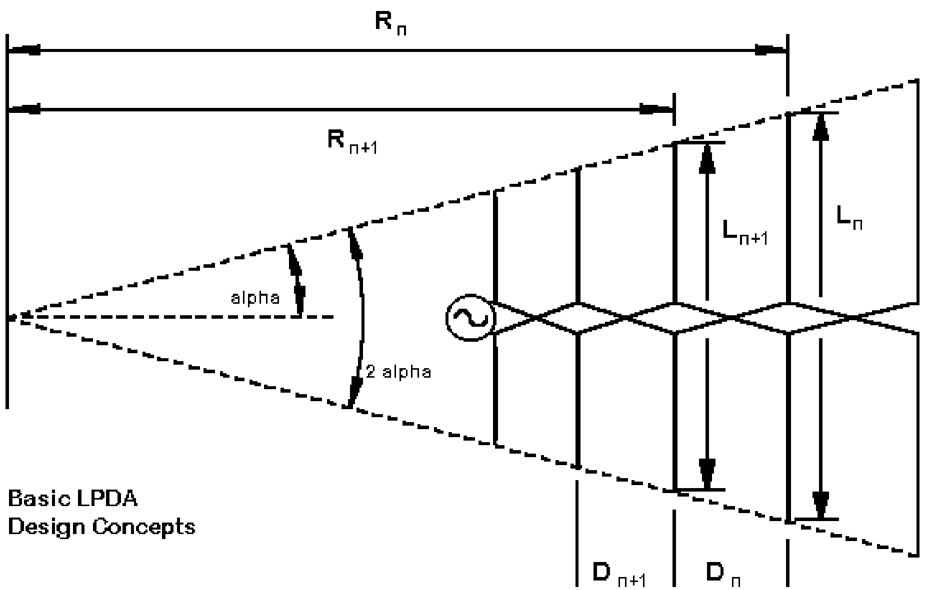

Fig. 8-15

Up to the 1960s (and beyond, in many circles), antenna designers derived smaller arrays used alone or as driver cells from empirical experimentation. This situation did not change with the advent of antenna modeling software, although the experimentation moved from the shop to the computer desk. For larger phased arrays, the development of frequency-independent antenna theory saw the emergence of the log periodic dipole array (LPDA). A sequence of elements would operate over a defined frequency range if the element lengths and the spacing values adhered to mathematical calculations. **Fig. 8-14** shows the basic terms of the LPDA.

Note that we feed every element via a phaseline that undergoes reversal between each pair of elements. However, remember that each element receives energy not only from the direct feed from the phaseline, but as well from the mutual coupling between adjacent elements. Under these conditions, three inter-related factors determine the elements in an LPDA. The angle α defines the outline of an LPDA and permits every dimension to be treated as a radius or as the consequence of a radius (R). The most basic structural dimensions are the element lengths (L), the distance or radial distance of each element (R) from the apex of angle α, and the distance between elements (D). The distance of an element from the angle apex is considered to be large enough so that the curve for radius approximates the straight line of the element. A single value, τ, can be defined in terms of all of the components in the following manner:

$$\tau = \frac{R_{n+1}}{R_n} = \frac{D_{n+1}}{D_n} = \frac{L_{n+1}}{L_n}$$

Elements n and n+1 are successive elements in the array working toward the apex of angle α. The value of τ is always less than 1.0; although effective LPDA design requires values as close to 1.0 as may be feasible.

The value of τ defines the relationship between successive element spacing values, but it does not itself determine the initial spacing between the longest and next longest elements upon which to apply τ successively. The initial spacing also defines the angle α for the array. Hence, we have two ways to determine the value of σ:

$$\sigma = \frac{1 - \tau}{4 \tan \alpha} = \frac{D_n}{2 L_n}$$

D_n is the distance between any two elements of the array and L_n is the length of the longer of the two elements.

LPDAs are very stable if they use large enough values of τ and if the design optimizes the value of σ. However, amateur arrays tend to be small and sparsely populated. As a consequence, amateur-band LPDAs rarely have a frequency range of more than 2:1 (for example, 14 to 30 MHz) with significant gain and front-to-back ratio. (See model 8-5.ez for a sample high-performance LPDA.)

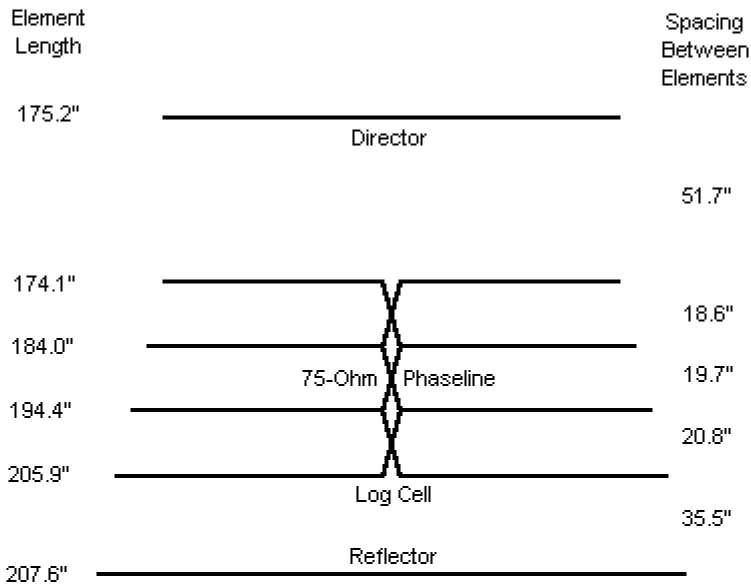

Fig. 8-16 A 6-Element 10-Meter Log-Cell Yagi

These introductory concepts only hint a both the possibilities and the complexities of practical LPDA design. A fuller treatment of LPDA basics for practical amateur-band arrays appears in Volume 1 of *LPDA Notes*. In Volume 2 of the same work, many chapters cover the advanced development of large phased driver sections in beams that also feature a parasitic director and a parasitic reflector. One name that we apply to these arrays is the log-cell Yagi. However, as suggested by the outline sketch in **Fig. 8-16**, we might easily call such arrays supplemented LPDAs.

The sample 10-meter log-cell Yagi uses a 4-element LPDA at its core. Unlike the simple 2-element phased drivers of the sample arrays in this chapter, the 4-element log cell derives from careful calculation according to LPDA methods. The value of τ is about 0.945, while the value of σ is 0.05. (See model 8-6.ez.)

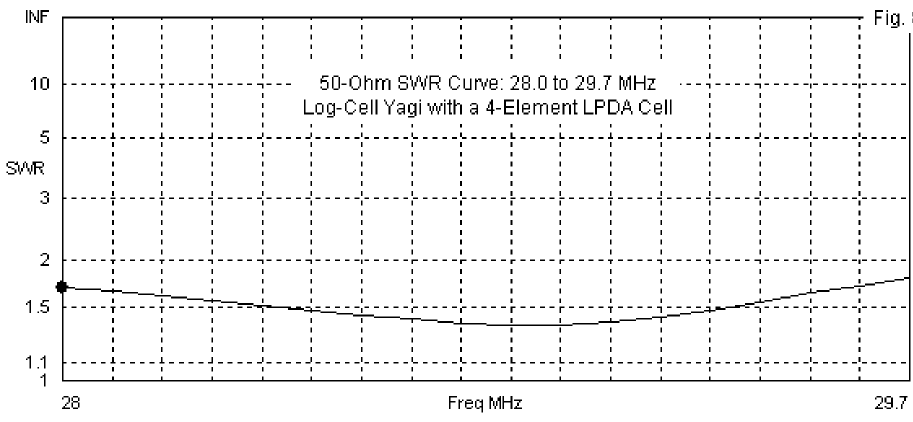

Fig. 8-17

To complete such an array, the designer experimentally determines the proper length and spacing for each of the parasitic elements. The goal is not to exceed the gain of a wholly parasitic Yagi having the same boom length. In fact, the sample log-cell Yagi has a free-space gain fitting to a 12' boom, namely, about 8.2 dBi. Instead, the use of a log cell increases the operating bandwidth of the array. The front-to-back ratio remains above 20 dB from 28.0 to 29.7 MHz, while the 50-Ω SWR is below 2:1for the same frequency span, as shown in **Fig. 8-17**. We may, of course, design log-cell Yagis with longer booms and higher gain just by increasing the value of σ and adjusting the parasitic elements for the revised log cell. In each case, the beam will approximately match the performance of a Yagi with the same boom length, but increase the operating bandwidth significantly.

LPDAs and log-cell Yagis carry us well beyond the limits that I set for this volume. However, they do serve as samples of what lies beyond the second element in a 2-element phased array. Our goal in this volume has been to understand the basics of element phasing. We have also tried to understand the nature and limits of what we may accomplish by phasing elements to form a directional beam—along with the fundamental techniques by which we may achieve our goal.

Along the way, we noted that every directional beam is a phased array, regardless of whether we use any means to supplement parasitic coupling by directly feeding energy to each element. We also noted, in Chapter 4, the general limits of performance that we might obtain from geometry alone, that is, from a wholly parasitic 2-element horizontal array. However, the 2-element Yagi-Uda beam has so many variations that it invites separate study. For example, no other beam has undergone so many attempts to shorten the elements while retaining as much performance as possible. As well, we may construct such beams from an almost inexhaustible supply of local as well as professional materials.

As a result, the 2-element parasitic array deserves extended study on its own ground. That will be the subject of Volume 2. However, let's pause one more time for a practical matter—converting some of the sample models used in this volume into antennas that you can build for yourself.

9. Converting Uniform- to Stepped-Diameter Elements

Many of the antennas used as samples (and provided as sample models) throughout the chapters in this volume are very practical designs. However, they are not ready for construction, since they have two limitations. First, they use uniform-diameter elements to simplify the models. Second, they use a design frequency of 28.5 MHz, which may or may not place them on the operating band that you desire.

In this brief supplemental chapter, we shall go through a two-step process. First, we shall see how within entry-level NEC software to convert a uniform-diameter model into one that uses a desired stepped-diameter schedule. Second, we shall add a few notes about scaling the initial model to another band and then selecting a stepped diameter schedule for the new frequency range.

The Initial, Intermediate, and Final 10-Meter Models

Fig. 9-1

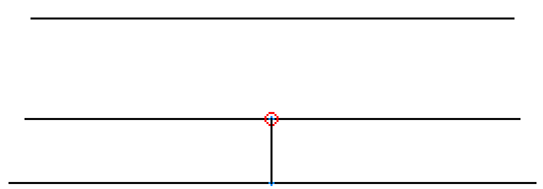

General Outline: Antenna to be Converted to
a Stepped-Diameter Schedule

Fig. 9-1 outlines the model that we shall use as our subject. It comes from the preceding chapter as the short-boom, 3-element array with a phased driver pair designed for wide-band service. (See model 9-1.ez.)

Fig. 9-2 shows the EZNEC model wire table for the initial model. The array uses 0.5” diameter aluminum elements. Wire 1 and 2 form the phased driver pair, while wire 3 is the director. We need not show other details, since nothing will change with respect to element spacing, the phaseline or the feedpoint. The phaseline for this model uses a 250-Ω, 1.0-VF parallel transmission line.

Wires

Wire Create Edit Other EZNEC Wire Table for Initial Model Fig. 9-2

Coord Entry Mode Preserve Connections Show Wire Insulation

Wires

No.	End 1				End 2				Diameter	Segs
	X (in)	Y (in)	Z (in)	Conn	X (in)	Y (in)	Z (in)	Conn	(in)	
1	0	-102	0		0	102	0		0.5	21
2	25	-96	0		25	96	0		0.5	21
3	64	-93.5	0		64	93.5	0		0.5	21
*										

Since we may not obtain the element strength that we need with a uniform-diameter element, we normally use stepped-diameter elements in actual construction. Since the element diameter decreases as we move away from the element center, the overall weight is less. **Fig. 9-3** shows the proposed structure of the elements that we plan to build.

Fig. 9-3

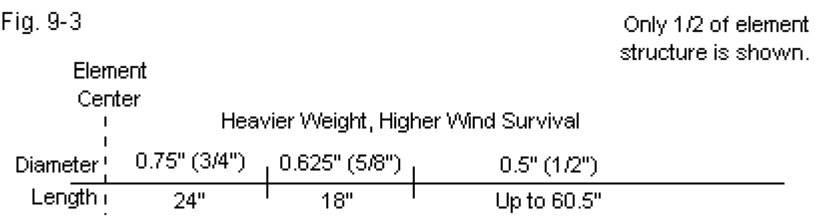

Proposed Stepped-Diameter Element Structure

Driven elements require a split at the center. The gap is part of the element length. The director may use a 48” section of ¾” tubing. The successively smaller section add 2”-3” to each length to fit inside the preceding section. Less than about 2” of overlap may weaken the junction and more than about 3” adds unnecessary weight to the element. (In large beam elements, we may find some sections doubled for added strength.)

My selection of the section lengths and diameters is based on the wind load that the element might be expected to sustain without damage. There are programs such as YagiStress that permit element design to any desired wind load. However, *The ARRL Antenna Book* Yagi chapter contains a wide variety of designs for most upper amateur bands. Most designs appear for medium and heavy duty, that is wind loads in the 60-70 mph range and in the 80+ mph range. You may adopt the appropriate element structure and change only the tip lengths to suit an alternative array design, such as the phased arrays in this volume. However, before we design the new elements, we must be sure that we know what performance curves we wish to replicate.

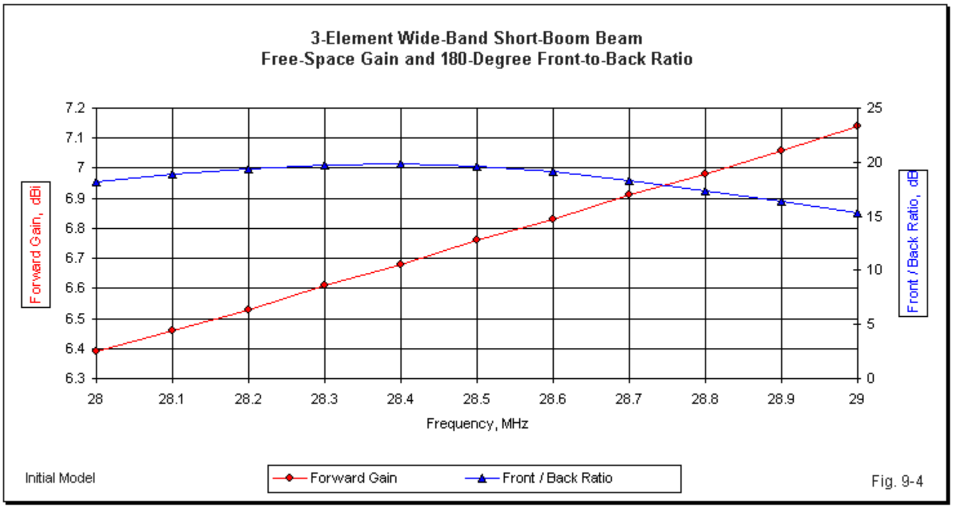

Fig. 9-4 shows the free-space gain and the 180° front-to-back curves from 28 to 29 MHz for the initial model with uniform-diameter elements. The gain runs from about 6.4 dBi to about 7.15 dBi across the passband. The front-to-

back ratio peaks just below the design frequency. The resistance, reactance, and 50-Ω SWR appear in **Fig. 9-5**. Note that the SWR reaches a minimum value at the design frequency, but rises more rapidly above that frequency than below it. Now we know the sort of performance curves that we wish to obtain from the stepped-diameter model of the same array—without changing the phase line or the element spacing.

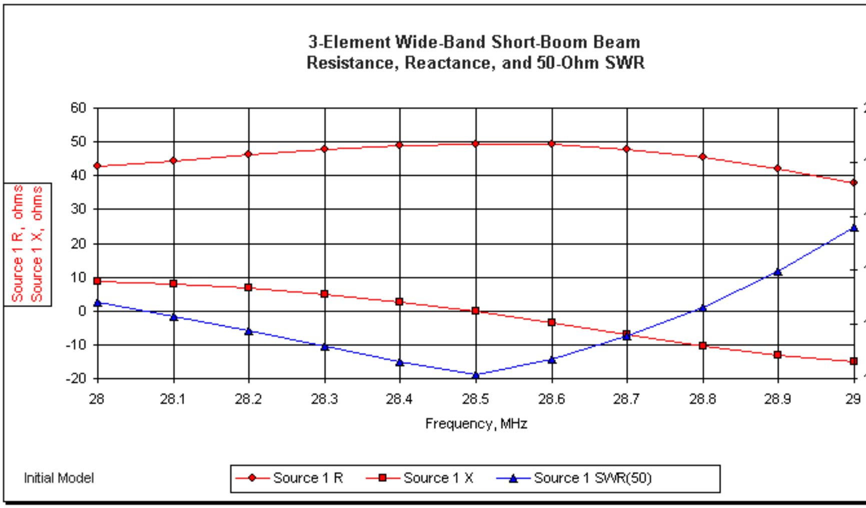

Fig. 9-5

The next step in the conversion process requires that we set up the elements using the stepped-diameter sections. For this step, we need to enable the Leeson or stepped-diameter correction function that is available both in EZNEC and in NEC-Win Plus. The corrections will prove important in telling us how to adjust the element lengths, which we shall do only by changing the outer dimension of the tip section.

Fig. 9-6 shows the wire table with the elements established. (Note that models show only the exposed sections of the tubes and do not show the potion inside the preceding section.) I have set up this model to make evident the tip limits for each element by pairing the left-of-center and the right-of-center element sections. Hence, each element ends with two wires that do not connect to other wires. (See model 9-2.ez.)

Wires

Wire Create Edit Other — Stepped-Diameter Elements Before Adjustment — Fig. 9-6

Coord Entry Mode Preserve Connections Show Wire Insulation

Wires

No.	End 1				End 2				Diameter	Segs
	X (in)	Y (in)	Z (in)	Conn	X (in)	Y (in)	Z (in)	Conn	(in)	
1	0	-24	0	W3E1	0	24	0	W2E1	0.75	5
2	0	24	0	W1E2	0	42	0	W4E1	0.625	2
3	0	-24	0	W1E1	0	-42	0	W5E1	0.625	2
4	0	42	0	W2E2	0	102	0		0.5	6
5	0	-42	0	W3E2	0	-102	0		0.5	6
6	25	-24	0	W8E1	25	24	0	W7E1	0.75	5
7	25	24	0	W6E2	25	42	0	W9E1	0.625	2
8	25	-24	0	W6E1	25	-42	0	W10E1	0.625	2
9	25	42	0	W7E2	25	96	0		0.5	5
10	25	-42	0	W8E2	25	-96	0		0.5	5
11	64	-24	0	W13E1	64	24	0	W12E1	0.75	5
12	64	24	0	W11E2	64	42	0	W14E1	0.625	2
13	64	-24	0	W11E1	64	-42	0	W15E1	0.625	2
14	64	42	0	W12E2	64	93.5	0		0.5	5
15	64	-42	0	W13E2	64	-93.5	0		0.5	5
*										

The outer length limits of each element initially use the values from the uniform-diameter model. However, the effective element length in terms that have an affect on array performance is not that same as for the uniform-diameter elements. Since the elements taper to smaller diameters along their length (as measured from each element center point), they "play" shorter than their physical length. That is, a tapered-diameter element the same length as a roughly comparable uniform-diameter element will have a self-resonant frequency that is higher. The taper of the elements in this example is relatively small. The more radical the taper from the center to the end, the shorter the effective length of the element compared to a uniform-diameter element of the same overall length.

The effective length of the element is not simply the length of an element with the average of the diameters of the sections. The calculations are complex, and both EZNEC and NEC-Win Plus use the highly effective system worked out by Dave Leeson—hence, the name Leeson corrections. **Fig. 9-7** shows the equivalent uniform-diameter elements that EZNEC would substitute for the tapered diameter elements. These substitutes are necessary for NEC-2, since that core does not handle tapered-diameter elements with good accuracy. NEC-4 is quite usable without corrections for gentle tapers, but may show some error if the stepped-diameter schedule has large steps or moves from a very large to a very small diameter over the element length.

Stepped Diameter Correction

Edit Other Stepped-Diameter Elements Before Adjustment Fig. 9-7

Wires

No.	End 1				End 2				Diameter	Segs
	X (in)	Y (in)	Z (in)	Conn	X (in)	Y (in)	Z (in)	Conn	(in)	
1	0	-23.5028	0	W3E1	0	23.5028	0	W2E1	0.569753	5
2	0	23.5028	0	W1E2	0	41.1298	0	W4E1	0.569753	2
3	0	-23.5028	0	W1E1	0	-41.1298	0	W5E1	0.569753	2
4	0	41.1298	0	W2E2	0	99.8867	0		0.569753	6
5	0	-41.1298	0	W3E2	0	-99.8867	0		0.569753	6
6	25	-23.4804	0	W8E1	25	23.4804	0	W7E1	0.577041	5
7	25	23.4804	0	W6E2	25	41.0906	0	W9E1	0.577041	2
8	25	-23.4804	0	W6E1	25	-41.0906	0	W10E1	0.577041	2
9	25	41.0906	0	W7E2	25	93.9215	0		0.577041	5
10	25	-41.0906	0	W8E2	25	-93.9215	0		0.577041	5
11	64	-23.471	0	W13E1	64	23.471	0	W12E1	0.580375	5
12	64	23.471	0	W11E2	64	41.0742	0	W14E1	0.580375	2
13	64	-23.471	0	W11E1	64	-41.0742	0	W15E1	0.580375	2
14	64	41.0742	0	W12E2	64	91.4389	0		0.580375	5
15	64	-41.0742	0	W13E2	64	-91.4389	0		0.580375	5

Note that the length limits of these equivalent elements are just about 2" shorter than the actual lengths of the originals. In passing, we may note that the effective diameter of the elements varies from 0.57" to 0.58". Since each tip section has a slightly different length, the small changes do affect the final value of the effective element diameter. Despite the fact that the effective diameter is greater than the original uniform-diameter 0.5" model, the elements are still electrically shorter than the originals. This fact shows the degree to which the taper itself influences the electrical performance of a linear element. The more extreme the taper of a linear element, the greater will be the degree of electrical shortening.

If we leave the effective length of the elements short, we shall not replicate the performance curves of the original uniform-diameter version of the antenna. For example, **Fig. 9-8** provides the free-space gain and the 180° front-to-back performance curves for the un-adjusted model. Compare the graph to **Fig. 9-4**. The new model shows a bit lower gain, and the frequency of the front-to-back peak value has moved to near the upper limit of the passband.

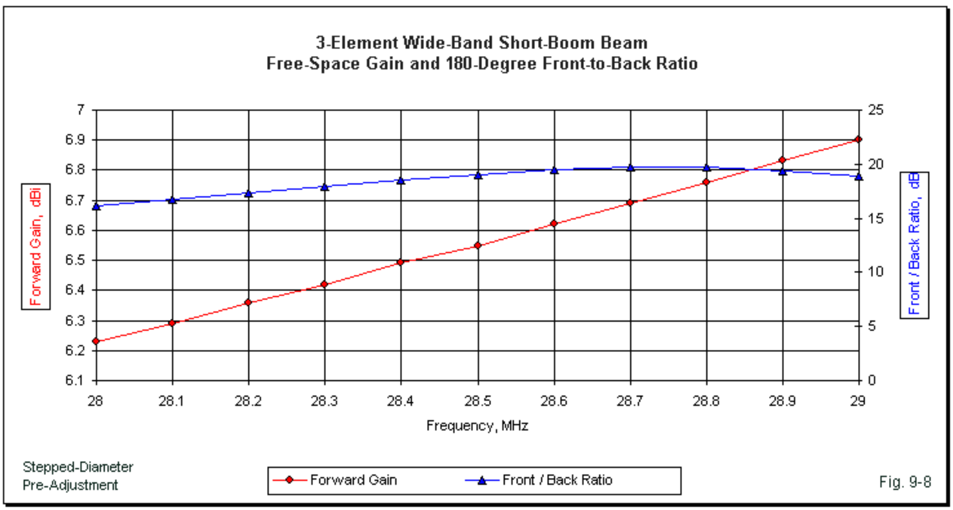

Fig. 9-9 provides the comparable data for the feedpoint resistance, reactance, and 50-Ω SWR. Compare the curves to those in **Fig. 9-5**. The SWR minimum value occurs at 28.9 MHz. As well, the source resistance at 28.0 MHz is below 40 Ω, compared to a higher figure for the original model. The performance curves for this revised model may be acceptable in many circumstances. However, the curves are considerably offset from the originals. If we wish to restore the performance curves, we must adjust the element lengths. (Since the adjustments will be small, we shall not need to adjust the element spacing or the length of the phaseline between the driver elements.)

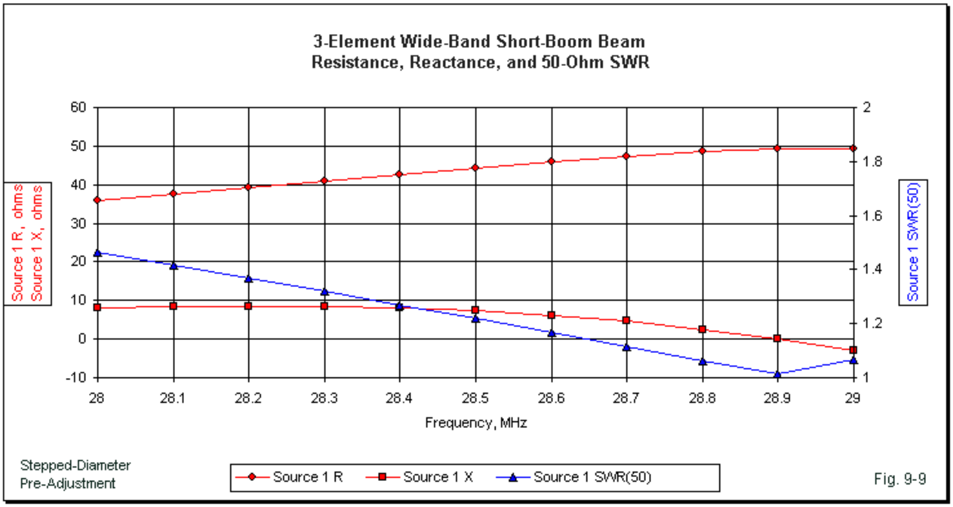

Wires

Wire Create Edit Other "Final" Element Length Adjustments Fig. 9-10

Coord Entry Mode Preserve Connections Show Wire Insulation

Wires

No.	End 1				End 2				Diameter	Segs
	X (in)	Y (in)	Z (in)	Conn	X (in)	Y (in)	Z (in)	Conn	(in)	
1	0	-24	0	W3E1	0	24	0	W2E1	0.75	5
2	0	24	0	W1E2	0	42	0	W4E1	0.625	2
3	0	-24	0	W1E1	0	-42	0	W5E1	0.625	2
4	0	42	0	W2E2	0	102.5	0		0.5	6
5	0	-42	0	W3E2	0	-102.5	0		0.5	6
6	25	-24	0	W8E1	25	24	0	W7E1	0.75	5
7	25	24	0	W6E2	25	42	0	W9E1	0.625	2
8	25	-24	0	W6E1	25	-42	0	W10E1	0.625	2
9	25	42	0	W7E2	25	96.5	0		0.5	5
10	25	-42	0	W8E2	25	-96.5	0		0.5	5
11	64	-24	0	W13E1	64	24	0	W12E1	0.75	5
12	64	24	0	W11E2	64	42	0	W14E1	0.625	2
13	64	-24	0	W11E1	64	-42	0	W15E1	0.625	2
14	64	42	0	W12E2	64	94.5	0		0.5	5
15	64	-42	0	W13E2	64	-94.5	0		0.5	5
*										

We might use the 2" differential between the effective and the actual element lengths of the tip sections as a starting point in adjusting the elements. However, since the effective diameter is larger than the original elements in the uniform-diameter model, we can expect the required changes to be smaller than 2". In fact, the increments of change turn out to be variable among elements, as shown in **Fig. 9-10**.

The phased driver elements each required an increase of 0.5". The director required a full 1" increase. (Note that these values are for each end of the element. Hence, the total length change is twice the value shown. For this exercise, I limited the increment of end-length change to 0.5" per step.) The need to change element lengths by different amounts is normal for the final adjustment process.

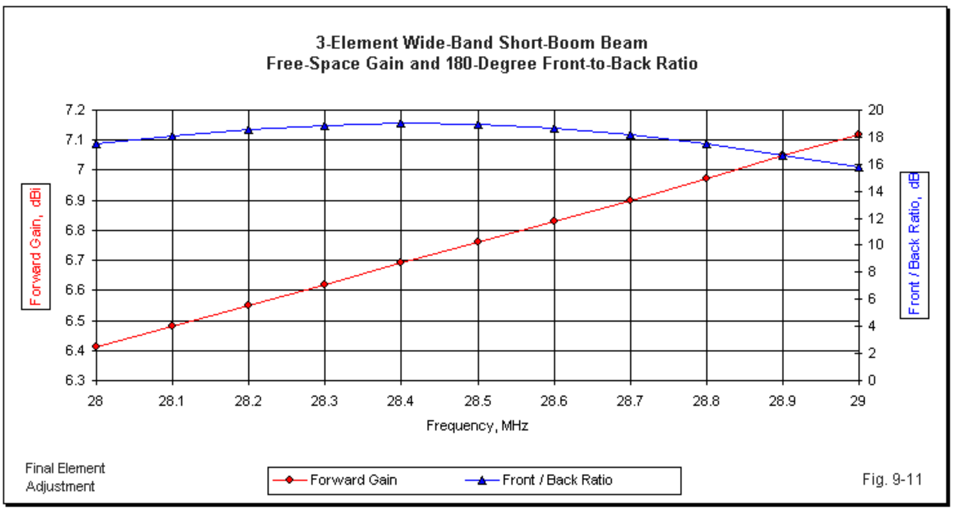

Fig. 9-11

Fig. 9-11 provides a view of the changes in the gain and front-to-back performance curves. Peak gain at 29 MHz is once more greater than 7.1 dBi. As well, the front-to-back curve peaks closer to the center of the band. (Had I used a finer increment of length change in the exercise, the curve peak might easily have come to rest at 28.5 MHz.) **Fig. 9-12** shows the improvements in the feedpoint data curves. The SWR shows its minimum value at 28.6 MHz. This point is slightly high, but the passband edge SWR values are now much closer to each other, with a 1.36:1 peak value.

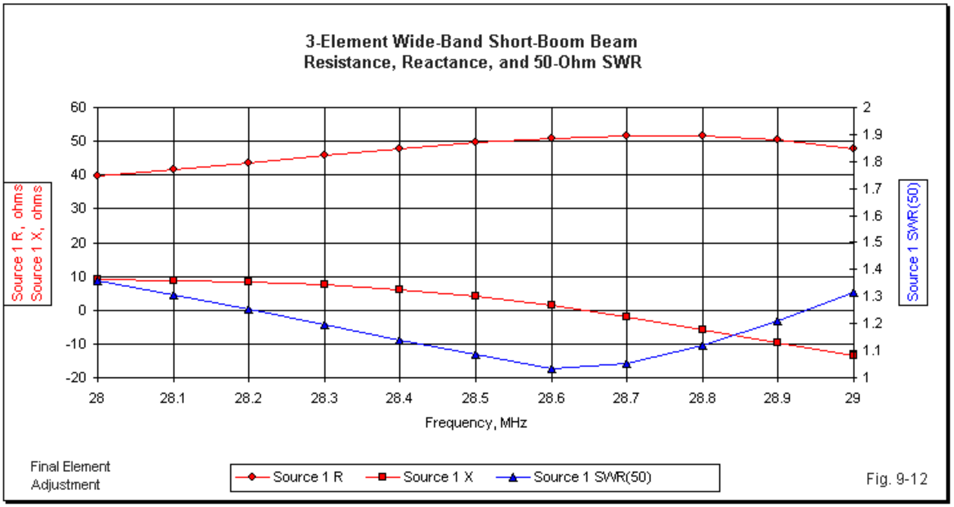

If I selected the stepped-diameter schedule shown in **Fig. 9-3**, I likely would cease my efforts at this point and begin to cut tubing. For all such beams, I would use 6063-T832 tubing, which is not only strong, but nests very closely but smoothly with adjacent sizes.

Scaling and Setting a 20-Meter Version of the Array

Suppose that we wish to build a 20-meter version of the 3-element array. We might be tempted to scale the stepped-diameter version of the 10-meter array. However, that direction of effort would leave us with completely wrong element sections for a usable stepped diameter 20-meter element. Therefore, we need to retreat further to the uniform-diameter version of the 10-meter array.

To scale an antenna requires that we proportionally scale the element length, the element spacing values, and the element diameter. The ratio of a 20-meter wavelength to a 10-meter wavelength is about 2:1. However, we can be much more precise by using the old design frequency (28.5 MHz) and the new design frequency (14.175 MHz). The ratio is about 2.011:1. Therefore, the new uniform-diameter array will have the dimensions shown in **Fig. 9-13**. (See model 9-4.ez.)

Wires

Wire Create Edit Other 10-Meter Uniform-Diameter Array Directly Scaled to 20 Meters Fig. 9-13

Coord Entry Mode Preserve Connections Show Wire Insulation

Wires

No.	End 1				End 2				Diameter	Segs
	X (in)	Y (in)	Z (in)	Conn	X (in)	Y (in)	Z (in)	Conn	(in)	
1	0	-205.079	0		0	205.079	0		1.00529	21
2	50.2646	-193.016	0		50.2646	193.016	0		1.00529	21
3	128.677	-187.989	0		128.677	187.989	0		1.00529	21

Fortunately, EZNEC performs all of the math tasks required, although a hand calculator would make short work of the task. Since all proportions remain the same, the 250-Ω phaseline with its half-twist remains intact at the new spacing between the two driver elements (50.26"). The new element diameter value is so close to 1" that we might easily change it to that value without changing the performance perceptibly.

The 20-meter band has only about 70% of the bandwidth of the 10-meter passband. Therefore, slight irregularities that we passed without notice regarding the performance curves become significant within the more restricted 20-meter passband. **Fig. 9-14** provides a case-in-point: the slight off-center location of the peak front-to-back ratio value becomes a more significant de-centering on the new band. The SWR curve, shown in the data collection in **Fig. 9-15**, is well centered. As we develop a stepped-diameter version of the array, we shall want to keep in mind any value location adjustments and make them as we finalized the element lengths.

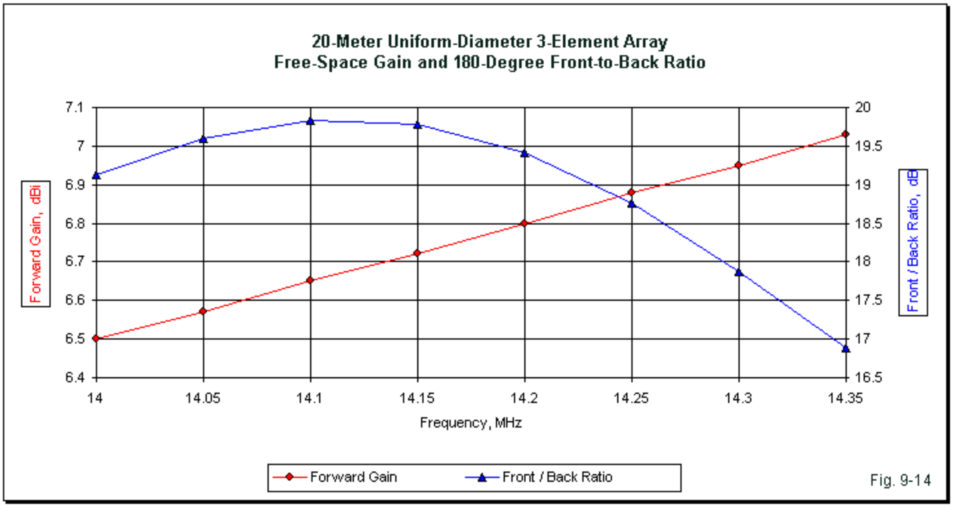

Fig. 9-14

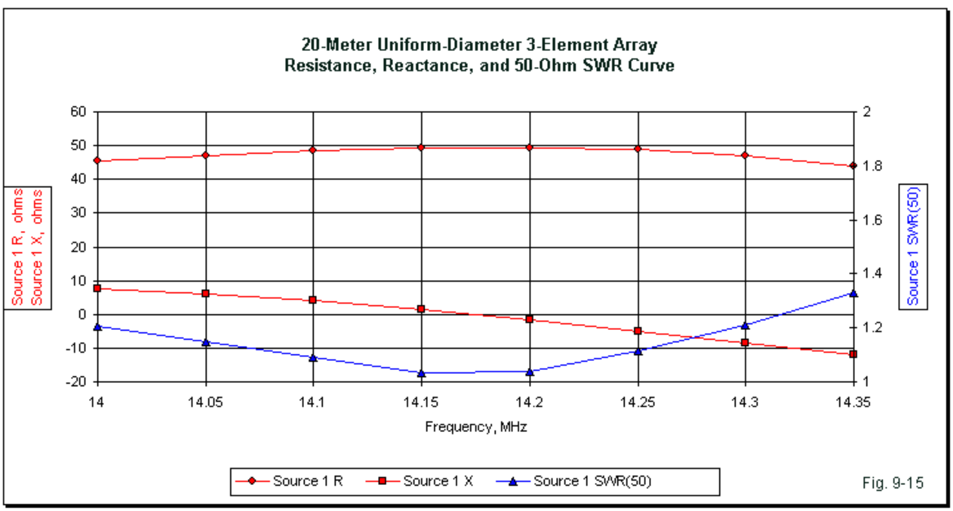

Fig. 9-15

The next step in our development process is to adopt an element taper schedule and to initially apply to it the uniform-diameter model element length values. **Fig. 9-16** shows the resulting wire table. Note the far more complex structure of the individual elements. (See model 9-5.ez.)

Wires

Wire Create Edit Other — Stepped-Diameter 20-Meter Array Wire Table — Fig. 9-16

☐ Coord Entry Mode ☐ Preserve Connections ☐ Show Wire Insulation

Wires

No.	End 1				End 2				Diameter	Segs
	X (in)	Y (in)	Z (in)	Conn	X (in)	Y (in)	Z (in)	Conn	(in)	
1	0	205.1	0		0	154	0	W2E1	0.5	2
2	0	154	0	W1E2	0	134	0	W3E1	0.625	1
3	0	134	0	W2E2	0	92	0	W4E1	0.75	2
4	0	92	0	W3E2	0	72	0	W5E1	0.875	1
5	0	72	0	W4E2	0	48	0	W6E1	1	1
6	0	48	0	W5E2	0	-48	0	W7E1	1.25	5
7	0	-48	0	W6E2	0	-72	0	W8E1	1	1
8	0	-72	0	W7E2	0	-92	0	W9E1	0.875	1
9	0	-92	0	W8E2	0	-134	0	W10E1	0.75	2
10	0	-134	0	W9E2	0	-154	0	W11E1	0.625	1
11	0	-154	0	W10E2	0	-205.1	0		0.5	2
12	50.25	193	0		50.25	154	0	W13E1	0.5	2
13	50.25	154	0	W12E2	50.25	134	0	W14E1	0.625	1
14	50.25	134	0	W13E2	50.25	92	0	W15E1	0.75	2
15	50.25	92	0	W14E2	50.25	72	0	W16E1	0.875	1
16	50.25	72	0	W15E2	50.25	48	0	W17E1	1	1
17	50.25	48	0	W16E2	50.25	-48	0	W18E1	1.25	5
18	50.25	-48	0	W17E2	50.25	-72	0	W19E1	1	1
19	50.25	-72	0	W18E2	50.25	-92	0	W20E1	0.875	1
20	50.25	-92	0	W19E2	50.25	-134	0	W21E1	0.75	2
21	50.25	-134	0	W20E2	50.25	-154	0	W22E1	0.625	1
22	50.25	-154	0	W21E2	50.25	-193	0		0.5	2
23	128.67	188	0		128.67	154	0	W24E1	0.5	2
24	128.67	154	0	W23E2	128.67	134	0	W25E1	0.625	1
25	128.67	134	0	W24E2	128.67	92	0	W26E1	0.75	2
26	128.67	92	0	W25E2	128.67	72	0	W27E1	0.875	1
27	128.67	72	0	W26E2	128.67	48	0	W28E1	1	1
28	128.67	48	0	W27E2	128.67	-48	0	W29E1	1.25	5
29	128.67	-48	0	W28E2	128.67	-72	0	W30E1	1	1
30	128.67	-72	0	W29E2	128.67	-92	0	W31E1	0.875	1
31	128.67	-92	0	W30E2	128.67	-134	0	W32E1	0.75	2
32	128.67	-134	0	W31E2	128.67	-154	0	W33E1	0.625	1
33	128.67	-154	0	W32E2	128.67	-188	0		0.5	2

The element structure for 20 meters requires a considerably larger number of sections, as shown in **Fig. 9-17**. These sections—again taken from an ARRL Yagi design—yield a relatively heavy-duty element for higher wind loads. Note especially the transition from 1.25" to 1" tubing. Within the 1.25" tube is another tube that is 1.125" in diameter (or the 1.25" tube has a wall thickness of 0.125" or just under that value). When planning the tube cutting, we must remember to include an additional 2" to 3" for insertion into the preceding larger tubing section.

Fig. 9-17

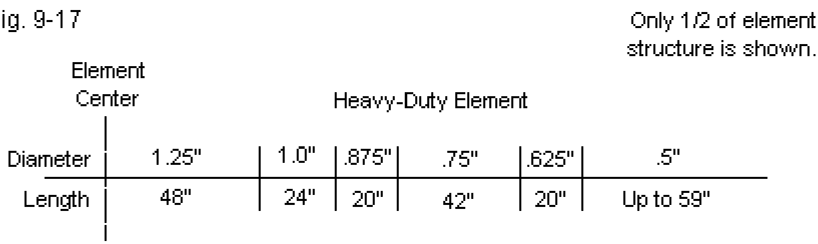

Proposed Stepped Diameter Element Structure for 20 Meters

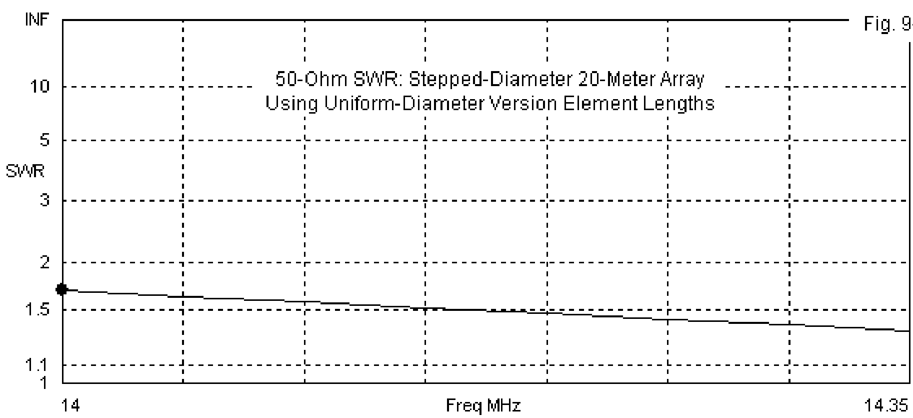

Fig. 9-18

Wires

Wire Create Edit Other — Final 20-Meter Array Wire Table — Fig. 9-19

☐ Coord Entry Mode ☐ Preserve Connections ☐ Show Wire Insulation

Wires

No.	End 1				End 2				Diameter	Segs
	X (in)	Y (in)	Z (in)	Conn	X (in)	Y (in)	Z (in)	Conn	(in)	
1	0	213	0		0	154	0	W2E1	0.5	2
2	0	154	0	W1E2	0	134	0	W3E1	0.625	1
3	0	134	0	W2E2	0	92	0	W4E1	0.75	2
4	0	92	0	W3E2	0	72	0	W5E1	0.875	1
5	0	72	0	W4E2	0	48	0	W6E1	1	1
6	0	48	0	W5E2	0	-48	0	W7E1	1.25	5
7	0	-48	0	W6E2	0	-72	0	W8E1	1	1
8	0	-72	0	W7E2	0	-92	0	W9E1	0.875	1
9	0	-92	0	W8E2	0	-134	0	W10E1	0.75	2
10	0	-134	0	W9E2	0	-154	0	W11E1	0.625	1
11	0	-154	0	W10E2	0	-213	0		0.5	2
12	50.25	201	0		50.25	154	0	W13E1	0.5	2
13	50.25	154	0	W12E2	50.25	134	0	W14E1	0.625	1
14	50.25	134	0	W13E2	50.25	92	0	W15E1	0.75	2
15	50.25	92	0	W14E2	50.25	72	0	W16E1	0.875	1
16	50.25	72	0	W15E2	50.25	48	0	W17E1	1	1
17	50.25	48	0	W16E2	50.25	-48	0	W18E1	1.25	5
18	50.25	-48	0	W17E2	50.25	-72	0	W19E1	1	1
19	50.25	-72	0	W18E2	50.25	-92	0	W20E1	0.875	1
20	50.25	-92	0	W19E2	50.25	-134	0	W21E1	0.75	2
21	50.25	-134	0	W20E2	50.25	-154	0	W22E1	0.625	1
22	50.25	-154	0	W21E2	50.25	-201	0		0.5	2
23	128.67	196	0		128.67	154	0	W24E1	0.5	2
24	128.67	154	0	W23E2	128.67	134	0	W25E1	0.625	1
25	128.67	134	0	W24E2	128.67	92	0	W26E1	0.75	2
26	128.67	92	0	W25E2	128.67	72	0	W27E1	0.875	1
27	128.67	72	0	W26E2	128.67	48	0	W28E1	1	1
28	128.67	48	0	W27E2	128.67	-48	0	W29E1	1.25	5
29	128.67	-48	0	W28E2	128.67	-72	0	W30E1	1	1
30	128.67	-72	0	W29E2	128.67	-92	0	W31E1	0.875	1
31	128.67	-92	0	W30E2	128.67	-134	0	W32E1	0.75	2
32	128.67	-134	0	W31E2	128.67	-154	0	W33E1	0.625	1
33	128.67	-154	0	W32E2	128.67	-196	0		0.5	2

Since we initially used the uniform-diameter lengths for the elements, we do not expect this antenna to perform well within the new passband. **Fig. 9-18** provides a simple SWR curve to show that the antenna is short and everything requires lengthening. **Fig. 9-19** shows by how much we must lengthen the three elements in the array. The average increase per element end is 8". (See model 9-6.ez.)

If we check back to **Fig. 9-17**, we can see that each element-end plays about 8" short of the uniform-diameter physical length value. We may wish to cast a quizzical eye at the fact that our new final values required the full increase, whereas the 10-meter array required lesser increases when we created stepped-diameter elements. Part of the answer lies in the more extreme stepping between the element center section (1.25") and the tip sections (0.5"). The other part of the answer lies in the fact that the stepped element effective diameter is less than the uniform-diameter element value (0.8" to 0.83", in contrast to 1.0"). Under these conditions, we can expect to require greater element lengthening to restore the performance curves.

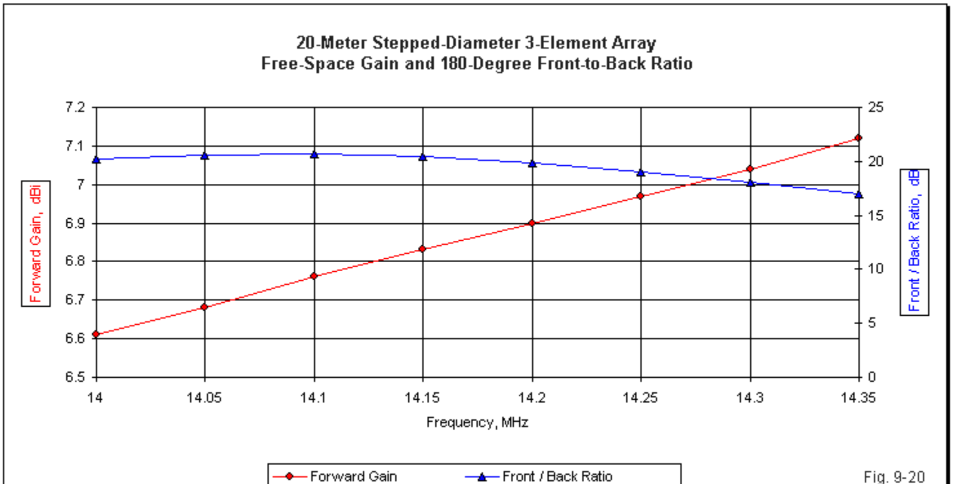

Fig. 9-20

Neither the gain nor the front-to-back curves have moved much from their uniform-diameter positions, as shown in **Fig. 9-20**. Therefore, we might like to tweak this model further, using increments smaller than the 0.5" values that I used in this exercise. Still, the overall performance is numerically superior to the uniform-diameter version of the antenna, but not in any way that a user could detect during operation.

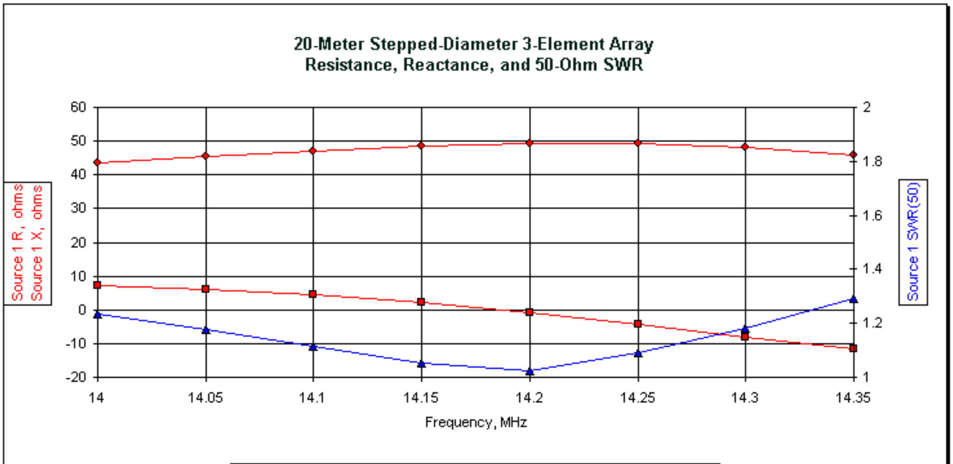

Fig. 9-21

The feedpoint impedance data in **Fig. 9-21** shows well-behaved values, in contrast to the curve in **Fig. 9-18**, taken before we made the semi-final element length adjustments. Although the minimum value occurs just above the band's center frequency, the band-edge values are very well matched. One might expect to see 50-Ω SWR values that never rise above 1.3:1. We may conclude our work here—or we may continue to tweak the model to the limits of what we accomplish in our own shops with careful construction.

Conclusion

I have taken us through the conversion and scaling processes for several reasons. First, too many relatively inexperienced modelers give up on design models if the model does not match the materials at hand. I hope that showing the progression of development steps allows such modelers to perfect better working designs that suit both the operating band and the desired stepped-diameter tubing schedule.

Second, this volume contains a considerable number of highly usable designs for phased arrays, even though all of the analytical work used 10 meters as a test bed. Although the process samples in this chapter used a single design as their focal point, the same principles and techniques apply to every design in the volume. A similar set of considerations will apply to the second volume, which concentrates on wholly parasitic beam designs. They, too, will use a standardized uniform-diameter element for 10 meters. However, the parasitic beams are also adaptable to stepped-diameter elements and changes in the operating band.

Other Publications

We hope you've enjoyed this Volume 1 of the **2-Element Horizontal Beams.** You'll find many other very fine books and publications by the author L.B. Cebik, W4RNL in the ***antenneX Online Magazine BookShelf*** at the web site shown below.

Published by
antenneX Online Magazine
http://www.antennex.com/
POB 271229
Corpus Christi, Texas 78427-1229
USA

ISBN: 1-877992-81-X